The neural basis of stop-signal inhibition in healthy individuals and in schizophrenia patients

Matthew Edward Hughes
BSc(Psyc)(Hons)

Submitted to the University of Newcastle, October 2009, in fulfillment of the degree of Doctor of Philosophy

This thesis contains no material which has been accepted for the award of any other degree or diploma in any university or other tertiary institution and, to the best of my knowledge and belief, contains no material previously published or written by another person, except where due reference has been made in the text. I give consent to this copy of my thesis, when deposited in the University Library, being made available for loan and photocopying subject to the provisions of the Copyright Act 1968.

Matthew Edward Hughes

Acknowledgements

Thanks must first go to my primary supervisor, Professor Pat Michie, for her inspiration and unwavering support, encouragement and confidence in me during this process, and to my secondary supervisor, Dr Ross Fulham for his assistance and conversations regarding data analysis, which I have found invaluable. I would also like to thank a former supervisor, Dr Bill Budd, and Dr Patrick Johnson, for their assistance and friendship (and cigarettes!) that I have enjoyed throughout.

Acknowledgements and thanks must also go to the many others who were integral to the studies detailed here, notably the Schizophrenia Research Institute (SRI) for supporting this work financially, the staff at Hunter Imaging (John Hunter Hospital, Newcastle) particularly Gary O'Conner and Steve Hudson for their assistance with data acquisition, and to Gavin Cooper at the University of Newcastle for programming the experiments.

This process has been made considerably easier by my network of family and friends, who have supported me throughout, especially my mother Vicki, father Robert and his partner Kerry, and my brothers Andrew and Luke without whom I would never have made it. Additionally, I would like to thank my oldest friends, especially Fraser, Robert, Drew, Colin and Trent for their support and good humour. And to my more recently acquired friends from the various labs I have worked and studied in, in particular Alyna, Vanessa, Juanita, Rowena and Sharna for all the conversation and joking around. Special thanks must go to Kathryn for her support, friendship, yoga sessions, tennis games and general fun – high times indeed! Finally, I would like to thank Christina for her love and support during the final stages of writing, and for ignoring my innumerable foibles.

Table of Contents

LIST OF FIGURES VII

LIST OF TABLES IX

GLOSSARY OF ABBREVIATIONS XIV

ABSTRACT XVI

CHAPTER 1: EXECUTIVE CONTROL 1

1.1. Control of cognition 1
1.1.1. Introduction 1
1.1.2 Control and the executive system 1
1.1.3 Definition of executive control 2
1.1.4 Roles and types of executive functions 3
1.1.5 Inhibition as a core feature of cognition 4

1.2. Behavioural inhibition paradigms 5
1.2.1. Behavioural inhibition 5
1.2.2. Go/No-go paradigms 8
1.2.3 The stop-signal paradigm 9
1.2.4 The race model 11
1.2.5 Estimating SSRT 14
Average SSRT 15
SSRT at the mean of the inhibition function 15
SSRT at the median of the inhibition function 15
1.2.6 Inhibition functions 16
1.2.7 Caveats to stop-signal inhibition indices 17
1.2.8 Appropriate setting of stop-signal delays 17

CHAPTER 2: THE FUNCTIONAL NEUROANATOMY OF BEHAVIOUR 19

2.1. Cortico-basal ganglia-thalamocortical pathways 19
2.1.1. Introduction 19
2.1.2. Cortico-basal ganglia-thalamo-cortical circuitry 19
2.1.3. Direct, indirect and hyperdirect cortico-basal ganglia-thalamocortical pathways 23

2.2. The functional neuroanatomy engaged during stop-signal inhibition 26
2.2.1. Overview 26
2.2.2. Rodent lesion evidence 28
2.2.3. Human lesion and TMS evidence 32
2.2.4. Human neuroimaging evidence 34
2.2.5. Stopping in Parkinson's Disease 36
2.2.6. ERPs elicited during stop-signal inhibition 39
2.3.1 Outstanding issues and present studies 47

CHAPTER 3: EXPERIMENT 1 50

3.1. Introduction **53**

3.2. Methods **55**
3.2.1. Participants and Procedures 55
3.2.2. Tasks and Stimuli 56
Stop-signal task: fMRI acquisition 56
Stop-signal task: Inhibition function 58
MR image acquisition 59
MR image pre-processing 59
Data Analysis: Behavioural data 59
Data Analysis: MRI data 60
Region of interest (ROI) analyses 61

3.3. Results **62**
3.3.1. Behavioural data: fMRI session 62
Inhibition function data 63
3.3.2. Functional brain activation 63
Relationship between performance measures and functional brain activation 69
Small volume correction (SVC) analyses 69

3.4. Discussion **70**
3.4.1. Behavioural data 70
3.4.2. Whole brain activation 71
Right inferior frontal gyrus 71
ACC 73
PreSMA 74
Right inferior parietal lobe 75
Cerebellum 75
3.4.3. Conclusion 77

CHAPTER 4: EXPERIMENT 2 ..... **79**

4.1 Introduction **79**

4.2 Methods **87**
4.2.1. Participants and Procedures 87
4.2.2. Tasks and stimuli 87
Behavioural variables 89
Stimulus presentation 91
4.2.3. fMRI session 92
Participants 92
MR image acquisition 92
MR image pre-processing 92
Modeling: First level analyses 93
Group level analyses 94
Determining functional neuroanatomy 94
Region of interest (ROI) analyses 94
4.2.4. ERP session 95
Participants 95
EEG data recording 95
ERP data preprocessing 96
ERP trial averaging 96
ADJAR correction procedure for stop-signal task group average waveforms 96
Measurement of components from Stop and Stop Failure ERP waveforms 97
4.2.5 Correlation of Stop>Go contrasts with Stop related components 98

4.3. Results 98
4.3.1. fMRI session 98
4.3.1.1 Behavioural data 98
Reaction time (RT) data 98
Pre- and Post- event RT differences 99
Stop-signal trial data 100
4.3.1.2. fMRI data 101
Stops > Baseline 101
Simple correlation: SSRT and Stops > Baseline 102
Stop Failures > Baseline 106
Small volume correction (SVC) with a priori ROIs 108
Stops > Stop Failures 110
Stop Failures > Stops 112
ROI analyses: Analysis of parameter estimates 113
4.3.3. ERP session 116
4.3.3.1. Behavioural data 116
RT data 116
Pre- and Post- event RT differences 117
Stop-signal trial data 119
4.3.3.2. Go ERPs 119
4.3.3.3. Stop–signal ERPs 121
Other features of stop-signal ERPs 124
Central features of stop-signal ERPs 124
Auditory evoked N1: average waveform analyses 125
Stop-signal N1 latency 126
Stop-signal N1 Amplitude 126
Mean Stop-signal N2 amplitude 127
Stop-signal P3 128
Stop-signal P3 peak latency 129
Stop-signal P3 peak amplitude 130
Stop-signal P3 mean amplitudes (170 – 400 ms) 130
Relationships between peak measures and stopping indices 131
4.3.3.4. Comparison of fMRI and ERP behavioural data 134
4.3.3.5. Correlation of Stop>Go contrasts with Stop related ERP measures 135

4.4. Discussion 135
4.4.1. Basic behavioural findings 135
4.4.2. fMRI findings 137
4.4.3.ERP findings 144
ADJAR efficacy 145
Stop signals elicit N1 and P3 potentials 145
4.4.4. Integration of fMRI and ERP findings 150
4.4.5. Conclusions 151

CHAPTER 5: A BRIEF INTRODUCTION TO SCHIZOPHRENIA 153

5.1. What is schizophrenia? 153
5.1.1. Introduction 153
5.1.2. Prevalence and incidence 154
5.1.3. Diagnostics 154
Symptomatology 154
Positive symptoms 156
Negative Symptoms 157
Diagnosis 158
5.2. Underlying causes of schizophrenia 158

5.2.1. Theories 158
5.2.2. Neurotransmitter systems and schizophrenia 160
The role of dopamine in schizophrenia 160
Dopaminergic pathways and antipsychotics 161
The role of glutamate in schizophrenia 166

5.3. Neuropsychological functioning in schizophrenia 168
5.3.1. Neuropsychological measures as diagnostic criteria 168
5.3.2. Neuropsychological impairment in schizophrenia 169
5.3.3. Executive functions, attention and memory impairments in schizophrenia 170
5.3.4. Some types of executive functions 172
5.3.5. What is probed during executive function tasks? 174
5.3.6. Performance requirements for executive function tasks 177

5.4. Behavioural inhibition as a discrete impairment in schizophrenia 178
5.4.1. Behavioural findings 178
5.4.2. Further evidence for response inhibition impairments in schizophrenia 180
5.4.3. Go/No-go evidence 181
5.4.4. ERP evidence 181
5.4.5. Neuroimaging evidence 183

5.5. Stop-signal evidence 186
5.5.1. Studies of stop-signal inhibition 186
5.5.2. Stopping in at-risk groups 186
5.5.3. Stopping in patients with a diagnosis of schizophrenia 188
5.5.4. Neuroimaging evidence 189

CHAPTER 6: EXPERIMENT 3 191

6.1. Introduction 191

6.2. Method 194
6.2.1. Research overview 194
6.2.2. Participants 194
Patient medication details and symptom ratings 195
6.2.3. Tasks and stimuli 196
Stimulus presentation 198
6.2.4. Behavioural variables 198
6.2.5. fMRI data 199
MR image acquisition 199
MR image pre-processing 199
Identifying ‘bad scans’ 200
Modeling: First level analyses 200
Modeling: Second level analyses 201
Small volume correction (SVC) analyses 202
6.2.5. ERP data 202
EEG data recording 202
ERP data preprocessing 203
ERP trial averaging 203
ADJAR correction and Group averaging procedure for stop-signal group average waveforms 203
Component measures analyses for Go, Stop and Stop Failure waveforms 203
Integration of fMRI and ERP data 204
Latency and amplitude measures of Stop-N1, Stop-P3 and the Stop P3-N1 latency were correlated with Stops > Go contrast maps and explored in an SVC analysis using a priori ROIs outlined previously. Additionally, the mean of a potential identified in the N2 latency range in Stop Failure ERPs for both

groups was correlated with Stop Failure > Go contrast maps for each group separately, testing for a negative relationship. This data was (post-hoc) explored by application of an ACC ROI constructed from AAL maps in an SVC analysis. 204

6.3. Results 204
6.3.1. Trial type proportions for fMRI and ERP sessions....204
6.3.2. fMRI session....206
6.3.2.1. Age, gender and education 206
6.3.2.2. Behavioural data analyses 206
RT data 207
SSRT and SSD analyses 207
Errors 208
Pre and post-event RT analyses 208
Relationships between behavioural variables and symptom profiles....210
6.3.2.3. fMRI data 210
Go > Baseline: one-sample t-tests 210
Go > Baseline: Matched sample t-tests....210
Stops > Go contrast: One sample t-tests 212
Matched samples t-tests of Stop > Go contrast....216
Number of activated voxels in Go > Stops and Stops > Go contrasts for patient and controls groups..220
Stop Failures > Go: One sample t-tests 220
Matched sample t-tests 224
Simple correlation: SSRT and Stops > Go 229
6.3.3. ERP session 232
6.3.3.1. Age and education 232
6.3.3.2. Behavioural data analyses 233
RT data 233
Error analyses 233
SSD and SSRT....233
Relationships between behavioural variables and symptom profiles....234
Pre and post event RTs differences....234
6.3.3.3. Go stimulus ERP analyses....235
Go-N1 data 237
Peak Go-N1 amplitude and latency analyses....238
Parietal sites: Go-N1 peak amplitude 238
Parietal sites: Go-N1 peak latency....238
Mean Go-N1 amplitude analysis 238
Scalp topography analysis: mean Go-N1 amplitudes 238
Peak Go-P3 amplitude and latency analyses 239
Parietal sites: Go-P3 peak amplitude 239
Parietal sites: Go-P3 peak latency 240
Scalp topography analysis: mean Go-P3 amplitudes....240
6.3.3.4. Stop and Stop Failure ADJAR correction waveforms....240
6.3.3.5. Stop-signal ERP analyses 242
Auditory evoked N1: average waveform analyses 245
Stop-signal N1 peak latency and amplitude measures: At Cz only 246
Stop-signal N1 peak amplitude and latency measures: Across fronto-central sites....246
Inter-relationships between N1 measures, age and symptomatology 248
Mean N2 amplitude measures 250
P3 peak amplitude and latency measures....250
Latency measures 250
Peak amplitude analyses....251
Mean amplitudes: Scalp topography analysis (Group x Hand x Inhibition x AP x Laterality ANOVA) 252
Relationship between stop-signal P3 measures and symptomatology....253
Relationships between SSRT and ERP amplitude and latency measures....253

Relationships between ERP measures and Stops>Go contrasts 253
6.3.4. Between session behavioural analyses 254

6.4. Discussion....255
6.4.1. Overview 255
6.4.2. Behavioural Data 256
SSRT....256
Pre and post event RTs 260
6.4.3. fMRI data 261
Stopping data 261
Go data....263
6.4.4. ERP data 264
ADJAR efficacy 264
Go and stop-signal waveforms 265
N1 findings 266
Stop-signal N1 modulation 267
N1 Latency 270
P3 findings....270
N2 findings 273

CHAPTER 7: DISCUSSION AND CONCLUSIONS....275
7.1 Introduction 275
7.2 Key findings 275
7.3 Neuroimaging data 277
7.4 Electrophysiological data 280
7.5 Stopping in patients with schizophrenia 282
7.6 How this thesis has added to the literature 284
7.7 Limitations of studies 286
7.8 Future directions....288

REFERENCES....290

List of Figures

Figure 1.1. Go and No-go trials in a simple Go/No-go variant..... 9
Figure 1.2. Stop-signal paradigm trial types. 10
Figure 1.3. Models used to describe inhibition. 12
Figure 1.4: The race model (adapted from Logan & Cowan, 1984). 13
Figure 2.01. The parallel cortico-basal ganglia-thalamo-cortical circuits (adapted from Alexander et al., 1986) 20
Figure 2.02. The 'direct', 'indirect' and 'hyperdirect' cortico-basal ganglia-thalamocortical pathways (adapted from Nambu et al., 2002). 24
Figure 3.1. Brain activation revealed by the Stop vs. Go contrast slicing up through cerebellar and cerebral cortices from left to right and top to bottom. 67
Figure 3.2. Correlation between Stop vs. Go contrast values in right inferior frontal gyrus ROI and average SSRT across delays. 69
Figure 4.01. Stop-signal task trials. 89
Figure 4.02. Regression of PI and SSRT. 101
Figure 4.03. Cortical activation for Stops > Baseline contrast (thresholding at $p < .001$, 10 contiguous voxels) with views of right hemisphere (left), superior midline (centre) and left hemisphere (right) activation. 103
Figure 4.04. Brain areas in Stops > Baseline contrast maps showing significant positive correlations with SSRT (thresholding at $p < .01$, and 10 contiguous voxels)..... 103
Figure 4.05. Negative correlation between Stops > Baseline contrast maps and SSRT (thresholding at $p < .01$, and 10 contiguous voxels), showing right hemisphere (on left), mid-line sagittal (middle), and left hemisphere (on right) views. 106
Figure 4.06. Cortical activation for Stop Failures > Baseline contrast (thresholding was $p < .001$, 10 contiguous voxels) with views of the right hemisphere (left), superior midline (centre) and left hemisphere (right) activation. 107
Figure 4.07. Brain regions showing significant activation in the contrast of Stops > Stop Failures (thresholding was $p < .01$, and 10 contiguous voxels). 112
Figure 4.08. Scatterplots of mean parameter estimates against SSRT for ROIs that were significantly correlated with SSRT, in addition to the correlation of MFG parameter estimates and SSRT 115
Figure 4.09. Left and right hand grand average Go ERPs at frontal (F3, Fz, F4), central (C3, Cz, C4) and parietal sites (P3, Pz, P4). 120
Figure 4.10. Scalp correction waveforms estimated by the ADJAR procedure at midline and lateral frontal (F3,Fz,F4), central (C3,Cz,C4) and parietal sites (P3,Pz,P4) for left and right Stops and Stop Failures. 122
Figure 4.11. Plots of uncorrected stop-signal ERPs, ADJAR correction waveforms, and ADJAR corrected stop-signal ERPs at Cz for left and right hands. 123
Figure 4.12. Stop-signal ERPs for left and right hands. 125
Figure 4.13. Scatterplots depicting relationships observed between SSRT and left hand Stop-P3 amplitude (on left), and SSRT and right hand Stop-P3 (on right) at Fz. 132
Figure 4.14. Scatterplots of the difference between Stop-P3 and Stop-N1 peak latency and SSRT for left and right hands at Fz. 133
Figure 6.01. Go > Baseline contrasts (right is right). 212

Figure 6.02. Cortical activation for Stops > Go in control and patient groups 215
Figure 6.03. Subcortical and anterior cingulate (ACC) activation revealed in Stops > Go 216
Figure 6.04. Prefrontal and subcortical areas revealing greater activation in the controls > patients contrast above threshold activation 218
Figure 6.05. PFC activation surviving threshold ($p < .05$, 10 contiguous) when Stops > Go contrasts were compared for patients > controls. 219
Figure 6.06. Within group activation for (A) controls (top panel views: right hemisphere cortex, superior cortical surface, and left hemisphere cortex), and (B) patients (bottom panel views: right hemisphere cortex, axial slice emphasizing STN activation,, and left hemisphere cortex). 223
Figure 6.07. Control group activation shown by axial slices through the cortex for the Stops > Stop Failure contrast (thresholding was $p < .01$, 10 contiguous voxels). 228
Figure 6.08. Left and right hand correct grand average Go ERPs for control and patient groups. 236
Figure 6.09. Outcome from ADJAR correction procedure at Cz for (A) left hand, and (B) right hand, Stop and Stop Failure grand average ERP waveforms for control and patient groups. 242
Figure 6.10. Left hand ADJAR corrected Stop and Stop Failure grand average ERP waveforms for control and patient groups. 244
Figure 6.11. Right hand ADJAR corrected Stop and Stop Failure grand average waveforms for control and patient groups. 245
Figure 6.12. Scatterplots of Stop-N1 latency and total SANS scores for left and right hands at Fz (top panel) and Cz (bottom panel). 249

List of Tables

Table 3.1 62
Behavioural Data obtained from Scanning Sessions. RT means displayed are calculated from median RTs from individual participants. 62
Table 3.2 63
Mean Stop-signal Delay (SSD) and Mean Probability of Inhibition (P(I)) at each delay. .. 63
Table 3.3 64
Group brain activation for the Stops > Passive contrast. 64
Table 3.4 65
Group brain activation for the Go > Passive contrast. 65
Table 3.5 68
Group Brain Activation Revealed in the Stop vs Go Contrast 68
Table 3.6 68
Non-parametric Group Brain Activation Revealed in the Stop vs Go Contrast. 68
Table 4.01 97
Latency ranges over which component measures were extracted for statistical analysis 97
Table 4.02 99
Mean group data for behavioural indices (with standard deviations in parentheses) from fMRI sessions 99
Table 4.03 100
Group means of participant median pre and post event RTs in ms collapsed over left and right hands (with standard deviations in parenthesis). 100
Table 4.04 102
Activation table for Stops > Baseline (thresholding was $p < .001$, 10 contiguous voxels) 102
Table 4.05 104
Brain areas revealing positive SSRT correlated BOLD variance in Stops > Baseline contrasts (thresholding was $p < .01$, 10 contiguous voxels) 104
Table 4.06 105
Brain areas revealing negative SSRT correlated BOLD variance in Stops > Baseline contrasts (thresholding was $p < .01$, 10 contiguous voxels) 105

Table 4.07 107
Activation table for Stop Failures > Baseline (thresholding was p < .001, and 10 contiguous voxels) 107
Table 4.08 109
Small volume correction (SVC) output for right hemisphere *a priori* regions of interest (ROIs) 109
Table 4.09 111
Activation table for Stops > Stop Failures (thresholding was p < .01, and 10 contiguous voxels) 111
Table 4.10 113
Activation table for Stop Failures > Stops (thresholding was p < .01, and 10 contiguous voxels) 113
Table 4.11 114
Means and standard deviations of parameter estimates extracted in right hemisphere brain regions defined by AAL probability maps and their Pearson's correlation (r) with SSRT (one-tailed) 114
Table 4.12 115
Correlation matrix of parameter estimates extracted from *a priori* ROIs that were significantly correlated with SSRT, r (sig.) 115
Table 4.13 117
Mean scores on behavioural indices (with standard deviations in parentheses) from ERP sessions 117
Table 4.14 118
Group mean pre and post event RTs (with standard deviations in parentheses) collapsed over left and right hands 118
Table 4.15 127
Summary of group mean (N = 12, with standard deviation in parentheses) Stop-N1 and Stop Failure-N1 peak amplitude and latency measures of N1 (time window = 50 – 150 ms) at Fz and Cz for left and right hand events 127
Table 4.16 128

Summary of group mean (with standard deviation in parentheses) Stop and Stop Failure N2 mean amplitude measures (across the time window 180 – 320 ms) at midline electrodes averaged for left and right hand events (N = 14) 128
Table 4.17 129
Summary of group mean (with standard deviation in parentheses) Stop and Stop Failure peak amplitude and latency measures of P3 (time window = 170 – 600 ms) at Fz, Cz and Pz for left and right hand events (N = 11) 129
Table 4.18 131
Summary of group mean (with standard deviation in parentheses) Stop and Stop Failure P3 mean amplitude measures (across the time window 170 – 400 ms) at midline electrodes averaged for left and right hand events (N = 14) 131
Table 6.01 195
Antipsychotic medication summary for the patient group 195
Table 6.02 196
Mean ratings (with standard deviations in parentheses) on SAPS and SANS sub-scales, total global scores for the patient group 196
Table 6.03 205
Mean numbers and proportions (with standard deviations in parentheses) of trial types by experimental session 205
Table 6.04 208
Left and right hand fMRI session behavioural data for patient and control groups 208
Table 6.05 209
Patient and control group median pre and post event RTs for left and right hands 209
Table 6.06 211
Brain areas surviving thresholding from matched samples t-tests, Controls > Patients and Patients > Controls, in a comparison of Go > Baseline contrast maps (thresholding was $p < .01$, and 10 contiguous voxels) 211
Table 6.07 213
Control group activation for Stops > Go contrast (thresholding was $p < .01$, and 10 contiguous voxels) 213
Table 6.08 214

Patient group activation for Stops > Go contrast (thresholding was p < .01, and 10 contiguous voxels) 214
Table 6.09 217
Areas surviving thresholding in a matched-samples t-test contrast testing differences in Stop > Go related activation for Controls > Patients 217
Table 6.10 219
Areas surviving thresholding in a matched-samples t-test contrast testing differences in Stop > Go related activation for Patients > Controls 219
Table 6.11 220
Total voxels surviving thresholding (at p < .05, 5 contiguous voxels) for left, right and combined Go > Stops and Stops > Go contrasts for patient and control groups 220
Table 6.12 221
Control group activation for Stop Failures > Go one sample t-test (p < .01, and 10 voxels) 221
Table 6.13 222
Patient group activation for Stop Failures > Go one-sample t-test (p < .01, and 10 voxels) 222
Table 6.14 224
Areas surviving thresholding in a matched-samples t-test contrast testing differences in Stop Failures > Go related activation for Controls > Patients. 224
Table 6.15 225
Areas surviving thresholding in a matched-samples t-test contrast testing differences in Stop Failures > Go related activation for Patients > Controls 225
Table 6.16 226
Control group activation for a repeated-measures t-test contrast of (Stops > Go) > (Stop Failures > Go; p < .01, and 10 voxels) 226
Table 6.17 228
Control group activation for a repeated-measures t-test contrast of (Stop Failures > Go) > (Stops > Go; p < .01, and 10 voxels) 228
Table 6.18 229

Control group t-maps arising from the negative correlation of SSRT with Stops > Go contrast maps (thresholding was p < .01 and 10 contiguous voxels)..... 229
Table 6.19..... 230
Patient group t-maps arising from the correlation of SSRT with Stops > Go contrast maps (thresholding was p < .01 and 10 contiguous voxels)..... 230
Table 6.20..... 231
SVC analyses for control group Stops > Go and Stop Failures > Go contrast t-maps 231
Table 6.21..... 232
ERP session behavioural data (hand-wise) for patients and control groups 232
Table 6.22..... 235
Control and patient group pre and post event RTs for left and right hand events 235
Table 6.23..... 237
Group means at parietal sites P3 and P4 for Go-N1 peak amplitude and latency (controls = 11, patients = 9), and for mean Go-N1 amplitude (controls = 13, patients = 10)..... 237
Table 6.24..... 251
Group mean stop-signal P3 peak latency measures (in milliseconds, ms) for control (N = 12) and patient (N = 7) groups used in fronto-central midline electrode analysis. Standard deviations are in parentheses 251
Table 6.25..... 252
Group mean stop-signal P3 peak amplitude measures (in microvolts, μV) for control (N = 12) and patient (N = 7) groups used in fronto-central midline electrode analysis. Standard deviations are in parentheses 252

Glossary of abbreviations

AAL……automated anatomical labeling
ACC……anterior cingulate cortex
ADJAR……..adjacent response technique
ADHD……attention deficit hyperactivity disorder
BA……..Brodmann Area
BOLD……blood oxygenation level dependent
DBS……deep brain stimulation
DLPFC……...dorsolateral prefrontal cortex
DSM……...Diagnostic and Statistical Manual of Mental Disorders
EEG……electroencephalogram
EOS……early onset schizophrenia
EPI……..echo-planar imaging
EPS…….extra-pyramidal symptoms
ERP…….event-related potential
FEF…….frontal eye fields
fMRI……...functional magnetic resonance imaging
FWHM……full width at the half-maximum
GABA…….gamma amino butyric acid
GABAergic…….using GABA as a neurotransmitter
GLM……...general linear model
GoRT……median Go reaction time
GP……...globus pallidus
GPe……..globus pallidus (*pars externa* - external capsule)
GPi……..globus pallidus (*pars interna* - internal capsule)
HRF…….....hemodynamic response function
IFG……..inferior frontal gyrus
IPL……..inferior parietal lobe
ISI……...interstimulus interval
M1……...primary motor cortex (or sensorimotor cortex)
MFG……....middle frontal gyrus
MNI…….Montreal Neurological Institute
MRT……median reaction time
NMDA……N-methyl D-asparate
N1……first negative-going ERP component
N2……second negative-going ERP component
OCD……obsessive-compulsive disorder
OFC……orbital frontal cortex
PCP……..phencyclidine
PET……..positron emission tomography
PD……Parkinson's Disease
PI…….probability of inhibition (also P(i))
PFC……..prefrontal cortex
PMC…….premotor cortex
PR…….probability of responding (also P(r))

P3…….third positive going ERP component
preSMA……...pre-supplementary motor area (or anterior supplementary motor area)
ROI……..region of interest
RTs……..reaction times
SANS……...scale for the assessment of negative symptoms
SAPS……....scale for the assessment of positive symptoms
SFG……..superior frontal gyrus
SMA……supplementary motor area
SNr……..substantia nigra *pars reticulate*
SOA……stimulus onset asynchrony
SSD…….stop-signal delay
SSRT……...stop-signal reaction time
STN…….subthalamic nucleus
STG…….superior temporal gyrus
STR…….striatum
SVC…….small volume correction
Thal…….thalamus
TMS……transcranial magnetic stimulation
VLFPC……ventrolateral prefrontal cortex
VTA……ventral tegmental area
WCST……Wisconsin card sorting test
ZRFT……...z relative finishing time

Abstract

The capacity to inhibit planned or on-going action enables individuals to flexibly control behaviour in response to changing task demands or a change in goals. This capacity, termed *response inhibition*, is a core function of the executive control system and is often studied in laboratory settings using the stop-signal paradigm, which was used for studying response inhibition throughout this thesis. The stop-signal paradigm (Logan & Cowan, 1984) is increasingly being used by research groups to study response inhibition largely due to the indices of behavioural control afforded by stop-signal procedures, notably the speed of response inhibition processes and the capacity to trigger these processes.

Lesion, transcranial magnetic stimulation and neuroimaging experiments have linked stopping to activity in the right inferior frontal gyrus (IFG), and some evidence indicates a role for the subthalamic nucleus (STN). These brain areas are thought to form a network which acts by suppressing thalamo-cortical output to motor cortex. Event-related potential studies have linked stopping to amplitude enhancement of an N1-P3 complex during successful inhibition trials compared to unsuccessful inhibition trials.

The primary aim of this thesis was to investigate the spatio-temporal dynamics of stop-signal inhibition in healthy individuals using electrophysiological and neuroimaging methods, and secondly, to investigate the neural basis of impaired stopping in patients with a diagnosis of schizophrenia – the first of its kind using the stop-signal paradigm. Several previous behavioural studies have reported slowed stop-signal response inhibition processes in patients with schizophrenia, but an impaired capacity to trigger response inhibition processes has also been reported.

In each of the three neuroimaging studies detailed herein, stopping was related to activation in right IFG and STN, and in one study a model for the difficulty of inhibition was proposed, which predicted activity in this network. Consistent with previous reports, stopping processes in patients with schizophrenia were slower compared to controls, and right IFG and STN were uniquely underactivated in the patient group. Additionally, one study revealed a link between response inhibition speed and both Stop-P3 amplitude, and the latency difference between N1 and P3 potential peaks elicited on stop-signal trials.

Chapter 1: Executive control

1.1. Control of cognition

1.1.1. Introduction

The brain systems that are engaged in humans for overt modulation of processing in other structures may be termed control processes. While some brain processes are controllable, other processes are uncontrollable; once begun, they go on to completion and cannot be stopped. These are appropriately termed ballistic processes. Therefore, brain processes may be broadly classed as control, controllable, and uncontrollable or ballistic processes. This discussion is concerned with control processes, commencing with a brief overview of control theory and the major roles of controlled processing in humans. In this section a working definition of control processes is proposed to provide a frame of reference within which to understand control. The final half of the discussion is concerned with a specific inhibitory function: the inhibition of on-going action.

1.1.2 Control and the executive system

Most cognitive processes are automatic in the sense that they occur spontaneously without any cognitive effort, for example, the orienting response we all produce when a sudden flash of light or loud noise is perceived or reading of a common word when it is seen. Orienting to sudden, violent stimuli is usually described as being a naturally selected trait that is a survival instinct (Sokolov, Nezlina, Polyanskii & Evtikhin, 2002). In contrast, word reading is automatised due to repeated performance over time (Schneider & Shiffrin, 1977; Shiffrin & Schneider, 1977), eventually becoming independent of intention requiring few resources or effort. The low level sensory processes linked to perception of such stimuli are ballistic in the sense that they cannot be stopped, but orienting and word reading responses are controllable via cognitive effort. Suppressing automatic behaviours and responses, or sequencing them into an organized larger set of cognitions or behaviours requires cognitive control. Such automatic behaviours cannot be readily "turned off".

Exactly how control is implemented in the brain is not known. However theorists have proposed models describing how it may occur. Prominent among these are a

supervisory attention system (Norman & Shallice, 1986) whereby anterior (supervisory) areas override automatic or routine processing in posterior (subordinate) systems when situations arise requiring control for a successful outcome. Other models posit a *central executive* (Baddeley, 1986) that activates and inhibits processing in subordinate systems to achieve intended outcomes (Logan & Cowan, 1984; Roberts & Pennington, 1996). Despite differences in these views of control, both express a hierarchical notion of processing, whereby central processes exert control over processing in subordinate structures. The dominant position of the central system, or central executive, has led to this (theoretical) system being termed the 'executive system', which carries out 'executive functions' via 'executive processes'.

While the exact nature of the executive system is not well understood, and highly controversial given the implied notion of a homunculus (Baddeley, 1996; Hazy, Frank & O'Reilly, 2007), it is widely accepted that the frontal lobes provide the cortical basis for controlled processing (Fuster, 1997; Fuster, 2000; Stuss, 2006). The advent of functional neuroimaging tools has enabled researchers to investigate executive control in a more thorough and direct manner, and findings from these investigations have only served to strengthen the link between frontal cortex and executive control.

1.1.3 Definition of executive control

There is still much debate regarding the nature of executive functions, and consequently also lacking is a solid definition and definitive taxonomy of cognitive processes that may be considered executive processes. For the purposes of this thesis, a twofold definition of executive control will be assumed. Executive functions must satisfy both:

1. a set of processes that act by enhancing activation or inhibiting activation of subordinate or downstream processes, including those related to the optimization and monitoring of performance.
2. a set of processes that are intentionally engaged by individuals for performance of any cognitive or behavioural task

This definition is intended to capture the intentional or volitional nature of processes that act in a top-down manner to directly influence processing in subordinate systems, as those that are of the executive system. These processes operate by enhancing or inhibiting activation in subordinate systems, hence the term 'executive', and relate to intentional control of thought and behaviour. Acts of control may include the instigation and modulation (enhancing or inhibiting) of processing in subordinate systems. It must be stressed that the definition relates to intended or directed processing, not processing that proceeds in an automatic or stimulus driven manner (i.e., prepotent and non-declarative processes).

1.1.4 Roles and types of executive functions

Executive functions underpin performance of day-to-day activities such as driving, working and shopping for groceries, and thus serve multiple psychological roles. Primarily, control processes have roles in on-going behaviour whereby processing in subordinate brain systems is selectively activated or inhibited for correct and/or optimized performance, and are especially important for processing during novel situations (Stuss, 2007). Additionally, executive processes serve an emergent role whereby moment-to-moment processing aimed at achieving a sub-goal occurs in an integrated sequential manner to realise higher overarching goals. Such goal-directed activity is the highest order of processing, representing the capacity of humans to operate effectively in the world – the attempt to make internal representations (or goals) manifest as external events or objects. It follows that individuals engage in a series of *acts of control* in order to realise higher goals (Logan & Cowan, 1984), whether the intended goal is to hit a ball with a racket, write a PhD thesis, court a mate, promote a political agenda, or paint a scene, etc.

Some theorists have argued that the executive system operates as a unitary construct (Duncan, Emslie, Williams, Johnson & Freer, 1996; Duncan & Owen, 2000) with a primary role in 'adaptive encoding' (Duncan & Miller, 2002) whereby frontal cortex as a whole adapts to task goals. In contrast, others have proposed a modular view of executive functioning (Stuss, 2006; Stuss, Shallice, Alexander & Picton, 1995; Shallice, 2002), whereby distinct frontal structures are engaged for distinct operations. The latter 'fractional' view of executive processing is strongly supported by lesion studies indicating

that unique cognitive operations require integrity of unique frontal areas (Aron, Fletcher, Bullmore, Sahakian & Robbins, 2003a; Mayr, Diedrichsen, Ivry, & Keele, 2006; Stuss, 2006).

Although a definitive taxonomy of executive control functions is a matter of serious debate (for a recent review see Jurado & Rosselli, 2007) and is beyond the scope of this thesis, processes that are often described as executive functions include maintenance and updating of task rules and goals in working memory (Miyake et al., 2000), task-switching (Rogers & Monsell, 1995), manipulation of representations in working memory (Perry et al., 2001), planning (Shallice, 1982), selective and sustained attention (Kane & Engel, 2002), performance monitoring (Carter et al., 1998), and the intentional inhibition of thought and action (Logan & Cowan, 1984).

1.1.5 Inhibition as a core feature of cognition

Roberts and Pennington (1996) have proposed that what is common among tasks tapping executive functions is a competitive dynamic between relevant and irrelevant representations in working memory. For correct responding, irrelevant representations must be inhibited in favour of relevant representation. However, 'inhibition' can refer to various unrelated processes, e.g,, from suppressing irrelevant representations from entering working memory, to suppressing processing of an irrelevant stimulus dimension in favour of processing a relevant dimension of the same stimulus (e.g., Stroop task performance), or even the outright inhibition of an action that is in-progress (for review see Nigg, 2000). While the model presented by Roberts and Pennington (1996) appears to refer to a unitary inhibitory mechanism to account for the functions of the executive, the diverse modes of inhibition indicate a modular view of inhibitory capacities that may account for executive functioning (Nigg, 2000).

Use of the term 'inhibition' is notoriously loose in the literatures, referring to everything from Freudian-like repression, to neurochemical modulation at the synapse (Aron, 2007). This holds true even within the cognitive literature, despite attempts to delineate facets of cognitive and behavioural inhibition (e.g. Nigg, 2000). Cognitive theories point to the role of inhibition in cognitive and behavioural processing, both in development and normal functioning (Harnisfeger, 1995), and moreover, some theories of

psychiatric disorders point to the role of impaired inhibitory control arising from dysfunction in the neural circuits underpinning inhibitory capacities in the emergence of clinical pathologies (Casey, Durstan & Fossella, 2001; Dillion & Pizzagalli, 2007; Nigg, 2000; Verbruggen & Logan, 2008).

In her influential review, Harnisfeger (1995) defines cognitive inhibition as the ability to suppress the activation of irrelevant trace items in working memory during task performance, and suggests that inhibitory control is a crucial marker of cognitive development and normal cognitive functioning. Equally crucial in development is behavioural inhibition, defined as resisting temptation, delaying gratification, impulse control and motor inhibition. Harnishfeger describes models (Bjorkland & Harnishfeger, 1990; Harnishfeger & Bjorkland, 1993) proposing a developmental trajectory in which infants are unable to inhibit prepotent responses but gradually learn to control behaviour by initially directing themselves via external commands, and, at a later stage of development, by internal speech. Maturing cognition is indicated by more efficient processing (faster spread of activation), and the capacity to suppress irrelevant representations from working memory, and inappropriate responses and actions from day-to-day behaviour. Hence intentional inhibition, a prototypical executive function, is vital in both development and aging as it enables us to gain control of ourselves in development, and stay in control throughout the lifespan.

1.2. Behavioural inhibition paradigms

1.2.1. Behavioural inhibition

From the above review, it can be seen that a key facet of executive functioning is the intentional inhibition of thought and action (Aron, 2007; Harnishfeger, 1995; Nigg, 2000; Roberts & Pennington, 1996). This capacity involves the ability to interrupt and cancel processing in subordinate systems (Logan & Cowan, 1984) and relates not only to overcoming prepotent or non-declarative processes, but also the cancellation of on-going processes, no matter the stage of processing, i.e., whether processes to be inhibited are

related to preparation processes (i.e.. readying for action), or processes responsible for the execution of responses (i.e. performing action).

Many neuropsychological tests of executive function have been criticised for their heavy loading on multiple component processes, e.g. working memory and selective attention in the Wisconsin Card Sorting Test (Miyake et al., 2000). Tasks developed by cognitive psychologists suffer less from this problem, and are based on highly articulated models that can predict changes in dependent variables when task factors are manipulated. One such task is the stop-signal paradigm, (Logan & Cowan, 1984; Logan, 1994), which is traditionally used to measure response inhibition. This paradigm enables researchers to index the ability of individuals to stop (or inhibit) inappropriate or no longer relevant thought and/or behaviour, but is traditionally used as a behavioural paradigm. Variants of this paradigm are used in the experiments detailed in later chapters of this thesis, which were aimed at understanding the spatial and temporal properties of the neural networks responsible for the inhibition of on-going action, and whether patients with schizophrenia reveal impaired and/or differential network activation during this act of control compared to healthy controls, as suggested by previous research (Badcock, Michie, Johnson & Combrinck, 2002; Davalos, Compagon, Heinlein & Ross, 2004; Enticott, Ogloff & Bradshaw, 2008; Ross, Wagner, Heinlein & Zerbe, 2008).

The necessity to stop planned or on-going response activation processes arises when a current thought or behaviour is rendered inappropriate due to a change in current goals, or more commonly, a change in environmental contingencies, that may arise from within or external to a behaving individual. Imagine you are waiting at traffic lights, anxiously anticipating a green signal that will allow you to get to work on time. You are, as always, running late, not having consumed the necessary quantity of caffeinated beverages required for efficient processing at that hour. Finally, the lights change and you begin to activate your intended behaviour – to engage or enhance the processes that will lead to your car lurching forward in a controlled fashion. However, the green signal to go is for a right turn[1], presented in the form of a green right-pointing arrow, not the desired green circle stimulus – the universal symbol for drivers to proceed. To avoid an accident, harassment

[1] Under Australian law, drivers must use the left side of the road for travel, hence in this example the driver is turning right from the left hand turning lane.

and embarrassment, the go related activation must be cancelled. That is, the go response processes must be stopped completely and suddenly to halt the action. Note that in the example given, a cue to proceed leads to the instigation of processes that, if not suppressed, will lead to an overt and observable response. Also note that after or during the processing of this go stimulus, another stimulus arises, this time as an internal contingency, instructing you to cancel the instigation of the go response behaviour, "…I'm not going right – STOP!"

It is quite evident that the earlier a crucial stimulus is detected, the easier it is to alter behaviour. Hence our ability to implement control over our behaviour hinges on the relative time of detecting a stimulus which instructs or stimulates us to countermand a planned response, or one that is about-to-be-executed. The timing of an inhibition stimulus illustrates two distinct aspects of executive motor control. If the intention to act is formed as a motor plan but not launched prior to the detection of a signal to stop, the planned response is easily inhibited since it is still under the command of the (central) executive system. However, if response execution processes have been activated – indicated by increased activation of subordinate processes that lead to overt behaviour - it is less likely the response will be inhibited.

De Jong and colleagues (1990, 1995) have argued that if response execution processes have begun, a different control mechanism is engaged by the executive to inhibit responding in a non-selective manner. This mechanism is thought to be engaged to inhibit response related processes downstream of central response execution processing, i.e. downstream of the neural outflow from sensor motor cortex (M1). If this outflow has not commenced, then what is required is selective inhibition of central response activation (preparation and/or planning) processes. But if outflow from M1 has commenced, then engagement of the non-selective mechanism is required. De Jong described this as a peripheral inhibitory mechanism. The claim of a peripheral inhibition mechanism has been controversial, with other groups suggesting the data indicate the graded activation of a single central inhibition mechanism (Band & van Boxtel, 1999). But what cannot be doubted is that on successful inhibition trials where inhibition processes are instigated relatively late compared to the instigation of response activation processes, then inhibition is effected at a later stage of response readiness. Both De Jong et al. and van Boxtel and

colleagues (2001) report that response inhibition processes are effective even when target muscles are executing the go response. This corroborative evidence indicates that responses may be inhibited at later stages of response activation processing than response preparation or selection that occur prior to response execution, and may have theoretical implications for the neural mechanism(s) evoked to suppress responding.

Paradigms that are most commonly used to investigate response inhibition include the Go/No-go paradigm and the Stop-signal paradigm. In the following descriptions of these paradigms, the stage of response readiness where inhibition is effected will be emphasized, supporting the notion that No-go inhibition is easier than stop-signal inhibition, at least for the way in which these experimental paradigms are usually operationalised.

1.2.2. Go/No-go paradigms

Go/no-go paradigms[2] reflect situations when an inhibition stimulus is detected prior to the launch of overt response activation process. There are two tasks/trial types (see Figure 1.1); a Go task and a No-go task. The Go task is usually a simple or choice reaction time task, and requires behaving participants to elicit fast, accurate responses indicated by Go stimuli. In contrast, for the No-go task, No-go stimuli instruct no response. The Go task constitutes the majority of experimental trials such that over successive trials overt responding becomes prepotent. That is, the go response becomes dominant whereby the participant is increasingly likely to make an overt response no matter what stimulus is presented. The only index of inhibitory control derived from experiments using go/no-go paradigms is error rates which are manipulated by increasing the proportion of go trials and by using short stimulus onset asynchronies (SOAs; the time between successive trial onsets).

[2] This refers to classical Go/No-go paradigms involving only the requirements to respond when a Go stimulus is presented and to not respond when a No-go stimulus is presented. Some researchers have investigated No-go inhibition using more complex paradigms such as that employed by Garavan and colleagues (1999). In that paper, the letters 'X' and 'Y' were presented amongst a stream of other letters; participants were required to respond to these (targets) only if the previous target letter was not the current letter. Hence participants were only required to respond if X and Y alternated, but if the current letter was identical to the previous target, then no response (No-go) was required.

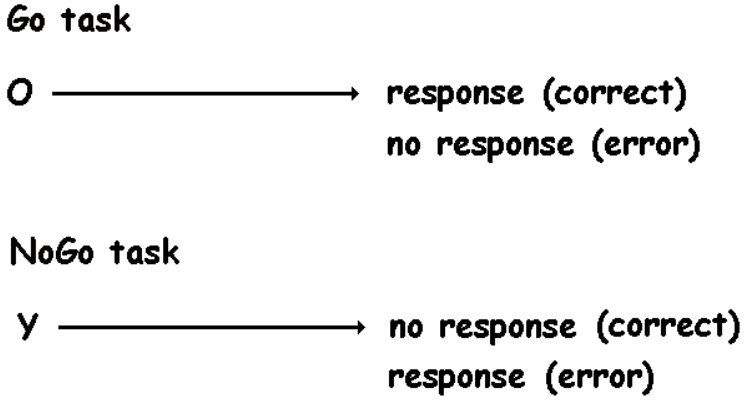

Figure 1.1. Go and No-go trials in a simple Go/No-go variant. The Go stimulus is the letter 'O', and the No-go stimulus is the letter 'Y'. Go stimuli instruct a reaction time response (usually a button press). A failure to respond during Go trials is called an error of omission. Responding during No-go trials is called an error of commission.

What is important for this discussion is that only one stimulus is presented on each trial and that during No-go trials, participants are not instructed to respond. On each trial, stimuli instruct the behaving participant to either respond or not to respond. Hence Go/No-go experiments may operationalise situations requiring inhibitory control where inhibition stimuli are detected in the early stages of response activation processes, even prior to the commencement of these processes. However, it is possible that if responding is highly prepotent, or when participants are anticipating the timing of stimulus presentation, response activation processes may have evolved somewhat – response execution processes may even have been instigated – prior to No-go stimulus presentations. In such cases, inhibition may also be required at late stage of response readiness.

1.2.3 The stop-signal paradigm

Stop-signal paradigms[3] comprise two tasks which are performed concurrently. The primary task, as elaborated by Logan and Cowan (1984), is a choice reaction time task where participants are required to make fast, accurate responses to alternate primary

[3] This thesis is concerned with non-selective 'stop-all' response inhibition, which requires suppression of all active responses (Logan, 1994). Another common type of stop-signal paradigm operationalises 'selective-stopping' where stop-signals instruct response inhibition on some but not all stop-signal trials (see De Jong, Coles & Logan, 1995; Logan, 1994).

stimuli. These stimuli are mapped to alternate responses such as left and right hand responses. Primary stimuli are often called Go stimuli (see Figure 1.2), and are presented stochastically and with equal probability. For example, the letters O and X presented visually instructing left and right hand button press responses, respectively. The primary task usually constitutes the majority of trials in stop-signal experiments.

A stop-signal task trial commences with the presentation of a Go stimulus, initiating response activation processes, however, at some interval after the onset of the Go stimulus another stimulus is presented. This stimulus, the stop-signal (often a tone), instructs the participant to inhibit response activation processes instigated by the Go stimulus. This is the stop-signal task (see Figure 1.2).

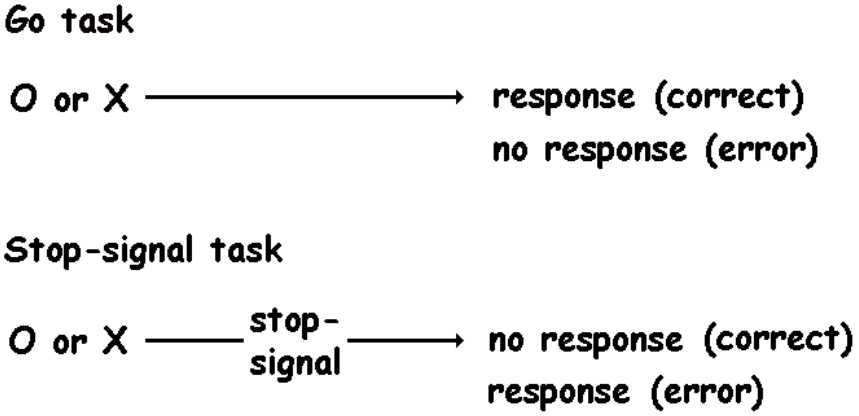

Figure 1.2. Stop-signal paradigm trial types. The Go task begins with the presentation of a primary stimulus which activates response activation processes. In this example, the letter O is mapped to a left hand response and the letter X is mapped to a right hand response. The correct response is that cued by the primary stimulus, whereas no response is called an error of omission and an incorrect response may be termed an incorrect Go error. Stop-signal task trials also begin with the presentation of go stimuli, however, after a short delay a stop-signal is presented, instructing the participant to inhibit response activation processing cued by the preceding Go stimulus. Successfully inhibited responses are called Stops, indicated by no response, whereas any response is called a Stop Failure, or a commission error.

The interval between the onset of primary stimulus presentation and stop-signal presentation is called the *stop-signal delay*. Varying the stop-signal delay is the primary method of manipulating inhibition difficulty; increasing stop-signal delay increases the likelihood that participants will respond to the target stimulus (probability of responding,

P(r)), while decreasing the delay increases the likelihood that the primary task response will be inhibited (probability of inhibition, P(i)). The relationship between P(r)/P(i), stop-signal delay and GoRT is accounted for by a race model, which was formally articulated by Logan and Cowan (1984).

In his compendium of the stop-signal paradigm, Logan (1994) calls the latencies of responses on the primary task *no-signal reaction times* (no-signal RT) and the latencies of responses to Go stimuli on the stop-signal task, *signal-respond reaction times* (signal-respond RT) which are the result of *stop failures*. While clear for those familiar with the nomenclature, these terms will not be used in this thesis as they were deemed ambiguous by proof readers. Instead, no-signal reaction times will be called Go reaction times (GoRTs), and signal respond reaction times will be called Stop Failure reaction times (Stop Failure RTs). In addition incorrect Go reaction times will be called incorrect Go reaction times (IncorrectGoRTs), and no response Go trials (errors of omission) will be called Go misses or missed Go trials. This nomenclature is less confusing for all readers, and more precise for those unfamiliar with the literature.

1.2.4 The race model

Race models are the simplest models of neural interaction that have been used to describe inhibitory interactions between competing response alternatives, consisting of two accumulators that race to some threshold by accumulating sufficient activation for execution (Burle, Vidal, Tandonnet & Hasbroucq, 2004). The accumulator reaching response threshold first wins the race and is thus executed. What is important about this model is that the accumulators are stochastically independent, i.e., they do not interact.

In their seminal paper, Logan and Cowan (1984) formally articulated response inhibition on the stop-signal paradigm using a race model (sometimes called the horse race model of inhibition, see Figure 1.4). In numerous experiments, race models account for behavioural data very well, however, such models do not parallel the neural circuitry involved which appear to involve direct inhibitory connections. Direct inhibitory interactions between competing response alternatives is not accounted for by race models. For this reason, Boucher and colleagues (2007) compared the ability of a race model and an interactive model (see Figure 1.3B) to account for behavioural and neurophysiological data

recorded from fixation (inhibitory) and movement neurons from the frontal eye fields and superior colliculus during an antisaccade task. Both models predicted behavioural findings, but only the interactive model could account for the neurophysiological data. In this thesis, only the behavioural predictions from the stop-signal task are of interest, hence the classical race model (see Figure 1.3A and Figure 1.4) will be dealt with.

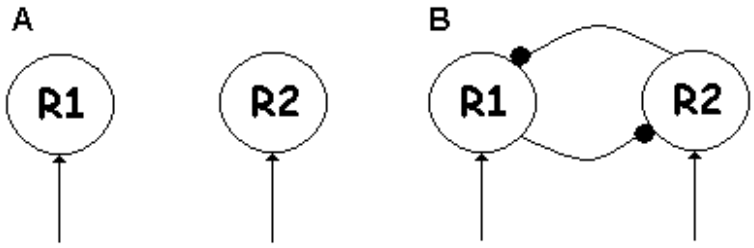

Figure 1.3. Models used to describe inhibition. (A) A simple race model consisting of two accumulators (denoted by R1 and R2) that race to accumulate sufficient activation for execution; the losing response is not executed. (B) An interactive model where accumulators increase activation via upstream inputs, and inhibit the other accumulator as a function of these inputs. The accumulator reaching the required threshold first is executed. Hence the speed of response execution is partly dependent on response competition, but this results in direct inhibition of a competitor, not just determining position at a bottleneck.

In the race model, the processes modeled are Stop-signal task response activation processes cued by Go stimulus presentation (a Go response), and Stop-signal task response inhibition processes; these competing processes are independent and vary randomly in latency. The set of processes that win the race determines whether the response is executed or inhibited. If the Go response cued activation processes win, an overt response is executed, but if the stop-signal cued response inhibition processes win, response activation processes are inhibited (no overt response). What is important in determining the outcome of the race is the relative finishing times of these sets of processes. The latency of stop-signal cued inhibition processes is called the *stop-signal reaction time* (SSRT), and is the major dependent variable derived from stop-signal task experiments (Band, van der Molen & Logan, 2003; Logan, 1994).

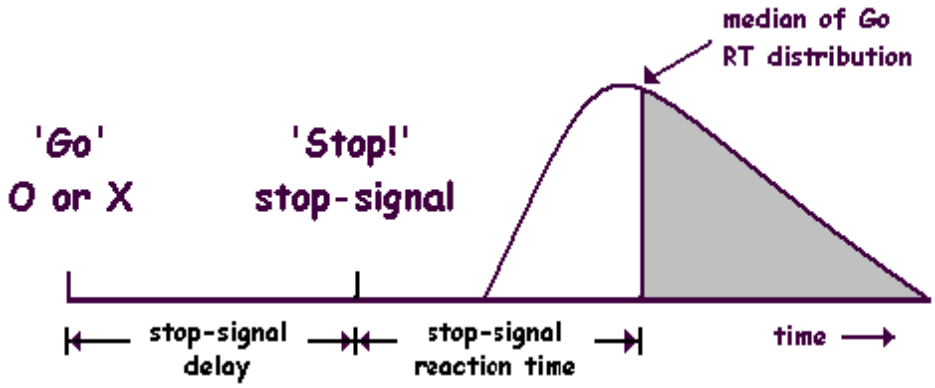

Figure 1.4. The race model (adapted from Logan & Cowan, 1984). The Go task requires fast, accurate responses mapped to visual go stimuli (O or X). On a small proportion of trials (approx. 25%) a stop-signal (usually a tone) is presented just after a go stimulus, requiring response activation processing cued by the go stimulus to be inhibited. The delay between the onset of go stimuli and stop-signals is the stop-signal delay; participants produce a probability of responding (P(r), white portion under the Go RT distribution curve) at a given stop-signal delay. The grey portion under the Go RT curve is the probability of inhibition, P(i).

As stated previously, the race model assumes these processes operate independently, therefore when experimental data are modeled they are treated as discrete random variables. This implies that response inhibition is probabilistic. If we assume momentarily that SSRT is constant, as the race model does, it can be seen from Figure 1.4 that at a given stop-signal delay, the finishing time of inhibition processes cut off part of the GoRT distribution. The area under the distribution to the left of the line reflects the probability that response activation processes will finish first, P(r), while the area under the distribution to the right of the line reflects the probability that response inhibition processes will win the race, P(i). Hence stop-signal delay influences the outcome of the race by handicapping one set of processes in favour of the other set of processes. Increasing stop-signal delay increases P(r), while decreasing stop-signal delay increases P(i). Similarly, an increase in median GoRT will result in an increase in P(i), whereas a decrease in median GoRT will result in an increase in P(r). It follows that the GoRT distribution traces out a probability density function. In the stop-signal literature this is often referred to as an inhibition function.

A core feature of the race model is that it permits two valuable indices of inhibitory control. These indices include estimates of the speed of inhibition processes, and an estimate of the capacity of a participant to trigger inhibition processes. The speed of inhibition processes is the speed of the unobservable response to the stop-signal, SSRT. The capacity of participants to trigger inhibitory responses is indicated by the slope of inhibition functions generated by plotting the probability of inhibiting primary task responses over a range of stop-signal delays.

1.2.5 Estimating SSRT

One obstacle in the study of behavioural inhibition is that inhibition responses are covert and thus unobservable. Unlike measuring overt response reaction times, the surreptitious nature of inhibition processes does not permit direct measurement of SSRT. Stop-signal procedures overcome this difficulty by application of the race model. The model implies that at a given stop-signal delay, P(r) cuts off some proportion of the cumulative no-signal reaction time distribution and so corresponds to some definite GoRT, $t_{P(r)}$. In turn, this GoRT, $t_{P(r)}$ corresponds to the sum of the stop-signal delay, t_d, plus SSRT, t_s:

$$t_{P(r)} = t_d + t_s \qquad (1)$$

Therefore, an estimate of stop-signal reaction time at a given stop-signal delay is given by:

$$t_s = t_{P(r)} - t_d \qquad (2)$$

To accomplish this, the distribution of GoRTs from an experiment is first rank ordered and expressed as a percent cumulative distribution. P(r) at some stop-signal delay is determined by summing the number of times a stop failure was incurred at some specific stop-signal delay and dividing this sum by the number of stop-signal task trials at that delay. P(r) is then converted to a percentage and the GoRT corresponding to P(r) x 100 in the cumulative distribution of Go RTs is the estimated value of $t_{P(r)}$. As t_d is known, equation (2) is easily solved for t_s. This single measure of SSRT has been termed 'observed

SSRT' ($SSRT_{obs}$; Band et al, 2003). Band and colleagues (2003) describe this observed value as being distinct from the actual or 'internal' SSRT ($SSRT_{in}$).

Average SSRT

However, a common feature of stop-signal experiments is that SSRT decreases with increasing stop-signal delay, hence estimating SSRT at a single stop-signal delay is unreliable. A more valid estimate is obtained by averaging SSRT estimates over a range of stop-signal delays ($SSRT_{avg}$; Band et al, 2003).

SSRT at the mean of the inhibition function

Another estimate of SSRT is derived by subtracting the mean (or median) GoRT from the mean of the inhibition function ($SSRT_{mean}$; Band et al, 2003; Logan & Cowan, 1984). For an accurate estimate, equal numbers of stop-signal delays should be distributed about the midpoint of the inhibition function (see below for more detail on inhibition functions). That is, at P(r) = .5, there should be data concerning P(r) at an equal number of stop-signal delays on either side of this point. Estimation accuracy is enhanced by obtaining larger numbers of data points distributed about P(r) = .5. This is given through the following relationship:

$$SSRT_{mean} = \text{mean no-signal RT} - [(P(r)_2 - P(r)_1)t_{d2} + (P(r)_3 - P(r)_2)t_{d3} + (P(r)_4 - P(r)_3)t_{d4}]/(P(r)_4 - (r)_1) \quad (3)$$

where $P(r)_n$ is the probability of responding at stop-signal delay, t_n.

SSRT at the median of the inhibition function

This estimate is the difference between the median GoRT and stop-signal delay at the median of the inhibition function (Logan & Cowan, 1984). The delay estimate is obtained by regression of P(r) onto a range of stop-signal delays and reading off the delay when P(r) = .5 and the median of the GoRT distribution is simply the RT at the 50^{th} percentile on the no-signal RT distribution ($SSRT_{med}$; Band et al., 2003).

Other estimates are obtainable such as that of Colonius (1990) where the entire distribution of SSRTs from a data set are calculated and the median discerned from this distribution, however this method is of little use when sub-optimal experimental conditions are in use as is generally the case (Band et al., 2003).

1.2.6 Inhibition functions

The probabilistic nature of inhibition on the stop-signal task is described by an inhibition function; the relationship of P(r) (or P(i)[4]) to stop-signal delay. The function is generated by assessing the probability of inhibiting primary task responses over a range of delays and plotting P(r) against stop-signal delay. In functional terms, the slope of an inhibition function indexes the capacity to trigger inhibition processes; steeper slopes indicate a greater capacity to trigger inhibition. Furthermore, the difficulty a participant or group has in controlling a measured behaviour is demonstrable through a comparison of inhibition functions (Logan and Cowan, 1984; Logan, 1994).

The shape of the function is influenced by both the mean and variability of the no-signal RT distribution. The mid-point of the function, where P(i) = P(r) = .5, depends on the mean of the GoRT distribution; assuming estimated SSRT remains constant, a shift in mean Go RT of *x* ms results in a shift of the inhibition function to the right of *x* ms on the horizontal abscissa. The steepness of the function depends on the variability (standard deviation, σ) of the GoRT distribution. To correct inhibition functions for these influences (mean (or median) GoRT and σ), the point on the GoRT distribution that the response to the stop-signal occurs at each delay is expressed as a Z score (ZRFT, Z relative finishing time; Logan & Cowan, 1984):

$$ZRFT = (\text{mean GoRT} - t_d - t_s)/\sigma \qquad (4)$$

where t_s is calculated using equation 2.

This transformation is sufficient to align all inhibition functions so long as a central SSRT estimate is used (Band et al, 2003; Logan & Cowan, 1984). A group difference in

[4] P(r) = 1-P(i). P(r) data is most commonly presented (Logan, 1994).

inhibition function slopes that is still present after ZRFT transformation is taken as an indication of a true group difference in stopping performance.

1.2.7 Caveats to stop-signal inhibition indices

Band and colleagues (2003) used Monte Carlo simulations to test the influence of experimental design on SSRT and inhibition functions. Design variations focused on the setting of stop-signal delays which included tracking inhibition performance using a Levitt rule (Levitt, 1971) and using fixed stop-signal delays set relative to the onset of Go stimuli on stop-signal task trials. It was found that $SSRT_{med}$ and $SSRT_{av}$ were always accurate measures of $SSRT_{obs,}$ while $SSRT_{mean}$ was not accurate when fixed stop-signal delays were used. Hence stop-signals should be set relative to the onset of Go stimuli while attempting to sample around P(r) = .5 in contrast to having delays fixed relative to the onset of Go stimuli.

Band and colleagues also found that ZRFT transformations of inhibition functions were not sufficient to account for the variability in stopping performance between groups. Most importantly, ZRFT transformations did not correct for the variability in no-signal RT distributions. Other factors including the variability in the distribution of SSRTs in a data set had an effect on inhibition function slopes leading the authors to conclude that inhibition function slopes are not a reliable index of stopping behaviour unless GoRT distributions are essentially homogenous.

These findings from Band and colleagues (2003) reinforce the robustness of SSRT as an index of response inhibition, but appear to invalidate the use of inhibition function slopes. Nonetheless recent evidence from rodent lesion studies conducted by Eagle and colleagues (2003a/2003b/2008), have linked lesions in remote brain areas to dissociable stopping deficits indicated by SSRT and the slope inhibition functions. These findings suggest that separate neural regions may control the speed and triggering of stopping processes.

1.2.8 Appropriate setting of stop-signal delays

Important considerations for stop-signal experiments include the choice of stop-signal delays, in addition to the ratio of stop-signal trials to no-signal trials in the

experiment. Increasing the proportion of stop-signal trials make such trials more predictable and has been shown to result in participants delaying primary task responses to facilitate inhibition success (Logan, 1994). However, one needs to consider the trade-off between this proportion and the time taken for participants to perform all experimental trials. Logan (1994) suggests using approximately 25% stop-signal trials as a compromise.

Inhibition success is also facilitated when stop-signal delays are presented at fixed delays relative to the onset of primary stimuli (Badcock et al., 2002; Logan, 1994; Ollman, 1973), largely due to the adoption of strategies by participants aimed at enhancing inhibition success. The optimum method of setting stop-signal delays is to use a tracking procedure such as that proposed by Levitt (1971) such that inhibition success is steady at around 50%.

This thesis is concerned with the spatial and temporal dynamics of the neural networks that are responsible for stop-signal inhibition, and whether these networks are dysfunctional in patients with schizophrenia. Outlined above is a broad description of executive functioning, with a focus on response inhibition and the stop-signal inhibition. The next chapter is a brief review of the literature on the neural networks that underpin executive control processes, with a detailed focus on response inhibition operationalised in Stop-signal and Go/No-go paradigms.

Chapter 2: The functional neuroanatomy of behaviour

2.1. Cortico-basal ganglia-thalamocortical pathways

2.1.1. Introduction

Decades of anatomical, pharmacological, histochemical and lesion studies in both animals and humans, indicate that behavioural control is implemented via activation within discrete cortico-subcortical pathways that involve diverse cortical areas, especially the frontal and limbic cortices, in addition to basal ganglia and thalamic nuclei (for reviews see Alexander, De Long & Strick, 1986; Mink, 1996; Nambu, Tokuno, & Takada, 2002; Temel, Blockland, Steinbusch & Visser-Vandewalle, 2005). However, the functionality of individual pathways and how they interact to execute controlled thought and behaviour is not well understood. Indeed, the study of rudimentary neural connectivity, neurotransmitters and their action at receptors within the cortical and subcortical areas comprising these pathways, are some of the most intensively researched areas in neuroscience. With the knowledge of basic brain function and organisation gained in these fields, in addition to that derived from decades of research by cognitive psychologists, cognitive neuroscientists have attempted to explain higher order cognitive and behavioural abilities (or processes) in terms of the functionality of these cortico-subcortical pathways. The importance of understanding the neurocognitive and neurobehavioural functionality of this neural circuitry cannot be understated as such knowledge represents the doorway to understanding directed, conscious thought and ensuing behaviour, and hence the nature of the supposed 'mind of man'. Furthermore, understanding normal brain function at this level enables researchers to target research efforts regarding the neural basis of cognitive and behavioural dysfunction in psychopathology (Casey, et al., 2001; Ring & Serra-Mestres, 2002; Temel et al., 2005).

2.1.2. Cortico-basal ganglia-thalamo-cortical circuitry

Current theories of neurocognitive function propose that exertion of cognitive and/or behavioural control commences with activation of cortical efferents that input to the basal ganglia (Alexander, et al., 1986; Alexander & Crutcher, 1990; Casey et al., 2001;

Miller & Cohen, 2001; Mink, 1996). These inputs arise from either of motor (primary motor cortex, M1; supplementary motor area SMA; premotor cortex, PMC), oculomotor (frontal eye fields, FEF), dorsolateral prefrontal (DLPFC) and ventrolateral orbital prefrontal (VLPFC), or anterior cingulate (ACC) and mesial orbital frontal (OFC) cortices (Alexander, et al., 1986; Temel et al., 2005). 'Basal ganglia' is a generic term that refers to a group of highly interconnected subcortical nuclei, including the striatum (STR; caudate, putamen and nucleus accumbens), the internal and external segments (or capsules) of the globus pallidus (GPi and GPe, respectively), the substantia nigra pars reticulata (SNr), and the subthalamic nucleus (STN), in each hemisphere (Alexander et al., 1986; Temel et al., 2005).

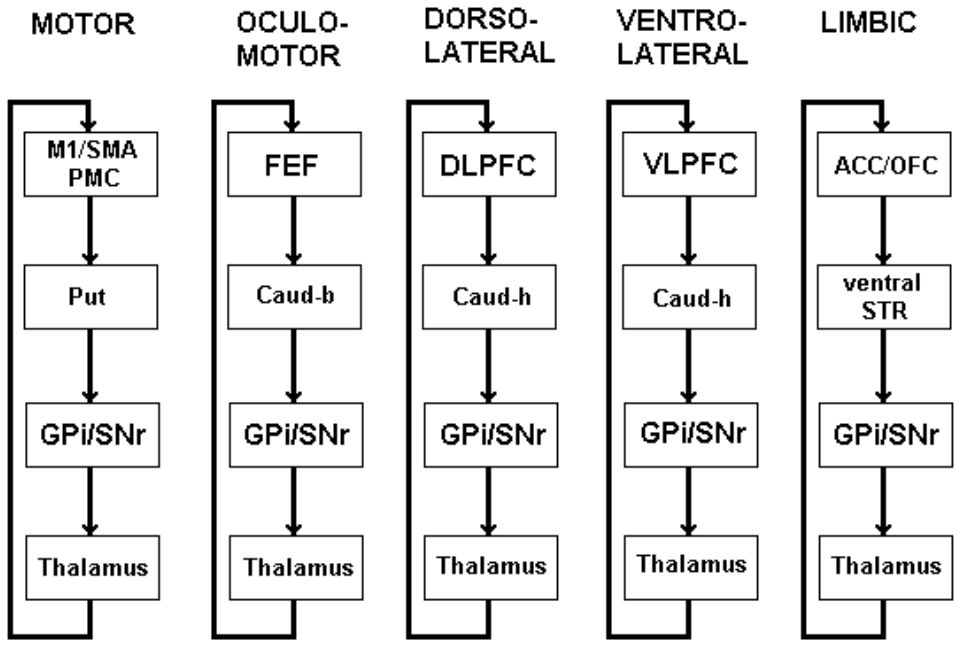

Figure 2.01. The parallel cortico-basal ganglia-thalamo-cortical circuits (adapted from Alexander et al., 1986). M1 = primary motor cortex; SMA = supplementary motor area; PMC = premotor cortex; FEF = frontal eye-fields; DLPFC = dorsolateral prefrontal cortex; VLPFC = ventrolateral prefrontal cortex; ACC = anterior cingulate cortex; OFC = orbital frontal cortex; Put = putamen; Caud-b = caudate body; Caud-h = caudate head; Ventral STR = ventral striatum; GPI = internal capsule of globus pallidus; SNr = substantia nigra pars reticulata.

Basal ganglia output nuclei (GPi and SNr, GPi/SNr) target the thalamus, notably dorsomedial, mediodorsal and ventrolateral thalamic nuclei, then project back (via thalamo-cortical projection neurons) to virtually identical cortical areas to those from where cortico-basal ganglia inputs originate (Alexander et al., 1986; Alexander & Crutcher, 1990; Nambu et al., 2002; Temel et al., 2005). Due to apparent re-entrant connectivity of these circuits (cortex-basal ganglia-thalamus-cortex) they are termed 'closed' circuits.

Cortical input to basal ganglia is excitatory, using glutamate as a neurotransmitter, and received from distributed cortical areas that are largely convergent upon striatal nuclei, and to a lesser extent, STN (Temel et al., 2005; see Figure 2.1). Both STR and STN efferents project to GPi and SNr (GPi/SNr), which are the major output nuclei of basal ganglia, in addition to GPe (Alexander et al., 1986; Temel, et al., 2005). However, STN and STR efferents have distinct modulating effects on GPi/SNr and GPe due to differences in neurotransmission: STR efferents, unlike STR afferents, are inhibitory (GABAergic), whereas STN efferents and afferents are excitatory (glutamatergic)[5].

The main basal ganglia pathways, linking the cortex to striatal and subsequently thalamic nuclei, reveal a tapering of efferent volume at each nuclear station, and form five functionally and structurally segregated neural circuits (or 'loops'), usually termed frontostriatal circuits. These circuits run in parallel to one another, and follow the same general route through the brain: cortex – striatum – globus pallidus – thalamus – cortex, with GPi/SNr output also modulated by cortico-STR-GPe-STN (Alexander et al, 1986), and cortico-STN-GPi/SNr (Nambu et al., 2002) connectivity. Most cortico-basal ganglia projections are focussed on STR, which includes the caudate nucleus, putamen, and nucleus accumbens, and so with reference to their cortical origin, the circuits are often termed the motor, oculomotor, prefrontal (including DLPFC and VLPFC) and limbic (ACC and OFC) striatal circuits, or collectively, frontostriatal circuits or sometimes cortico-basal ganglia-thalamocortical circuits referring to basal ganglia function as whole.

Understanding of the precise connectivity within the primary circuits remains elusive, but research to date indicates a similarity in the architecture of individual circuits,

[5] STR efferents also transmit peptides, including Substance P (STR-GPi/SNr projections) and enkephalin (STR-GPe projections), though these are co-localised presynaptically with glutamate and GABA; STR-GPi/SNr projections also transmit dyorphins. The action of these neurochemicals is not relevant to this discussion.

especially between the motor and prefrontal-association circuits. The main differences between the circuits lie in their locus of cortical origin, in addition to the exact striatal, pallidal and thalamic channels targeted by individual circuits[6]. The parallel segregation of structure and function existing between the individual circuits is thought to enable simultaneous processing in multiple cognitive and/or motor domains (Temel et al., 2005).

The prefrontal circuits primarily involve input from DLPFC and VLPFC but also from temporal and parietal cortex, and are thought to be necessary for cognitive control (Temel et al., 2005). In primates, cortical input innervates the caudate nucleus in addition to the most anterior parts of the putamen (rostral of the anterior commissure). These stations then send projections to dorsomedial GPi and rostral SNr (GPi/SNr), which then project to ventroanterior (VA) and centromedial (CM) nuclei of the thalamus (Temel et al., 2005). From these thalamic nuclei, efferents then project back to DLPFC and VLPFC, closing the circuit. Striatal efferents are also sent to anterior GPe, which is reciprocally connected to mediodorsal STN that also sends excitatory efferents to GPi/SNr through which it can modulate thalamocortical output (Nambu et al., 2002; Temel et al., 2005).

The motor circuits are responsible for motor control and are almost identical in their organisation and connectivity to the prefrontal-association circuits described above (Alexander & Crutcher, 1990). Cortical input arises from M1, PMC, SMA, primary somatosensory cortex (S1) and somatosensory association cortices and is directed to rostrocaudal putamen (Temel et al., 2005). From this basal ganglia station, efferent neurons topographically innervate posterior and ventrolateral parts of GPi and GPe, in addition to posterolateral SNr (Temel et al., 2005). Terminals from GPi/SNr and GPe project to the ventrolateral (VLN), anterior ventral (AVN), and centromedial (CMN) nuclei of the thalamus. Cortical and GPe input to STN is also topographically organised and directed to dorsolateral STN, which subsequently innervates (topographically) GPi/SNr, and also GPe via reciprocal connections with this pallidal nucleus (Temel et al., 2005).

Limbic circuitry is responsible for emotional, motivational and affective processes (Temel et al., 2005). Cortical input is from the limbic cortices, but also arises from the

[6] The evidence suggests further specialisation within each primary basal ganglia-thalamo-cortical circuit whereby functionally and structurally segregated sub-loops endure throughout each primary cortex-striatal-pallidal-loop (e.g. motor circuit) at each neural station from cortex to thalamus (Alexander & Crutcher, 1990), including STN (Temel et al., 2005); in the motor circuit, sub-loops demarcate orofacial, forelimb and hindlimb channels, further enabling the co-ordination of multiple functions.

amygdala, hippocampus and paralimbic cortices, each projecting to the ventral striatum, including the nucleus accumbens and ventromedial portions of the caudate and putamen, but also part of the olfactory tubercle (Temel et al., 2005). Striatal efferents project to the ventral pallidum[7], which is the major output station of the limbic circuit, and subsequently project to the mediodorsal nucleus of the thalamus. The circuits are closed by projections to ACC and OFC (Temel et al., 2005). The ventral striatum does not innervate GPe, but is reciprocally connected with medial STN, which modulates ventral pallidal activity and hence thalamocortical output (Nambu et al., 2002; Temel et al., 2005).

2.1.3. Direct, indirect and hyperdirect cortico-basal ganglia-thalamocortical pathways

Of the primary pathways, most studied are the motor and oculomotor circuits, largely because activation effects in these can lead to overt movement and are thus more easily quantifiable for the purposes of research. In contrast, activation effects in the cognitive-association and limbic pathways are largely of a cognitive, affective and motivational nature, and thus more difficult to measure (Temel et al., 2005).

In the motor and association circuits, each primary circuit is comprised of two sub-loops existing within the basal ganglia that function by exerting opposing influences, one excitatory and one inhibitory, on thalamocortical output. Past views of voluntary behaviour have emphasised the interaction of these sub-loops, termed the 'direct' (cortico-STR-GPi/SNr-thalamus) and 'indirect' (cortico-STR-GPe-STN-GPi/SNr-thalamus) cortico-basal ganglia thalamo-cortical pathways, to explain controlled behavioural responses (for review see Mink, 1996). More recent conceptualisations of basal ganglia function, informed by fresh evidence from histochemical, electrophysiological (using chronically implanted electrodes) and structural neuroimaging investigations, emphasise the role of cortico-STN-GPi/SNr connections and the inhibitory influence on thalamocortical output afforded by this 'hyperdirect' pathway (see Figure 2.2, Nambu et al., 2002).

Controlled behaviour is thought to be executed by focussed inhibition and disinhibition of GABAergic thalamocortical projections that selectively disinhibit M1 pyramidal neurons related to the wanted behaviour (motor program) only (Mink, 1996;

[7] Rat brains differ in prefrontal circuit connectivity, whereby corticostriatal projections from the prefrontal pathways innervate the core of the nucleus accumbens, which then sends efferents to the ventral pallidum. In the rat brain, prefrontal circuit connectivity largely parallels that of the limbic circuits.

Nambu et al., 2002). This proceeds via concomitant activation of three parallel pathways that operate within the basal ganglia-thalamocortical motor circuit, arising form corollary M1 inputs to the striatum and STN. Initially, STN is excited via a glutamatergic signal from the pyramidal layer (layer 5) of M1 that in turn excites GPi/SNr, consequently inhibiting extensive areas of the thalamus. This cortico-STN-thalamocortical loop is called the 'hyperdirect' pathway due to fast neural conduction time within the pathway (Nambu, Takada, Inase, & Tokuno et al., 1996; Nambu et al., 2002).

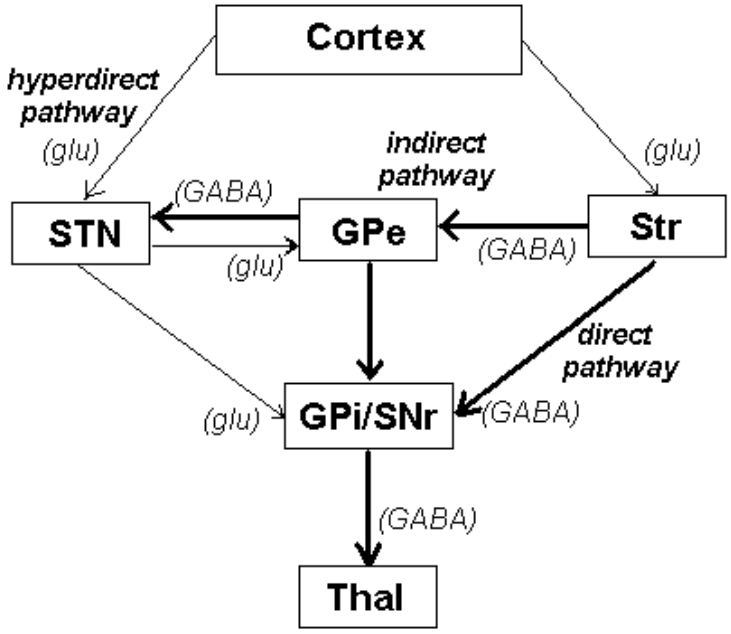

Figure 2.02. The 'direct', 'indirect' and 'hyperdirect' cortico-basal ganglia-thalamocortical pathways (adapted from Nambu et al., 2002). The direct pathway proceeds via cortico-STR-GPi/SNr-thalamus; the indirect pathway proceeds via cortico-STR-GPe-STN-GPi/SNr-thalamus; the hyperdirect pathway proceeds via cortico-STN-GPi/SNr-thalamus. Bold lines indicate GABAergic (inhibitory) connections and lighter font lines indicate glutamatergic (excitatory) connections. STN = subthalamic nucleus; GPe = external capsule of the globus pallidus; Str = striatum; GPi = internal capsule of the globus pallidus; SNr = substantia nigra pars reticulata; Thal = thalamus; glu = glutamate; GABA = gamma aminobutryric acid.

Slower (neural conduction time), but more potent STR GABAergic efferents arrive slightly later via the 'direct' pathway (cortico-STR-GPi/SNr), selectively targeting

GPi/SNr-thalamocortical output neurons related only to the wanted motor program, while competing programs remained suppressed. Such GABAergic inhibition of GPi/SNr disinhibits thalamocortical projections and consequently their M1 pyramidal neuron targets, permitting selective cortico-spinal outflow of the wanted motor program to alpha motor neurons; this aspect of thalamocortical disinhibition is analogous to the release of the thalamo-cortical 'brake' (Mink, 1996). Alpha motor neurons innervate target muscles (e.g. finger/thumb effectors in the case of typical Go responses in Stop-signal and Go/No-go paradigms). Hence excitation of these populations can effect overt movement (for review see Mink, 1996).

Striatal GABAergic discharge also inhibits GPe via STR-GPe efferents, lowering GPe basal firing rate and consequently diminishing the basal GABAergic effect of GPe efferents on STN and GPi/SNr, raising the basal firing rate of these latter nuclei in the process (Mink, 1996). Disinhibition of STN further activates GPi/SNr via glutamatergic STN-GPi/SNr connections, resulting in powerful thalamocortical inhibition, thus decreasing M1 excitation after a response is executed (Mink, 1996). This effect is primarily conveyed via the 'indirect' pathway (i.e., cortico-striatal-GPe-STN-GPi/SNr pathway), so named for the induced ('indirect') effects (i.e., increased basal STN-GPi/SNr firing) on the thalamus arising from STR GABAergic inhibition of GPe (Alexander & Crutcher, 1990).

A 'centre and surround' model of inhibition/disinhibition has been proposed to account for the effects sequential to the hyperdirect, direct and indirect pathways on thalamo-cortical projections during the execution of controlled behaviour outlined above (Alexander & Crutcher, 1990; Mink, 1996; Nambu et al., 2002). Initial hyperdirect signals inhibit widespread thalamic areas, then a later arriving direct pathway signal focally disinhibits selected thalamo-cortical M1 projections in a functional 'centre', while maintaining inhibition in surrounding thalamic areas, thereby releasing (disinhibiting) only the selected motor program.

It should be noted that the functional integrity of the striatum is contingent upon ascending dopaminergic input from substantia nigra pars compacta (SNc). These dopaminergic connections comprise the nigrostriatal (dopaminergic) pathway and are not part of the basal ganglia, but none-the-less have important roles in basal ganglia function (Temel et al., 2005). This involvement affects striatal efferents, tending to increase STR-

GPi activity and decrease STR-GPe activity. Therefore, dopaminergic input from SNc enhances conduction in the direct pathway, and inhibits conduction in the inhibitory indirect pathway, thus enhancing the flow of information processing in the basal ganglia (Alexander & Crutcher, 1990). Loss of nigrostriatal neurons leads to Parkinson's Disease, which is linked to enhanced STN activity, hence inhibition of M1, and decreased STR activation, making movement difficult.

In summary, it is thought that executive motor control is implemented via neural activation within sub-loops (or pathways) that exist within the primary motor cortico-basal ganglia-thalamocortical pathway; similar sub-loops exist within the primary oculomotor, prefrontal-association and limbic primary pathways (Alexander & Crutcher, 1990; Temel et al., 2005). These sub-loops are termed the direct, indirect and hyperdirect basal ganglia-thalamocortical pathways, which act in a highly coordinated manner to produce controlled behaviour (Nambu et al., 2002; Temel et al., 2005). The cortico-STN-GPi/SNr hyperdirect sub-loop initially suppresses all motor-related activation in thalamic nuclei, after which a volley of cortico-STR-GPi/SNr efferent activity conveyed via the direct sub-loop disinhibits thalamocortical projections selectively to release a wanted motor program. In this manner, the hyperdirect and direct sub-loops of the motor circuit produce controlled behaviour via 'centre-surround' inhibition/disinhibition of thalamic nuclei to execute a wanted response (Nambu et al., 2002). Immediately following response execution, the indirect cortico-STR-GPe sub-loop suppresses motor activity in the thalamus by inhibition of GPe, which raises the basal firing rate of GPi/SNr and STN, suppressing thalamocortical projections that were previously activated.

2.2. The functional neuroanatomy engaged during stop-signal inhibition

2.2.1. Overview

Understanding the neural basis of executive control is arguably the most challenging question in basic cognitive neuroscience and substantial research efforts are geared toward elucidating clues. While this is a significant question alone, it is amplified when considering the ever-increasing number of research papers detailing cognitive and

behavioural control dysfunction in psychiatric and psychological disorders (Casey et al., 2001; Nigg, 2000; Ring & Serra-Mestres, 2009; Verbruggen & Logan, 2008). Salient among these are reports of response inhibition impairments, where the stop-signal paradigm has been crucial, in part because stop-signal procedures afford greater utility for understanding control by way of indices of response inhibition not obtainable through the use of other behavioural paradigms. But more significantly, the unambiguous way that response inhibition is operationalised in the stop-signal paradigm is thought to be a prevailing factor in revealing control dysfunction (Aron, 2007; MacLeod, Dodd, Sheard, Wilson, & Bibi, 2003), i.e., inhibition of responses that are *in-progress*. To this end, stop-signal investigations have revealed behavioural control impairments in patients with ADHD (Bekker et al., 2005b; Dimoska, Johnstone, Barry & Clarke, 2003; Overtoom et al., 2002), OCD (Chamberlain, et al., 2007; Menzies et al., 2007), Parkinson's Disease (Gauggel, Reiger, & Feghoff, 2004; van den Wildenberg et al., 2006) and schizophrenia spectrum disorders (Badcock et al., 2002; Bellgrove et al., 2006; Davalos et al., 2004; Enticott et al., 2008; Ross et al., 2008), and children at risk of developing schizophrenia (Davalos et al., 2004; Ross et al., 2008). Additionally, at least one study has indicated that SSRT may be related to impulsive behaviour (Logan, Schachar, & Tannock, 1997).

Cortico-basal ganglia-thalamocortical response control has traditionally been studied in the motor system (Alexander & Crutcher, 1990; Mink, 1996; Nambu et al., 2002), however, recent evidence indicates that other response control functions, notably response inhibition, may operate via non-motor cortico-basal ganglia-thalamocortical association routes (Aron & Poldrack, 2006; Aron, Behrens, Smith, Frank, & Poldrack, 2007a; Aron et al., 2007b; Eagle et al., 2008). Response inhibition differs from controlled response execution whereby for the latter, a correct response is executed and incorrect responses are suppressed in the thalamus, whereas for response inhibition, all active response channels in the thalamus are suppressed. Response inhibition may be effected via either the hyperdirect pathway, or the indirect pathway. However, indirect pathway effects are conveyed through several basal ganglia nuclear stations, STR and GPe, whereas the hyperdirect pathway passes through STN only, a shorter and faster route through the basal ganglia (Nambu et al., 2002; Temel et al., 2005) enabling fast and urgent response inhibition that is required for stopping (Aron & Poldrack, 2006; Aron et al., 2007a).

The following literature review details current knowledge of cortical and basal ganglia structures engaged during response inhibition. In so doing, this review is focussed primarily on evidence derived from stop-signal paradigm research, drawing on rodent lesion studies (Baunez et al., 2001; Eagle & Robbins, 2003a; Eagle & Robbins, 2003b; Eagle et al., 2008), behavioural studies with PD patients (Gauggel et al., 2004; van den Wildenberg et al., 2006), and studies with healthy participants using TMS (Chambers et al., 2006; Chambers et al., 2007), neuroimaging (Aron & Poldrack, 2006; Aron et al., 2007a; Li, Yan, Sinha & Lee, 2008; Vink et al., 2005) and event-related potentials (Bekker et al., 2005a; De Jong et al., 1990; Dimoska et al., 2006; Dimoska et al., 2008; Kok, Ramautar, Ruiter & Ridderinkof, 2004; Ramautar, Kok, Ridderinkof, 2004).

2.2.2. Rodent lesion evidence

Work with lesioned rodents performing stop-signal and response selection paradigms have been crucial in elucidating putative roles of the basal ganglia in behavioural control processes. In a series of papers, Trevor Robbins and his colleagues have detailed the findings from their extensive research of cortico-basal ganglia-thalamocortical involvement in executive control using lesion rat models, employing sham area and experimental area lesions (Baunez et al., 2001; Eagle et al., 2008; Eagle et al., 2003a; Eagle et al., 2003b). The lesioning technique involves use of neurotoxins to produce targeted excitotoxic fiber-sparing lesions in discrete brain areas. Lesions are applied by insertion of an injecting device into (bilateral) target brain areas and injection of a phosphate buffered saline (PBS) solution containing neurotoxin, e.g. ibotenic acid or quinolinic acid. Sham operated animals are injected with PBS only, controlling for the effect of surgery on experimental animals. Using this technique, the group has employed several reaction time paradigms, including simple and/or multi-choice reaction time tasks to investigate the roles of basal ganglia nuclei in response selection (Baunez et al., 2001; Brown & Robbins, 1991), and likewise, the stop-signal paradigm, to investigate response inhibition (Eagle & Robbins, 2003a; Eagle & Robbins, 2003b; Eagle et al., 2008).

The role of STN in pre-potent response control was first directly investigated by Baunez et al. (2001), who compared the performance of groups of trained rats with excitotoxic lesions of STN or sham areas on either a simple RT task (SRT) or a choice RT

task (CRT) to index response selection (4 groups of rats). For both SRT and CRT tasks, a trial began when a rat poked its nose into a central hole, which was flanked by a hole on the left and the right (three holes in total). After a variable *fore-period* (0.5 – 1.25 s) a tone was presented instructing rats to perform a nose poke into one of the lateral holes. The target hole was indicated by a change in lighting intensity (increase or decrease) at the beginning of the fore-period for SRT, and at tone presentation for CRT. The time taken for rats to remove their nose from the central hole after tone presentation was the *RT*, and the time taken from tone presentation until the rat poked its nose into a lateral hole was the *movement time*. Pre-lesion data showed that CRT was significantly longer than SRT, but this effect was abolished by STN lesions, which also elicited more incorrect responses, but had no effect on the fore-period effect (longer fore-periods were linked to faster RT) and had no effect on movement times. STN lesioned rats performing the SRT task also made more premature responses (during the fore-period) to the incorrect side, particularly when the required response was opposite to a correct (rewarded) response on the previous trial. This data contrasted with the findings of a previous study by this group (Brown & Robbins, 1991) in which rats performed the same paradigm, but this time with and without unilateral striatal lesions, induced by dopamine depletion. In this study, the fore-period effect was impaired in rats with striatal lesions, who also showed a response bias toward the side ipsilateral to the lesion site.

The authors described the pattern of deficits stemming from STN lesions as being evidence of a dysfunctional limited capacity response buffer that, in a correctly functioning state, is cleared of a previously rewarded response at the commencement of a new trial each trial. Clearing of this hypothetical response buffer is implicated in response preparation and response selection processing, and could be accomplished by STN action on the thalamus that can suppress all active responses (Nambu et al., 2002).

In a recent paper, Eagle and colleagues (2008) detailed the findings of a stop-signal study where they used this lesion based experimental paradigm approach to investigate the roles of OFC, infra-limbic cortex and STN in stop-signal inhibition in trained groups of rats. The stop-signal variant required rats to make regular Go responses, involving a left lever press to start the trial, followed by a reaction-time right lever press which was the Go response. The lever was presented for a limited but variable 'hold' period so that rats had to

make speeded responses to get a food pellet reward. Stop-signals were tones, presented on 20% of trials between left and right lever presses instructing rats to withhold the response throughout the hold period. In an initial baseline session, rats responded on trials where the stop signal delay was set to zero, with the purpose of establishing an on-going response control baseline indexed by the number of successful inhibitions (PI). In subsequent sessions, rats responded to the same stimuli but tones were presented over a range of stop-signal delays (e.g. mean GoRT – 300), but only one delay was used in each session. This procedure permitted the generation of inhibition functions and estimation of SSRT. Baseline and experimental sessions were performed before and after surgery, and after testing was complete, the size of lesions were estimated by independent raters after Cressyl violet staining of sectioned brain slices from the animals to reveal the extent of lesion.

Stop-signal inhibition deficits were revealed in animal groups with OFC and STN lesions, however the deficits revealed in each group - and therefore brain area - were unique. Only OFC lesions slowed SSRT, and the size of lesion and SSRT were significantly correlated (Spearman's r = .5), whereas STN inactivation made withholding of on-going responses more difficult on stop-signal task trials at all delays, indicated by a greater number of stop failures and consequently, flatter inhibition functions at each delay in the post-surgery condition. However, when these animals did inhibit successfully it was done with similar speed as sham controls, but less often. STN lesioned animals also exhibited faster mean GoRTs than controls indicating a lack of suppressive influence in normal controlled reaction time responding.

These findings indicate a clear role for PFC in stop-signal inhibition, especially given that lesions to rat OFC slowed SSRT and the extent of excitotoxic damage to this cortical area was correlated with SSRT slowing. STN involvement is less clear given that lesions to STN had no effect on SSRT. Notwithstanding this, STN involvement appears to have a role in stopping as rats with lesions to this structure exhibited flatter inhibition functions, which is thought to reflect an impaired capacity to trigger stopping processes (Logan, 1994). However, these findings should be interpreted cautiously given the results of Monte Carlo simulations conducted by Logan and colleagues (Band et al., 2003) who found that inhibition functions were an unreliable index. Nonetheless, given the location

and connectivity of STN (Temel et al., 2005), this finding is worthy of further investigation.

Interestingly, a previous behavioural study has linked flatter inhibition functions to a discrete impairment displayed by patients with schizophrenia (Badcock et al., 2002). This study was comparable in design to the rat studies previously described, excepting for the use of a choice RT Go task and the presentation of the entire range of stop-signal delays within the same experimental session. It was found that patients with schizophrenia uniquely exhibited flatter inhibition functions in comparison to both psychiatrically healthy and non-schizophrenic psychotic control groups. The findings of Eagle and colleagues (2008) suggest that this response inhibition impairment may be linked to underactivation of STN, but no studies have so far investigated this.

More tangible clues to basal ganglia involvement in the stopping process were provided by Eagle and Robbins (2003a, 2003b) in earlier papers using the same stop-signal paradigm variant as per Eagle et al. (2008). However, in these instances, lesions were applied to discrete parts of STR in rats; the medial dorsal striatum (2003a) and the nucleus accumbens core (2003b). In the latter study, lesions were also applied to medial prefrontal cortex; neither lesion site in this study (2003b) had any effect on performance of rats. In contrast, rats with lesions to medial dorsal striatum (2003a) exhibited severe performance deficits, revealed in both Go task and Stop-signal task performance. GoRT was unaffected, but rats made more errors of omission indicating an inability to initiate Go responses. In addition, inhibition functions were flatter in this group, but the authors indicated this was likely a result of more variable GoRT. Most pertinent to this discussion was that these rats exhibited significantly slower SSRTs than sham lesioned controls indicating direct involvement of medial dorsal STR in the stop response. In a further aspect of this study, Eagle and Robbins (2003a) administered d-amphetamine to investigate changes in inhibitory control in a pharmacological challenge study; rats with STR lesions showed a dose specific response, whereby low doses (0.3 mg/kg) normalized SSRT while higher doses (0.3 mg/kg) slowed SSRT indicating a dose dependent effect.

These data are very significant in consideration of previous findings indicating fronto-STR connectivity in development of inhibitory control processes (Bunge & Wright, 2007; Casey, Tottenham, Liston & Durston, 2005; Liston et al., 2006), and in child ADHD,

in which dysfunctional STR circuitry is thought to be a contributory factor (Booth et al., 2005; Casey et al., 2007). Indeed, several studies have revealed slower SSRTs in children (Dimoska, Johnstone, Barry, & Clarke, 2003; Schachar, R., Tannock, R., Marriott, M., & Logan, G., 1995; Tannock, Schachar & Logan, 1995) and adults (Bekker et al., 2005b; Aron, et al., 2003b) with ADHD, which is normalized by administration of methylphenidate (Ritalin®; Aron et al., 2003b; Tannock et al., 1995). Underscoring the specificity of these findings, a recent publication detailed findings of a study comparing inhibitory control in boys (aged 6-12 yrs) with ADHD on tasks tapping response inhibition (inhibition of prepotent responses and on-going responses in separate tasks) and also interference control (Scheres et al., 2003). Compared to the placebo ADHD group, those receiving methylphenidate exhibited better control. However, the effect was only significant for performance on the response inhibition tasks.

2.2.3. Human lesion and TMS evidence

Widespread areas of frontal cortex have been reported as having significant roles in human response inhibition, including middle and inferior PFC, but also medially in anterior supplementary motor area (preSMA) and anterior cingulate cortex (ACC). In neuroimaging studies, PFC activations are often bilateral but mostly right lateralised, and accompanied by activations within parietal cortex, which have lead to almost clichéd reports of a right fronto-parietal network involvement in response inhibition. Of these frontal structures, right inferior frontal gyrus (IFG) has the clearest role in stopping, though SMA cannot be ruled out as mediating this form of behavioural inhibition.

The first direct demonstration of right IFG involvement in stop-signal inhibition was published by Rieger and co-workers (2003) who compared performance of patients with cortical and basal ganglia lesions to orthopedic controls using a variant that selectively adapted stop-signal delay to ensure that inhibition was successful on 50% of stop-signal trials. It was found that patients with bilateral and right inferior frontal lesions, in addition to patients with lesions to the basal ganglia, had slower SSRTs compared to patients with left inferior frontal lesions, patients with lesions outside frontal cortex and controls. The non-specific nature of the basal ganglia lesions in this group did not permit isolation of discrete nuclear involvement in these processes. These findings were extended by Aron and

colleagues (2003a), who found that for patients with right frontal lesions, the proportion of grey matter loss in right IFG predicted SSRT whereas no relationship was observed between the extent of lesions to left IFG and SSRT. In an exploratory partial correlational analysis, it was found that damage to right *pars opercularis*[8] resulted in particular marked impairment, indicating this subgyral formation may be especially important for stop-signal inhibition.

Studies using repetitive transcranial magnetic stimulation (TMS[9]) have also revealed significant relationships between SSRT and *pars opercularis* of right IFG (Chambers et al., 2006; Chambers et al., 2007). Chambers and associates (2006) investigated stopping in participants both with and without TMS applied to fronto-parietal regions implicated in response inhibition (*pars opercularis* of IFG, mid-dorsolateral MFG, and the angular gyrus located in IPL). In this experiment, a range of stop-signal delays centred around 50% inhibition success were determined from the results of an initial practice session and used in a subsequent session that followed cortical deactivation produced via TMS. Its was found that IFG deactivation selectively impaired response inhibition, indicated by longer SSRT, but also impaired withholding of responses, indicated by fewer Stops at each stop-signal delay after TMS. In a more recent study (Chambers et al., 2007), this research team compared involvement of dorsal premotor cortex (dPMC) to IFG in both hemispheres during performance of a combined stop-signal and flanker task paradigm to investigate putative roles of these cortical regions in stopping (via stop-signal performance) and response conflict (via flanker task performance). Effects were observed only in right hemisphere regions, but a double dissociation was observed between response inhibition and response conflict: TMS applied to IFG impaired stopping, but not the capacity to suppress competing responses on the flanker task whereas TMS applied to PMC impaired the capacity to suppress competing responses but not stopping.

[8] Inferior frontal gyri are composed of three sub-gyral formations; *pars opercularis, pars triangularis and pars orbitalis* (Mai, Assheuer & Paxinos, 2004).
[9] TMS is applied to a cortical area of interest over adjacent scalp to disrupt normal brain function in a reversible manner in that region.

2.2.4. Human neuroimaging evidence

The earliest fMRI studies using stop tasks provided the first indications that right IFG was engaged during stopping (Rubia et al., 2001a; Rubia et al., 2003). Using an epoch-based design, Rubia and co-workers (2001a) investigated generic activation across three versions of a stop task that included a simple RT task for Go trials and a visual stop stimulus (presented on 50% of trials) that was invariantly presented 250 ms after the Go stimulus. Three tasks were used to control for visual stimulation and motor output by varying the number of Go and Stop stimuli presented, and onset-to-onset times of Go stimuli across tasks. Unique Stop-related activation was reported in right IFG (extending into the *insula*), right IPL, and medially in pre-SMA and ACC. Shared BOLD variance was revealed within right MFG and bilateral middle temporal cortex that was mutually attributable to a No-go task conducted in the same experiment. In a later study, Rubia and co-workers (2003) employed event-related fMRI procedures to investigate the stop response in more detail, but this time a typical stop-signal variant was used; the primary task was this time a choice reaction time task (right or left thumb button presses as instructed by Go stimuli), and the time between Go stimulus onset and Stop stimulus onset was varied for each participant to ensure a 50% inhibition success rate on Stop trials. When Stops were contrasted with Stop Failures it was found that successful inhibition was related to activation of right IFG only.

Recent neuroimaging research using a typical stop-signal paradigm has further elucidated the stop-signal response inhibition brain network, but has revealed a contrasting relationship between STN and SSRT to that observed in the previously mentioned rodent work of Eagle et al. (2008). Aron and Poldrack (2006) modelled Stops, Stop Failures, Go and Go errors to explain BOLD intensity variance in image time-series that were acquired while participants responded to stimuli from a paradigm variant that adjusted stop-signal delays to ensure a 50% inhibition success rate. Compared to baseline, Stops were related to activation in a right lateralised fronto-parietal brain network that included cortical BOLD changes in IFG, preSMA, IPL and subcortically within STN, globus pallidus and thalamus. A region of interest analysis was performed where the average parameter estimates within right frontal and subcortical areas defined by probability maps were extracted and correlated with SSRT. It was revealed that only right IFG and STN were significantly

related to SSRT. Crucially, this was an inverse relationship indicating that greater activation in this network was related to shorter (faster) SSRTs.

In a later paper, Aron and colleagues (2007a) showed that both right IFG and preSMA were structurally connected to STN using diffusion weighted imaging (DWI), and suggested these brain areas are part of the motor (SMA-STN) and association (IFG-STN) cortico-basal ganglia thalamocortical networks that can suppress thalamocortical output in a manner paralleling the hypothesised glutamatergic 'hyperdirect' cortico-basal ganglia-thalamo-cortical network suggested by Nambu and colleagues (1996; 2002).

However, when Stops were contrasted against Stop Failures, Aron and Poldrack (2006) observed bilateral putamen activation and consequently proposed this result may be due to either response inhibition processes mediated via the indirect sub-loop, or slower Go processes during Stops. In support of this, Aron pointed to the study of Vink and co-workers (2005) who not only observed enhanced dorsal putamen activation during Stops compared to Stop Failures, but also revealed a strong inverse relationship between striatal activation and slowed Go responding when stop-signal presentation became increasingly likely. This group also compared Go trials that were linked to a high chance of stop-signal presentation (slow GoRT) compared to Go trials with a low probability of stop-signal presentation and observed bilateral putamen activation in addition to cortical activation within an SMA/ACC region and the right insula[10]. In addition, Vink performed a parametric analysis investigating regions responsive to Stop-signal probability in Go trials and showed this same network (bilateral striatum, SMA/ACC and right insula) was positively correlated with increasing likelihood of a stop-signal trial.

In combination Aron and Vink's findings strongly suggest indirect pathway involvement in the strategic control (slowing) of Go responding in anticipation of a stop-signal, and moreover, that such control is cortically mediated by SMA/ACC and right insula cortex.

In Aron et al's previously mentioned study, Aron and Poldrack (2006), a relationship between stop-signal delay and inhibition network activation was observed. Specifically, they found that longer stop-signal delays were linked to increased activation

[10] This cluster were identified as merging into *pars orbitalis* of (BA47) right IFG (MNI co-ordinates reported were: 42 18 -4) after MNI to Talairach conversion and entering into the Talairach daemon.

within right preSMA, right GP and rSTN, but not right IFG suggesting that activation within the hyperdirect motor sub-loop is linked to harder inhibition, i.e., when an on-going response is closer to execution. Additionally, Aron noted that the IFG-basal ganglia network discriminated harder from easier response inhibition across subjects, but was activated regardless of stop-signal delay interval and was thus related to SSRT but not stop-signal delay. Hence when response activation has proceeded further to (or through) the end stage of response execution, the preSMA-STN-pallidal pathway is more necessary for successful inhibition.

2.2.5. Stopping in Parkinson's Disease

Involvement of STN in motor control has been known for over one hundred years; autopsies of patients exhibiting sudden jerky lateralised movements revealed lesions in STN contralateral to the side of hyperkinesia (also called hemiballismus). In a series of papers published in the 1950s, Malcolm Carpenter first described hyperkinesia in a patient due to hemorrhagic lesioning of STN, and subsequently examined the effect of lesions to STN in primates, observing the same hyperkinetic symptoms present in humans with STN lesions (cited in Temel et al., 2005).

In recent times, most investigations of STN functioning have been motivated by PD concerns as death of dopaminergic nigrostriatal projections to GPe impairs basal level firing of this nucleus resulting in disinhibition of GPi/SNr and STN. Treatment of PD traditionally involves therapeutic administration of a dopamine derivative called levodopa to enhance functioning of the dopaminergic system and thereby normalise basal ganglia function (Chen et al., 1999; Kraft et al., 2009; Tedroff, 1997; Tedroff et al., 1996). Over the last 15-20 years, experiments have shown that electrical stimulation of STN, GPi, or thalamic nuclei delivered through chronically implanted electrodes, reduces PD symptoms in monkey PD models (Benazzouz, Gross, Féger, Boraud & Biolac, 1993), in addition to human PD patients (Limousin et al., 1995; Limousin et al., 1998). The site of stimulation depends upon diagnostic symptomatology, but all deep brain stimulation (DBS) impairs normal functioning in the structure receiving stimulation. This is done to normalise functioning in structures downstream from the site of stimulation and thereby normalise

functioning of cortico-basal ganglia-thalamocortical circuitry, and is quite effective for a majority of patients fitted with DBS devices[11].

Patients with PD serve as a useful model of impaired basal ganglia function, specifically as a model of STN hyperactivity. Moreover, symptom reducing drug therapies and subcortical DBS in PD patients offer additional paradigms of research, whereby patients may be tested in 'on' and 'off' medication or stimulation conditions.

Three PD studies of response inhibition have been published. In the first of these, Cooper and co-workers (1994) found that PD patients were impaired during No-go inhibition, indicated by increased error rates compared to controls, but also exhibited slowing on both simple and choice RT tasks. In contrast to the lesioned rats of Baunez et al. (2001), slowing was proportional across simple and choice RT tasks. Later, Gauggel, Reiger and Feghoff (2004) compared PD patients with orthopaedic controls on Stop-signal paradigm performance which using a tracking algorithm to ensure 50% inhibition probability. SSRT was significantly slower in the PD group, and could not be accounted for by general slowing indicated by GoRT, or by cognitive decline measured by neuropsychological tasks known to be sensitive to the neuropathology of PD (including general intelligence and executive function). These findings indicate that stopping is very sensitive to the integrity of basal ganglia function, more so than response initiation processes, and other cognitive functions.

In the third study, basal ganglia function in PD was more directly assessed by van den Wildenberg and co-workers (2006) who compared performance of patients with STN targeted stimulators to other patients whose stimulators targeted thalamic nuclei (the ventral intermediate nucleus, Vim). The latter group was subdivided into groups with tremor symptoms (Vim-PD) and without symptoms (Vim non-PD). Patients responded to stimuli on a stop-signal variant employing a typical choice RT paradigm where stop-signal delays were adjusted adaptively (using 50 ms increments) to ensure a 50% inhibition rate; stop-signal delay was increased after Stops and decreased after Stop Failures. Participants also performed a Go/No-go task with equi-probable Go and No-go trials, however the Go task was a simple RT task, enabling a comparison of simple and choice RT, the latter obtained

[11] Other basal ganglia nuclei are sometimes targets for DBS, including STR and GPe for treatment of patients with basal ganglia disorders such as Huntingtons Disease or basal ganglia lesions

from performance on the stop-signal paradigm. Response speed and accuracy on Go/No-go task performance was unaffected by stimulation in all groups. However stop-signal paradigm findings differed. Both STN and Vim PD DBS patients exhibited faster SSRT during stimulation, but only STN DBS patient's choice RT was faster during the 'on' condition. Vim non-PD were unaffected by stimulation. While supporting the notion of STN having a role in response inhibition, this was not specific to STN DBS; stimulation of a thalamic motor nucleus (Vim) in patients exhibiting essential tremor reduced SSRT also. However, only STN DBS group exhibited faster choice RT. The authors interpreted these findings as indicating a primary role for STN in response selection, whereas SSRT acceleration may be due to more general therapeutic effects of DBS on cortico-basal ganglia-thalamocortical pathways, probably by normalisation of cortico-STN projection neuron function which is immediately upstream of STN.

These rat lesion and human neuroimaging studies have revealed some vital clues as to the possible agent (Band & Boxtel, 1999) of stop-signal response inhibition, particularly the studies revealing a relationship between a cortical area and SSRT: Eagle et al. (2008) in rat OFC, Aron and colleagues (2003a; 2006; 2007a) in human right IFG. Each species specific region may thus be tenable 'agents' of stopping. In view of Aron's findings, Eagle et al. (2008) tentatively speculated that rat OFC and human IFG may be analogous regions in rat and human PFC, but noted there was little or no evidence to indicate homology between these regions aside from each belonging to PFC within their respective species.

However, Eagle's findings showed that bilateral lesions to the STN did not slow SSRT, and post-test histological preparations revealed that lesion size in STN was also not related to SSRT. These results seem to conflict with Aron's finding that SSRT predicted BOLD signal changes in STN during Stops across subjects, and also conflicts with Aron's conclusion that faster SSRTs are contingent upon STN activation. What Eagle did find however, was that STN lesions impaired the ability of rats to inhibit cued responses on stop-signal trials, indicated by significantly flatter inhibition functions. Despite the large impairment revealed in the performance of the STN lesion group, when rats successfully inhibited they did so at a speed not different to that of sham controls. These findings clearly indicate that STN has a significant role in stop-signal inhibition, however it remains unclear

exactly what that the role is. Eagle et al. (2008) suggested a putative role in selection, either overt response selection, or a more fundamental role that may include stimulus selection.

2.2.6. ERPs elicited during stop-signal inhibition

The act of stopping has been linked to elicitation of several ERP components including N1 and N2 potentials, for which different authors have advocated various roles (for N1 see Bekker et al., 2005a, De Jong et al., 1990, and Dimoska & Johnstone, 2008; for N2 see van Boxtel et al., 2001; Dimoska, Johnstone & Barry, 2006; Ramautar et al., 2004). However, most researchers contend that the stopping process itself is revealed as a late positive deflection (a P3) that is largest over frontal and central electrode sites in tone-locked Stop waveforms (Bekker et al., 2005a; De Jong et al., 1990; Dimoska & Johnstone, 2008; Kok et al., 2004; Ramautar et al., 2004). Despite general agreement on this issue, exactly how this component reveals stopping remains contentious, largely stemming from the problem of how to isolate unique stopping related potentials.

Isolation of potentials elicited by stop-signals is difficult because stop-signal trials involve the presentation of two stimuli in rapid succession: first a primary task stimulus and shortly thereafter, a stop-signal. The proximity of stop-signals to primary task stimuli necessarily results in potentials elicited by each stimulus overlapping on stop-signal trials, making straightforward interpretation of tone-locked waveforms difficult. Some of the disagreement in the literature regarding the attribution of a definitive stopping potential may be attributable to the various methods employed by research teams to account for this overlap.

In the first study to report stop-signal ERPs, De Jong and colleagues (1990) pioneered a method to account for differential primary task activation overlap between different Stop and Stop Failure waveforms. This was done by aligning Stop and Stop Failure ERPs (locked to the onset of primary task stimuli) with Go ERP comparison waveforms (locked to Go stimulus onsets) computed from trials coming from either the left or right portions of the GoRT distribution. The line demarcating left and right portions of this distribution was defined by the PI at the mean stop-signal delay of a given stop-signal ERP. Stop comparison waveforms were computed from Go trials coming from the right hand portion (slow GoRT) as they would likely be inhibited, and Stop Failure comparison

waveforms were computed from the left hand portion (fast GoRT) as they would likely escape inhibition.

A performance tracking algorithm utilizing a Levitt rule (Levitt, 1971) was used to set stop-signal delays to obtain stop-signal trial data corresponding to inhibition probabilities (PIs) cutting off approximately 29%, 50% and 71% of the GoRT distribution, described as 'early', 'middle' and 'late' stop-signal delays[12], respectively. In accordance with the predictions of the race model, these conditions yielded longer stop-signal delays as PI decreased. Thus six Go trial comparison waveforms were computed; three for the Stop conditions and three for Stop Failure conditions. To compare differences between Stop and Stop Failure waveforms, trial type Go ERPs were subtracted from corresponding stop-signal trial ERPs forming Stop and Stop Failure difference waveforms for each of early, middle and late conditions.

Unfortunately, ERP data were not the primary focus of this investigation, hence minimal analyses were conducted; and for each condition only midline ERP data (Fz, Cz and Pz) for Stop and Stop Failure difference waveforms were reported. A clear N1 component (maximal at Cz) was elicited during both Stops and Stop Failures, but was reduced in Stop Failures compared Stops in the late condition. In addition, a substantial late positive deflection, described by De Jong as P3, was revealed during Stops. This potential was also maximal at Cz and began about 150 ms post stop-signal onset. Given the timing of the P3 wave in comparison to the calculated finishing time of the stopping process (SSRT), which was approximately 200 ms in this experiment, and that P3 was largely absent during Stop Failures, P3 onset was interpreted as reflecting the onset of inhibition processes.

A later study challenged De Jong and co-worker's (1990) interpretation that stopping is revealed in P3 potentials. Van Boxtel van der Molen, Jennings and Brunia (2001) proposed that response inhibition is manifested in ERP waveforms as a negative deflection (N2) with a frontal maximum (i.e., Fz). This hypothesis largely stemmed from studies with Go/No-go paradigms that have revealed larger N2 potentials for No-go compared to Go ERPs. Van Boxtel and colleagues collected ERP data using a variant with

[12] By example, for the 'early' stop-signal delay, the left hand portion of the GoRT distribution accounted for 29% of the total area under the GoRT distribution representing those trials that would theoretically escape inhibition manifesting Stop Failures, while the remaining 71% lying to the right represented those trials that would be inhibited, manifesting Stops.

visual stop-signals that included a No-go condition (not further reported on here) and an algorithm that tracked performance such that about half of stop-signal trials resulted in Stop Failures. A response device that measured response force was used so that stop-signal trials on which a 'partial response' was executed (a response where some force was exerted on the device but not that normally associated with a typical response) could be recorded. Stop-signal ERPs were locked to the onset of stop-signals (only frontal sites reported), but differences in primary task overlap was not accounted for. N2 amplitude in stop-signal waveforms paralleled the level of force measured; Stops revealed small N2s, while partial Stop[13] and Stop Failure ERPs revealed N2s that were progressively larger. P3 effects were not reported.

This pattern of stop-signal N2 enhancement was interpreted as reflecting greater inhibitory pressure: Van Boxtel proposed that inhibition was more effortful during Stop Failures than Partial Stops, which in turn involved a greater attempt to suppress responding than did Stops. This interpretation has some merit, in that the attempt to inhibit an on-going response may be greater as inhibition failure becomes more imminent, but relies more upon argument than data. This is particularly relevant in consideration of Go/No-go investigations employing auditory No-go stimuli that have found considerably smaller No-go N2 than N2 elicited by visual stimuli (Folstein & van Petten, 2006), thereby weakening the N2 response inhibition hypothesis. This was amply demonstrated by Falkenstein, Hoorman and Hohnsbein (1999) who compared Go and No-go waveforms elicited by visual and auditory stimuli (visual and acoustically presented letters). Despite similar behavioural performance across visual and auditory modalities, No-go N2 was remarkably attenuated in the auditory condition compared to the visual condition, and moreover, N2 modality specific scalp topographies were different. Falkenstein and colleagues suggested their results indicate that N2 reflects a modality specific inhibition mechanism that is not related to response inhibition, i.e., non-motor inhibition.

Van Boxtel and colleagues (2001) suggested that N2 augmentation on Partial Stop and Stop Failure trials may reflect larger motor potentials manifested on those trials compared to Stop trials. This compromise interpretation suggests that the greater positivity

[13] Partial Stops are thought to be those where the stopping process is effective after the commencement of motor outflow from M1 (De Jong et al., 1990). De Jong and colleagues also recorded these trials, but only reported ERP data for Stops where no force was recorded, and Stop Failures.

of Stops reflected greater inhibition of motor activation, which is consistent with the observations and interpretation of De Jong et al. (1990).

In a study focussing on stop-signal ERPs, Kok, Ramataur, De Ruiter, Band, and Ridderinkoff (2004) also used visual go stimuli and stop-signals, but computed difference waveforms to isolate stop-signal related potentials. In this instantiation, stop-signal delays were jittered between 10-300 ms after primary task stimulus onsets in 18 evenly spaced steps with each delay having equal likelihood of presentation. Jittering the stimulus onset asynchrony of stimuli that onset closely to one another has the effect of low pass filtering the overlap of potentials of the first stimulus on the second. This technique has the effect of offsetting positive and negative phases of waveforms such that after linear summation, the phase differences cancel one another out[14]. Residual overlap in stop-signal waveforms was accounted for by computing difference waveforms, but was performed differently to De Jong et al. (1990), and so is worth describing.

Stop and Stop Failure ERP waveforms were first collapsed into three stop-signal delay bins (early, middle, and late stop-signal delay bins), resulting in three Stop and three Stop Failure sub-averages, which were then averaged producing Stop and Stop Failure grand averages. 'Fast' and 'slow' grand average Go ERPs were computed from the appropriate parts of the GoRT distribution. In contrast to De Jong's difference waveform computations, to account for different levels of motor activation distorting stop-signal ERPs, Go ERPs were aligned with stop-signal ERPs such that the latter occurred in synchrony with Go ERPs at appropriate stop-signal delays; Stop ERPs were synchronized at an earlier time point than Stop Failure ERPs against their respective Go ERP averages. Difference waveforms were then computed by subtraction. This technique is comparable to the Adjacent response technique (Woldorff, 1993, see below), but is less temporally resolved.

Stop and Stop Failure difference waveforms both exhibited N2 and P3 potentials that were both larger and of longer latency in Stop Failures compared to Stops; P3 peaked at around 300 ms in the grand average Stop difference waveform, and at about 450 ms for the Stop Failure homologue. Furthermore, the respective scalp topographies were clearly

[14] This does not necessarily hold for lower frequency potentials, especially those which are of a frequency lower than the jitter range (Woldorff, 1993).

distinguishable, whereby Stop P3 revealed a central distribution (Cz maximum), whereas Stop Failures revealed a centro-parietal distribution (maximal at Pz). Interestingly, while an N2 was observable in difference waveforms for Stops and Stop Failures, this was significant (relative to zero) only in the Stop Failure difference waveform, and maximal at Cz. Topographical analyses were consistent with these findings, revealing a central distribution for Stop Failure N2.

The authors suggested that the latency differences between Stop and Stop Failure P3s reflect differences in the timing of the response to the stop-signal, and paralleling the interpretation of De Jong et al. (1990), Kok suggested that the onset of Stop-P3 may be indicative of the finishing time of stopping processes.

In a later study, this group investigated stop-signal ERP probability effects by comparing the performance of participants during two stop-signal conditions: in one condition, stop-signals were presented on 50% of trials and on 20% of trials in the other (Ramautar, Kok, Ridderinkhof, 2004). For both conditions, five fixed stop-signal delays were used whereby stop-signals were presented (randomly) at 100 ms,…, 300 ms after the onset of primary task stimuli. Stopping in the low probability stop-signal condition was considered to require more forceful inhibitory effort as it was anticipated that participants would bias performance toward response activation on the primary task due to the preponderance of go trials, and thus ERP differences would differ between these conditions. Specifically, it was hypothesised that Stop-P3 in the low probability condition would reveal a more anterior distribution than in the high probability condition.

Consistent with this hypothesis, GoRTs were faster and Stop Failures more common in the low probability condition compared to the high probability. Additionally, Go related N2 and P3 components were of shorter latency in the low probability condition. These findings support the hypothesis that participants bias responding toward Go stimuli in the low probability condition and presumably require greater inhibitory effort for successful inhibition. Importantly however, SSRT did not differ between high and low probability conditions.

Stop-signal ERPs largely paralleled those of Kok et al. (2004), whereby stop-signals elicited N2 and P3 potentials which were larger and peaked later for Stop Failures than for Stops. Additionally, Stop P3 had a more anterior focus than Stop Failure P3, though this

was mostly driven by a posterior parietal maximum present in low probability Stop Failures, whereas high probability Stop Failure P3 revealed a fronto-central maximum that was similar to both low and high probability Stop P3 topographies. A visual comparison of the scalp topographies presented in this paper and the groups' earlier paper (Kok et al., 2004) suggest a more anterior distribution of Stop P3 in both conditions and for Stop Failure P3 in the high probability condition in this paper than those published in Kok et al.

These findings seriously challenge the hypothesis espoused by van Boxtel and colleagues (2001) that N2 reflects stop-signal inhibition: Stop N2 was larger in the high probability condition than the low probability condition. Presuming that presenting stop-signals less frequently requires greater inhibitory effort for successful inhibition than when stop-signals are more common, which was supported by Go trial and stop-signal inhibition probability findings, it seems improbable that N2 is indicative of stopping. In contrast, Stop P3s were larger in the low probability condition compared to the high probability, suggesting a relationship between this component and stop-signal inhibition.

Dimoska, Johnstone and Barry (2006) further disputed the notion that N2 reflects response inhibition while endorsing the P3-inhibition hypothesis using a novel approach to delineate overlapping activation present in stop-signal and go trials. In addition to Go response activation overlap, this group also attempted to account for ERP differences in auditory processing, which was not accounted for in the studies of De Jong et al. (1990), Kok et al. (2004), and Ramautar et al. (2004). Two tones of different frequency were presented on 60% of trials over a range of stimulus onset asynchronies (MRT – 0, …, MRT – 600) defining two trial types; stop-signal trials (1500 Hz tone) and 'ignore-signal trials' (1000 Hz tone). Tones on stop-signals were typical, instructing response inhibition, however ignore-signal trial tones instructed a fast accurate Go response, hence participants had to discriminate the trial type instructed by tonal frequency, i.e., go response execution or stop-signal response inhibition. The RT distribution of correct ignore trials was divided into fast and slow RT trials in the typical manner; determined by the PI cut-off of this distribution resulting from stop-signal trials.

N2 was smaller for Stop ERPs than the corresponding ignore trials across midline sites (Fz, Cz and Pz), but larger for Stop Failures than comparable Ignore ERPs, notably at Pz. These findings further negate the assertion that N2 is commensurate with response

inhibition. In contrast, P3 was larger across midline sites for Stops compared to corresponding Ignore trial P3, whereas Stop Failure and corresponding Ignore trial P3 comparisons revealed no difference at Fz and Cz, but a significant reduction was observed at Pz in Stop Failure waveforms. In addition, Stop Failure P3 peaked later than Ignore P3.

In a subsequent analysis, participants were divided into fast and slow go trial responders, to explore the notion that faster go responders require greater inhibitory effort to suppress responding than slower responders. The fast response group exhibited faster RTs across all trials (Go, Ignore and Stop Failure RTs) in addition to an increased probability of Stop Failures, but no differences in SSRT were observed between the groups, thus supporting the assumption of independence between stop and go processes in race model theory. Larger N2 was observed for slow responders compared to fast responders across all trials, but no differences were observed between trials. In contrast, P3 was larger for faster responders, and also significantly larger during Stops for the fast group, while no group differences were observed between Ignore P3.

In a later paper, this group used the same methodology to investigate stimulus probability effects by varying the frequency of stop-signals between experimental conditions (Dimoska & Johnstone, 2008). Specifically, this study was motivated by the hypothesis that enhanced Stop potentials may ensue from the rarity of stop-signal trials compared to go trials, as it is well established that reducing the probability of any stimulus results in an enhancement of potentials elicited by that stimulus compared to when it is more frequently presented. Tones were presented on 60% of all trials, but in one condition 30% of these trials were stop-signals (1500 Hz tone) and 70% were ignore tones (1000 Hz tones), and in a second condition 70% were stop-signals and 30% were ignore tones. It was noted that for a potential to truly reflect inhibition processing, a Stop related interaction must be observed between trial type (Stop, Ignore) and probability (rare, frequent), such that Stop potentials must reveal an enhancement in the rare condition that is significantly greater than an enhancement observed for Ignore potentials. N1, N2 and P3 potentials were observed across the scalp; N2 was largest in the frequent condition and was not further reported on for tone-locked ERPs. N1 and P3 Stop potentials were larger across the scalp than Ignore potentials, irrespective of the probability of stop and ignore trials. Importantly for the Stop-P3 inhibition hypothesis, trial X condition interaction with scalp sites revealed

that there were scalp topography differences over frontal and parietal regions for stop signals that were larger for rare than frequent stop-signals but these effects were not evident for ignore-signals. These results were interpreted as indicating that activation of inhibition processes on stop-signal trials is independent of probability effects and therefore support the association of stop P3s with inhibition.

Bekker and co-workers (2005a) criticized the methodology proposed by De Jong et al. (1990) to account for primary task processing overlap, noting that the linear subtraction effectively adds a positive component to the Stop – Go difference waveform. This occurs due to the inverted polarity of the late P3 potential in the Go comparison waveform. For this reason, Bekker suggested that the resulting enhancement of Stop P3 compared to Stop Failure P3 observed by De Jong and colleagues may stem directly from the difference waveform computation rather than from the presence of stop-signal inhibition processing.

These authors also suggested that overlap removal using the jittered SOA approach (low pass filtering), as per the method of Kok et al. (2004) and Ramautar et al. (2004) (see also Pliszka, Liotti, & Woldorff, 2000, and Dimoska et al., 2003) does not remove all the overlap, hence primary task activation overlap is still present in stop-signal task ERP averages. More pointedly, Bekker indicated that averages with different stop-signal delays computed using this approach, have rendered within them different amounts of overlap. Hence observable differences revealed in comparisons of such averages, as in a comparison of Stop and Stop Failure ERPs, could be rooted in differential primary task distortion arising from differential stop-signal delay linked overlap and not in the process of interest, in this case stop-signal inhibition.

With these concerns in mind, Bekker and colleagues (2005a) used the 'adjacent response' (ADJAR) technique developed by Woldorff (1993) to remove primary task activation overlap from stop-signal ERPs. The ADJAR procedure can account for stop-signal ERP contamination by modeling the primary task related overlap and then removing it from Stop and Stop Failure ERPs by subtraction. An important outcome from the application of ADJAR procedures is that baselines are flattened in corrected ERPs, demonstrating overlap removal.

A comparison of corrected Stop and Stop Failure waveforms showed that Stops were linked to enhanced N1 and P3 potentials compared to Stop Failures, with maximal

differences revealed at FCz and Cz, respectively. Corrected waveforms were also compared to uncorrected waveforms; these analyses revealed that N1 enhancement in Stops compared to Stop Failures was present only in corrected data, and that P3 enhancement in Stops was larger in uncorrected waveforms. Noting that N1 is sensitive to selective attention (Hillyard et al., 1973), Bekker hypothesised that N1 enhancement in Stops compared to Stop Failures reflects the devotion of attentional resources to searching the environment for stop-signals, and that failure to do so results in inhibition failure. Hence N1 amplitude, or the difference between Stop and Stop Failure N1, may be predictive of inhibition success.

The findings of Bekker and colleagues (2005a) mark a turning point in stop-signal ERP studies enabling unambiguous interpretation of stop-signal potentials: removal of go response activation distortion in stop-signal ERPs which has confounded the results of previous studies. To this end, application of the ADJAR correction procedure is marked not only by flattened baselines, but also an augmentation of stop-signal N1 potentials and an attenuation of stop-signal P3 potentials.

2.3.1 Outstanding issues and present studies

The following chapters detail the findings of three experiments investigating the neural basis of stop-signal inhibition using a combination of behavioural, fMRI and ERP methods. The first two experimental chapters (Chapters 3 and 4) utilize healthy young adults to address outstanding issues in the literature regarding the mechanism(s) engaged during stop-signal task performance (detailed below), while the final experimental chapter (Chapter 6) details an investigation into the neural basis of stopping impairments that have been reported in patients with schizophrenia. The latter chapter is preceded by a brief overview of schizophrenia (Chapter 5) as a disorder and the neuropsychological account of schizophrenia, ending with a review of the existing literature on response inhibition in this group. The final chapter provides an overview of the experiments conducted for this thesis and discusses the implications stemming from this work. It should be noted that Chapters 4 and 6 were written in a style intended to represent separate publications.

The review of the literature in this chapter raises two basic questions that will be addressed in the following two experimental chapters of this thesis. The first question regards the sustained processing requirements for stop-signal task performance. Sustained

or tonic processes are those that are continuously active during performance, which contrasts with phasic processes that are engaged specifically for performance of a particular trial type, but may not be required for performance of all trial types, e.g., response inhibition processes are not required for go trial performance. Sustained processing may be examined using epoch-based (or 'blocked') fMRI designed studies whereas phasic processes are best examined using event-related fMRI designs. The only epoch-based design in the stop-signal literature is that by Rubia and colleaguies (2001a). This early study used a non-standard stop-signal paradigm involving a single fixed SSD with visual stop-signals and SSRTs were not estimated. Chapter 3 addresses these issues by employing a standard stop-signal variant involving visual go stimuli and auditory stop-signals that were set using an adaptive algorithm attempting to titrate successful inhibition at 50%. Additionally, SSRT was estimated and related to functional activation within right IFG. This study was submitted to Human Brain Mapping in 2005, but was not accepted for publication. It is to be read as a stand alone document.

The second experiment (Chapter 4) builds upon the first by using an event-related fMRI design to examine stop-signal inhibition, however, the millisecond resolution of event-related potentials (ERPs) are also exploited. In combination, these techniques enable a detailed assessment of both the spatial and temporal properties, respectively, of phasic brain activation elicited during stop-signal task performance. Crucially however, this study addresses the question of task difficulty in stop-signal paradigms. A model of task difficulty for stop-signal experiments is introduced, which has deep implications for many previous stopping experiments where stopping difficulty was not accounted for. In the experiment, task difficulty was varied between participants such that the likelihood each participant could successfully inhibt a cued go response on a given stop-signal task trial was determined by individual SSRT. Hence SSRT was predictive of stopping difficulty and thereby was used as a predictor for regression analyses on fMRI activation data and the peak amplitudes and latencies of ERP components elicited by stop-signals.

The final experimental chapter likewise employed event-related fMRI and ERPs to examine stop-signal inhibition, but the primary aim was to investigate the neural basis of recent reports of stopping impairments in patients with schizophrenia. To this end, patients with a diagnosis of schizophrenia were compared to a group of healthy controls matched

for age, gender and years of education to the patient group. Importantly for this experiment, stopping difficulty was equal for all participants enabling a direct and uncomplicated comparison between patient and control groups, and moreover, enabling a qualitative comparison with the previous experiment where stopping difficulty was varied. The relationships between SSRT, stopping related brain activation and stop-signal ERPs were also examined.

Chapter 3: Experiment 1

Right inferior frontal gyrus and the speed of inhibition processes: an fMRI study.

Hughes, M. E. [a,b,c], Budd, T. W. [a,b,c,f], Fulham, W. R. [a,b,c], Badcock, J. C. [d,e], Michie, P. T. [a,b,c,f].

[a]Functional Neuroimaging Laboratory, School of Behavioural Sciences, University of Newcastle, Callaghan, NSW, AUS

[b]Neuroscience Institute of Schizophrenia and Allied Disorders (NISAD), Sydney, NSW, AUS

[c]Hunter Neuroscience, Newcastle, NSW, AUS

[d]School of Psychiatry and Clinical Neurosciences, University of Western Australia, Perth, WA, AUS

[e]Centre for Clinical Research in Neuropsychiatry, Graylands Hospital, Perth, WA, AUS

[f]Centre for Mental Health Studies, James Fletcher Hospital, Newcastle, NSW, AUS

Short Title: fMRI during stop-signal inhibition

Abstract

fMRI was used to investigate the neural networks involved in response inhibition during performance of a standard stop-signal task (Logan & Cowan, 1984) where participants were required to inhibit an about-to-be-executed response in a visual choice reaction time (RT) task on detection of a stop-signal (tone). In a design contrasting a block of trials of the stop-signal task with a block of trials of choice RT only, activation was observed in a right lateralised network of neural areas commonly reported in studies of response inhibition, including bilateral (but predominantly right) inferior frontal gyri, right middle frontal gyrus, and right inferior parietal lobe; also activated were two areas in left posterior cerebellar cortex. Relationships between behavioural measures (choice reaction time, estimated stop-signal reaction time, and inhibition function slope) and the level of activation in a region of interest analysis were also determined. A significant correlation was found between estimated reaction time to the stop-signal and the level of activation in right inferior frontal gyrus. This finding confirms recent lesion data relating the speed of inhibitory processes to the volume of grey matter loss in right inferior frontal gyrus (Aron et al., 2003a).

Keywords: fMRI, stop-signal reaction time, right inferior frontal gyrus.

3.1. Introduction

The ability to stop responses which are about-to-be executed is a prototypical example of behavioural inhibition, and is one function of the executive system (Logan, 1994). The stop-signal paradigm as first elaborated by Logan and Cowan (1984) is designed to probe an individual's capacity for this form of behavioural control. Stop-signal paradigms involve the performance of two concurrent tasks. In the paradigm most intensively investigated by Logan and his colleagues, the primary task is a choice reaction time task to equally probable visually presented primary or Go stimuli, typically the letters O and X, which instruct left and right hand responses, respectively. On a small percentage of trials an auditory stop-signal (a tone) is presented at some time between the onset of the primary stimulus and the anticipated response time of the participant. The stop-signal instructs the participant to inhibit the primary task response about-to-be executed on that trial; this is the *stop-signal task*. Inhibition difficulty can be manipulated by increasing (harder) or decreasing (easier) the time between Go stimulus onset and stop-signal onset. This interval is termed the *stop-signal delay*.

The stop-signal paradigm is of special interest as the *race model* of stop-signal task performance developed by Logan and Cowan (1984) enables an estimate of the latency of the non-observable (internal) inhibitory response to be derived. This is a unique feature of the stop-signal paradigm compared to other response inhibition paradigms, such as the Go/No-go paradigm. The race model assumes that the Stop process triggered by the stop-signal races against independently triggered Go related processes. If the Stop process wins, action is inhibited; if the Go process wins, action is completed. The latency of the stop response, termed the *stop-signal reaction time* (SSRT), can be estimated using the simple assumptions of the race model. Stop-signal procedures also permit an estimation of a participant's ability in controlling inhibitory responses by generating an *inhibition function* (Logan, 1994; Band et al., 2003): an individual's probability of inhibiting responses over a range of stop-signal delays. The capacity to control inhibitory responses is defined by the slope of the inhibition function as a function of ZRFT, a transformation of stop-signal delays which controls for influence of the relative finishing times of the stop and go processes and variability in the Go task response times (Logan & Cowan, 1984; Logan,

1994). Several clinical disorders have been linked to performance deficits on stop-signal paradigms including schizophrenia (Badcock et al., 2002), children with an increased familial risk of schizophrenia (Davalos et al., 2004), child ADHD (Oosterlaan et al., 1998; Schachar & Logan, 1990), and disinhibition syndromes such as adult impulsivity (Logan et al., 1997). Although there is some controversy about the reliability of the ZRFT slope function as a measure of inhibitory control (Band et al., 2003), there is evidence that it can be dissociated from the speed of the inhibitory response since schizophrenia patients have reduced inhibitory control (ZRFT slope) but not prolonged speed of inhibitory response (Badcock et al., 2002) whereas children with ADHD show the reverse pattern (Oosterlaan et al., 1998; Schachar & Logan, 1990). Evidence of such double dissociations across clinical disorders constrain attempts to explain deficits in behavioural inhibition on stop-signal tasks in terms of a single factor (Baddeley, 2003) as only systems that contain a high degree of functional specialization can produce strong double dissociations (Shallice, 1988).

The neural networks involved in stop responses are poorly understood; only two neuroimaging investigations have studied this form of response inhibition (Rubia et al., 2001a; Rubia et al., 2003), and neither employed the stop-signal paradigm as originally articulated by Logan and Cowan (1984). Rubia and co-workers (2001a) investigated generic activation across three versions of a stop task where participants were told to press a button with their right thumb (a simple reaction time task) when a visual Go stimulus was presented, and to inhibit the response when a visual Stop stimulus (50% of trials) was presented 250 ms after presentation of the Go stimulus. Three tasks were used to control for visual stimulation and motor output by varying the number of Go and Stop stimuli presented, and onset to onset times of Go stimuli across tasks. Rubia reported activation in bilateral inferior frontal gyri (extending into the *insula*), right inferior parietal lobe, and medially in pre-supplementary motor area (preSMA) and anterior cingulate cortex (ACC). In a more recent investigation Rubia et al. (2003) employed event-related fMRI to study the stop response in more detail. The primary task was a choice reaction time task (right or left thumb button presses as instructed by Go stimuli), and the time between Go stimulus onset and Stop stimulus onset was varied for each participant to ensure a 50% inhibition success

rate on Stop trials. Rubia and colleagues found that successful inhibition was related to activation of right inferior frontal gyrus.

Evidence linking right inferior frontal gyrus in particular with inhibitory processing has also emerged from a recent lesion study by Aron and colleagues (2003a) using the stop-signal paradigm. For patients with right frontal lesions, the proportion of grey matter loss in inferior frontal gyrus, particularly portions of *pars opercularis*, predicted SSRT. No correlation was observed for patients with lesions in the same region of the left hemisphere. The relationship between SSRT and right inferior frontal gyrus was first suggested by Reiger et al. (2003) who found that patients with bilateral and right inferior frontal lesions (in addition to patients with lesions to the basal ganglia) had longer SSRTs compared to patients with left inferior frontal lesions, patients with lesions outside frontal cortex, and orthopedic controls. However, no evidence was presented on the relationship between the degree of damage to this area with SSRT. Activation of inferior frontal gyrus has also been reported in other tasks requiring motor inhibition or interference control including the Stroop task (Carter et al., 2000; Taylor et al., 1997), Go/No-go tasks (Durston et al., 2002), flanker tasks (Ullsperger & von Crammon, 2001), the Hayling test (Nathaniel-James et al., 1997) and Simon task (Forstmann et al., 2008).

The aim of the current study was to investigate the neural networks involved in Stop responses by employing fMRI to determine brain regions activated during performance of the version of the stop-signal task most extensively investigated by Logan and his colleagues (De Jong et al., 1995; De Jong et al., 1990; Logan & Burkell, 1986; Logan & Cowan, 1984; Logan et al., 1984; Williams et al., 1999), and further, to relate the degree of activation in regional brain areas to behavioural measures derived from the task including primary task Go reaction times, SSRT estimates and the slopes of inhibition functions.

3.2. Methods

3.2.1. Participants and Procedures

Eleven right-handed volunteers (aged 19-41, M = 27.25 years, SD = 7.4 years, 5 males and 6 females) were tested. Participants with a personal or family history of psychological or psychiatric disorders, a personal history of neurological disorders, brain

injury or substance abuse were excluded based on self-reported information acquired during a preliminary telephone interview and a semi-structured abridged clinical interview (mini-SCID) for DSM-IV Axis I disorders. The project was approved by the Human Research Ethics Committee of the University of Newcastle, the Hunter Area Research Ethics Committee, and the ethics committee of the Faculty of Science and Information Technology, University of Newcastle. Written and informed consent was obtained from all participants.

Participants attended the laboratory for three appointments: the first consisted of an interview to determine suitability for participation, and practice on the stop-signal task. During the second appointment, fMRI data were acquired. On the third appointment, detailed behavioural assessment of stop-signal task performance over a range of stop-signal delays was carried out with the purpose of providing estimates of individual inhibition functions. One participant was unable to attend the behavioural testing session (giving N = 10). Stop-signal delay resulting in 50% success rate in the practice runs of the first appointment were used as the initial settings of these parameters for the stop-signal tasks performed during fMRI scanning. Participants were instructed prior to practice and experimental sessions that accuracy and speed of responding were of most importance, not successful inhibition.

3.2.2. Tasks and Stimuli

Stop-signal task: fMRI acquisition

fMRI data were acquired during four imaging sessions, each of 8 min 47 s in duration. A session consisted of multiple blocks of three separate experimental conditions, each condition being a variation of the stimulus and response components of the stop-signal task (Logan and Cowan, 1984). In all conditions, a block consisted of 24 visual stimuli (a single letter, O or X; 100 ms duration, 50% probability), separated by a stimulus onset asynchrony (SOA) of 2000 ms, giving a block duration of 48 s. For the Stop (S) condition, participants were instructed to make speeded key presses with the left and right index finger to Go stimuli, O and X respectively. On 33% of trials, an auditory stimulus (1000 Hz, 100 dB square-wave tone of 50 ms duration) was presented between the onset of a visual stimulus and the anticipated response latency of the participant. This tone signaled subjects

to inhibit their response on that trial (Stop/signal trials). For all remaining Stop condition trials, no tone was presented (Stop/no-signal trials). The interval between the onset of visual stimuli and the occurrence of the tone (stop-signal delay) was selected adaptively for individual participants to ensure approximately 50% success rate in inhibiting responses (see below).

For the Go (G) condition, trials and stimuli were identical to the Stop condition except that subjects were instructed to respond regardless of whether a stop-signal was presented. For the Passive (P) condition, trials were identical to Stop and Go conditions but subjects were instructed to passively look at/listen to stimuli and refrain from responding. Rest intervals of 15 s preceded and followed each condition block in order to allow the haemodynamic response to return to baseline. Each session consisted of 8 blocks of the three conditions presented in a regular SGSPSGSP sequence. A greater number of Stop blocks relative to Go blocks and Passive blocks were required for a planned event-related analysis of Stop blocks alone which was not proceeded with for technical reasons.

All aspects of the tasks were controlled by software developed in-house written in C++. Primary stimuli (Os and Xs in white arial font) were presented within a small black square which was centred over a horizontal rectangle which differed in colour for each condition: red for Stop blocks, green for Go blocks, and aqua for Passive blocks. Instructions for each condition were centred above the rectangle: 'Attend to tones' for Stop blocks, 'Ignore tones' for Go blocks, and 'No response' for Passive blocks. An 'O' and ‘X’ were always displayed to the left and right respectively of the condition instructions to indicate left and right hand response mapping for Os and Xs. During rest intervals, the rectangle was grey, and the condition display presented condition instructions for the subsequent block.

Visual stimuli were back projected onto a screen (positioned approximately 2 m from the scanner bore entrance) that the subject viewed with a mirror mounted on the head coil (maximum horizontal and vertical extent on screen: 80 x 30 cm; viewing distance: 350 cm; visual angle approximately 0.25° x 0.36°). Auditory stimuli were delivered via 5 m lengths of plastic tubing to etymotic insert earphones. Plastic earmuffs (nominally 30 dB attenuation) were used to reduce external noise generated by the scanner. Participants lay supine in the scanner bore, holding a response key in each hand. Responses were monitored

via a fibre optic cable connected to a laptop computer that logged the timing of stimuli, keypress responses, and volume acquisition TTL pulses from the scanner with millisecond accuracy.

During the first and fifth blocks only within each session, when participants were attending to the stop-signal, the software adaptively changed the stop-signal delay so that inhibition success rate approached 50%. During these blocks, a mean reaction time (MRT) was determined by computing a running average of the reaction time to correctly responded Stop/no-signal trials. Following each Stop/signal trial, stop-signal delay (relative to MRT) was incremented or decremented by 4 ms[15] depending upon whether the response was correctly inhibited. During each of the subsequent Go, Stop and Passive blocks the same sequence of primary stimuli, signal and no-signal trials, and stop-signal delay times were repeated to ensure comparable stimulus presentation in all conditions. MRT and stop-signal delay for each session were used as initial parameter estimates for the subsequent session.

Stop-signal task: Inhibition function

Participants performed 9 blocks of 72 trials. Stimulus delivery was identical to those in the fMRI tasks except that the stop-signal tones were delivered via standard headphones and were presented at 6 different delays within each block based on the methods of Badcock et al. (2002). In the first block, a practice block, participants were instructed to ignore stop-signals and respond as quickly and accurately as possible to Go stimuli on all trials. In the subsequent block, stop-signals instructed participants to inhibit the response cued by primary stimuli on that trial (stop-signal task block); stop-signal delays were set at 0, 100, 200, 300, 400, and 500 ms (4 trials at each delay within blocks) prior to MRT to primary stimuli in the practice block. In subsequent blocks (all stop-signal task blocks), stop-signal delays were set relative to MRT to primary stimuli from the preceding block. While the primary purpose of this session was to obtain data on individual subject's inhibition functions, it also provided an opportunity to obtain estimates of SSRT.

[15] While this step size is smaller than traditionally used, it nonetheless titrated stop-signal task performance approaching the desired chance level (i.e., 50% successful inhibitions).

MR image acquisition

Magnetic resonance images were acquired using a Siemens Vision 1.5 T whole-body MR scanner equipped with a Siemens quadrature head coil. Prior to all experimental runs a magnetization prepared rapid acquisition gradient echo (MPRAGE) sequence (TR = 9.7 ms, TE = 4 ms, flip angle = 12°, 224 x 256 matrix, FoV = 250 mm, voxel size = 0.98 mm^3 was employed to acquire a 164 slice, high resolution T1-weighted anatomical image for later registration into standardised stereotactic space (MNI). During stimulus presentation, 145 whole brain EPI images (TR = 3.839, TE = 70 ms, flip angle = 90°, FoV = 256 mm, 64 x 64 matrix, voxel size = 4 mm^3) were acquired as 32 contiguous and ascending slices (no gap) positioned according to the anterior-posterior commissural line, maximizing brain volume imaged.

MR image pre-processing

Image processing and subsequent statistical analyses were performed using SPM99 (Wellcome Department of Neurology, London). Differences in EPI slice acquisition timing were corrected using the middle slice (16) as a reference. All EPI image time series were then realigned to the first EPI image and a mean realigned EPI image was co-registered to each participant's T1 image. T1 images were then normalized to the SPM99 T1 template and the transformation parameters were then applied to all EPI images. Accuracy of registration between functional and structural data was assessed by visual inspection of the overlay of each individual subjects mean EPI and T1 image. These realigned and spatially normalised images were then smoothed, using an 8-mm Full-Width Half-Maximum Gaussian filter, high-pass filtered (<276 s), scaled to the global mean intensity and corrected for first-order auto-correlation.

Data Analysis: Behavioural data

Median reaction times (RTs), correct response rate, error and miss rates were computed for individual subjects for Go/no-signal and Go/signal trials in Go blocks, and for Stop/no-signal trials in Stop blocks of the fMRI sessions. For Stop/signal trials in Stop blocks, three measures were obtained: the percentage of successfully inhibited trials and the median RT for Stop Failures (Stop Failure RT; responses to Stop/signal trials in Stop

blocks represent a failure to inhibit the response in progress). Estimation of SSRT was based on the procedures outlined by Logan (1994): RTs on correctly responded Stop/no-signal trials (Stop/Go RTs) were rank ordered and the RT cutting off the distribution nearest the probability of responding over Stop/signal trials was determined. Mean stop-signal delay was subtracted from this RT estimate giving SSRT. Data collected during the inhibition function session provided an estimate of the slope of the inhibition function over those stop-signal delays (SSD) where the function was linear (MRT-400, MRT-300, MRT-200, and MRT-100 ms). In addition, a Z transformed relative finishing time (ZRFT) conversion was applied to the stop-signal delays in order to control for influence of the relative finishing times of the stop and go processes and variability in the Go task response times using the procedure outlined by Logan and Cowan (1984; see also Band et al., 2003; ZRFT = (Go RT – SSD – SSRT)/$SD_{RT.}$). An estimate of SSRT was also derived from this session by averaging the estimated SSRT at stop-signal delays of MRT - 100, MRT - 200, MRT - 300, and MRT - 400 ms.

Data Analysis: MRI data

Statistical parametric mapping was carried out using an epoch-based general linear model approach (SPM99). The BOLD signal for each participant was high-pass filtered (276 sec) and experimental conditions were modeled using a boxcar function convolved with the SPM99 canonical haemodynamic response function. The six motion correction parameters (yaw, pitch, roll and x, y and z translations) were included as a covariate of no interest in the general linear model to control for variance in BOLD signal associated with head motion. For each participant, t statistic images were then generated to reveal those voxels in brain regions where significant increases in BOLD activity occurred for STOP relative to PASSIVE conditions (Stop vs. Passive contrast), GO relative to PASSIVE conditions (Go vs. Passive contrast) and STOP relative to GO conditions (Stop Vs. Go contrast). Statistical thresholding in each contrast was set to $p < 0.001$ (uncorrected), using a voxel cluster criterion of 10 contiguous voxels. Group brain activation was assessed for each contrast according to the random effects model (SPM99). Activation maxima co-ordinates for each significant cluster were converted from MNI space to Talairach space, using a standard routine (Brett et al., 2002b) and the corresponding anatomical loci

identified using the Talairach Daemon (gyral loci; Brodmann Area, BA, loci; Lancaster et al., 2000) and cross-checked with a standard stereotactic atlas (Talairach & Tournoux, 1988).

The validity of the uncorrected SPM99 findings were further investigated by subjecting the data (one scan per subject) to a one sample t-test using the SnPM toolbox (Wellcome Department of Neurology, London) for SPM99. This non-parametric approach uses randomisation tests (here 2048 permutations) which inherently account for the multiple comparisons problem (Nichols & Holmes, 2002). A corrected t threshold of $p < .05$ and variance smoothing of 10 mm FWHM were used in this analysis.

Region of interest (ROI) analyses

ROIs were defined according to the suprathreshold clusters in the Stop vs Go contrast (primary effect of interest) for each participant and mean BOLD activity calculated using marsbar-0.23 region of interest toolbox for SPM (Brett et al., 2002a). Mean BOLD responses for each ROI were then correlated with Stop/GoRT (scanning session), SSRT (inhibition function session), and the slope of inhibition functions (inhibition function session). The results from these analyses were verified by performing simple regression analyses using SPM. Only correlations revealing significantly activated clusters in the same neural areas as defined by the ROI were considered valid. Further, given that previous studies (Aron et al., 2003a; Aron et al., 2004a; Reiger et al., 2003) have identified right inferior frontal subgyral formations with inhibition, separate *a priori* ROIs corresponding to *pars triangularis*, *pars opercularis*, *pars orbitalis* as well as the immediately adjacent regions of the right *insula* were defined using the Automated Anatomical Labeling maps (AAL; Lancaster et al., 2000). These ROI images were then smoothed using a 2.5 mm FWHM filter and used to effect a small volume correction using SPM99 (SVC; Friston, 1997) based on the total number of voxels within each ROI. Using this method, significance thresholding for all activation clusters were adjusted separately for multiple comparisons ($p < .05$).

3.3. Results

3.3.1. Behavioural data: fMRI session

Participants responded more slowly during Stop blocks relative to Go blocks: Stop/GoRTs were significantly longer than Go/no-signal RTs $F(1,10) = 13.310$, $p = .004$ as well as Go/signal $F(1,10) = 10.472$, $p = .009$ (see Table 3.1). Median RTs on Go/signal and Go/no-signal trials did not differ indicating that the presence of the auditory signal had no impact on GoRTs in Go Blocks. Stop Failures, that is responses on Stop/signal trials, were significantly faster (by 41 ms) than Stop/GoRTs, $F(1,10) = 9.671$, $p = .011$ (see Table 3.1). While over 5% fewer errors were committed during Stop/no-signal trials than Go trials, the difference was not significant when compared with the error rate when a tone was present $F(1,10) = 3.67$, $p = .084$, or absent $F(1,10) = .065$, $p = .804$.

The overall rate of inhibition was 57.38%, which was higher than the desired 50% success rate; this was primarily due to technical difficulties encountered during testing of two participants. Removing these two participants resulted in an overall inhibition success rate of 52.95%. Due to these difficulties, estimates of SSRTs from the scanning sessions were not used in further analyses as they were not considered to be reliable estimates.

Table 3.1

Behavioural Data obtained from Scanning Sessions. RT means displayed are calculated from median RTs from individual participants.

Trial type	Mean RT (ms)	Correct (%)	Errors (%)	Misses (%)
STOP BLOCKS				
Stop/GoRT	483 (63)	93.77 (5.18)	6.23 (3.91)	3.52 (5.03)
Stop Failure RT	442 (43)	- -	- -	- -
GO BLOCKS				
Go/no-signal	425 (49)	88.21 (11.93)	11.79 (11.93)	4.40 (5.39)
Go/signal	426 (48)	88.64 (8.95)	11.36 (5.35)	3.13 (3.76)

Inhibition function data

Mean slope estimates for inhibition probability as a function of stop-signal delay and ZRFT were -.0235 and .299, respectively (see Table 3.2). The mean SSRT was 270 ms (*SD* = 37 ms) which is within the range described by Logan and Cowan (1984). Once again it was found that Stop Failure RTs (*M* = 523, *SD* = 90) were significantly faster than correct Go responses (*M* = 550, *SD* = 99), F(1,9) = 15.294, p = .004.

Table 3.2

Mean Stop-signal Delay (SSD) and Mean Probability of Inhibition (P(I)) at each delay.

	MRT - 400	MRT - 300	MRT - 200	MRT - 100
Mean SSD	161	253	355	454
Mean P(I)	0.85	0.63	0.28	0.12

3.3.2. Functional brain activation

The Stop vs. Passive and Go vs. Passive contrasts yielded a distributed pattern of large clusters of activation in largely overlapping brain regions but with additional regions of activation in the Stop vs. Passive contrast (see Table 3.3) which are not seen in the Go vs. Passive contrast (see Table 3.4), in particular, right middle and inferior prefrontal regions. Overlapping brain regions include bilateral primary motor cortex (M1), somatosensory cortex, inferior parietal lobes and cerebellar areas, and on the left, inferior and middle frontal gyri, superior temporal gyrus (BA22/BA41), insula and thalamus. In addition, both contrasts show significant activation in medial structures either in or adjacent to anterior cingulate/SMA.

Table 3.3

Group brain activation for the Stops > Passive contrast.

Brain region	BA	N-voxels	t score	Talairach co-ords of peak		
Right Hemisphere						
Inferior Frontal Gyrus	13	64	9.65	32	7	-9
Inferior Frontal Gyrus	44	35	7.18	53	12	10
Inferior Frontal Gyrus	9	13	6.12	51	7	33
Inferior Frontal gyrus	47	75	5.39	38	21	-8
Middle Frontal Gyrus	10	28	5.70	38	45	11
Middle Frontal Gyrus	9	12	4.59	46	33	30
Precentral Gyrus	4	27	6.16	59	-16	39
Precentral Gyrus	4	12	5.62	44	-9	52
Supramarginal Gyrus	40	147	8.00	59	-41	30
Inferior Parietal Lobe	40	16	5.37	65	-40	22
Inferior Parietal Lobe	40	31	5.05	44	-48	52
Postcentral Gyrus	2	58	7.84	44	-23	44
Superior Temporal Gyrus	38	52	7.57	50	11	-12
Superior Temporal Gyrus	22	13	5.09	55	15	-4
Thalamus	-	26	8.04	8	-17	6
Putamen	-	84	7.28	20	4	2
Subthalamic Nucleus	-	14	5.76	14	-10	-3
Cerebellar Declive	-	454	10.24	28	-59	-21
Cerebellar Declive	-	13	7.04	4	-76	-11
Cerebellar Culmen	-	63	8.35	8	-65	-9
Left Hemisphere						
Medial Frontal Gyrus	6	542	9.28	-2	14	45
Inferior Frontal Gyrus	47	29	6.92	-30	23	-3
Inferior Frontal Gyrus	9	24	6.01	-46	3	29
Middle Frontal Gyrus	6	82	6.72	-30	-11	48
Middle Frontal Gyrus	10	81	6.13	-34	49	3
Precentral Gyrus	4	32	6.05	-46	-13	47
Precentral Gyrus	6	10	4.94	-48	0	42
Insula	13	42	5.82	-40	4	-2
Cingulate Gyrus	32	11	5.15	-8	17	29
Inferior Parietal Lobe	40	58	7.04	-40	-46	50
Inferior Parietal Lobe	40	13	5.54	-50	-31	46

Brain region	BA	N-voxels	t score	Talairach co-ords of peak		
Postcentral Gyrus	2	27	6.64	-51	-22	36
Superior Temporal Gyrus	22	74	11.17	-50	8	0
Superior Temporal gyrus	41	55	5.55	-57	-17	6
Putamen	-	-	10.38	-26	8	-4
Thalamus	-	37	5.69	-14	-9	6
Pulvinar	-	13	5.47	-24	-23	9
Cerebellar Culmen	-	281	8.75	-34	-59	-24
Cerebellar Culmen	-	17	5.80	-4	-51	-18
Cerebellar Pyramis	-	59	7.05	-26	-73	-27
Cerebellar Declive	-	43	5.73	-10	-79	-20

Table 3.4

Group brain activation for the Go > Passive contrast.

Brain region	BA	N-voxels	t score	Talairach co-ords of peak		
Right Hemisphere						
Precentral gyrus	4	38	8.95	34	-22	56
Precentral Gyrus	4	15	6.20	57	-15	41
Precentral Gyrus	4	16	5.59	38	-21	49
Precentral Gyrus	44	16	5.24	53	7	14
Superior Frontal Gyrus	6	34	8.47	8	8	53
Cingulate Gyrus	32	353	7.81	8	15	31
Insula	13	24	6.25	42	0	9
Middle Frontal Gyrus	6	30	5.92	24	-7	48
Inferior Parietal Lobe	40	17	5.79	32	-45	37
Postcentral Gyrus	3	14	5.68	30	-34	51
Paracentral Lobule	31	42	6.59	2	-11	48
Globus Pallidus	-	42	6.14	14	-8	-3
Cerebellar Dentate	-	459	10.89	22	-52	-24
Cerebellar Pyramis	-	26	8.50	14	-75	-30

Brain region	BA	N-voxels	t score	Talairach co-ords of peak		
Left Hemisphere						
Middle Frontal Gyrus	6	12	6.68	-20	-7	54
Insula	13	69	6.16	-40	4	-4
Insula	13	15	5.63	-38	18	8
Precentral Gyrus	4	14	6.34	-34	-13	52
Inferior Frontal Gyrus	9	10	5.97	-51	5	27
Inferior Parietal Lobe	40	47	6.80	-44	-29	42
Postcentral Gyrus	3	15	6.84	-44	-21	53
Postcentral Gyrus	2	22	5.66	-51	-29	36
Postcentral Gyrus	40	14	5.66	-34	-36	52
Superior Temporal Gyrus	22	29	5.89	-46	-8	2
Superior Temporal Gyrus	38	13	5.63	-50	-2	-5
Superior Temporal Gyrus	41	12	5.22	-53	-21	8
Thalamus	-	40	11.39	-20	-19	8
Putamen	-	18	6.01	-24	-6	0
Pons	-	10	5.94	-18	-38	-28
Cerebellar Culmen	-	190	8.03	-16	-55	-16
Cerebellar Culmen	-	51	6.06	-30	-48	-21
Cerebellar Culmen	-	19	5.51	-32	-60	-26
Cerebellar Pyramis	-	44	6.68	-4	-77	-25
Putamen	-	18	6.01	-24	-6	0
Pons	-	10	5.94	-18	-38	-28

In contrast, the Stop vs. Go block contrast revealed a network of very focal activation in right lateralised cortical regions which have previously been linked to response inhibition (see Table 3.5 and Figure 3.1). These areas include bilateral (but predominately right) inferior frontal gyri bordering the *insula* (BA 47), right middle frontal gyrus (BA 46), and right inferior parietal lobe (BA 40). In addition, there were two areas activated in left cerebellar cortex: cerebellar tonsil and cerebellar declive.

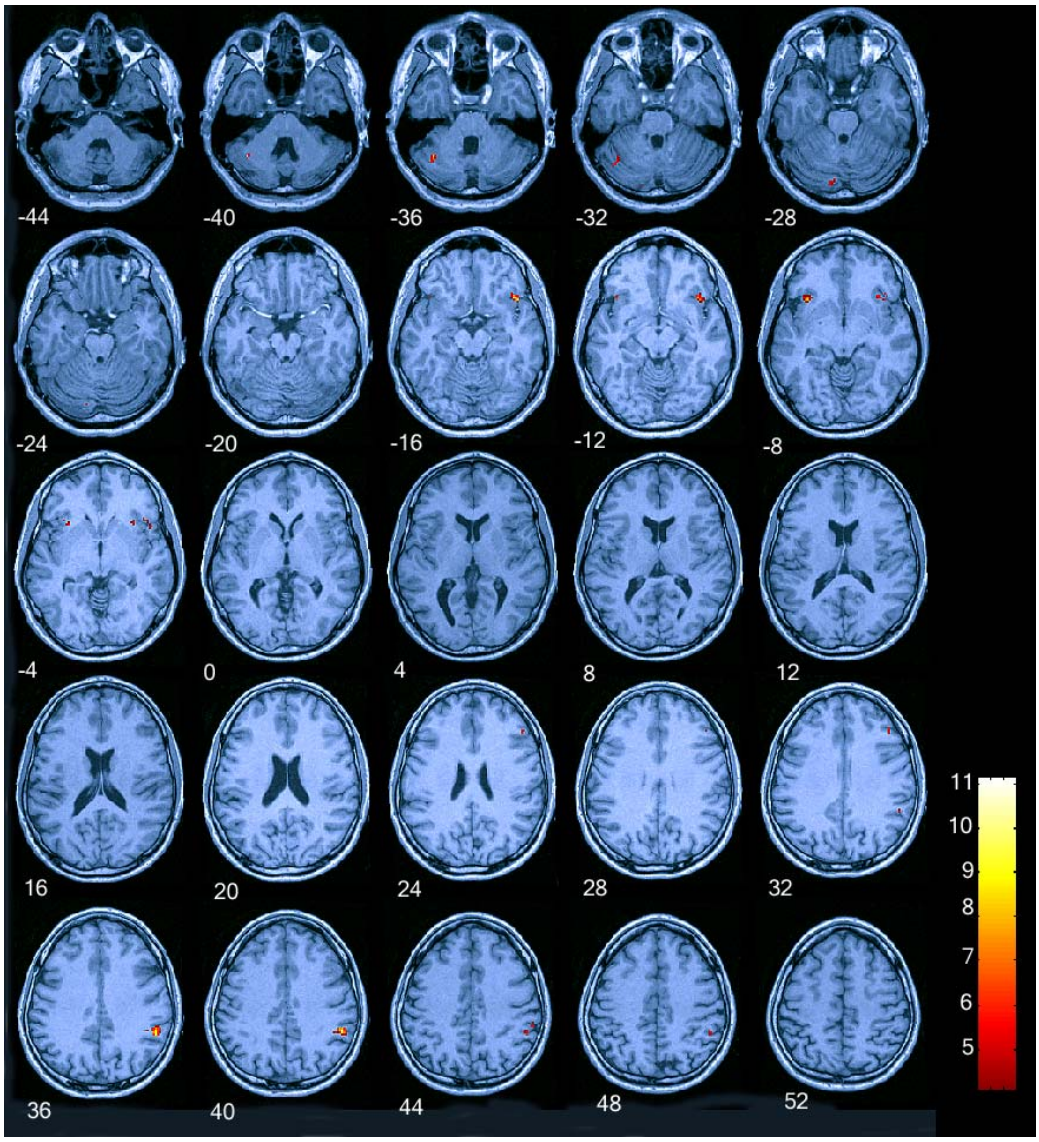

Figure 3.1. Brain activation revealed by the Stop vs. Go contrast slicing up through cerebellar and cerebral cortices from left to right and top to bottom. Numbers to bottom left of each slice depict axial slice location in Z direction (Talairach co-ordinates). Thresholding was: height, $p<.001$ (uncorrected); extent, 10 contiguous voxels. Activation clusters gradually revealed in order are left cerebellar tonsil, left cerebellar declive, RIFG, left inferior frontal gyrus, right middle frontal gyrus, and the right inferior parietal lobe. Colour bar to right denotes t score height.

Non-parametric analyses (see Table 3.6) largely confirmed these findings; the Talairach co-ordinates of activation peaks surviving this thresholding were almost identical

to those observed in the primary SPM99 analysis. Particularly significant was activation in RIFG, right inferior parietal lobe and left cerebellar declive. Right middle frontal gyrus activation was not significant in this analysis.

Table 3.5

Group Brain Activation Revealed in the Stop vs Go Contrast.

Brain Region	BA	Cluster Size	Peak t score	Talairach Co-ords		
Right Hemisphere						
Inferior Parietal Lobe	40	112	10.63	55	-39	39
Inferior Frontal Gyrus	47	100	9.15	44	21	-14
Middle Frontal Gyrus	46	18	5.41	51	36	18
Left Hemisphere						
Inferior Frontal Gyrus	47	53	7.4	-34	19	-8
Cerebellar Tonsil	-	55	11.13	-36	-58	-31
Cerebellar Declive	-	20	6.54	-14	-85	-21

Table 3.6

Non-parametric Group Brain Activation Revealed in the Stop vs Go Contrast.

Brain Region	BA	Cluster Size	Pseudo-t	$P(t_{max}>=u)$	Tal Co-ords		
Right Hemisphere							
Inferior Frontal Gyrus	47	10	6.07	0.005	46	20	-14
Inferior Parietal Lobe	40	5	5.48	0.026	60	-38	44
Left Hemisphere							
Inferior Frontal Gyrus	47	1	5.41	0.032	-34	18	-4
Cerebellar Declive	-	4	5.52	0.023	-8	-86	-26
Cerebellar Tonsil	-	1	5.32	0.040	-38	-60	-36

Relationship between performance measures and functional brain activation

For marsbar-0.23 based ROI analyses, the only significant Spearman's correlation was between average SSRT and the contrast of Stop vs. Go parameter estimates in the right inferior frontal gyrus activation cluster (see Figure 3.2A), $r_s(10) = -.552$, $p = .049$. This result was heavily influenced by a bivariate outlier (see Figure 3.2B); removing this participant resulted in a highly significant correlation, $r_s(9) = -.983$, $p < .001$. No other correlations between ROIs and performance measures on the stop-signal task met the criteria for significance.

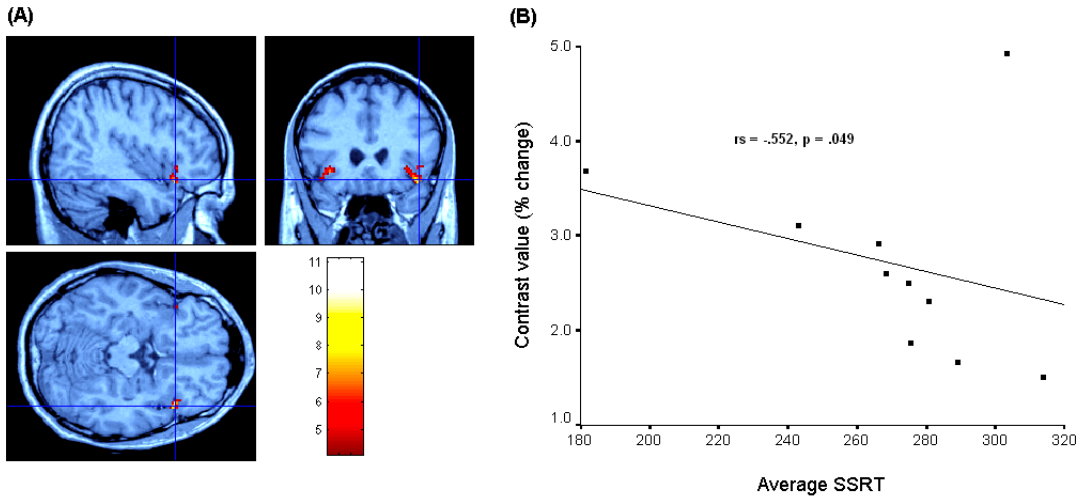

Figure 3.2. Correlation between Stop vs. Go contrast values in right inferior frontal gyrus ROI and average SSRT across delays. (A) Blue crosshairs define peak activated voxel in sagittal (top left), coronal (top right) and axial (bottom left) views of group (N = 11) activation in right inferior frontal gyrus. Height and extent thresholding used was $p < .001$ (uncorrected) and 10 contiguous voxels, respectively. (B) Scatter plot of participants mean contrast value within right inferior frontal gyrus ROI and average SSRT with fitted regression line. Note the outlier (top right). With the outlier removed, rs (9) = .983, p< .001.

Small volume correction (SVC) analyses

Significant activation maxima were detected in the AAL defined *pars orbitalis* ($p < .019$, 94 voxels) and the right *insula* ($p < .046$, 74 voxels), with the peak activated voxel located in *pars orbitalis*. When correction thresholds derived from these analyses were

applied to group data, only clusters in the right inferior frontal gyrus, right inferior parietal lobe and left cerebellar tonsil survived.

3.4. Discussion

3.4.1. Behavioural data

Performance on the stop-signal tasks during the fMRI and inhibition function sessions was consistent with the race model and previous reports (Band et al., 2003; Logan & Cowan, 1984; Logan et al., 1984). The finding that responses escaping inhibition (Stop Failures) were faster than Stop/no-signal responses (Stop/GoRT) is in accord with the race model of Logan and Cowan (1984). The model proposes that Stop Failures result from the primary task process finishing before the stop process. For the particular instantiation of the stop-signal paradigm employed in the current study, the model assumes that the stop process is equivalent to a simple RT (and therefore expected to be faster than primary choice RT task responses) but is handicapped by the stop-signal delay. Hence it is fast primary task responses that typically escape inhibition consistent with our data. While SSRT estimates were a little slower than those described by Logan and Cowan (1984, 200-250 ms), the variability of the estimated times puts them within the same range. As expected, the probability of inhibiting a response varied with stop-signal delay with the probability of inhibiting a response decreasing as stop-signal delay increased.

It was also found that Stop/no-signal trials were significantly slower than both Go/no-signal and Go/signal trials. This is despite participants being instructed that the adaptive nature of the software adjusted stop-signal delay to increase inhibitory difficulty when participants slowed reaction time responses over successive trials and that fast accurate responding was primary during the Stop condition, not inhibition performance. There are at least two possible explanations of this finding. It may be due to participants slowing responses to facilitate inhibitory performance during Stop blocks relative to Go blocks (Logan, 1994), or it could be attributed to the increased working memory load and top-down control associated with the addition of the secondary task of attending to stop-signals during Stop blocks. The middle frontal gyrus activation (albeit weak) in the Stop vs. Go contrast is consistent with the latter interpretation as this area (BA 46) is known to have

a primary role in working memory processes (Smith & Jonides, 1999) and when there are increased requirements for top-down control (MacDonald et al., 2000).

3.4.2. Whole brain activation

As anticipated, the contrast of Stop vs. Go blocks revealed a right lateralised pattern of cortical activation. Activated areas in the uncorrected SPM analysis included bilateral (but predominantly right) inferior frontal gyrus (both BA 47) bordering the *insula*, right middle frontal gyrus (BA 46), and right inferior parietal lobe (BA 40). Not anticipated was the left lateralized cerebellar activation in the posterior cerebellar tonsil and posterior cerebellar declive. The tonsil activation was most marked. Despite the low power of the study due to the small N, non-parametric (with correction for multiple comparisons) and small volume correction analyses confirmed significant activation in the right inferior frontal gyrus extending into the right *insula* and with a peak in *pars orbitalis*, right inferior parietal lobe and the left cerebellum. These analyses suggest that this network of neural areas is robustly activated in stop-signal inhibition and delineates the principal differences between the Stop vs. Passive and Go vs. Passive contrasts. The additional and overlapping areas of activation reported for these latter contrasts may be attributed to primary task processes (stimulus processing, in particular auditory, response selection, response preparation and response execution) and somatosenory processes, not present in the Passive condition. Activations associated with these processes were eliminated in the Stop vs. Go contrast.

Right inferior frontal gyrus

A significant correlation was observed between average SSRT and the level of activation in right inferior frontal gyrus. This correlation was of moderate size in the full sample but was very substantial (-.983) with one outlier removed. That is, increased activation in the right inferior frontal gyrus ROI during Stop blocks was strongly associated with faster SSRTs. These results implicate right inferior frontal gyrus as having a critical role in the speed of inhibitory control in the stop-signal task. Activation in other ROIs including right inferior parietal lobe and left cerebellum were unrelated to stop signal task

performance, either speed of the inhibitory response (SSRT) or inhibitory control (inhibition function slope).

The association between right inferior frontal gyrus activation and SSRT is consistent with the findings of Aron and colleagues (2003a) who, in a lesion study, found that smaller volumes of grey matter loss in right inferior frontal gyrus resulted in shorter SSRTs[16]. While Aron et al. (2003a; 2003b) assert that the speed of inhibitory processing was most closely related to *pars opercularis* volume[17], our functional study places the peak of activation in the adjacent *pars orbitalis*. Therefore, the current study offers the first functional neuroimaging evidence linking activation of right inferior frontal gyrus to the *speed of inhibition processes.* Additionally, a recent lesion study by Aron et al. (2004a) found that damage to right inferior frontal gyrus (specifically the *pars opercularis*) results in increased switch costs in a task-switching paradigm. Therefore, the right inferior frontal gyrus may be critical for the speed of inhibitory processes in both cognitive (inhibition of cognitive set) and motor domains (inhibition of on-going responses; Aron et al., 2004b).

Rubia et al. (2003) have observed activation in a similar area in right inferior frontal gyrus in an event-related comparison of successful vs. unsuccessful stop trials and have argued that this area is crucial for successful *inhibitory control*. Data on the speed of the inhibitory response (from estimated SSRT) and its relationship to activation of right inferior frontal gyrus or other areas were not reported. However, the evidence noted earlier of a double disassociation between the inhibitory response speed and inhibitory control (in individuals with schizophrenia vs. ADHD; Badcock et al., 2002; Oosterlaan et al., 1998) suggests that speed and control of inhibitory responses reflect distinct aspects of behavioural inhibition and therefore are potentially mediated either by separate areas within right inferior frontal gyrus or type of activation (tonic vs phasic) within right inferior frontal gyrus. Our block design, which would be more sensitive to tonic activation of brain areas associated with stopping (Garavan et al., 2003), demonstrated a relationship between right

[16] While a recent study by Dimitrov and colleagues (2003) found no difference in SSRT between a group of patients with frontal lobe lesion patients and matched controls, none of their lesion patients had damage to BA 47.

[17] Although Aron and his colleagues report that speed of inhibitory response was most closely related to *pars triangularis* volume in their 2003 paper (Aaron et al., 2003a), in an erratum (Aron et al., 2003c) and a later paper (Aaron et al., 2004b), they note that their 2003 paper erroneously referred to the *pars opercularis* as the *pars triangularis*.

inferior frontal gyrus activation and speed but not control, whereas Rubia et al's event related design with the capacity to measure phasic activation (Garavan et al., 2003) demonstrated a relationship between right inferior frontal gyrus activation and control (although it is not known whether event-related RIFG activation is related to speed of the inhibitory response). Therefore, one possible interpretation of these data is that phasic activation of right inferior frontal gyrus is related to control but tonic activation is related to speed; other studies have demonstrated that differential tonic and phasic activations within the same brain structure underpin different functions (Simões-Franklin, Hester, Shpaner, Foxe & Garavan, 2009). Further research using suitable designs will be necessary to determine whether there is parcellation of right inferior frontal gyrus according to type of inhibition function (speed vs. control) or whether these separate functions are controlled by tonic vs. phasic right inferior frontal gyrus activation. However, it must be acknowledged that the block design of the current study does not allow us to distinguish inhibition related processes from other cognitive and motor processes that distinguish Stop blocks from Go blocks such as increased attentional demands, response selection and execution complexity, response competition and error monitoring.

ACC

No activation was observed in ACC at the thresholding used ($p < .001$ uncorrected, 10 contiguous voxels), although at lower thresholds ($p \leq .005$ uncorrected, 10 contiguous voxels) ACC activation was present. ACC is known to have primary roles in error detection (Fassbender et al., 2004; Fiehler et al., 2004; Garavan et al., 2003; Garavan et al., 2002; Hester et al., 2004; Kiehl et al., 2000; Menon et al., 2001; Rubia et al., 2003) and response competition (Carter et al., 1998; van Veen et al., 2004). As approximately equal numbers of successful inhibitions and stop failures (errors) occurred in the stop-signal task performed in the scanner, activation was expected in this medial cortical region. However, ACC is also known to be activated during 'difficult' inhibition (Garavan et al., 2002) trials where the response to the primary stimulus on the previous trial is relatively fast. Therefore, it is possible that an event-related analysis of stop-failures combined with manipulation of inhibition difficulty will provide a more sensitive index of ACC activation than the paradigm employed here.

PreSMA

While previous groups have argued that preSMA is critical for response inhibition in go/no-go tasks (Ball et al., 1999; Humberstone et al., 1997; Garavan et al., 1999; Mostofsky et al., 2003), the contrast of Stop vs. Go in the current study suggests that stopping on-going responses in the stop-signal task does not activate preSMA significantly more than executing responses in a choice reaction time task. Medial frontal activation was present in both the Stop vs. Passive and Go vs. Passive contrasts, extending from SMA proper into preSMA anteriorly, and inferiorly into cingulate gyral regions. In the contrast of Stop vs. Go, preSMA activation was not observed even at more liberal thresholding ($p < .01$ uncorrected, 10 contiguous voxels). This contrasts with the findings of Rubia et al (2001a) who reported activation in this medial frontal region in a block design.

One possible explanation for the discrepancy between the current findings and those of Rubia and colleagues is related to performance differences by participants in the two studies. MRT for the equivalent of stop/no-signal trials reported by Rubia were long (average RT of 620 ms over three versions of the stop-signal tasks in contrast to an average RT of 328 ms in two versions of Go/No-go tasks reported in the same paper), given that the primary Go task was a simple reaction time task requiring right thumb responses. Furthermore, inhibition success was high (93% on all three stop tasks). The slow reaction times and high inhibition success rate suggests participants may have strategically delayed responses very substantially in order to facilitate inhibition performance. The high percentage (50%) of stop trials utilized in Rubia's study may have encouraged the use of such a strategy (Band et al., 2003; Logan, 1994). Further, neurophysiological studies in non-human primates have shown that preSMA neurons are highly active while a response is withheld over a delay period (Matsuzaka et al., 1992), and PET studies have found greater preSMA activity when responses are covertly guided compared to responses that are externally guided by cues (Deiber et al., 1996; Deiber et al., 1991). In addition, preSMA is known to have a significant role in response preparation (Watanabe et al., 2002). These findings appear to support the possibility that preSMA activation reported by Rubia et al. (2001a) resulted from participants delaying responses in order to facilitate inhibitory performance. A recent fMRI study has shown that preSMA has a significant role in the

estimation of stimulus duration (Coull et al., 2004). Therefore, it is also possible that preSMA activation was observed by Rubia et al. (2001a) because participants were, in addition to delaying responses, estimating the stop-signal delay (duration) which was fixed at 250 ms. Delaying strategies were circumvented to some extent in the current study, although not entirely, via the use of an adaptive algorithm which varied stop-signal delay to achieve an inhibition probability of approximately 50%.

Right inferior parietal lobe

Right inferior parietal lobe (BA 40) activation is consistently reported in studies of response inhibition; this region is thought to form part of a posterior attentional network subserving the frontal lobes, probably as a sensory-motor interface (Mattingley et al., 1998). Specifically, the right inferior parietal cortex plays a role in visual-spatial attention processes required for task performance (Maguire et al., 2003; Posner & Peterson, 1990). Our data are consistent with this explanation as attentional demands are greater during the Stop condition than the Go condition due to the additional task demand of attending to stop-signals. However, despite recruitment during successful inhibition (Garavan et al., 2002; Rubia et al., 2003), inferior parietal cortex has also been linked to error-related processes. On the basis of ERP data, Garavan et al. (2002) suggested that activity in this area on failed inhibition trials reflects late activation of inhibitory responses, a hypothesis which is in accordance with the predictions of race model.

Cerebellum

Cerebellar activation is often not seen in neuroimaging studies of response inhibition simply because this area is not imaged. Even when activation is significant in response inhibition tasks, the role of cerebellar cortex is not interpreted (Liddle et al., 2001). In a study of response inhibition which reported cerebellar activation, Mostofsky and colleagues (2003) suggested that lateralised left posterior cerebellar activity during no-go responses reflects either response preparation or response inhibition processes.

While the traditional view of cerebellar function has limited this region to roles in motor control, research over the last several years has implicated cerebellar involvement in a diverse array of both motor and cognitive functions (Ivry, 2000), including time

discrimination (Smith et al., 2003), signaling the difference between predicted and actual sensory consequences of actions (Blakemore et al., 2001), probabilistic reasoning (Blackwood et al., 2004), tool learning (Tamada et al., 1999), the omission of anticipated events (Tesche & Karhu, 2000) and attentional functions (Gottwald et al., 2003).

The cerebellar activation observed in the present study could be attributed to a combination of two of these functions: motor control and probabilistic reasoning. As previously mentioned, it is often the case in stop-signal experiments that participants delay primary task responses in order to facilitate inhibition success (Logan, 1994). Hence it is likely that participants control responses on-line until they think it is 'safe' to respond. This interpretation involves the participant inferring the probability that a stop-signal will be presented on a given trial; on trials that the participant thinks it likely a stop-signal will be presented (if no stop-signal has been presented on preceding trials), the planned response would be held on-line longer than on trials where the participant thinks it less likely that a stop-signal will be presented (if a stop-signal was presented on the preceding trial). Hence participants may have counted the number of trials preceding the current trial, which did not contain a stop-signal, and varied primary task response time on the current trial accordingly. In this interpretation the timing, or level of motor control exerted to produce a correct response is related to probabilistic inference. This is not unlike the findings of Blackwood and colleagues (2004) who used tasks where trains of alternate stimulus types were presented (e.g. blue circles and red circles) from one of two stimulus sets (e.g. one containing 60% blue circles and 40% red circles, and the other containing 60% red circles and 40% blue circles). Participants were required to indicate from which stimulus set the stimuli in each train were likely to have come and thus were required to count the number of each stimulus type presented. It was found that activation in a lateral portion of the left cerebellum (Talairach co-ordinates -32 –62 –28), in close proximity to cerebellar activation in the present study (Talairach co-ordinates -36 –58 –31), was particularly related to deciding from which set the stimulus train was presented (probabilistic reasoning). In this case, not unlike the former, the correct response is related to probabilistic reasoning.

Lateralisation of cerebellar activation to the left side may also be due to the contralateral connections between cortical regions and cerebellar regions (Middleton & Strick, 1994). Thus, functional links are thought to exist between right inferior frontal gyrus

and the left cerebellum (Tamada et al., 1999), and between left inferior frontal gyrus and the right cerebellum (Roskies et al., 2001). The former link could be of particular relevance to the current findings considering the known role of cerebellar cortex in motor control; control may be modulated in cerebellar cortex via the activities of right inferior frontal gyrus. Further research is needed to investigate the functional link between these areas in relation to higher order motor control.

3.4.3. Conclusion

In conclusion, a network of predominantly right hemisphere cortical regions and left cerebellar regions was found to be activated during stop-signal inhibition. Cortical areas activated included areas implicated in previous response inhibition studies: bilateral inferior frontal gyri, right middle frontal gyrus, and right inferior parietal lobe with the most robust activations in right inferior frontal gyrus and right inferior parietal lobe. However, a significant correlation between average SSRTs and mean activity in right inferior frontal gyrus provides the first functional neuroimaging evidence that the level of activation in this cerebral region is critical for the speed of inhibition of on-going motor responses.

Acknowledgements

Matthew Hughes is supported by a NISAD Postgraduate Scholarship for Schizophrenia Research. The research was supported by grants awarded by the University of Newcastle Research Grants committee and by the Neuroimaging Consortium of the National Health and Medical Research Council Network for Brain Research into Mental Disorders. We are grateful to Steve Hudson and Gary O'Connor for assistance with MRI data acquisition.

Chapter 4: Experiment 2

4.1 Introduction

Studies investigating the neural basis of response inhibition have consistently emphasised prefrontal cortex (PFC) in this aspect of executive control. However, a localised neocortical agent (driver of response inhibition processes) and site (neural area where motor output is suppressed) of response inhibition has remained elusive. While studies often report distributed prefrontal activation patterns, right-lateralised activation loci observed in inferior frontal gyrus (IFG: Aron et al., 2003a; Aron & Poldrack, 2006; Experiment 1; Rubia et al., 2001a; Rubia et al., 2003), middle frontal gyrus (MFG: Kawashima et al., 1996; Watanabe et al., 2002; Zheng et al., 2008; de Zubicaray et al., 2000), and preSMA (Aron & Poldrack, 2006; Aron et al., 2007a; Mostofsky et al., 2003; Vink et al., 2005) are most commonly attributed roles in response inhibition. These areas are thought to instigate inhibition processes (the driver) and send output to basal ganglia structures, particularly striatal nuclei (Li et al., 2008; Vink et al., 2005) and the subthalamic nucleus (STN: Aron & Poldrack, 2006; Aron et al., 2007; Li et al., 2008; see also Experiment 1) which are capable of inhibiting motor output (the site) by suppressing thalamocortical afferents that project to motor cortex (M1; Alexander & Crutcher, 1990; Nambu et al., 2002).

One factor impeding clarification of these issues is the variability in inhibition difficulty posed by different paradigms in combination with paradigm variants that have been used to investigate response inhibition. Usually go/no-go or stop-signal paradigms are used which has led to response inhibition being defined in the literature as both the inhibition of *prepotent* responses (Roberts & Pennington, 1996) and the inhibition of *on-going* responses (Logan & Cowan, 1984; Nigg, 2000). In traditional go/no-go paradigms[18], no-go inhibition trials require participants to override a prepotent response tendency built up over previous go trials, hence inhibition difficulty is manipulated by varying the number of go trials preceding a no-go trial (Roberts & Pennington, 1996). The inhibition difficulty

[18] Other Go/No-go paradigms have been used to facilitate stronger Go response prepotency such as that employed by Garavan and colleagues (1999) where No-go stimuli were conditional (see Chapter 1).

of stop-signal trials may also be influenced by go response prepotency as per no-go trials, but is primarily manipulated by stop-signal delay (SSD) variation. Thus both go response prepotency and SSD influence the difficulty of inhibition, but these factors do not uniquely determine inhibition difficulty. For example, an SSD that evokes a high proportion of Stop Failures (commission errors) from one participant may not evoke the same proportion of Stop Failures from another participant. Hence SSD may influence inhibition difficulty for an individual, but is not an intrinsic measure of difficulty. So what is inhibition difficulty?

Inhibition difficulty may be construed as the ratio (henceforth termed 'inhibition difficulty ratio') comparing the time necessary for inhibition processes to effect inhibition (inhibition processing time) to the time given for this to be accomplished. It is not possible to estimate inhibition processing time using go/no-go paradigms, however the stop-signal paradigm does afford this estimation using the assumptions of the race model (Logan & Cowan, 1984). As described in chapter 1, this is called the stop-signal reaction time (SSRT), and is usually around 200 ms[19] for an individual (Logan, 1994), but varies across individuals. In stop-signal studies, the inhibition difficulty ratio is therefore SSRT compared to the time between stop-signal onset and the anticipated RT (median go reaction time, GoRT), i.e., inhibition difficulty ratio = SSRT/(GoRT – SSD). Experimenters manipulate inhibition difficulty by changing the denominator of the ratio (GoRT – SSD): increased difficulty is implemented by increasing SSD, reducing the denominator and consequently reducing the probability of response inhibition (PI); decreasing SSD increases the denominator, thus reducing difficulty, and consequently increasing PI. Therefore the inhibition difficulty ratio and SSD are inversely proportional to PI.

In go/no-go studies, the time given to inhibit go responding is equivalent to anticipated GoRT, not unlike a stop-signal trial where SSD equals zero. Assuming that inhibition processing time is equivalent for stop-signal and go/no-go paradigms (i.e., about 200 ms), then the inhibition difficulty ratio is this time compared to the anticipated response time (inhibition difficulty ratio = SSRT/GoRT), the latter usually being in the order of 350-400 ms for go/no-go (recognition) reaction time tasks[20] (Laming, 1968). This

[19] As noted by Logan (1994) this typical estimate of SSRT is akin to that observed for simple reaction time tasks when responses are cued by auditory stimuli.

[20] In his pioneering work, Donders (1969) found that simple reaction times (responding upon presentation of a single stimulus) were shorter than recognition reaction times (responding only to selected stimuli), while

interval is substantially longer than typical SSRT, therefore effecting quite a low inhibition difficulty ratio. Hence high PIs (few commission errors) would be anticipated, and are usually reported in go/no-go studies, but PI decreases with increasing go trial prepotency (e.g. de Zubicaray et al., 2000; Durston et al., 2002).

When go responses are highly prepotent in go/no-go paradigms, participants anticipate go stimulus presentation, and may (incorrectly) pre-emptively launch go response processes prior to stimulus presentation – but a no-go stimulus is presented. In this circumstance, the no-go stimulus becomes a stop-signal, since the go response is *in-progress*, and becomes a signal to inhibit on-going go response activation. Therefore, response prepotency can be thought of as generating a pseudo SSD, equating to the interval between pre-emptive launch of stop-signal processes and the onset of the no-go stimulus.

Many neuroimaging experiments employing the stop-signal paradigm have demonstrated that right IFG is critical for stopping, using both blocked (Rubia et al., 2001a; see also Experiment 1) and event-related (Aron & Poldrack, 2006; Aron et al., 2007; Chikazoe et al., 2007; Rubia et al., 2003) experimental designs. The importance of right IFG has also been demonstrated using TMS (Chambers et al., 2006) and in patients with frontal lesions (Aron et al., 2003a; Regier et al., 2003). In particular, a subgyral structure of right IFG, *pars opercularis*, is thought to be most crucial for stopping (Aron et al., 2003a; Aron & Poldrack, 2006; Aron et al., 2007a; Aron et al., 2007b). Aron and colleagues (2003a) found that in patients with frontal lesions, grey matter loss in right *pars opercularis* was most predictive of SSRT slowing, and in a later neuroimaging study, Aron & Poldrack (2006) reported that larger BOLD responses in *pars opercularis* were predictive of faster SSRT. In Experiment 1 on the other hand, it was found that activation of pars orbitalis was predictive of faster SSRT.

IFG has also been linked to no-go inhibition, but usually only when response prepotency is high (Garavan et al., 1999; Liddle et al., 2001; Menon et al., 2001). Durston and colleagues (2002) observed a linear relationship between BOLD signal intensity increases in IFG (albeit left IFG) and the number of go trials preceding a no-go trial,

---

choice reaction times (selecting among possible responses depending upon the stimulus presented) were longer than both simple and recognition reaction times. Laming (1968) concluded that recognition reaction times were around 384 ms.

suggesting that IFG is sensitive to increasing no-go inhibition difficulty triggered by pre-emptive launching of go responses with increasing go response prepotency.

Notwithstanding this, MFG activation was reported in most of the aforementioned studies as well, and one event-related fMRI study reported that right MFG was the only PFC region that was commonly recruited for stop-signal and no-go inhibition (Zheng et al., 2008). Additionally, in the previously mentioned lesion study of Aron and colleagues (2003a), it was reported that grey matter loss in MFG was predictive of SSRT slowing, although when IFG damage was controlled for, the correlation between MFG and SSRT was not significant. An analysis of the literature suggests that MFG typically dominates inhibition contrast activation patterns in go/no-go neuroimaging studies when no-go and go trials are equally common or have low go response prepotency (low inhibition difficulty ratio: De Zubicaray et al., 2000; Kawashima et al., 1996; Rubia et al., 2001a; Watanabe et al., 2002). Indeed, a go/no-go fMRI study using a block design, found that both MFG activation and RT increased as the number of no-go trials compared to go trials in each block increased (De Zubicaray et al., 2000), suggesting lower go response prepotency was linked to greater reliance on MFG for no-go inhibition. Together these findings indicate that IFG is recruited for increasing inhibition difficulty (high inhibition difficulty ratio), whereas MFG is most necessary during situations of low inhibition difficulty, but is engaged no matter how difficult the inhibition task is. In support of both these assertions, lesion and neuroimaging experiments have reported that MFG (Aron et al., 2003a; Zheng et al., 2008) and IFG (Aron et al., 2003a; Aron & Poldrack, 2006; Aron et al., 2007a; see also Experiment 1) are predictive of SSRT. But as noted previously, lesion (Aron et al., 2003a) and neuroimaging studies (Aron & Poldrack, 2006; Aron et al., 2007a) suggest that *pars opercularis* of right IFG, is uniquely predictive of SSRT.

In addition to these PFC regions, many studies have reported basal ganglia involvement in response inhibition, notably the STN[21] (Aron & Poldrack, 2006; Aron et al., 2007a; Eagle et al., 2008; Li et al., 2008) and striatum (Eagle et al., 2003a; Li et al., 2008; Vink et al., 2005). The most informative findings have been revealed in stop-signal studies that have related performance variables to the function of basal ganglia nuclei, though the

[21] STN activation was linked to stopping in Experiment 1, but only when Stop blocks were compared to Passive blocks and not when Stop blocks were compared to Go blocks (see Chapter 3).

findings are conflicting. Aron and his colleagues (2006; 2007a) reported that faster SSRT predicted greater BOLD signal intensity in STN, whereas a Cambridge group led by Trevor Robbins found, using rodent lesion models, that lesions to STN did not affect SSRT, but did affect animals' ability to trigger stop-signal inhibition processes, (see Chapter 2: Eagle et al., 2008). Adding to these inconsistencies, Li et al. (2008) found stopping elicited larger BOLD responses in STN for participants with slower SSRT compared to participants with faster SSRT. However, this group also reported that participants with faster SSRT had greater striatal activation compared to those with slower SSRT. Another rodent study by the Robbins group directly tested the relationship between striatal function and SSRT, and reported that medial striatal lesions in rats slowed SSRT, but also slowed GoRT, produced more go trial omissions and flattened inhibition functions (Eagle et al., 2003a), indicating generalised impairment due to lesioning. It should be noted however, that impairing striatal function should also alter STN function through disruption to the indirect pathway (see Chapter 2).

Some clues to the nature of striatal involvement in stopping was provided by Vink and colleagues (2005), who observed a strong correlation between BOLD signal increases within striatal nuclei and slowing of go RTs in anticipation of a stop-signal trial, thus implicating the striatum in the facilitation of stopping by strategic slowing of go responses. Vink also reported greater striatal activation during Stops compared to Stop Failures, a finding also reported by Aron and Poldrack (2006); Vink did not report RTs for Stop Failure trials, but fast RTs are consistently observed for Stop Failures, as predicted by the race model (Logan, 1994), and thus Vink's latter finding further supports the notion of striatal engagement in strategic slowing of Go responses.

On the whole, these findings indicate a significant role for STN in stopping, whereas striatal involvement may be limited to suspension of go response activation to facilitate stopping. If this is true, and STN is related to faster inhibition processing as proposed by Aron and Poldrack (2006), then the findings of Li and colleagues (2008) indicate that in that study, participants with faster SSRTs strategically slowed responding (greater striatal activation) more than participants with slower SSRTs to reduce the difficulty of inhibition, thereby lessening the requirement for fast inhibition and hence STN engagement. It should be noted that Li et al. (2008) did not report that pre-performance

instructions to participants included the requirement to respond as fast as possible which may have favoured the adoption of such strategic responding. Stahl and Gibbons (2007) have described such slowing as a 'wait criterion', i.e., waiting after go stimulus presentation for a stop-signal to facilitate stopping. Given the neuroimaging findings of Vink et al. (2005) and Aron and Poldrack (2006) such waiting is presumably mediated by the striatum. Hence it is possible that STN activation may be contingent upon the difficulty of inhibition and not solely on SSRT.

The current investigation was designed to test the hypothesis that activation within the proposed hyperdirect right IFG-STN network is contingent upon inhibition difficulty. For most stop-signal studies, including the neuroimaging studies outlined above, inhibition difficulty is manipulated using performance tracking algorithms that set SSDs adaptively to produce equal numbers of Stops and Stop Failures (i.e., PI = .5). The purpose of this approach is primarily to obtain reliable estimates of SSRT (Band et al., 2003), but implies, quite necessarily, that the time given to inhibit on-going go response processes is equivalent to SSRT, and thus the inhibition difficulty ratio as defined above is equal to one. But more importantly, the inhibition difficulty ratio is equivalent for each participant, despite variation in SSRT between participants. In the current experiment, inhibition difficulty was manipulated by keeping the time given for stop-signal inhibition approximately constant between participants, accomplished by setting the onset of stop-signals relative to the anticipated time of responding (median go task reaction time, GoRT). Because participants were given equal time to initiate stop-signal inhibition processes and to inhibit go task activation, the inhibition ratio varied among participants. Race model theory implies that with this manipulation, participants with longer SSRTs would inhibit less often than participants with comparatively shorter SSRTs, due to differences in the inhibition difficulty ratio. Hence in this stop-signal variant, SSRT should predict inhibition difficulty; participants with longer SSRTs should have a relatively high inhibition difficulty ratio whereas participants with faster SSRTs should have a lower inhibition difficulty ratio. For this reason, it was hypothesised that SSRT in this stop-signal variant would be

inversely related to the probability of inhibition (PI), and assumed that SSRT was predictive of the difficulty of inhibition[22].

It was hypothesised that participants would generically activate a network including right lateral MFG and IFG, but that slower SSRT (higher inhibition difficulty ratio) would predict greater activation in the right IFG-STN network, and moreover, that IFG activation would be specific to *pars opercularis*. Additionally, the notion that stopping is linked to slowing of RTs was tested. This experiment did not involve the go trial manipulations employed by Vink and colleagues (2005). Rather, the RTs of trials preceding Stops and Stop Failures were assessed. It was hypothesised that stopping would be mediated by slower go RTs preceding Stops than Stop Failures, and also that Stops would reveal greater striatal and STN activation than Stop Failures.

A further goal of this study was to examine the event-related potential (ERP) correlates of stop-signal inhibition. Some researchers have linked stopping to elicitation of a potential peaking at about 200 ms termed stop-signal N2 (Pliszka et al., 2000; van Boxtel et al., 2001), but this component can be larger for Stop Failures compared to Stops (van Boxtel et al., 2001; Ramautar et al., 2004), and is usually not observed when auditory stop-signals are used (Bekker et al., 2005; De Jong et al., 1990; Dimoska et al., 2006; Dimoska et al., 2008). Therefore, it is difficult to make a strong case for N2 involvement in stopping. Most researchers agree that a later positive deflection, P3 (Stop-P3) reflects stopping processes (Bekker et al., 2005a; De Jong et al., 1990; Dimoska & Johnstone, 2008; Kok et al., 2004; Ramautar et al., 2004). Stop-P3 is maximal at central midline electrodes (i.e., Cz of the 10-20 system), and peaks earlier and with greater amplitude at central sites than Stop Failure-P3, which is largest at parietal sites. Recent evidence indicates that stopping is also linked to an early negative potential, N1, that has a larger amplitude during Stops compared to Stop Failures (Bekker et al., 2005a). Näätänen (1987) distinguishes 'exogenous' modulation of N1 that is influenced by the physical and temporal parameters of a stimulus, from endogenous modulation that is influenced by particular stimulus contexts. Given that stop-signals do not differ between Stops and Stop Failures, the N1 enhancement during Stops compared to Stop Failures observed by Bekker and colleagues (2005a) must be

[22] PI was not considered to reflect inhibition difficulty because previous studies using patients with schizophrenia (Badcock et al., 2002) and rats with STN lesions (Eagle et al., 2008a) did not exhibit slower SSRT compared to controls, despite a reduced probability of inhibition.

endogenously driven. Bekker suggested that the component that is added to auditory evoked N1 distinguishing Stop-N1 from Stop Failure-N1 is elicited by selectively attending to the stop-signal during Stops, and is thus important for timely activation of the stopping process (Bekker et al., 2005a). Hence, while Stop-P3 is thought to reflect the actual stopping process, the role of Stop-N1 is thought to be linked to triggering that process.

Most relevant to the current ERP investigation is a recent stop-signal study by Bekker and colleagues (2005a) who used ADJAR correction procedures (Worldorff, 1993) to remove overlapping go stimulus ERP potentials - elicited by go task stimuli on stop-signal trials – from stop-signal ERP waveforms. This method was chosen above others as it aims to completely remove ERP overlap elicited by the primary Go task in stop-signal ERPs, which is not possible using difference waveform approach that has been employed in most stop-signal experiments to isolate stop related activation (e.g. De Jong et al., 1990; Dimoska et al., 2006; Dimoska et al., 2008; Kok et al., 2004; Ramautar et al., 2004). Bekker found that using ADJAR procedures resulted in enhancement of N1 amplitudes, and reduction of P3 amplitudes. An additional factor revealing the efficacy of ADJAR correction procedures not mentioned by Bekker is that the latency of the major potential removed from stop-signal-locked waveforms should correspond to the latency of the Go-P3 (which is removed) minus SSD.

In an extension of the work by Bekker et al. (2005a), the current study also examined the relationship of ERP latency and amplitude measures to SSRT. Specifically, it was hypothesised that faster SSRT would be linked to earlier peaking Stop-P3, but given that the latency of Stop-N1 reflects the speed of sensory processes, the relationship between SSRT and Stop-P3 latency was also examined with Stop-N1 subtracted from the latter. Larger Stop-P3 amplitudes have previously been reported when stop-signal probabilities are reduced compared to those elicited during more frequent stop-signal presentation, which has been interpreted as evidence of greater inhibitory pressure (Ramataur et al., 2004), but other data suggests this effect is largely due to probability effects and not inhibitory processes (Dimoska & Johnstone, 2008). Hence it was tentatively hypothesised that larger Stop-P3 amplitudes would be related to longer SSRT due to greater inhibitory pressure required for participants with slower SSRT in this stop-signal variant.

4.2 Methods

4.2.1. Participants and Procedures

Healthy right-handed volunteers (N = 16, aged 22 - 34, M = 27.6 years, SD = 3.6 years, 9 males and 7 females) were tested. Exclusion criteria for participation were a personal or family history of psychological or psychiatric disorders, a personal history of neurological disorders, brain injury or substance abuse, suffering from claustrophobia, and having ferromagnetic objects within or on the body. This information was obtained from potential participants by self-report. The project was approved by the Human Research Ethics Committee of the University of Newcastle, and the Hunter Area Health Research Ethics Committee. Written and informed consent was obtained from all participants according to the Helsinki declaration.

Participants first attended a practice session, and later, fMRI and ERP experimental sessions. The practice session consisted of an interview to determine suitability for participation and practice on the stop-signal paradigm. In the experimental sessions, participants responded to stop-signal paradigm stimuli whilst undergoing fMRI scanning and EEG recording sessions. The order of these sessions were not well counterbalanced; for the group data reported in fMRI session analyses, that session was the first experimental session for eleven participants, whereas for the group data reported in ERP session analyses, that session was the first experimental session for five of the group members.

4.2.2. Tasks and stimuli

Practice and experimental session data were acquired in six blocks of trials, each lasting 5 minutes and 30 secs. Each participant's median correct go reaction time (GoRT) estimated from the practice session was used as a seed (anticipated) response time for fMRI and ERP sessions, i.e., the same seed time was used for first block of each session. Prior to practice and experimental sessions, participants were instructed that speed and accuracy of responding were of equal importance to inhibition. It was also explained that the paradigm was such that many stopping errors (i.e. Stop Failures) would be incurred, and that responding to go stimuli should not be slowed in order to facilitate inhibition success rate.

Blocks began with a 5 sec countdown to focus participant's attention to the task which was followed by a sequence of 220 trials, each commencing with the presentation of a primary task (or go task) stimulus, the letters O or X, with equal likelihood of presentation. Stop-signals (1000 Hz, 50 ms, 85 dB, square wave tones with 5 ms rise to peak time, and 5 ms fall time) were presented during 30% of these trials (66 trials in each block) in a pseudo random fashion that ensured stop-signals were never presented on subsequent trials, i.e, the first trial following a stop-signal trial was always a go trial. The primary task stimulus onset asynchrony (SOA) was varied randomly between 1.2 – 3 seconds ($\underline{M}$ = 1.5 seconds), sampled from an exponential distribution. Six stop-signal delays (SSDs) were used in stop-signal task trials, with equal probability of presentation within each block, and across blocks. To exploit individual differences in SSRT, the length of each SSD was always set relative to the GoRT seed: GoRT-255, GoRT-235, GoRT – 215, GoRT – 195, GoRT - 175, GoRT-155 (see Figure 4.01). A range of SSDs served a twofold purpose: firstly, the time given to inhibit responding is distributed about a typically observed estimate of group SSRT (approximately 200 ms; Logan, 1994) ensuring that all participants would successfully inhibit at least some of the time; and secondly, to introduce jitter that is necessary for utilization of the ADJAR correction procedure (Woldorff et al., 1993). It was anticipated that participants with faster SSRTs would inhibit responses over a large proportion of the SSD range, while stopping would only be possible for those with comparatively slow SSRTs at shorter SSDs (i.e. approaching GoRT – 255 ms).

Consistent inhibition performance across experimental blocks was facilitated by using GoRT estimated in practice as the initial seed value of GoRT, and the GoRT from the preceding experimental block as seeds for the subsequent blocks Therefore, if GoRT increased within a run relative to seeded GoRT for that run, then SSDs increased by that amount in the subsequent run. The practice of controlling for relative changes in GoRT between experimental blocks was included to account for the natural slowing of reaction time during lengthy experimental testing sessions, and to counter response-slowing strategies that can be problematic in stop-signal experiments (Logan, 1994). This was important because fixed stop-signal delays were used (albeit only within blocks); according to the predictions of the race model a change in relative GoRT would result in a

concomitant increase in PI, and hence a change in inhibition performance (Logan & Cowan, 1984; Logan, 1994).

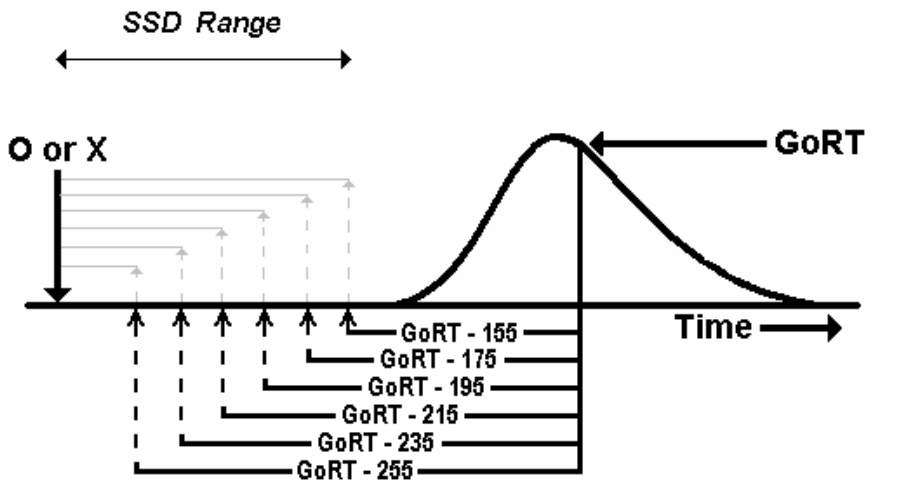

Figure 4.01. Stop-signal task trials. The initial setting of stop-signal delays (SSD Range) for experimental sessions was determined by setting stop-signals relative to a seeded median Go reaction time (GoRT), which was initially derived from the cumulative distribution of correct Go reaction times in a practice session.

Behavioural variables

The following variables were extracted from recorded behavioural data: median GoRT and the percentage of correct Go trials; median incorrect go reaction time (IncorrectGoRT) and the percentage of incorrect go trials (responding with the incorrect hand) and go trial misses (no response recorded on go trials); median Stop Failure RT (Stop Failure RT); the probability of inhibition (PI) and SSRT. On stop-signal trials, a Stop was coded if the following conditions were met: a response was recorded on the previous trial (always a correct go trial, see above) and no response was recorded on the current trial. This decision rule was adopted to ensure that participants were actively engaged in the stop-signal task and that an apparently successful inhibition trial was not actually a missed stop-signal trial. PI was calculated by dividing the number of Stops by the sum of all stop-

signal trials included (separately) in fMRI or ERP analyses[23] and corrected according to the procedures outlined by Tannock et al. (1995) to account for missed go trials. The calculation of SSRT was computed by first collapsing Stops into three appropriate SSD bins (trials with SSDs: 1. GoRT – 255 and GoRT – 235; 2. GoRT – 215 and GoRT – 195; 3. GoRT – 175 and GoRT – 155) and computing PI and a critical mean SSD (SSD_{crit}) for each bin[24]. By comparing the value of (1-PI) to the cumulative distribution of Go reaction times, a critical Go reaction time (Go_{crit}) was determined for each time bin, and a critical SSRT ($SSRT_{crit}$) estimated for each bin using the following formula:

$$SSRT_{crit} = Go_{crit} - SSD_{crit}$$

$SSRT_{avg}$ was then determined by computing the mean of all $SSRT_{crit}$ for each participant. Monte Carlo simulations have shown that this method of SSRT calculation is robust against violations of the race model (Band et al., 2003).

A further aim of the current experiment was to investigate the RT slowing prior to Stops that was reported by Vink and colleagues (2005). For this reason, the medians of the distributions of RTs preceding (pre-event RTs) and following (post-event RTs) Stops, Stop Failures, Go and IncorrectGo events were extracted. These RTs were constrained only in that the RT had to be from a Go response (i.e., correct go trial). The medians of the distributions of these RTs for the different events, and separately for pre and post event RTs were entered into a 4 x 2 ANOVA with factors Event Type and Time (see results for more detail). This analysis was not envisioned when the experiment was designed, but was inspired by the results of Vink, who in addition to the RT finding, also reported that preSMA and striatal activation predicted Go response slowing prior to Stops, and that striatal activation was greater in Stops when contrasted with Stop Failures. This latter result was very comparable to the findings of Aron and Poldrack (2006) who similarly reported

[23] In several instances, few or no Stops were recorded in the first an block in an experimental session (due to a change in relative GoRT from the practice session).To avoid SNR loss, these blocks were not included in images analyses or behavioural analyses of the fMRI experimental session, and were not included for behavioural analyses for the ERP experimental session.

[24] This was not performed at each SSD individually as it was occasionally the case that a participant did not have any Stops at the longest SSD.

greater striatal activation in Stops compared to Stop Failures, noting that Stop Failures are linked to faster RTs.

Stimulus presentation

All aspects of the tasks were controlled by Presentation® software (Version 0.70, www.neuro-bs.com). Visual (go task) stimuli (the letters O and X in white arial font) were presented within a small black square which was centred over a red horizontal rectangle. Instructions for the stop-signal task ('Stop on tone') were centred above the rectangle throughout all sessions. An 'O' and 'X' were always displayed to the left and right respectively of the instructions to indicate response mapping. A countdown period of 5 seconds was presented at the beginning of each experimental block, i.e., after the scanner had started. In this interval, the horizontal rectangle was green and the instruction centred over it was 'Countdown'. The appropriate numerals were displayed in the small black square as the countdown period progressed (i.e., 5, 4, 3, 2, 1).

For the fMRI session, visual stimuli (Os and Xs) were back projected onto a screen (positioned approximately 2 m from the scanner bore entrance) that the subject viewed with a mirror mounted on the head coil (maximum horizontal and vertical extent on screen: 80 x 30 cm; viewing distance: 350 cm; visual angle approximately 0.25° x 0.36°). Auditory stimuli were delivered binaurally through MRI compatible piezoelectric headphones. Participants' lay supine in the scanner bore, holding a response device in each hand. Responses and scanner TTL pulses were passed through a 'response box' (developed in-house) which was connected to a laptop computer which logged responses, the timing of stimuli, and slice acquisition (as TTL pulses).

For the EEG session, participants sat upright in a chair and viewed visual stimuli (Os and Xs) presented on a computer screen positioned approximately 1 metre away, subtending a visual angle of approximately 1°. The response system used and logging of events (stimuli and responses) were as per that used for the fMRI session. Auditory stimuli were presented binaurally through headphones (KOSS TD/65) worn by the participant.

4.2.3. fMRI session

Participants

Of the sixteen right-handed individuals participating in the study, the data from two of these were excluded due to image dropout artifacts, leaving a sample of fourteen participants for the fMRI session (aged 22 - 34, M = 27.4 years, SD = 3.8 years, 8 males and 6 females).

MR image acquisition

Magnetic resonance images were acquired using a Siemens Vision 1.5 T whole-body MR scanner equipped with a Siemens quadrature head coil. Prior to all experimental runs a magnetization prepared rapid acquisition gradient echo (MPRAGE) sequence (TR = 9.7 ms, TE = 4 ms, flip angle = 12°, 224 x 256 matrix, FoV = 250 mm, voxel size = 0.98 mm^3) was used to acquire a 164 slice, high-resolution T1-weighted anatomical image for later registration into a standardised stereotaxic space (MNI). During stimulus presentation, 92 whole brain EPI images (4 mm slice thickness, 32 slices, TR = 3.84, TE = 70 ms, flip angle = 90°, FoV = 256 mm, 64 x 64 matrix, voxel size = 4 mm^3) were acquired as interleaved slices (no gap) beginning at the top of the head and positioned according to the anterior-posterior commissural line, maximizing brain volume imaged.

MR image pre-processing

Image pre-processing and subsequent statistical analyses were performed using SPM2 (Wellcome Department of Neurology, London). The first 5 images from each imaging run were discarded[25] to allow for T1 saturation effects. Differences in EPI slice acquisition times were corrected using the central slice as a reference. Image time series were then realigned to the first EPI image and a mean realigned EPI image was created. Each participant's T1 image was co-registered to the mean image normalized to the T1 template provided with SPM2. The parameters from this transformation were then applied to all EPI images. Accuracy of registration between functional and structural data was assessed by visual inspection of the overlay of each individual subjects mean EPI and T1 image. Normalised EPIs were then smoothed with an 8 mm FWHM.

[25] This practice led to the loss of approximately 10 trials per run for each participant.

Modeling: First level analyses

FMRI time series were analysed by fitting a convolved canonical HRF and its temporal derivative to the onset of primary task stimuli (Os and Xs) for incorrect (inaccurate responses) Go trials, and likewise for the onset of tones for Stops (successfully inhibited stop-signal trials) and Stop Failures (where participants failed to inhibit go responses). Correct Go trials were not modelled explicitly, and thus constituted an implicit baseline (Baseline). Prior to model estimation, all images were globally scaled and time series were filtered to remove low frequency signals (<60 s). Missed go trials and missed stop-signal task trials (stop-signal task trials preceded a missed go trial) were not explicitly modelled and thus the variance in voxels attributable to these trials was permitted to contribute to the baseline of the general linear model. This approach was adopted as it was generally the case that such trials were infrequent and did not occur in all experimental blocks for all participants, and therefore estimation of parameters for these trial types, as individual regressors, was not possible.

Using standard notation, the voxel-wise GLM for this analysis was:

$$Y = \beta_0 + \beta_1 * X_1 + \beta_2 * X_2 + \beta_3 * X_3 + \xi$$

Where;

β_0 = parameter estimate for implicit baseline

β_1 = parameter estimate for incorrect Go

β_2 = parameter estimate for Stops

β_3 = parameter estimate for Stop Failures

ξ = error term

The following contrasts were performed: Stops > Baseline, Stop Failures > Baseline. Stops > Stop Failures and Stop Failures > Stops.

Group level analyses

Several random effects models were computed to investigate the stop-signal inhibition network at the group level. Initially, contrast images from each participant were submitted to one sample t-tests for the abovementioned contrasts.

To test which brain areas were progressively recruited across the group as stopping became more difficult, the contrast images from Stops > Baseline (β_2 - β_0) were submitted to a simple correlation model with SSRT as the explanatory variable. Regressing SSRT onto β_2 - β_0 images tested for a positive relationship between voxel-wise BOLD signal variance and SSRT to investigate whether SSRT predicted between participant variability in right IFG-STN. The negative correlation between SSRT and β_2 - β_0 images was also explored to investigate which brain areas participants with faster SSRTs engaged more during stopping.

Determining functional neuroanatomy

Anatomical loci were determined by converting cluster maxima to Talairach space and entering these co-ordinates into the Talairach Daemon. This output was cross-checked using the atlas of Talairach and Tournox (1988).

Region of interest (ROI) analyses

Similar to the procedure followed by Aron and Poldrack (2006), AAL probability maps (Tzourino-Mazoyer et al., 2002) were used to define areas that are part of the cortico-basal ganglia-thalamocortical circuitry involved in stopping. However, right IFG was decomposed into subgyral areas, including *pars triangularis*, *pars opercularis* and *pars orbitalis.* Also included were right MFG, right preSMA (clipped at y = 0), right pallidum (*pars interna* and *pars externa*), right putamen and right thalamus. Marsbar – 0.38 ROI toolbox for SPM (Brett et al., 2002a) was used to construct a 10 x 10 x 10 mm box centred at (10 –15 –5, MNI), which is thought to encompass right STN (Aron & Poldrack, 2006). This protocol enabled a thorough examination of the areas linked to stop-signal inhibition. Group t-maps were threshold at $p < .01$ (uncorrected) and small volume corrections (SVC; Worsley et al., 1996) were applied over individual ROIs. To further explore the data, Marsbar (Brett et al., 2002a) was used to extract the mean parameter estimates within these

ROIs estimated for Stops (β_2) which were subsequently correlated with SSRT. However, because MFG (40832 mm^3) is a large structure compared to the sub-gyral formations of IFG (AAL volumes: pars opercularis = 11192 mm^3; pars triangularis = 17208 mm^3; pars orbitalis = 13656 mm^3), and only mid-dorsolateral portions are observed in studies of response inhibition, mean parameter estimates for intact IFG (42056 mm^3) were also extracted. This was performed in order to establish the true relevance of IFG and MFG in stopping.

4.2.4. ERP session

Participants

Of the sixteen individuals who participated in the experiment, one did not return for the EEG recording session, and the data set from another participant had to be excluded due to technical difficulties encountered during recording which cut short the recording session, leaving a sample of fourteen participants (aged 22 - 34, M = 27.9 years, SD = 3.5 years, 7 males and 7 females). While largely overlapping (N = 12), this sample was different to that which comprised the final group fMRI data.

EEG data recording

The EEG was recorded using a Quik-Cap from 62 scalp electrodes positioned according to the 10/20 system (O2, O1, OZ, PZ, P4, CP4, P8, C4, TP8, T8, P7, P3, CP3, CPZ, CZ, FC4, FT8, TP7, C3, FCZ, FZ, F4, F8, T7, FT7, FC3, F3, FP2, F7, FP1, M1, PO3, P1, POZ, P2, PO4, CP2, P6, M2, CP6, C6, PO8, PO7, P5, CP5, CP1, C1, C2, FC2, FC6, C5, FC1, F2, F6, FC5, F1, AF4, AF8, F5, AF7, AF3, FPZ) and referenced to a nose electrode. Vertical and horizontal electro-oculograms (EOG) were recorded via electrodes positioned above and below the left eye, and on the outer canthi of each eye, respectively. EEG and EOG were continuously sampled at 500Hz/channel using a Synamps system (Neuroscan) with a band-pass of 0.01-30Hz using a 50Hz notch filter and gain of $2x10^4$.

ERP data preprocessing

Preprocessing of EEG data was performed using Scan 4.3. Continuous EEG files were visually inspected and sections of EEG contaminated with channel saturation or noise were excluded. Vertical eyeblink artifacts were corrected in the continuous EEG files using the algorithm developed by Semslitch, Anderer, Schuster and Presslich (1986) as implemented in Neuroscan software.

ERP trial averaging

ERP averages were created for Stops and Stop Failures by locking events to the onset of stop-signals (tones) for these trials, and go event averages were created by locking events to the onset of correct go trials only. All averages were created by extracting 1000 ms epochs around the onset of crucial stimuli (-200 ms to 800 ms), for left and right hand events separately, which were subsequently baseline corrected over the pre-stimulus interval (-200 – 0 ms). ADJAR-level 1 correction procedures (Worldorff, 1993) were applied to baseline corrected stop-signal averages (see below for outline of procedure).

ADJAR correction procedure for stop-signal task group average waveforms

The ADJAR procedure aims to account for the overlap by modelling it, then removing it by subtraction, permitting straight forward data interpretation. In more detail, jittered stop-signal delays over evenly spaced steps (in the current experiment these were 50 ms) are exploited by modelling the effect of primary task ERPs on stop-signals ERPs. Firstly, we obtained separate estimates of the left and right Go ERPs. We then determined four separate distributions of stop-signal events following left and right Go trials resulting in successful Stops and Stop Failures. Overlap from primary task left and right Go ERPs on stop-signal ERPs was then modelled by convolving (left-shifted) the Go ERP relative to stop-signal ERP in a manner corresponding to the stop-signal delay distribution for respective events separately for left and right Stops and Stop Failures. Convolved waveforms were then averaged to create an average convolution waveform that was subtracted from the relevant stop-signal ERP, creating a corrected stop-signal ERP.

Consequent corrected waveforms were baseline corrected over the pre-stimulus interval (-200 - 0ms) using Scan software. Averages were thus created from these ADJAR and baseline corrected waveforms separately for Stops and Stop Failures.

Measurement of components from Stop and Stop Failure ERP waveforms

In house software was used to extract maximum and minimum ERP component latencies and amplitudes for N1 and P3 within a time-window specified by the user, in addition to mean amplitudes across a specified window (see Table 4.01). Because a N2 peak was difficult to discern in some individual waveforms, N2 amplitude was measured as a mean amplitude. Appropriate windows were determined by visual inspection of the grand average waveforms for Stops and Stop Failures. In order to examine scalp topography differences in stop P3 and N2 were measured at selected lateral and midline sites over frontal, central and parietal areas while N1 was measured at lateral and midline frontal and central sites only as auditory N1 is often difficult to distinguish at parietal sites.

Table 4.01

Latency ranges over which component measures were extracted for statistical analysis

Component measure	Latency range of extraction (ms)
N1 peak amplitude	50 - 150
N1 peak latency	50 - 150
N2 mean amplitude	180 - 320
P3 peak amplitude	170 - 600
P3 peak latency	170 - 600
P3 mean amplitude	170 - 400

Stop-signal P3 amplitude and latency data at F3, Fz, F4, C3, Cz, C4, P3, Pz and P4 were entered into multi-factorial ANOVAs examining effects of Inhibition (levels Stop and Stop Failure), Hand (levels left and right), Laterality (levels ipsilateral, midline, and contralateral to response hand) and Anterior-Posterior extent (AP; frontal, central and parietal sites) on stop-signal potential measures shown in Table 4.01. These factors were

also used for an analysis of mean Stop-signal N2 amplitudes. Stop-signal N1 analyses were identical, excepting only that AP included levels frontal and central sites only as auditory N1 is often small at parietal sites. All statistical effects reported for these analyses are those surviving Greenhouse-Geisser correction (corrected degrees of freedom are reported for all F-values where appropriate). Relationships between SSRT and peak component measures (latency and amplitude) were assessed using correlational (simple) regression models.

4.2.5 Correlation of Stop>Go contrasts with Stop related components

Peak amplitude and latency ERP measures found to be related to SSRT were correlated with Stop>Go contrast maps for the group of participants who completed both sessions (N=12). Significant areas of correlation were determined by application of *a priori* ROIs to resultant t-maps. Only those areas significant at both the voxel-level and cluster-level were considered significant.

4.3. Results

4.3.1. fMRI session

4.3.1.1 Behavioural data

A summary of behavioural indices derived from fMRI sessions are presented in Table 4.02; all statistical tests were two-tailed unless otherwise stated.

Reaction time (RT) data

Median GoRT, IncorrectGoRT, and StopFailure RT were entered into a one-way repeated measures ANOVA with three levels of Event Type, which was significant, $F(1.193,15.509) = 13.116$, $p = .002$. Bonferroni comparisons (significance criterion was $p = .0167$ for each contrast) confirmed that GoRT was significantly slower than Stop Failure RT, $t(14) = 10.17$, $p < .001$, and IncorrectGoRT, $t(14) = 3.84$, $p = .002$, whereas Stop Failure RT and IncorrectGoRT did not differ, $t(14) = -.24$, *ns*.

Table 4.02

Mean group data for behavioural indices (with standard deviations in parentheses) from fMRI sessions

Index*	Measure
Go trials	
Mean GoRT (ms)	404 (38)
Mean IncorrectGoRT (ms)	368 (57)
Mean percent correct go trials	90 (5)
Mean percent incorrect go trials	5 (4)
Mean percent go trial misses	5 (5)
Mean percent go trial errors	10 (5)
Stop-signal trials	
Mean Stop Failure RT (ms)	370 (34)
Mean SSRT (ms)	191 (41)
SSRT range (ms)	136 – 275
Mean PI (proportion)	.59 (.20)
PI range (proportion)	.17 - .85
Mean Stop SSD (ms)	196 (41)
Stop SSD range (ms)	152 – 275
Mean Stop Failure SSD (ms)	215 (45)

*GoRT = median correct go trial reaction time; IncorrectGoRT = median incorrect go trial reaction time; SSRT = stop-signal reaction time; PI = probability of inhibition; SSD = stop-signal delay.

Pre- and Post- event RT differences

Median RTs for trials preceding and following Go, IncorrectGo, Stop, and Stop Failure events (pre and post event RTs) were extracted (see Table 4.03 for group data). Pre and post trial RTs were entered into a 4 x 2 ANOVA comprising factors Event Type (Go/Incorrect Go/Stop Failures/Stops) and Time (Pre/Post). Event Type approached significance, $F(2.113,27.467) = 3.059$, $p = .061$, due to RTs before and after Stops being marginally longer than RTs surrounding other events (refer to Table 4.02). Although the interaction was not significant, pre and post trial RTs were entered into separate one-way

ANOVAs, revealing a significant effect for pre-event RTs, $F(1.526,19.839) = 5.554$, $p = .018$, but not for post-event RTs, $F(1.491,19.384) = 0.072$, *ns*. Bonferroni planned comparisons of pre-Stop and pre-StopFailure RTs, and of pre-Go and pre-IncorrectGo RTs were assessed using repeated measures t-tests to investigate how recent trial history affected the outcome of go and stop-signal trials ($p < .025$ to account for multiple comparisons). Only the difference between pre-Stop RT and pre-Stop Failure RT was significant, $t(13) = 3.457$, $p = .004$, indicating that stopping was mediated by slower responses on the preceding trial.

Table 4.03

Group means of participant median pre and post event RTs in ms collapsed over left and right hands (with standard deviations in parenthesis).

Event	Pre-	Post-
Go	394 (36)	398 (41)
Incorrect Go	390 (40)	397 (41)
Stop Failures	397 (40)	397 (38)
Stops	407 (40)	400 (35)

Stop-signal trial data

For stop-signal trial data, a repeated measures t-test showed that stop-signal delays for Stops were significantly shorter than for Stop Failures, $t(14) = 7.526$, $p < .001$ (see Table 4.01), as predicted by the race model. Substantial individual differences were observed in participant SSRTs, which varied over a range of 139 ms, but mean SSRT (191 ms) was within the range described by previous reports (Logan, 1994). Additionally, SSRT and PI were highly correlated (see Figure 4.02), $r(14) = -.953$, $p < .001$, hence SSRT predicted the difficulty of control in this stop-signal paradigm variant[26].

[26] The wide dispersion of participant SSRT was important for testing the hypothesis that more difficult inhibition is related to greater activation in the right IFG-STN network; if different neural networks are recruited to effect inhibition depending upon the urgency of control, then relating these behavioural data, which comprise high and low rates of inhibition across participants, to image data, should reveal progressive recruitment of brain areas required when inhibition becomes more difficult.

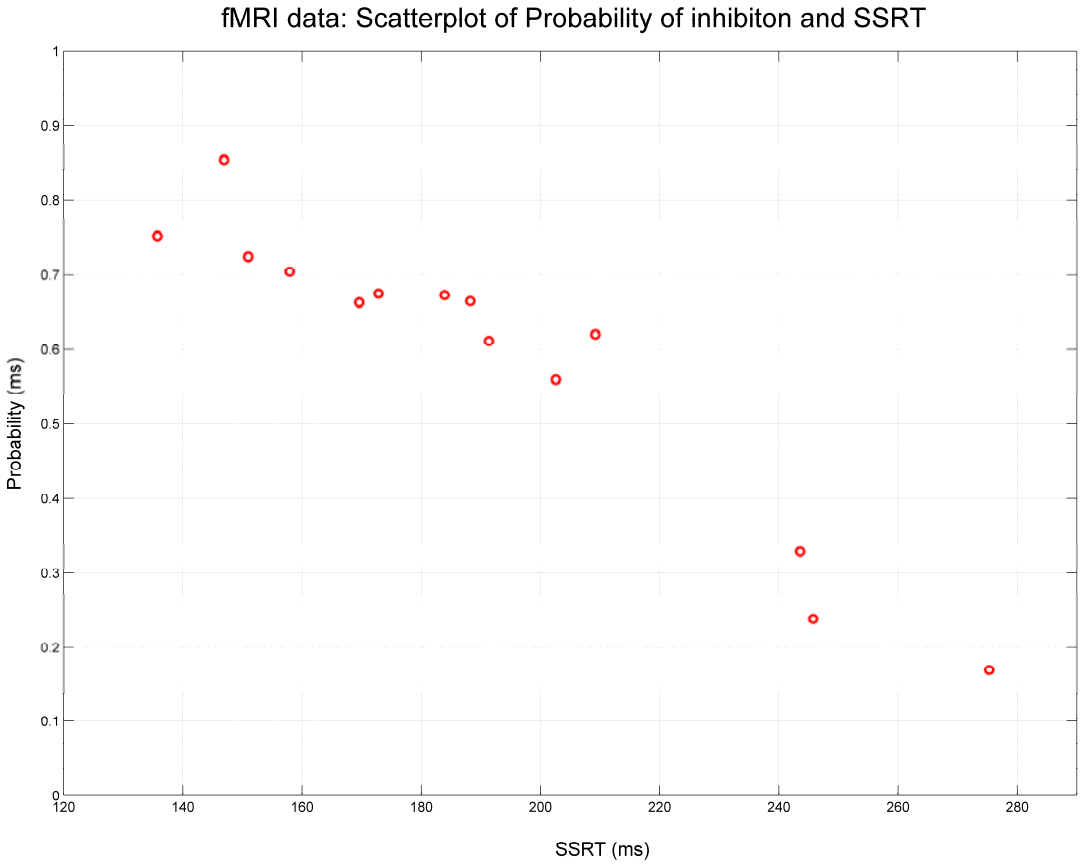

Figure 4.02. Regression of PI and SSRT. Participants who found the task easier tend towards the top left corner of the plot, while participants who found the task harder are clustered toward the bottom right.

4.3.1.2. fMRI data[27]

Stops > Baseline

Group brain activation in the random effects comparison of Stops > Baseline revealed a right lateralised activation pattern (for whole brain activation see Table 4.04 and Figure 4.03) that included right IFG (*pars triangularis*), MFG, TTG, and IPL, left SMA and bilateral STG; temporal lobe activations (STG and TTG) are involved in the sensory aspects of processing the stop-signal, and will not be considered further. At a more liberal

[27] For most of the following tables summarising brain activation, some cells in the 'No. Voxels' (number of voxels) column are empty. This is because the peak of activation is contiguous with a cluster containing a higher peak voxel t-score, as is the case with SPM2 output.

threshold ($p < .01$, 10 contiguous voxels), additional clusters were revealed within the left mid-cingulate, left MFG (middle and caudal portions) left IPL, right SMA and right dorsal thalamus, bilateral cerebellar cortex and right PONS.

Table 4.04

Activation table for Stops > Baseline (thresholding was $p < .001$, 10 contiguous voxels)

Brain Area*	BA	No. Voxels	t - score	MNI Co-ords
Right hemisphere				
STG	22	161	8.25	64 -44 12
STG	22		7.28	56 -8 0
TTG	41		5.43	52 -28 8
IFG/MFG	46	43	7.48	40 36 16
MFG	9		5.87	44 32 32
MFG	6	13	5.53	36 0 60
IPL	40	16	4.84	36 -48 44
Left hemisphere				
STG	42	259	7.68	-60 -32 12
STG	41		6.24	-48 -32 12
STG	22		5.94	-56 -48 12
SMA	6	16	5.56	-8 -8 68

*Superior temporal gyrus (STG); transverse temporal gyrus (TTG); inferior frontal gyrus (IFG); middle frontal gyrus (MFG); inferior parietal lobule (IPL); posterior supplementary motor area (SMA proper).

Simple correlation: SSRT and Stops > Baseline

The primary motivation for this study was to test the hypothesis that a right IFG-STN network, which is thought to mediate stopping (Aron & Poldrack, 2006; Aron et al., 2007a), would be positively related to SSRT (that is, longer SSRT associated with increased activation). When the relationship between SSRT and Stop > Baseline contrast maps (positive tail) was examined, at the standard thresholding ($p < .001$, 10 contiguous voxels), activation was observed within left precuneus and right cerebellum (culmen) only, so a more liberal thresholding criteria ($p < .01$, 10 contiguous voxels) was utilised. At this height, many areas were significantly positively related to SSRT (see Figure 4.04, Table

4.05), including bilateral precueus, cuneus, posterior cingulate, cerebellum, IFG (*pars opercularis*), MFG, ACC, postcentral gyrus, and thalami/STN. Additional right lateralised activation was observed in the fusiform gyrus, supramarginal gyrus, and STN/SN. Left lateralised activation included SMA, lingual gyrus, PCG, parahippocampal gyrus, insula and claustrum. It should be noted that IFG activation in this correlation map is posterior (in *pars opercularis*) to that observed in the Stops > Baseline contrast (in *triangularis*).

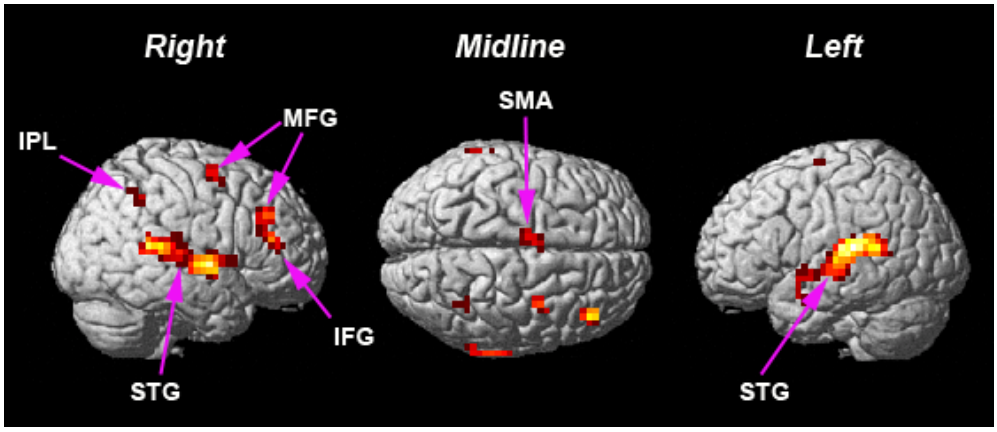

Figure 4.03. Cortical activation for Stops > Baseline contrast (thresholding at p < .001, 10 contiguous voxels) with views of right hemisphere (left), superior midline (centre) and left hemisphere (right) activation.

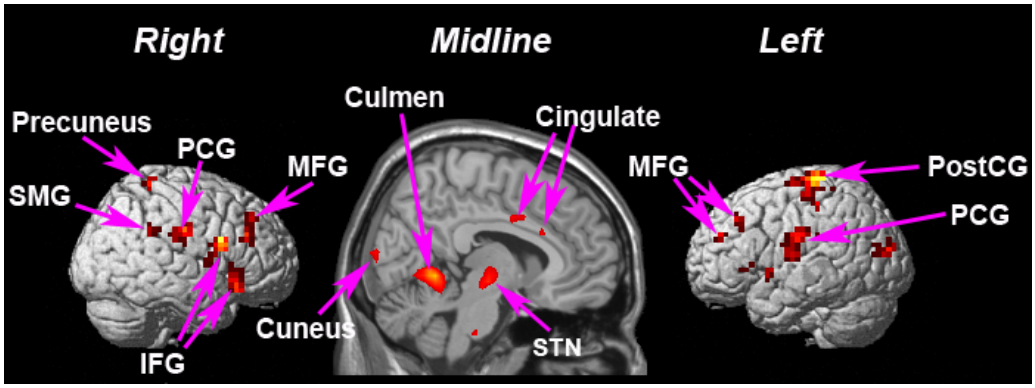

Figure 4.04. Brain areas in Stops > Baseline contrast maps showing significant positive correlations with SSRT (thresholding at p < .01, and 10 contiguous voxels).

Table 4.05

Brain areas revealing positive SSRT correlated BOLD variance in Stops > Baseline contrasts (thresholding was $p < .01$, 10 contiguous voxels)

Brain Area*	BA	No. Voxels	t - score	MNI Co-ords
Right hemisphere				
Precuneus	7	28	6.75	16 -60 44
Cingulate gyrus (posterior)	31		3.08	20 -48 28
Cingulate gyrus (posterior)	31		2.81	24 -48 36
Cerebellar culmen	-	64	6.55	12 -52 -4
IFG	46	180	5.97	36 32 20
IFG	44		4.70	52 12 20
MFG	9		4.54	32 36 40
ACC	24	10	4.24	12 20 24
PostCG	3	15	4.15	16 -40 68
Fusiform gyrus	37	16	4.05	40 -48 -12
Cuneus	18	33	4.04	4 -92 12
Cuneus	18		2.87	0 -80 4
SMG	40	12	3.93	48 -44 32
Thalamus (ln)	-	33	3.92	16 -8 4
STN/SN	-		3.86	8 -16 -8
Left hemisphere				
PostCG	3	134	8.81	-20 -36 72
SFG/SMA	6		4.07	-16 -16 68
Cingulate gyrus (posterior)	31		3.47	-16 -36 44
Lingual gyrus	19	12	5.50	-28 -60 -4
Cuneus	19	36	5.10	-24 -84 16
PCG	6	40	4.69	48 -12 32
Thalamus/STN	-	86	4.36	-8 -8 0
ACC	25		4.29	-4 0 -4
Parahippocampal gyrus	30		3.92	-16 -40 4
PCG	4	68	4.25	-52 -16 24
PCG	13		4.13	-48 -12 12
PostCG	2		3.86	-36 -32 32
MFG	9		3.37	-40 32 40
Insula	13	19	4.04	-40 4 -4
Cuneus	18		3.82	-8 -96 4
ACC	32	53	4.00	-12 24 28
ACC	24		3.97	-12 8 32
SFG	9	17	3.69	-12 48 24
MFG	10		3.47	-28 44 28
Claustrum	-	13	3.35	36 4 -8

Brain Area*	BA	No. Voxels	t - score	MNI Co-ords
IFG	47	15	3.26	-32 28 0
Cerebellar culmen	-	15	3.21	-24 -48 -28
Cerebellar declive	-		3.17	-20 -60 -20
Precuneus	7	11	3.20	-12 -56 48
Lingual gyrus	18	10	3.07	-16 -84 -8
Lingual gyrus	18		2.92	-8 -88 -8

*Inferior frontal gyrus (IFG); middle frontal gyrus (IFG); anterior cingulate cortex (ACC); precentral gyrus (PCG); supramarginal gyrus (SMG) post-central gyrus (postCG); superior frontal gyrus (SFG); posterior supplementary motor area (SMA); subthalamic nucleus (STN).

The t-map of significant negative correlations (observed by examining the negative tail of the relationship between SSRT and Baseline > Stops contrast) revealed an interesting activation pattern (see Table 4.06, Figure 4.05) that included bilateral ACC, frontal eye fields (FEF), STG, and cerebellar activations, in addition to right lateralised lingual gyrus, MFG/PCG, SPL, and IPL, and left lateralised MTG and SFG. In contrast to Aron and Poldrack (2006), decreasing SSRT did not predict increased BOLD signal in either right IFG or STN.

Table 4.06

Brain areas revealing negative SSRT correlated BOLD variance in Stops > Baseline contrasts (thresholding was $p < .01$, 10 contiguous voxels)

Brain Area*	BA	No. Voxels	t - score	MNI Co-ords
Right hemisphere				
ACC	32	27	4.42	8 44 4
FEF	8	39	4.27	0 36 60
Lingual gyrus	18		4.07	8 -88 -20
MFG/PCG	6	35	3.89	28 8 56
MFG	6		3.84	36 12 52
SPL	7	31	3.60	40 -60 56
IPL	40		2.94	48 -64 44
STG	22	14	3.13	64 -24 4

Brain Area*	BA	No. Voxels	t - score	MNI Co-ords
Left hemisphere				
MTG	21	33	5.35	-56 0 -32
ACC	32		3.79	-12 44 8
SFG	6		3.22	-12 24 64
MedialFG/FEF	8		2.95	-4 52 48
STG	22	20	3.96	-60 -4 0
STG	22		3.82	-64 -12 0
Cerebellar tuber	-	10	3.78	-48 -64 -32
Cerebellar tonsil	-		3.75	-48 -60 -40

*Anterior cingulate cortex (ACC); frontal eye fields (FEF); middle frontal gyrus (MFG); precentral gyrus (PCG); superior parietal lobule (SPL); inferior parietal lobule (IPL); superior temporal gyrus (STG); middle temporal gyrus (MTG); superior frontal gyrus (SFG); medial frontal gyrus (medialFG).

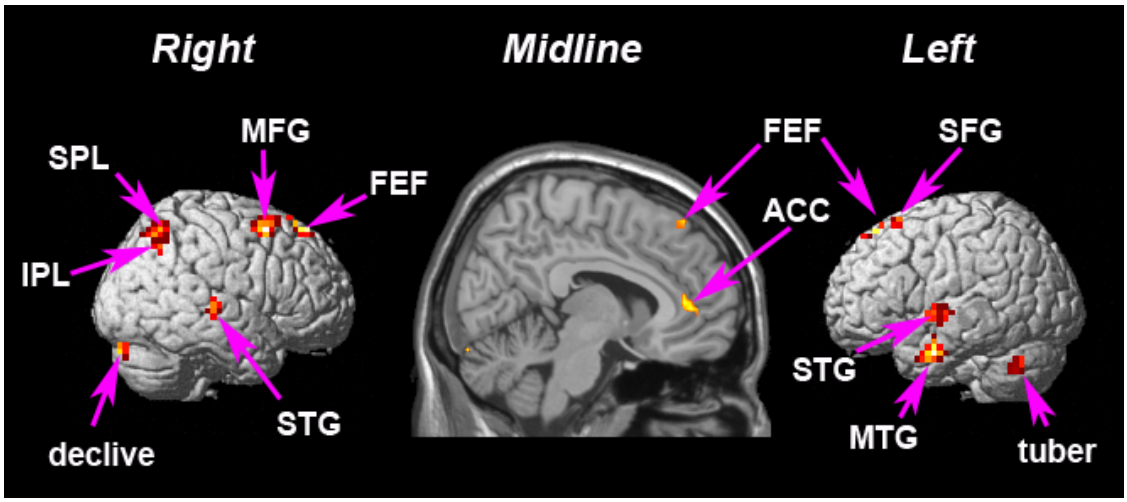

Figure 4.05. Negative correlation between Stops > Baseline contrast maps and SSRT (thresholding at p < .01, and 10 contiguous voxels), showing right hemisphere (on left), mid-line sagittal (middle), and left hemisphere (on right) views.

Stop Failures > Baseline

The contrast of Stop Failures > Baseline also revealed a right lateralised activation pattern (for whole brain activation see Table 4.07, Figure 4.06) that included cluster peaks within right hemisphere IFG, MFG (middle and caudal), in addition to preSMA and SMA-

proper. Left lateralised activation was observed in the anterior insula, transverse temporal gyrus (TTG) and rostral MFG, while STG were bilaterally activated. At a more liberal threshold ($p < .01$, 10 contiguous voxels), additional activation was observed within bilateral ACC, IPL and cerebellar cortex.

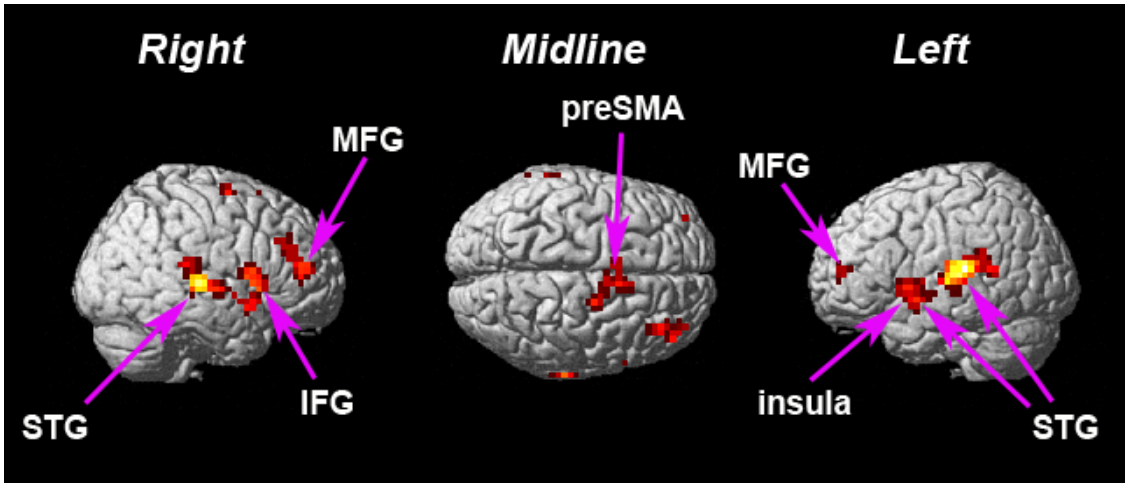

Figure 4.06. Cortical activation for Stop Failures > Baseline contrast (thresholding was $p < .001$, 10 contiguous voxels) with views of the right hemisphere (left), superior midline (centre) and left hemisphere (right) activation.

Table 4.07

Activation table for Stop Failures > Baseline (thresholding was $p < .001$, and 10 contiguous voxels)

Brain Area*	BA	No. Voxels	t - score	MNI Co-ords
Right hemisphere				
STG	41	167	6.84	52 -24 4
IFG	44		6.18	56 12 12
STG	22		6.02	68 -24 4
MFG	10	49	5.90	40 44 16
MFG	10		4.89	36 36 28
preSMA	6	60	5.43	4 0 64
MFG	6		5.31	20 -8 64
preSMA	6		5.21	8 8 60

Brain Area*	BA	No. Voxels	t - score	MNI Co-ords
Left hemisphere				
STG	42	167	8.15	-60 -32 12
TTG	41		7.16	-48 -28 12
STG	13		4.90	-52 -44 20
MFG	10	10	7.14	-32 52 8
STG	22	47	6.29	-48 4 -8
Insula	13		5.63	-44 8 0

*Superior temporal gyrus (STG); inferior frontal gyrus (IFG); middle frontal gyrus (MFG); anterior supplementary motor area (preSMA); transverse temporal gyrus (TTG).

To confirm that right IFG-STN was positively related to SSRT only for Stops, correlation t-maps were also computed for the correlation of SSRT and Stop Failures > Baseline. In this analysis, no significant voxels or clusters were revealed in the right IFG-STN network in either of the positive or negative correlation maps at the standard thresholding or at the lower thresholding (no table or figure provided). However, it should be noted that the negative correlation predicted activation within right ACC (MNI co-ords: 8 40 12), and the positive correlation predicted activation in the left posterior cingulate (MNI co-ords: -12 -36 40) at the standard thresholding.

Small volume correction (SVC) with a priori ROIs

Application of SVCs to *a priori* ROIs (see Table 4.08) further demonstrated the sensitivity of specific PFC and basal ganglia structures to SSRT in this instantiation of the stop-signal paradigm. Of most interest were differences in the pattern of BOLD signal effects between the Stops > Baseline contrast and the regression of SSRT onto the same Stops > Baseline contrast maps. The Stops > Baseline contrast revealed consistent effects (i.e. significant at both the voxel and cluster levels) within mid-dorsolateral MFG and *pars triangularis* of IFG, while a posterior region of MFG contained a significant voxel level effect. In contrast, the regression map showed that SSRT explained between-subject variance in the Stops > Baseline contrast maps within similar potions of mid-dorsolateral MFG and *pars triangularis*, but only at the voxel level. However, for this effect map, consistent effects were observed within *pars opercularis* of IFG and STN, while *pars*

orbitalis was significant at the cluster level only. No effects were observed for preSMA in either effect maps. Hence the major differences between these effect maps were that consistent effects were observed within mid-dorsolateral portions of MFG and IFG (*pars triangularis*) for Stops > Baseline, whereas for the effect map describing the regression of SSRT onto Stops > Baseline contrast maps, consistent effects were observed in a posterior portion of IFG (*pars opercularis*) and STN.

For the Stop Failures > Baseline contrast, consistent effects were observed in *pars opercularis, pars triangularis* (but marginally at the voxel level), MFG and preSMA, but not STN.

Table 4.08

Small volume correction (SVC) output for right hemisphere *a priori* regions of interest (ROIs)

ROI	t-score	FWE	MNI coords
Stops > Baseline			
Pars opercularis	-	-	-
Pars triangularis	5.88†	.006	40 36 12
	5.41	.013	44 32 28
Pars Orbitalis	-	-	-
MFG	7.48†	.001	40 36 16
	5.87	.016	44 32 32
	5.53	.029	36 0 60
preSMA	-	-	-
Putamen	-	-	-
Pallidum	-	-	-
Thalamus	-	-	-
STN	-	-	-
SSRT correlation (+ve) with Stops > Baseline			
Pars opercularis	4.70†	.039	52 12 20
Pars triangularis	5.27	.021	36 32 24
Pars Orbitalis	3.41†	-	-
MFG	5.97	.019	36 32 20
preSMA	-	-	-
Putamen	-	-	-
Pallidum	-	-	-
Thalamus	-	-	-
STN	3.86†	.020	8 -16 -8

ROI	t-score	FWE	MNI coords
Stop Failures > Baseline			
Pars opercularis	6.18†	.002	56 12 12
	5.48	.008	56 16 4
Pars triangularis	4.63†	.052	56 20 4
	4.63	.052	36 32 28
Pars Orbitalis	-	-	-
MFG	5.90†	.015	40 44 16
preSMA	5.43†	.008	4 0 64
	5.21	.011	8 8 60
Putamen	-	-	-
Pallidum	-	-	-
Thalamus	-	-	-
STN	-	-	-

† indicates corrected cluster.
Middle frontal gyrus (MFG); anterior supplementary motor area (preSMA); subthalamic nucleus (STN).

Stops > Stop Failures

No significant activations were detected at the standard thresholding, so more liberal thresholding criteria ($p < .01$, 10 contiguous voxels) were used. Most noticeable in this contrast (see Table 4.09, Figure 4.07) was substantial striatal (putamen) activation, which was bilateral but more substantial in the left hemisphere. Other peaks were revealed in left superior parietal lobule (SPL), IFG, lingual and hippocampal gyri. Right hemisphere activations were observed within the precuneus, paracentral lobule, globus pallidus (GP) and cerebellum, while bilateral effects were observed within middle occipital gyrus (MOG).

Table 4.09

Activation table for Stops > Stop Failures (thresholding was $p < .01$, and 10 contiguous voxels)

Brain Area*	BA	No. Voxels	t - score	MNI Co-ords
Right hemisphere				
SPL	7	22	4.46	24 -64 44
MOG	19	23	4.17	36 -84 0
MOG	19		3.79	32 -88 12
Putamen	-	23	3.92	20 12 8
Putamen	-		3.24	24 8 -4
Lingual gyrus	18	13	3.71	12 -56 0
Parahippocampal gyrus	30		2.83	20 -48 4
Left hemisphere				
IFG	45	14	4.85	-44 12 20
PCG	6		2.89	-40 0 28
Precuneus	7	24	4.85	-4 -48 52
Paracentral lobule	5		4.74	-12 -36 48
Precuneus	7	20	3.93	-28 -56 48
Precuneus	7		2.96	-16 -60 52
Putamen	-	77	3.87	-20 8 -8
Putamen	-		3.84	-20 20 0
GP (ln)	-		3.51	-16 0 0
Cerebellar culmen	-	14	3.64	-24 -36 -20
MOG	18	10	3.29	-32 -96 -4
MOG	19		3.27	-32 -88 8

*Superior parietal lobule (SPL); middle occipital gyrus (MOG); inferior frontal gyrus (IFG); precentral gyrus (PCG); globus pallidus (GP).

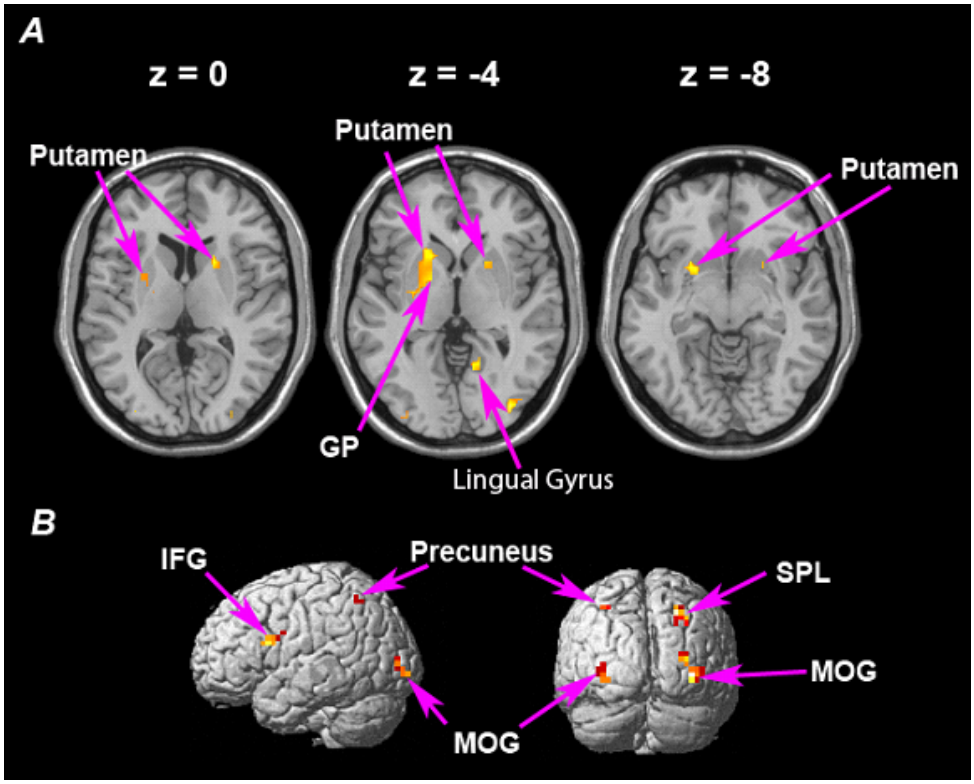

Figure 4.07. Brain regions showing significant activation in the contrast of Stops > Stop Failures (thresholding was $p < .01$, and 10 contiguous voxels). (A) Top panel: Subcortical and medial cortical activation shown on slices equally spaced from z = 0 to z = -8 (MNI coordinates). (B) Bottom panel: Frontal, parietal and occipital cortical activation shown on a rendered brain.

Stop Failures > Stops

No significant activations were detected at the standard thresholding in this contrast either, so the liberal criteria ($p < .01$, 10 contiguous voxels) were again used. At this thresholding, significant activation was revealed in right SFG, posterior cingulate, middle temporal gyrus (MTG) and ACC peaks, in addition to left post central gyrus and cerebellar cortex (see Table 4.10).

Table 4.10

Activation table for Stop Failures > Stops (thresholding was $p < .01$, and 10 contiguous voxels)

Brain Area*	BA	No. Voxels	t - score	MNI Co-ords
Right hemisphere				
SFG	9	26	3.77	12 52 24
Cingulate gyrus (posterior)	31	16	3.52	20 -44 20
Cingulate gyrus (posterior)	23		2.88	8 -36 20
MTG	21	18	3.51	52 4 -16
ACC	32	16	3.50	20 36 8
Left hemisphere				
Cerebellar tonsil	-	19	3.60	-16 -32 -52
PostCG	40	19	3.33	-52 -24 20
PostCG	40		3.08	-60 -20 16

*Superior frontal gyrus (SFG); middle temporal gyrus (MTG); anterior cingulate gyrus (ACC); post-central gyrus (postCG).

ROI analyses: Analysis of parameter estimates

To further investigate the relationship between SSRT and brain activation, mean parameter estimates for Stops for AAL probability maps used for SVCs were extracted using the marsbar ROI toolbox for SPM2 (Brett, et al., 2002a). These mean estimates from individual participants were correlated with SSRT and SSD. Of most interest was the relationship between SSRT and the brain areas that are thought to be involved in stop-signal response inhibition, particularly right lateralised pars opercularis, STN, preSMA, putamen, GP and thalamus (Aron & Poldrack, 2006; Aron et al., 2007a; Vink et al., 2005). However, given that MFG has also been linked to stopping (Aron et al., 2003) and no-go inhibition (De Zubicaray et al., 2000; Kawashima et al., 1996; Rubia et al., 2001; Watanabe et al., 2002), the AAL map defining this region and that defining the whole of IFG were included.

SSD was not significantly correlated with any ROI data.

Table 4.11

Means and standard deviations of parameter estimates extracted in right hemisphere brain regions defined by AAL probability maps and their Pearson's correlation (r) with SSRT (one-tailed)

Brain Area*	Mean parameter estimate (SD)	r (significance)
IFG	.181 (.319)	.581 (.015)
pars Opercularis	.198 (.393)	.638 (.007)
pars Orbitalis	.163 (.340)	.552 (.020)
pars Triangularis	.183 (.337)	.407 (.074)
MFG	.202 (.223)	.076 (.398)
preSMA	.219 (.332)	-.006 (.491)
GP	.116 (.362)	.355 (.106)
putamen	.195 (.390)	.469 (.045)
STN	.103 (.535)	.697 (.003)
thalamus	.039 (.289)	.349 (.111)

* inferior frontal gyrus (IFG); middle frontal gyrus (MFG); anterior supplementary area (preSMA); globus pallidus (GP); subthalamic nucleus (STN).

Interestingly, mean parameter estimates for MFG and preSMA as defined by AAL probability maps produced the largest mean responses for Stops across participants, but were uncorrelated with SSRT, whereas IFG with a moderately large parameter estimate revealed a strong relationship with SSRT (see Figure 4.09 for scatterplots). The strongest relationships with SSRT were found with *pars opercularis* and STN; it should be noted that these brain regions were the only estimates that were significant when non-parametric (Spearman's) correlation statistics were considered (*pars opercularis*: $\rho = .565$, $p = .018$; STN: $\rho = .464$, $p = .047$), while IFG was almost significant ($\rho = .455$, $p = .051$). Hence, *pars opercularis* was, overall, the best predictor of SSRT. ROI data was also correlated with SSD, but only thalamic activation revealed a non-significant relationship ($\rho = .429$. $p = .063$).

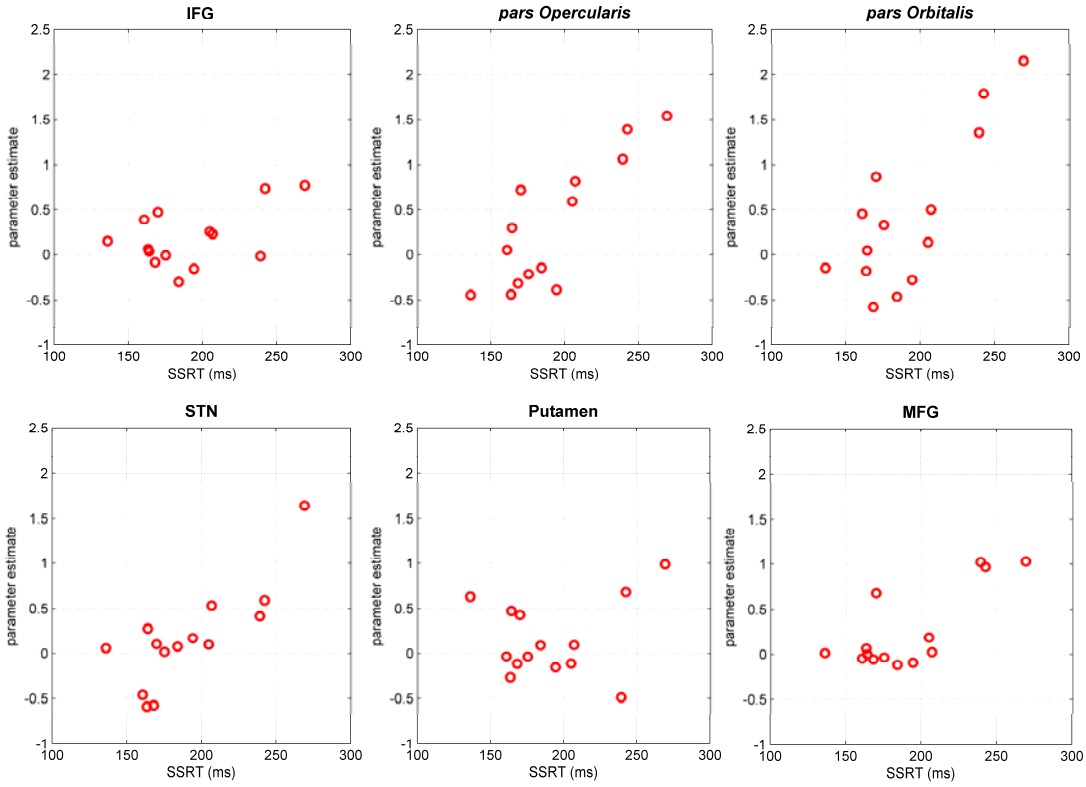

Figure 4.08. Scatterplots of mean parameter estimates against SSRT for ROIs that were significantly correlated with SSRT, in addition to the correlation of MFG parameter estimates and SSRT (correlation results presented in Table 4.11 above). Inferior frontal gyrus (IFG); subthalamic nucleus (STN); middle frontal gyrus (MFG).

To further investigate the relationship between brain activity and SSRT, the brain areas that were significantly correlated with SSRT were entered into a correlation matrix. It was found that activation in each of the areas were highly inter-correlated (see Table 4.12).

Table 4.12

Correlation matrix of parameter estimates extracted from *a priori* ROIs that were significantly correlated with SSRT, r (sig.)

	Opercularis	Orbitalis	Putamen	STN
Opercularis	1.0	-	-	-
Orbitalis	.701 (.003)	1.0	-	-
Putamen	.690 (.003)	.760 (.001)	1.0	-
STN	.579 (.015)	.713 (.002)	.819 (< .001)	1.0

Finally, these areas were entered into a partial correlation analysis with SSRT, initially controlling for *pars opercularis* activation. When this was performed, only STN remain significant (r = .521, p = .034) whereas the relationship between SSRT and BOLD signal variance in putamen (r = .051, p = .434) and *pars orbitalis* (r = .190, p =.267) was no longer significant. When *pars orbitalis* was controlled for, STN was still significant (r = .519, p = .035) and *pars opercularis* approached significance (r = .423, p = .075), while right putamen was uncorrelated (r = .092, p = .383). When STN was controlled for, *pars opercularis* was non-significantly correlated with SSRT (r = .402, p = .087), whereas the other areas exhibited no relationship (putamen: r = -.247, p = .208; *pars orbitalis*: r = .109, p = .361). Finally, when putamen activation was controlled for, both *pars opercularis* (r = .492, p = .044) and STN (r = .617, p = .012) remained significant, while *pars orbitalis* revealed a weak but non-significant correlation (r = .340, p = .128) with SSRT. These data indicate that STN accounted for most of the variance in SSRT and therefore was the best predictor of the variable, while *pars opercularis* was also robustly related to SSRT.

4.3.3. ERP session

4.3.3.1. Behavioural data

RT data

ERP session behavioural findings largely paralleled those revealed in fMRI session data analyses (see Table 4.13 for group ERP session data). A one-way ANOVA (factor Event Type: GoRT, IncorrectGoRT, StopFailure RT) revealed an effect of Event Type, $F(1.320,17.158) = 46.998$, $p < .001$, and similarly, Bonferroni planned comparisons using repeated measures t-tests ($p = .0167$, to correct for multiple comparisons) revealed that GoRT was significantly slower than Stop Failure RT, $t(14) = 12.51$, $p < .001$, and incorrect GoRT, $t(14) = 8.01$, $p < .001$, but Stop Failure RT and IncorrectGoRT differences did not reach the criterion for significance, $t(14) = -2.4$, $p = .031$.

Table 4.13

Mean scores on behavioural indices (with standard deviations in parentheses) from ERP sessions

Index*	Measure
Go trials	
Mean GoRT (ms)	405 (47)
Mean IncorrectGoRT (ms)	345 (43)
Mean percent correct go trials	89.5 (6.6)
Mean percent incorrect go trials	4.0 (3.5)
Mean percent go trial misses	6.5 (6.2)
Mean percent go trial errors	10.5 (6.6)
Stop-signal trials	
Mean Stop Failure RT (ms)	363 (41)
Mean SSRT (ms)	180 (29)
SSRT range (ms)	130 – 230
Mean PI (proportion)	.61 (.15)
PI range (proportion)	.34 - .83
Mean Stop SSD (ms)	202 (47)
Stop SSD range–(ms)	117 – 304
Mean Stop Failure SSD (ms)	217 (48)

*GoRT = median correct go trial reaction time; IncorrectGoRT = median incorrect go trial reaction time; SSRT = stop-signal reaction time; PI = probability of inhibition; SSD = stop-signal delay.

Pre- and Post- event RT differences

Visual inspection of pre and post event RT data (see Table 4.14) suggest little difference between pre and post RTs for correct Go and Stop Failure trials, but in contrast, incorrect Go trials were preceded by very fast responses after which participants slowed. Additionally, Stops were preceded by quite slow responses that sped up to a typical level after stopping was successful.

Table 4.14

Group mean pre and post event RTs (with standard deviations in parentheses) collapsed over left and right hands

Event	Pre-	Post-
Go	391 (45)	398 (45)
Incorrect Go	375 (48)	392 (52)
Stop Failures	392 (44)	395 (57)
Stops	413 (50)	394 (46)

The data were analysed as a 4x2 within subjects ANOVA comprising factors Event Type (Stop/Stop Failure/Go/incorrect Go) x Time (pre/post). A main effect was found for Event Type, $F(1.598,20.775) = 5.854$, $p = .014$, that was moderated by a significant Event Type x Time interaction $F(2.145,27.880) = 6.183$, $p = .005$. To explore the interaction in more detail, separate one-way ANOVAs (with a single repeated measures factor of Event Type) for pre and post event RTs were run. For pre-event RTs, there was a significant effect of Event Type, $F(1.348,17.518) = 30.750$, $p < .001$, but not for post-event RTs, $F(1.911,24.837) = .199$, *ns*). Planned comparisons using paired sample t-tests were conducted to compare pre-Stop RT and pre-Stop Failure RT, and also pre-Go RT with pre-incorrect GoRT. Only tests reaching a criterion of $p = .025$ (i.e., $p = FWE/k = 0.05/2$, where k is the number of comparisons), were considered significant. These analyses were largely consistent with fMRI session findings, whereby pre-Stop RT was significantly faster than pre-Stop Failure RT, $t(13) = 9.543$, $p < .001$, however, in the current analysis, pre-incorrect Go RT was also significantly faster than pre-Go RT, $t(13) = 3.108$, $p = .008$.

Bonferroni comparisons of pre-event and post-event RTs for each event type were also conducted using repeated measures t-tests; to account for the number of tests conducted, only tests reaching a criterion of $p = .0125$ (i.e., $p = FWE/k = 0.05/4$, where k is the number of comparisons), were considered significant. As anticipated, pre-Stop RTs were significantly slower than post-Stop RTs, $t(13) = 4.196$, $p = .001$. Surprisingly, pre-Go

RTs were significantly faster than post-Go RTs, $t(13) = 4.068$, $p = .001$, but no differences were observed between pre-IncorrectGo RTs and post-IncorrectGo RTs or for the event RTs surrounding Stop Failures.

Stop-signal trial data

Group mean SSRT (181 ms) was slightly faster than SSRT calculated for the fMRI session group, but was within the range described by previous reports (Logan, 1994). Additionally, a repeated measures t-test confirmed that stop-signal delay for Stops was significantly shorter than stop-signal delay for Stop Failures, $t(13) = -6.981$, $p < .001$.

4.3.3.2. Go ERPs

Four primary components were revealed in Go ERPs (see Figure 4.09) that are visible across the scalp. These include an early positive component, P1, peaking in the range 120-150 ms after go stimulus onset that is largest at central and midline sites, followed by a negativity that is most prominent at lateral parietal sites. This latter component, peaking just before 200 ms after go stimulus onset, is in the range of visual evoked N1, and is larger for right hand Go than left hand Go at lateral parietal sites, but the reverse is apparent at frontal sites, in addition to central midline and right central sites.

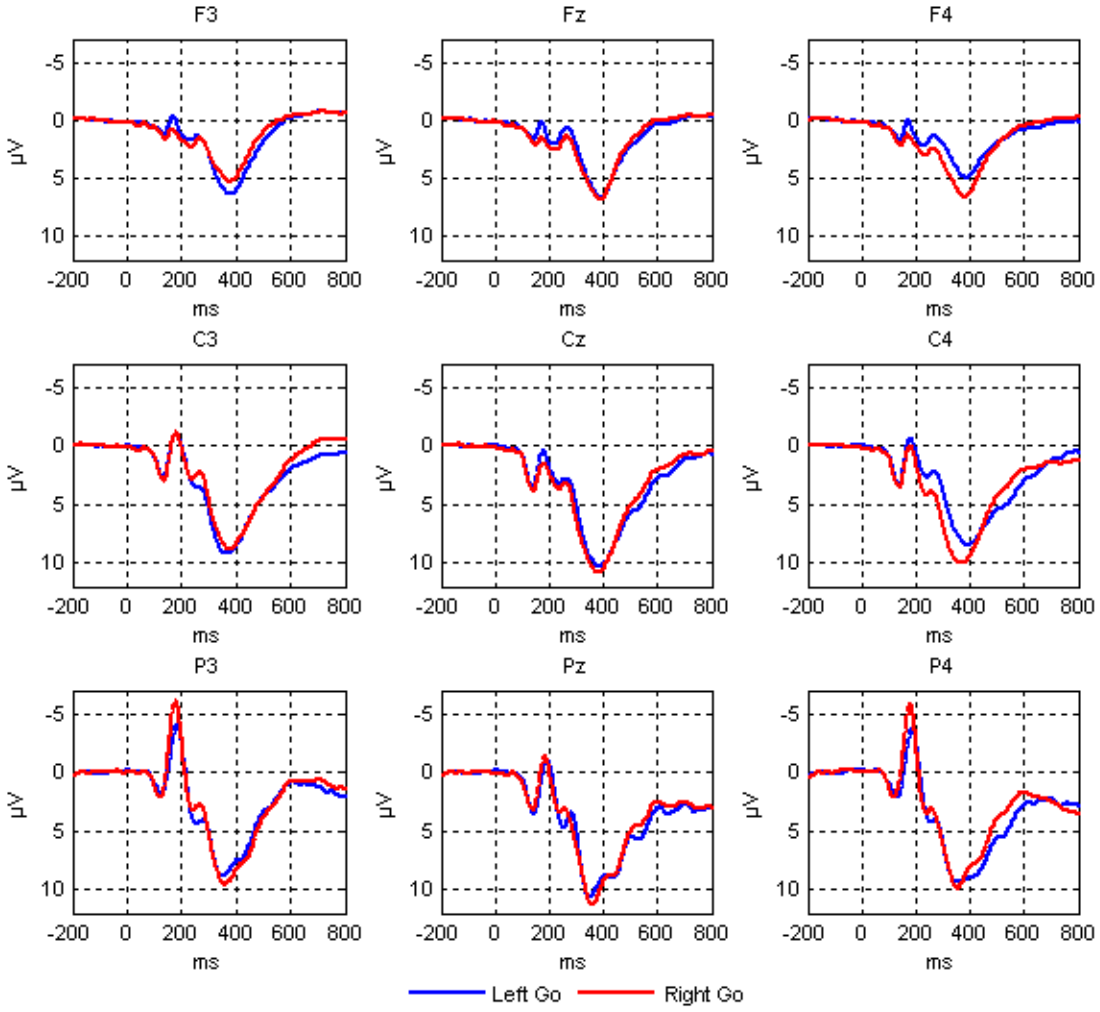

Figure 4.09. Left and right hand grand average Go ERPs at frontal (F3, Fz, F4), central (C3, Cz, C4) and parietal sites (P3, Pz, P4).

Following visual N1 is a small negative deflection peaking in the range 220-250 ms that is visible across the scalp, but is largest at Fz. This component is in the range of N2 that is often reported in studies of cognitive control (Bekker, Kenemans & Verbaten, 2004). Interestingly, left hand Go trials reveal a larger N2 at right frontal and right central sites compared to right hand Go, whereas right hand Go N2 is larger than left hand Go at left central sites, and across parietal sites. N2 is followed by the most salient potential in Go ERPs, a large positive deflection, referred to here as Go P3, peaking in the range 350-400m ms after go stimulus onset that is largest at central and parietal sites in. Interestingly, left

hand Go P3 is smaller (more negative/less positive) at right frontal and right central sites, and right hand Go is smaller at left frontal and left central sites, whereas they are equivalent at Fz and Cz. The consistency of these contralateral effects for both N2 and P3 components are indicative of lateralised readiness and motor potentials that precede response execution.

4.3.3.3. Stop–signal ERPs

The ADJAR method (Woldorff et al., 1993) was used to account for (visual) Go task related ERP overlap in (auditory) stop-signal ERPs. The main advantage of using ADJAR procedures to reveal potentials elicited during the stop-signal task is that late positive components elicited by primary task stimuli are removed from stop-signal ERPs, enabling a straightforward interpretation of the stop-signal ERP components (Bekker et al., 2005a). For this reason, it was anticipated that large positive components would be present in the ADJAR-derived correction (averaged convolution) waveform. Visual inspection of correction waveforms (see Figure 4.10 below) reveals a large positive potential peaking at about 200 ms after stop signal onset that was removed by the ADJAR method. This positive potential corresponds to the difference in the latency of Go-P3 (approximately 400 ms) minus Stop SSD (202 ms), underscoring the efficacy of ADJAR procedures for removal of go response activation overlap from stop-signal locked waveforms. There is some evidence that this positive potential onsets earlier for stop failures than stops consistent with a longer SSD for Stop Failures (217 ms) than Stops.

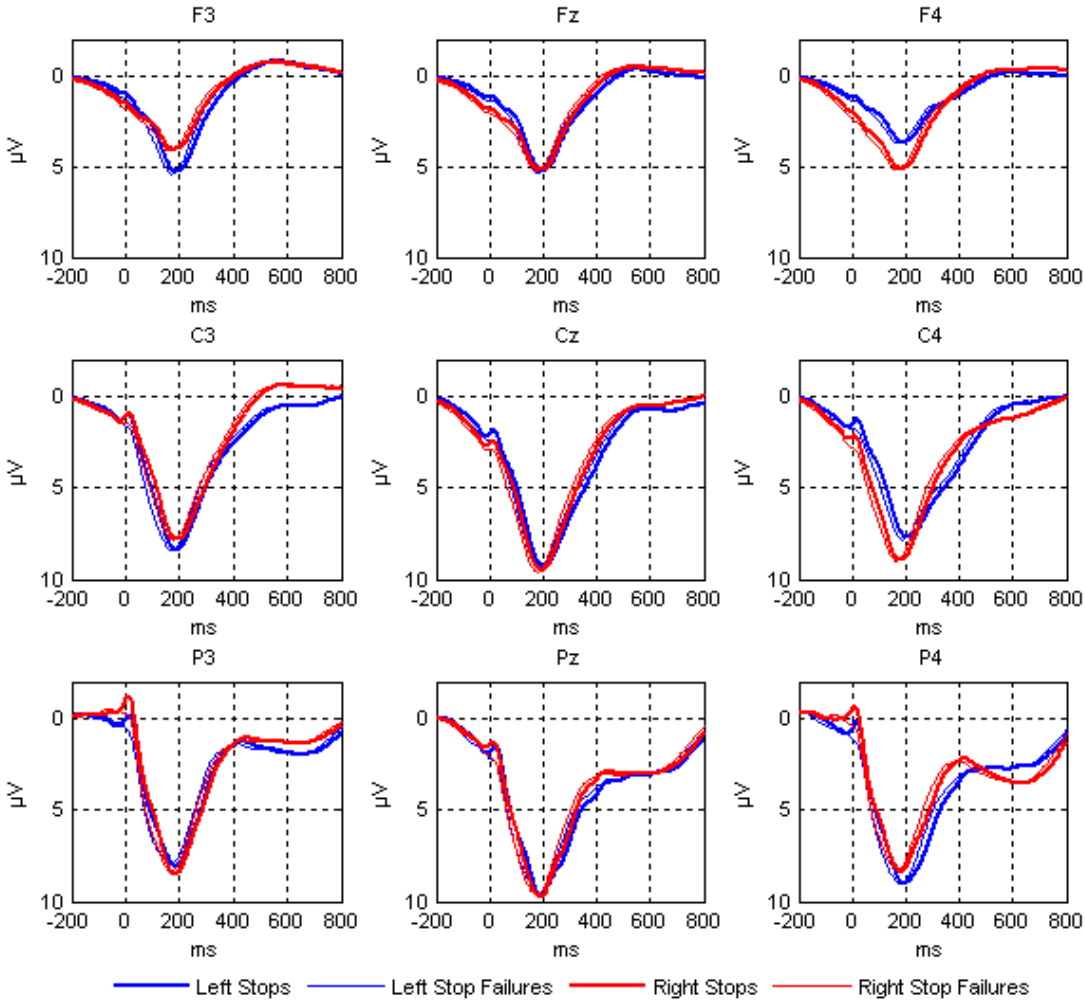

Figure 4.10. Scalp correction waveforms estimated by the ADJAR procedure at midline and lateral frontal (F3,Fz,F4), central (C3,Cz,C4) and parietal sites (P3,Pz,P4) for left and right Stops and Stop Failures.

Bekker et al. (2005a) and Woldorff et al. (1993) refer to another consequence of employing ADJAR procedures – flattening of corrected stop-signal locked ERP baselines. Inspection of baseline period activity in corrected stop-signal ERPs, the 200 ms period preceding time zero, presented in Figure 4.11 (see below), indicate that such flattening has indeed occurred.

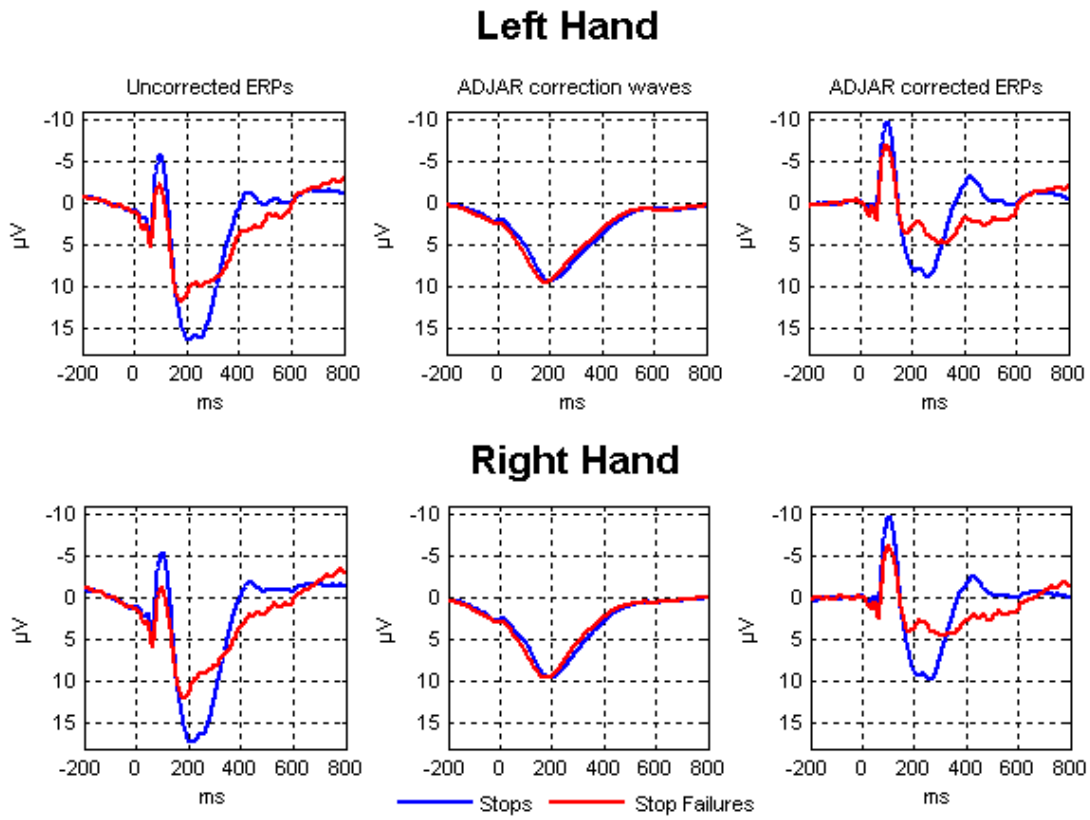

Figure 4.11. Plots of uncorrected stop-signal ERPs, ADJAR correction waveforms, and ADJAR corrected stop-signal ERPs at Cz for left and right hands. Note that application of the ADJAR procedure results in enhancement of N1 and attenuation of P3.

ADJAR corrected stop-signal ERPs (see Figure 4.12) reveal two salient components in each waveform - an early negative deflection peaking about 100 ms after stop-signal onset in all ADJAR corrected stop-signal ERPs (hereafter these will be called stop-signal ERPs/waveforms), followed by a positive component that peaks at about 250 ms for Stops and later than 300 ms for Stop Failures. These negative and positive potentials are in the latency range of N1 and P3 components reported in previous stop-signal experiments that have employed auditory stop-signals, and are the central features of analyses reported in this experiment. However, other features present in the waveforms that are different for

Stops and Stop Failures, are worth describing before reporting detailed analyses of stop-signal N1 and P3 potentials.

Non-central features of stop-signal ERPs

First, a sequence of high frequency positive and negative potentials that precede N1 were observed, the largest being a positive deflection that peaks about 50 ms after stop-signal onset. These are brainstem and mid-latency potentials that are not of interest in this experiment.

Stop ERPs reveal a further component: a large negative deflection across the scalp following P3 that peaks in the range 400-450 ms after stop-signal onset, but are of no interest in the current investigation as they peak well beyond the latency of inhibition processing.

Central features of stop-signal ERPs

Of most interest in this experiment were N1 and P3 potentials; analyses of these potentials are reported separately below, but are preceded by a description of each component in the relevant sections. (See Table 4.15 for a summary of N1 peak amplitude and latencies at Fz and Cz). Interestingly, Stop Failure P3s at fronto-central sites are interrupted by a clear negative potential that peaks about 250 ms after stop-signal onset. At the same sites, Stop ERPs produce an observable negative potential in the same latency range that appears as a notch just before the peak on the positive going arm of P3s, most clearly at central sites. These potentials are within the range of N2 described in previous stop-signal experiments. At parietal sites, no N2-type potential is observable in the same latency range for any stop-signal ERP. Given that N2 was difficult to discern in individual participant ERPs, N2 was measured as a mean amplitude over the interval from 180 – 320 ms (Table 4.16) as described earlier, and were analysed to test whether this component was larger for Stop Failures compared to Stops, as suggested by visual inspection (see Figure 4.12).

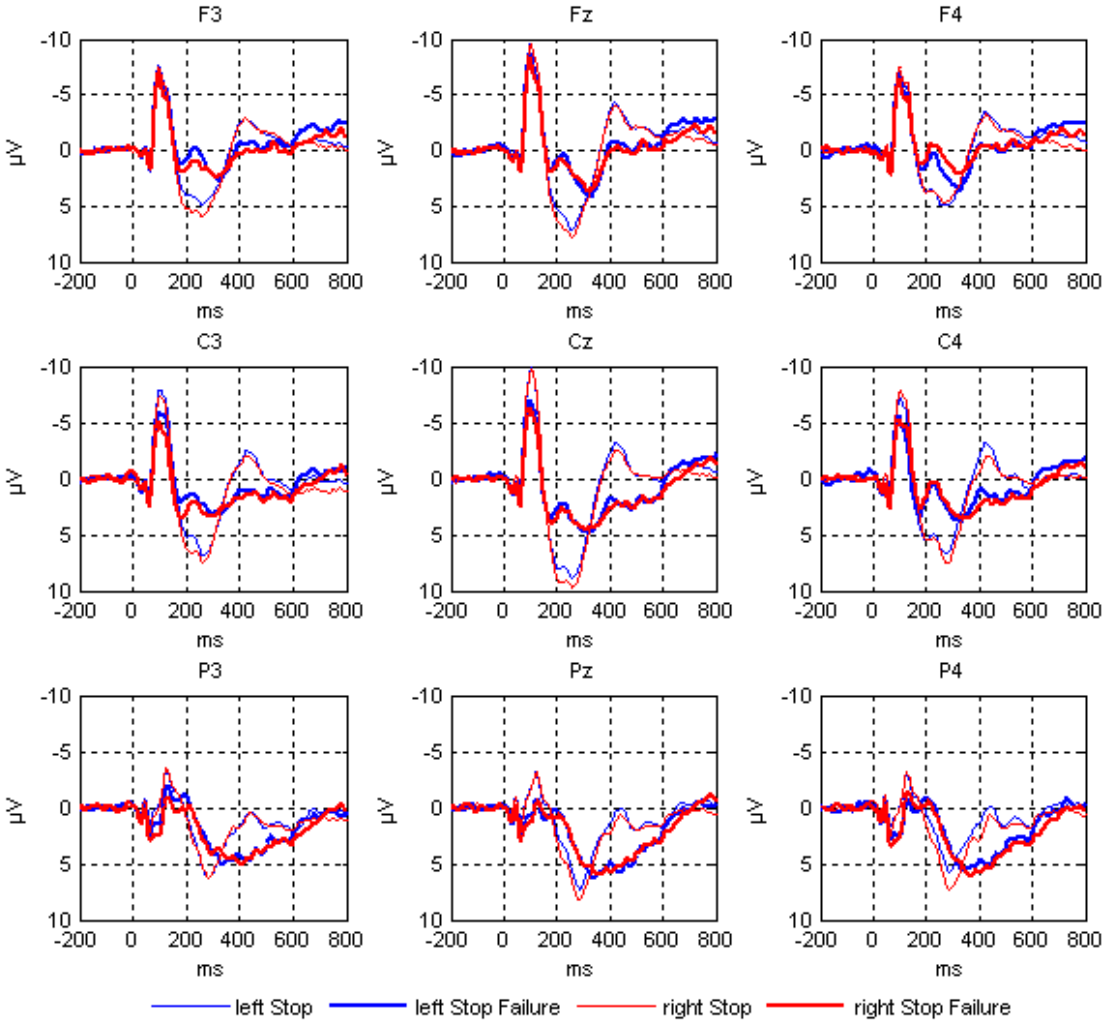

Figure 4.12. Stop-signal ERPs for left and right hands. Electrode positions are according to the 10-20 system.

Auditory evoked N1: average waveform analyses

Visual inspection of group average stop-signal waveforms suggests that N1 was largest at frontal and central sites, especially at the midline (i.e., Fz and Cz) where N1 peaked about 100 ms after stop-signal onset with an amplitude of approximately 10 μV in Stop ERPs. Stop Failure N1 morphology largely paralleled that of Stop N1 at frontal sites, but was substantially smaller in amplitude compared to Stop N1 at central and parietal sites.

Additionally, N1 morphology was largely invariant between left and right hand events for Stop and Stop Failure waveforms across the scalp, except at left lateral central and parietal sites (C3 and P3), where right Stop Failures had smaller amplitudes than left Stop Failures.

Amplitude and latency measures of stop-signal N1 peaks were extracted in the range 50- 150 ms after stop-signal onset, but were not distinguishable in the specified window in two participants leaving a sample of twelve participants.

Stop-signal N1 latency

No significant effects were observed.

Stop-signal N1 Amplitude

When amplitude measures were considered, main effects of Inhibition, $F(1,11) = 7.878$, $p < .017$, and Laterality, $F(1.773,19.506) = 24.274$, $p < .001$, confirmed that Stop-N1 (-9.9 μV) was significantly larger than Stop Failure-N1(-8.5 μV), and that midline stop-signal N1 (-10.6 μV) was enhanced compared to ipsilateral (-8.8 μV) and contralateral stop-signal N1 (-8.2 μV). These effects were moderated by Inhibition x Laterality, $F(1.626,17.888) = 13.676$, $p < .001$, and Inhibition x AP, $F(1,11) = 30.909$, $p < .001$, interactions which showed that Stop-N1 enhancement was significantly greater at midline and central sites compared to lateral and frontal sites, respectively. Finally, an Inhibition x Laterality x AP, $F(1.473,16.208) = 4.050$, $p = .048$, interaction showed that Stop-N1 enhancement was significantly greater at Cz where the difference was approximately 3.0 μV, whereas differences at other sites were 0.5-1.9 μV (mean = 1.4 μV).

Table 4.15

Summary of group mean (N = 12, with standard deviation in parentheses) Stop-N1 and Stop Failure-N1 peak amplitude and latency measures of N1 (time window = 50 – 150 ms) at Fz and Cz for left and right hand events

Event Type	Site	Amplitude (μV)	Latency (ms)
N1 (N = 12)			
Left Stops	Fz	-11.0 (2.2)	105 (11)
Right Stops	Fz	-11.0 (2.1)	105 (11)
Left Stop Failures	Fz	-10.6 (2.2)	106 (14)
Right Stop Failures	Fz	-9.8 (2.5)	106 (13)
Left Stops	Cz	-12.1 (4.1)	100 (11)
Right Stops	Cz	-12.2 (3.9)	106 (10)
Left Stop Failures	Cz	-9.6 (3.4)	101 (15)
Right Stop Failures	Cz	-8.7 (3.7)	104 (14)

Mean Stop-signal N2 amplitude

See Table 4.16 for a summary of stop-signal N2 mean amplitude data at midline electrodes. A main effect of Inhibition, $F(1,13) = 55.427$, $p < .001$, confirmed that mean Stop-signal N2 amplitude was more negative (less positive) for Stop Failures (5.18 μV) compared to Stops (2.04 μV).

Table 4.16

Summary of group mean (with standard deviation in parentheses) Stop and Stop Failure N2 mean amplitude measures (across the time window 180 – 320 ms) at midline electrodes averaged for left and right hand events (N = 14)

Event Type	Site	Mean amplitude (μV)
P3 (N = 14)		
Left Stops	Fz	5.7 (2.6)
Right Stops	Fz	6.4 (2.8)
Left Stop Failures	Fz	1.9 (2.7)
Right Stop Failures	Fz	2.0 (2.6)
Left Stops	Cz	7.6 (3.0)
Right Stops	Cz	8.4 (3.9)
Left Stop Failures	Cz	3.4 (3.7)
Right Stop Failures	Cz	3.7 (3.7)
Left Stops	Pz	4.5 (2.7)
Right Stops	Pz	5.5 (3.4)
Left Stop Failures	Pz	2.5 (3.6)
Right Stop Failures	Pz	2.6 (3.8)

Stop-signal P3

Peak amplitude and latency measures for P3s were extracted over the range 170-600 ms after stop-signal onset (see Table 4.17), but definable peaks within this window could only be detected at all nine sites assessed in ten participants. For this reason stop-signal P3 amplitudes were also measured by finding the mean amplitude over a shorter latency window (170 – 400 ms, see Table 4.18) in order to avoid the large negative component peaking after 400 ms in stop ERPs. These mean amplitude measures were analysed using the same ANOVA model.

Stop-signal P3 peak latency

A large main effect of Inhibition, $F(1,9) = 15.817$, $p = .003$, confirmed that Stop-P3s (260 ms) peaked earlier than Stop Failure-P3s (315 ms), while main effects of Laterality, $F(1.682,15.139) = 9.516$, $p = .003$, and AP, $F(1.450,13.049) = 7.479$, $p = .011$, revealed that stop-signal P3s peaked earliest at the midline compared to sites ipsilateral and contralateral to response hand and earlier at fronto-central compared to parietal electrodes, respectively. However, no interactions were observed.

Table 4.17

Summary of group mean (with standard deviation in parentheses) Stop and Stop Failure peak amplitude and latency measures of P3 (time window = 170 – 600 ms) at Fz, Cz and Pz for left and right hand events (N = 11)

Event Type	Site	Amplitude (μV)	Latency (ms)
P3 (N = 11)			
Left Stops	Fz	9.8 (3.2)	247 (44)
Right Stops	Fz	10.3 (3.9)	240 (39)
Left Stop Failures	Fz	7.2 (3.5)	307 (103)
Right Stop Failures	Fz	7.0 (2.9)	287 (107)
Left Stops	Cz	12.0 (3.9)	243 (47)
Right Stops	Cz	12.8 (4.9)	245 (38)
Left Stop Failures	Cz	9.3 (3.1)	330 (99)
Right Stop Failures	Cz	9.1 (3.9)	318 (105)
Left Stops	Pz	9.1 (2.4)	283 (39)
Right Stops	Pz	10.4 (3.8)	275 (32)
Left Stop Failures	Pz	10.1 (3.2)	353 (102)
Right Stop Failures	Pz	9.4 (3.8)	336 (76)

Stop-signal P3 peak amplitude

When amplitude measures were analysed, main effects of AP, $F(1.430,12.874) = 6.668$, $p = .016$, and Laterality, $F(1.997,17.970) = 51.611$, $p < .001$, confirmed that stop-signal P3s were smaller at frontal (7.6 μVs) compared to central (9.5 μVs) and parietal sites (9.1 μVs), and were larger at the midline (10.0 μV) compared to sites ipsilateral (8.0 μV) and contralateral (8.1 μV) to response hand, respectively. These effects were moderated by a Laterality x AP interaction, $F(2.497,22.474) = 6.136$, $p = .005$, revealing that stop-signal P3s were significantly larger at Cz compared to all other electrode sites investigated.

While the effect of Inhibition was not significant, $F(1,9) = 2.513$, $p = .147$, an Inhibition x AP interaction, $F(1.138,10.245) = 7.723$, $p = .017$, showed that Stop-P3 and Stop Failure-P3 amplitude differences were larger at frontal (2.3 μV) and central (2.5 μV) sites compared to parietal sites (0.7 μV), and a nearly significant Inhibition x Laterality interaction, $F(1.357,13.623) = 3.493$, $p = .077$, suggested that Stop-P3 enhancement was generally larger at the midline, but not significantly so. Finally, a Hand x Inhibition interaction, $F(1,9) = 9.634$, $p = .013$, revealed that the Stop-P3 and Stop Failure-P3 amplitude differences were much larger for right hand (1.8 μV) compared to left hand (0.9 μV) events.

Stop-signal P3 mean amplitudes (170 – 400 ms)

Analysis of mean stop-signal P3 amplitudes largely confirmed the peak amplitude analysis, whereby significant effects were observed for the spatial factors, Laterality, $F(1.360,17.868) = 26.832$, $p < .001$, and AP, $F(1.286,16.715) = 4.612$, $p = .039$, which were moderated by an Laterality x AP interaction, $F(2.915,37.891) = 7.554$, $p < .001$. Similarly, a Inhibition x AP, $F(1.465,19.047) = 13.360$, $p = .001$, was observed, however, in this analysis, Hand x Inhibition did not reach significance, $F(1,13) = 3.374$, $p = .089$.

What was most different in this analysis compared to that for peak amplitudes was a substantial main effect of Inhibition, $F(1,13) = 10.311$, $p = .007$, and an Inhibition x Laterality interaction, $F(1.622,21.082) = 4.580$, $p = .028$, which show that Stop-P3s were more positive than Stop Failure-P3s over the time-window assessed (170-400 ms post stop-signal), and that this difference was larger at midline sites compared to sites lateral to response hand, respectively. An Inhibition x Laterality x AP interaction that approached

significance, F(2.835,36.820) = 2.768, p = .058, suggested that midline enhancement of Stop-P3 compared to Stop Failure-P3 was greater at fronto-central sites compared to parietal sites.

Table 4.18

Summary of group mean (with standard deviation in parentheses) Stop and Stop Failure P3 mean amplitude measures (across the time window 170 – 400 ms) at midline electrodes averaged for left and right hand events (N = 14)

Event Type	Site	Mean amplitude (μV)
P3 (N = 14)		
Left Stops	Fz	3.7 (2.0)
Right Stops	Fz	4.2 (2.6)
Left Stop Failures	Fz	2.1 (2.3)
Right Stop Failures	Fz	2.0 (2.7)
Left Stops	Cz	5.0 (2.6)
Right Stops	Cz	5.7 (3.9)
Left Stop Failures	Cz	3.5 (2.9)
Right Stop Failures	Cz	3.7 (3.4)
Left Stops	Pz	3.8 (2.6)
Right Stops	Pz	4.6 (3.6)
Left Stop Failures	Pz	3.6 (2.8)
Right Stop Failures	Pz	3.6 (3.3)

Relationships between peak measures and stopping indices

To test the hypotheses that shorter latency P3 would be related to shorter SSRT and that longer SSRT would be related to enhanced P3 amplitude, Stop-P3 measures for all participants (Stop-P3 was discernable within the stop-signal P3 window at midline sites in all participants, hence N = 14), at Fz, Cz, and Pz were entered into a correlation matrix with

SSRT and assessed using Spearman's correlation coefficients (ρ). No relationships were observed between Stop P3 latency and SSRT at Fz, Cz or Pz. However, against the hypothesised relationship between SSRT and P300 amplitude, Spearman's statistics revealed non-significant *negative* correlations with both left (ρ = -.499, p = .070) and right (ρ = -.473, p = .088) Stop-P3 amplitude at Fz only (two-tailed tests). Scatterplots (see Figure 4.13) revealed one bivariate outlier in each plot, and upon subject-specific inquiry, it was found that these were drawn from the same participant's data. Excluding this participant from the data yielded highly significant negative correlations between SSRT and left (ρ = -.703, p = .008) and right (ρ = -.670, p = .012) hand Stop-P3 peak amplitudes at Fz, but not at Cz or Pz with the outlier excluded (all ρ < .2, ns). Pearson's statistics were also significant in this analysis for both left (r = -.648, p = .016) and right (r = -.711, p = .006) Stop-P3s (two-tailed tests) at Fz. No significant relationships were observed between Stop Failure-P3 amplitudes and SSRT.

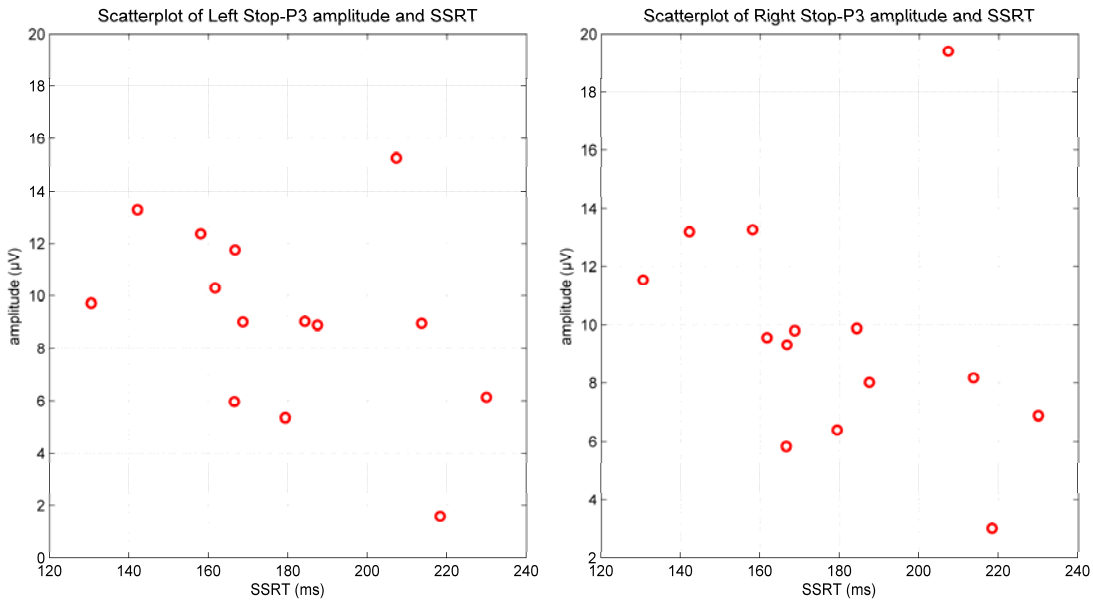

Figure 4.13. Scatterplots depicting relationships observed between SSRT and left hand Stop-P3 amplitude (on left), and SSRT and right hand Stop-P3 (on right) at Fz. Note outliers in top right of each plot.

To investigate the specific linkage of Stop-P3s and SSRT, other stop-signal task factors (GoRT, SSD and PI) were entered into the correlation matrix with the outlier from the previous analysis omitted. As would be anticipated, given the tight coupling between SSRT and PI in this paradigm, the correlation between PI and left hand Stop-P3 at Fz was significant ($\rho = .588$, $p = .035$), but right hand Stop-P3 although in the same direction was not significant ($\rho = .467$, $p = .108$). No other relationships were significant. To validate this was a Stop-P3 specific effect and not linked to earlier ERP stopping components, SSRT was correlated with N1 peak amplitude and latency measures at Fz, Cz and Pz. Again, no significant relationships were observed.

As foreshadowed in the Introduction, further analysis was conducted on latency measures, whereby the difference in P3 and N1 peak latencies for left and right hands were computed and correlated with SSRT (see Figure 4.14 for scatterplots of these relationships at Fz).

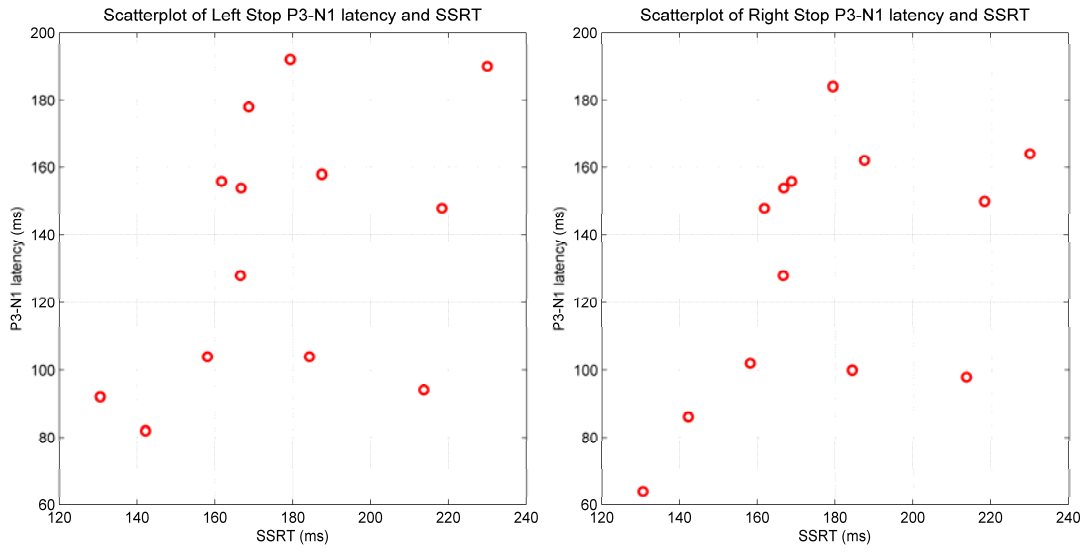

Figure 4.14. Scatterplots of the difference between Stop-P3 and Stop-N1 peak latency and SSRT for left and right hands at Fz.

This was rationalised by consideration of the fact that N1 indicates processing of the stop-signal and thus triggers stopping processes (Bekker et al., 2005a). Hence the endogenous act of stopping cannot begin until at least this point and, noting the difference between SSRT and P3 peak latency[28] (SSRT = 177 ms; left Stop-P3 latency = 243 ms, right Stop-P3 latency = 238 ms), stopping finishes prior to P3 peak latency. Hence the difference between P3 and N1 peak latencies may be a better psychophysiological indicator of stopping than Stop-P3 latency. If this is the case, it would be expected that shorter Stop-P3 minus Stop-N1 latency difference ('Stop P3-N1 latency') would be positively related to SSRT. Given this directional hypothesis, one-tailed tests were used. Significant relationships were observed between Fz Stop P3-N1 latency (right: M = 130 ms, SD = 37 ms; left: M = 137 ms, SD = 39 ms) and SSRT for both left (ρ = .490, p = .045) and right hands (ρ = .549, p = .026). Scatterplots of these relationships (see Figure 4.14) indicate a true relationship, but given the small sample size, they should be taken with caution. At Cz and Pz, the correlations were less consistent across hands in that significant relationships were observed for right hand Stops (Cz: M = 129 ms, SD = 36 ms; Pz: M = 153 ms, SD = 36 ms) at Cz (ρ = .527, p = .048) and Pz (ρ = .545, p = .041), but no significant relationships were observed for left hand data (all ρ < .310). Hence the Stop P3-N1 latency and SSRT correlation was only consistently observed at Fz.

4.3.3.4. Comparison of fMRI and ERP behavioural data

The consistency of the major behavioural variables (GoRT, SSD and SSRT) was assessed by comparing fMRI and ERP (session data for the twelve participants who participated in both sessions using paired samples t-tests. No significant differences were observed for GoRT, t(11) = .839, *ns*, SSD, t(11) = 1.104, *ns*, or SSRT, t(11) = 1.395, *ns*. Importantly, SSRT was moderately strongly correlated across sessions, r = .518, p = .042, while very strong correlations were observed for GoRT, r = .883, p < .001, and SSD, r = .934, p < .001, across sessions.

[28] Outlier from amplitude analysis omitted.

4.3.3.5. Correlation of Stop>Go contrasts with Stop related ERP measures

Stop-P3 peak amplitudes, and Stop P3-N1 latencies were correlated with Stop > Go contrast maps. Only when Stop P3-N1 latencies were correlated with Stop > Go was a significant relationship observed. This was within right *pars orbitalis* (MNI coords: 56 32 -4; t = 5.16; cluster sig. = .055; voxel FWE = .033).

4.4. Discussion

FMR BOLD imaging and ERPs were used to investigate the neural dynamics of stop-signal inhibition where the difficulty of inhibition varied across group members depending on an endogenous behavioural factor: the stop-signal reaction time, SSRT. A primary objective was to assess SSRT discrimination of hemodynamic and electrophysiological brain activation. There were four key findings: (1) a network including right lateral *pars opercularis* of IFG and STN was recruited for more difficult stopping whereas dorsolateral PFC, including portions of right MFG and *pars triangularis* of IFG, was generically engaged irrespective of task difficulty; (2) faster SSRT was related to larger P3 peak amplitudes at frontal electrodes (Fz) only; (3) faster SSRT was not related to shorter P3 peak latency, but was predicted by shorter latency differences between N1 (index of stop-signal detection) and P3 peaks (thought to reflect inhibition processing) at Fz. (4) Successful inhibitions (Stops) were preceded by slower RTs on the trial before Stops compared to the trial before Stop Failures (unsuccessful inhibition).

4.4.1. Basic behavioural findings

Task performance was very consistent across fMRI and ERP sessions (see Table 4.1 and Table 4.13) even though group members varied slightly between sessions. The only discrepancy between session performances was that IncorrectGoRT was significantly faster than GoRT in the ERP session (by 50 ms) only, although a similar difference was observed in the fMRI session (36 ms difference). The group data suggest this discrepancy occurred because of longer (368 ms vs 345 ms) and more variable (SD = 57 ms vs. 43 ms)

IncorrectGoRTs in the fMRI session compared to the ERP session. However, it should also be noted that ERP sessions contained twice as many trials as fMRI sessions, and thus IncorrectGoRTs, which were few, were better estimated in ERP sessions. Analyses of the major behavioural variables (GoRT, SSRT and SSD) for the cohort who participated in both sessions (N = 12) revealed no between session differences, and importantly, the session variables were strongly correlated.

In both experimental sessions, SSRT was within the range of previous reports, and behavioural data were consistent with race model predictions whereby Stop Failure RT was faster than GoRT, and SSD for Stops was shorter than SSD for Stop Failures.

Crucially for the stop-signal variant used in this study and the hypotheses tested herein, SSRT was highly correlated with PI (positive relationship). This correlation was a consequence of the protocol used for setting SSDs: stop-signals were set such that the time interval between stop-signal onset and the anticipated response time (GoRT – SSD) was kept constant between participants. In so doing, inhibition difficulty, defined according to the inhibition difficulty ratio (SSRT/(GoRT – SSD)), varied between participants contingent upon individual SSRT, i.e., SSRT was the only factor that varied between participants and was thus predictive of inhibition probability. This finding demonstrates that in this instantiation of the stop-signal paradigm, participants whose SSRT was slower found the stop-signal task more difficult than participants with relatively faster SSRT.

A wide distribution of SSRTs was observed, resulting in a range of inhibition difficulty (inhibition difficulty ratios). This was important for testing the main hypothesis for this investigation - that more difficult inhibition would involve recruitment of a right IFG-STN network - because if true, greater variability in inhibition difficulty should generate greater between-participant variability in the brain areas engaged for more difficult stopping. Consequently, any BOLD signal variance detected during Stops in associated neuroimaging data (discussed below) that is explained by longer SSRTs should be taken to represent neural areas that are responsible for more difficult inhibition.

Trial history effects indicated that stopping was influenced by suspension of on-going go response activation revealed by slower RTs on the average on the trial preceding Stops compared to Stop Failures in both experimental sessions. This finding is comparable to that of Vink and colleagues (2005) who varied the number of go trials preceding stop-

signal trials parametrically and showed that go trial RTs increased linearly as a stop-signal trial probability increased. This manipulation was not implemented in the current investigation, but the current findings nonetheless support the notion that stopping is linked to top-down modulation of go response time to facilitate successful inhibition.

In a study by Boehler and colleagues (2009), post trial effects were assessed. This group found that go RTs were slowed after stop-signal trials compared to go trials, regardless of the outcome of the stop-signal trial (successful or unsuccessful inhibition; Boehler et al., 2009). Boehler attributed this RT modulation to the action of a conflict mechanism. However, this effect was not observed in either session of the current study, and was not observed by Vink et al. (2005). Indeed, while Vink and colleagues did not directly analyse post trial effects, they did show that the fastest go trials were those directly following a stop-signal trial (see Figure 4.3 in Vink et al., 2005) and thus conflict with the findings of Boehler and colleagues (2009). One reason for this discrepancy may be that in Vink's study, and the current study, the trial following a stop-signal trial was always a go trial. Hence participants may have learnt this and responded normally on such trials. If this is true, then the post stop-signal task trial slowing observed by Boehler and colleagues (2009) may actually be linked to strategic top-down modulation of go response activation in anticipation of a subsequent stop-signal trial, and not due to conflict induced inhibition as argued by Boehler et al. Such Go response slowing would presumably be implemented by the SMA-striatal mechanism reported by Vink et al. (2005) as being directly involved in RT slowing, whereas conflict is thought to be resolved by a related but separate cortical mechanism involving ACC (Kerns et al., 2004).

4.4.2. fMRI findings

Neuroimaging data confirmed the importance of right PFC for stop-signal response inhibition. The network activated by all participants irrespective of task difficulty ('generic network') revealed by a random effects one-sample t-test of Stops > Baseline, included right MFG merging into IFG (*pars triangularis*), and IPL in addition to left SMA. SVC analyses confirmed that generic network PFC activation for stopping (based on the Stops > Baseline contrast) was predominantly observed in mid-DLPFC, especially MFG and anterior IFG (*pars triangularis)*, whereas more difficult inhibition (based on the simple

(positive) correlation map of SSRT with Stops > Baseline contrasts) was related to activation in more posterior IFG regions (*pars opercularis)*. In particular, inhibition difficulty, predicted by SSRT, was strongly correlated with BOLD signal variance in the proposed 'hyperdirect' stopping network (Aron & Poldrack, 2006) that includes right *pars opercularis* of IFG, but also right STN. These latter effects were further confirmed by a detailed correlation analysis of SSRT and the parameter estimates extracted from ROIs in areas that have previously been linked to stopping (Aron & Poldrack, 2006).

The difference in PFC activation between the group Stops > Baseline contrast revealed by a random effects one sample t-test model, and the simple (positive) correlation of the same contrast images entered into the t-test model and SSRT, suggests that different neural networks were recruited as participants found the stop-signal task increasingly difficult: right dorsolateral portions (MFG and anterior IFG – *pars triangularis*) were generically recruited, while more difficult inhibition required recruitment of more ventrolateral regions of right PFC (posterior IFG – *pars opercularis*). Moreover, STN was positively, not negatively, correlated with SSRT, and was not observed in the random effects t-test of Stops > Baseline suggesting this nucleus is engaged for stopping only when response inhibition is difficult.

The location of PFC generic network activation in right DLPFC is very comparable to that dominating PFC activation patterns in neuroimaging studies of no-go inhibition (De Zubicaray et al., 2000; Garavan et al., 1999; Garavan et al., 2002; Kawashima et al., 1996; Mostofsky et al., 2003; Rubia et al., 2001a; Watanabe et al., 2002), though is slightly anterior to the MFG area reported by Zheng and colleagues (2008) who performed a conjunction of stop-signal and no-go inhibition. De Zubicaray and colleagues (2000) described DLPFC activation in their study of no-go inhibition as being evidence of an inhibitory mechanism associated with working memory that may also have a significant role in response inhibition. However, the importance of inhibition in working memory have been seriously challenged (Aron, 2007; MacLeod et al., 2003), and given that no-go trials do not involve a cue to respond, no response activation is likely to proceed, and hence it is doubtful that intentional inhibition of response activation is required, whereas there is broad agreement that intentional inhibition of responding is required for stopping (Aron, 2007; MacLeod et al., 2003). Indeed, lesion (Aron et al., 2003a) and TMS (Chambers et al., 2006;

Chambers et al., 2007) studies have demonstrated that impairment of right *pars opercularis* function selectively impairs SSRT whereas dysfunction of MFG does not, suggesting that MFG is not involved in response inhibition. However, right DLPFC has been strongly linked to decision making (Fleck, Daeslaar, Dobbins & Cabeza, 2005; Knoch, Pascual-Leone, Meyer, Treyer, & Fehr, 2006) and response selection (Bunge, Hazeltine, Scanlon, Rosen & Gabrieli, 2002; Rowe, Toni, Josephs, Frackowiack & Passingham, 2000) which maps more directly onto no-go inhibition than response inhibition (Rubia et al., 2001a), and to generic stopping in the current experiment.

This DLPFC mechanism may also be active during difficult stop-signal inhibition, whereby selection of the stop response and coding of the stop stimulus into working memory are required, with the notable difference that response execution processes are also underway – a more difficult situation to control - requiring recruitment of the *pars opercularis*-STN response inhibition mechanism. Such an explanation is consistent with the current experiment, in which dorsolateral PFC regions including right MFG and IFG (*pars triangularis*) were activated generically by all participants, but when stop-signal inhibition was increasingly difficult, *pars opercularis* and STN were increasingly engaged, but were not generically activated by all participants. It is noteworthy that the IFG region generically activated was located in *pars triangularis*, whereas more difficult inhibition was related to BOLD signal variance within *pars opercularis,* but not *pars triangularis*.

Right *pars opercularis* and STN are thought to form a cortico-basal ganglia network that constitutes a fast acting 'hyperdirect' pathway (Aron & Poldrack, 2006) capable of suppressing thalamocortical behavioural (response) output initiated in the 'direct' pathway (Nambu et al., 2002). Hence the right *pars opercularis*-STN network is engaged *after* the launch of motor commands. ROI and SVC analyses of neural structures thought to have roles in response inhibition confirmed that right IFG is critical for stopping, demonstrated by a strong and consistent relationship between right IFG BOLD activity and SSRT, whereas other cortical structures purported to have roles in response inhibition, namely right MFG and pre-SMA, were not predictive of SSRT. These analyses also confirmed that STN is critical for difficult inhibition.

In a detailed analysis of mean parameter estimates extracted from right lateral *a priori* ROIs that took into account the subgyral structure of IFG, it was found that SSRT

was most strongly related to *pars opercularis*, but also significantly correlated with SSRT were *pars orbitalis*, STN and putamen. Controlling for BOLD signal correlated variance in any other ROI, STN remained significantly correlated with SSRT. *Pars opercularis*, while not so reliably related, maintained correlations with SSRT when BOLD variance was controlled for in other ROIs (always $r > .4$), though these were usually non-significant. It is possible that with increased power from a larger sample size, *pars opercularis* may have remained significant in these analyses, whereas the reverse case is less likely to be true for *pars orbitalis* and putamen. Overall, these data suggest that right *pars opercularis* and STN are the most crucial for difficult stop-signal inhibition.

The positive relationship between slower SSRT and right IFG-STN activation conflicts with other reports of stop-signal inhibition, including Experiment 1, where SSRT was inversely related to activation within right IFG, lesion studies linking grey matter integrity to SSRT (Aron et al., 2003a; Reiger et al., 2003) and most pertinently, the findings of Aron and his colleagues (2006; 2007a), who reported a negative correlation between SSRT and activation in right IFG and STN. This inconsistency can be explained by consideration of the differences between the stop-signal variants used in these reports and that employed in the current experiment. In Experiment 1 and those of Aron and colleagues (2006; 2007a), the difficulty of inhibition, that is, the time between stop-signal onset and the anticipated response time of each participant, was manipulated by varying stop-signal delay such that inhibition probability was held at approximately chance level for each participant. This approach can be thought of as tailoring stop-signal trials on a participant-by-participant basis to produce consistent inhibition difficulty across the group, in addition to equivalence of the relative finishing times of stop-signal and go processes between participants. This means that the time between stop-signal onset and the anticipated response time (GoRT in these experiments) equals SSRT. Using this approach, in Experiment 1 and Aron and colleagues (2006; 2007a), it was found that faster SSRT predicted BOLD enhancement in right IFG, though in different subgyral structures; Aron and colleagues (2006; 2007a) in *pars opercularis* (and right STN), and for Experiment 1, right *pars orbitalis*. The differences in functional localisation observed in these studies may be explained by differences in experimental design – Aron and colleagues (2006/2007a) used event-related designs whereas in Experiment 1, an epoch-based design was employed.

These designs are differentially sensitive to phasic and tonic processes, respectively, suggesting that the differences observed may be linked to inhibitory control differences, namely phasic and tonic inhibitory control processes. Nonetheless, these studies operationalised response inhibition difficulty at chance level success by keeping the time given for stopping equal to SSRT, and subsequently linked faster SSRT to greater activation in right IFG – an inverse relationship.

In the current study, stop-signal inhibition was investigated using a very different approach: the time given to inhibit responses was kept approximately equal for each participant. This was operationalised by setting stop-signal delays relative to GoRT. Therefore, inhibition difficulty varied as a function of individual SSRT, and moreover, inhibition necessarily occurred at different points in the go response activation cycle for each participant. That is, response inhibition occurred at varying points in the motor hierarchy contingent upon individual SSRT. For participants with shorter SSRTs, response inhibition was effective at a higher point in the motor hierarchy, closer to or during central processing operations (e.g., response planning or response selection stages) compared to participants displaying longer SSRTs whose stopping processes had to be effected at a lower point in the motor hierarchy, closer to or during response execution stages. By contrast, if adaptive SSD settings are used ensuring that PI is equivalent for each participant as per Aron et al. (2006; 2007a), stop-signal inhibition occurs at approximately the same point in the motor hierarchy for all. In the current study, participants with faster SSRT did not require right IFG-STN network because response execution was not underway, or at least to a lesser degree compared their colleagues with slower SSRTs. Hence the current findings indicate that the right *pars opercularis*-STN mechanism is critical only when response inhibition is very urgent, and is increasingly engaged as the requirement for inhibition becomes increasingly urgent, whereas a DLPFC mechanism that includes *pars triangularis* of IFG is generically recruited for stopping.

These findings conflict partly with those of Aron and Poldrack (2006) who performed a parametric analysis where SSD was modelled for each Stop event at the participant level, with the aim of examining the network activated when the stop signal occurs close to the point of response execution. The brain map depicting the positive correlation of SSD with Stop events for each participant was passed to a group level t-test

model, which revealed a network including pre-SMA, GP and STN, indicating these areas were linked to stopping at later stages of motor readiness – more difficult inhibition. *Pars opercularis* activation was not correlated with SSD, indicating this area was activated regardless of the timing of the stop-signal, and thus was not sensitive to inhibition difficulty. By contrast, in the current investigation it was found that activation in *pars opercularis* and STN were only evident when stopping was difficult, and that pre-SMA was not linked to stopping at all.

These findings are somewhat contradictory, but may be due in part to the method employed by Aron and Poldrack for the aforementioned analysis, or may result from paradigmatic differences. In the Aron and Poldrack study, SSDs were set adaptively ensuring a stopping probability of 50% and hence equivalent inhibition difficulty between participants. The network linked to stopping difficulty was assessed using parametric modelling of SSD described above, revealing a preSMA, striatal (GP) and STN network. It is possible that Stops on longer SSD trials may have resulted from strategic slowing of Go response activation processes to facilitate stopping, which is difficult to control for on a trial-by-trial basis in stop-signal experiments (Logan, 1994). In support of this hypothesis, Vink and colleagues (2005) directly related slowing of Go responding in anticipation of a stop-signal trial to increased activation within bilateral portions of preSMA and the striatum (extending across caudate and GP nuclei), which was interpreted as reflecting strategic slowing for the purposes of facilitating stopping success. Hence the current findings suggest that when inhibition difficulty is primarily a function of the speed of inhibition (rather than controlled by adaptive setting of SSD), a different role of the pars opercularis-STN network becomes evident.

When Stops were compared to Stop Failures, right IFG and STN were not significantly activated, but paralleling the findings of Vink and colleagues (2005) and Aron and Poldrack (2006), enhanced activation was observed within bilateral striatal nuclei (putamen and caudate). In their elegantly designed study, Vink and colleagues (2005) manipulated the number of go trials interspersing each stop-signal trial using a pseudo-randomised stop-signal paradigm. They found that as the number of go trials between successive stop-signal trials increased, RTs and striatal activation on successive go trials also increased, which they interpreted as strategic slowing in anticipation of a stop-signal

that is contingent upon context, i.e, the number of preceding go trials. In the current study, a more randomised stop-signal design was used compared to that employed by Vink, the only constraint being that stop-signals were not presented on successive trials. Similar behavioural and neuroimaging findings were observed in this study whereby RTs on trials preceding Stops were significantly slower than the RTs on trials preceding Stop Failures, and the contrast of Stops > Stop Failures revealed that Stops were linked to significantly greater striatal activation. These results are consistent with Vink's assertion that the striatum has a role in mediating successful inhibition by the strategic slowing of go responding.

Rodent studies have shown that lesions to the medial striatum slow SSRT (Eagle et al., 2003a), but ventral striatal lesions do not (Eagle & Robbins, 2003b). An ROI analysis in the current study revealed a significant relationship between right putamen (only right lateral ROIs were used) and SSRT, however this relationship could be explained by BOLD signal variance in *pars opercularis,* or STN, the latter being the best predictor of SSRT. In contrast, BOLD signal variance in right *pars opercularis* could not explain all the variance in SSRT that was predicted by the BOLD response in right STN, indicating that both right *pars opercularis* and STN are both critical for difficult inhibition.

These results can be understood by consideration of connectivity within basal ganglia circuitry (detailed in Chapter 2 but reiterated briefly here). It is well known that GABAergic striatal efferents project to the internal capsule of the globus pallidus (GPi) that function by inhibiting GPi which subsequently disinhibits the thalamus to release only a selected motor command (the direct pathway: Alexander & Crutcher, 1990; Nambu et al., 2002). But striatal efferents also project to the external capsule of the globus pallidus (GPe). Indeed all striatal cells project to GPe and only a subset of these cells actually project to GPi also (Levesque & Parent, 2005; Wu, Richard & Parent, 2000).

These striatal-GPe efferents function by inhibiting GPe using GABA as a neurotransmitter, which subsequently diminishes the tonic inhibition GPe normally applies to GPi and STN via GABAergic GPe-GPi and GPe-STN neurons, respectively. When tonic inhibition of GPi and STN is released, the basal firing rates of these nuclei increase, exerting inhibitory effects over thalamocortical output. This is the indirect pathway. The balance of activation between the direct and indirect basal ganglia pathways is thought to

control the execution of movement, and in the controlled sequencing of movements. Increased GABAergic GPi-thalamus inhibition initially provides control over a selected motor program that is being executed, but this activity is later increased by heightened STN-GPi activation, which results in powerful thalamocortical inhibition after response execution.

When inhibition is easier, activation in the indirect basal ganglia pathway (striatum-GPe-STN/GPi-thalamus) may be all that is necessary to suppress responding, supported by the current finding that striatal activation distinguished Stops from Stop Failures and therefore was reliably activated in all participants[29]. By contrast, in situations of more difficult inhibition, phasic stop-signal locked activation in the alternate hyperdirect IFG-STN pathway is critically involved for successful inhibition. In support of this distinction, striatal nuclei were linked to slowed go responses in this study and in Vink et al.'s (2005) investigation, but additionally, striatal activation is sometimes reported for no-go inhibition (e.g., Menon et al., 2001), although activation of caudate nuclei are mostly emphasised.

This study is the first to show that right IFG-STN is crucially engaged only in situations of difficult inhibition, and that such 'hyperdirect' cortico-basal ganglia control is distinguishable from indirect pathway control of thalamocortical motor output when inhibition is easier.

4.4.3.ERP findings

The primary intention of the ERP data was to investigate the components elicited by stop-signals, and secondly, to investigate whether individual SSRT was associated with both the peak amplitude and peak latency of these components. An ancillary intention was to assess the utility of ADJAR correction procedures (Worldorff, 1993) for removing overlap from stop-signal waveforms, components elicited by go stimuli presented on stop-signal task trials.

[29] It should be noted that indirect pathway STN activation is not a phasic response, but is induced slowly and therefore is not revealed in event-related analyses.

ADJAR efficacy

Particularly affecting stop-signal waveforms are late positive potentials (Go-P3) elicited by go stimuli that are superimposed on uncorrected stop-signal-locked waveforms (Bekker et al., 2005a). Therefore, if ADJAR procedures were effective at removing the overlap in the current experiment, then correction waveforms should reveal a positive maximum at a latency corresponding to the difference between Go-P3 peak latency (around 400 ms; see Figure 4.09) and SSD (Stop SSD = 202 ms, Stop Failure SSD = 217 ms; see Table 4.13). Indeed, correction waveforms revealed a positive maximum at about 200 ms after stop-signal onset, thereby supporting the efficacy of overlap removal in this experiment. Another important factor indicating the effectiveness of ADJAR procedures was that pre-stimulus baselines were flattened in corrected compared to uncorrected stop-signal waveforms (see Figure 4.11), which was observed by Bekker et al. (2005a) who were the first group to apply these procedures to stop-signal ERPs. Bekker also found that ADJAR had the effect of increasing N1 amplitudes and decreasing P3 amplitudes in corrected compared to uncorrected stop-signal waveforms which was replicated here for both stop and stop failure ERPs (see Figure 4.11).

Stop signals elicit N1 and P3 potentials

Both Stop and Stop Failure waveforms revealed large N1 and P3 components that have been observed in other stop-signal experiments employing auditory stop-signals (Bekker et al., 2005a; De Jong et al., 1990; Dimoska & Johnstone, 2008). Additionally on the basis of a visual inspection of the waveforms, a stop-signal N2 was evident for Stop Failures but *not* Stop ERPs. Analysis of the mean amplitude over the range of this component confirmed that N2 was more negative during Stop Failures compared to Stops, thus discounting the proposal that N2 is linked to stop-signal inhibition (Van Boxtel et al., 2001), but rather, corresponds to either error-related processes (Dimoska et al., 2006) or conflict processes (Donkers et al., 2004), which are greater for Stop Failures compared to Stops (Stahl & Gibbons, 2007).

N1 amplitudes were largest at frontal and central sites, and were enhanced during Stops compared to Stop Failures, but only at central sites. No latency differences were observed. N1 enhancement at Cz during Stops has been observed in previous stop-signal

ERP experiments using auditory stop-signals (Bekker et al., 2005a; Dimoska & Johnstone, 2008), and over visual sensory areas in an MEG experiment using visual stop-signals (Boehler et al., 2009). Noting that N1 is sensitive to selective attention (Hillyard, Hink, Schwent, & Picton, 1973; see also Schwent & Hillyard, 1975), Bekker and colleagues (2005a) suggested that successful stopping is contingent upon attention to the stop-signal. Hence, augmented N1 during Stops was proposed to reflect greater allocation of attentional resources toward detection of the stop-signal. In support of this hypothesis, the current investigation revealed significantly longer RTs on the trial directly preceding a Stop compared to the homologue for Stop Failures. This clearly indicates the engagement of additional processes prior to Stops that are either not engaged, or engaged to a lessor degree, prior to Stop Failures. Vink and colleagues (2005) have provided very convincing evidence that participants slow responding in anticipation of a stop-signal trial, whereby the probability of a stop-signal trial predicted go RT, but whether this ensues from strategic slowing or due to reallocation of attentional resources to stop signal detection that results in unintentionally slowed responding (lateral inhibition), is not known. Nonetheless, these data – larger Stop N1 and slower RTs preceding Stops – clearly indicate that greater attention is directed toward processing of the stop-signal during Stops compared to Stop Failures.

While there is support for the notion that participants were allocating a greater proportion of attentional resources to auditory processing during (and prior to) Stops compared to Stop Failures, it is questionable whether N1 enhancement observed both here and in Bekker et al. (2005a) is actually due to selective attention as indicated by the research of Hillyard and colleagues. The effect reported by Hillyard's research group (Hillyard et al., 1973; Schwent and Hillyard, 1975) was revealed using tasks where a single relevant tone is presented among a series of irrelevant tones. The amplitude of N1 in response to relevant tones was greater than N1 elicited by the same tones when irrelevant. N1 enhancement reported in these experiments is comparable to that of Dimoska and Johnstone (2008) who reported larger stop-signal N1 amplitudes during Stops compared to tones presented during trials that were not stop-signal task trials, so-called 'ignore trials'[30]. Tones presented on these 'ignore trials' varied in frequency to stop-signals, thus requiring

[30] Dimoska and Johnstone (2008) did not report any comparison between Stop N1 and Stop Failure N1.

participants to discriminate between the irrelevant tone presented on ignore trials and the stop-signal on stop-signal trials. Dimoska attributed N1 enhancement, observed at frontal and central electrodes in their experiment, to a 'processing negativity', which was first proposed by Näätänen and Michie (1979). These latter authors suggested that N1 enhancement observed in selective attention tasks results from superimposition of a negative component upon typical N1 (only modulated by exogenous physical stimulus parameters) that indexes a comparator process whereby an input stimulus is compared to a 'trace memory' of the relevant stimulus held in working memory (Näätänen, 1982). In outlining his theory of selective attention, Näätänen (1982) suggested that when the trace memory and relevant stimulus input are matched, N1 enhancement at the vertex (Cz) is revealed, but the input stimulus is excluded from further processing when it does not match the trace memory.

Although this theory is somewhat applicable for Dimoska and Johnstone (2008), it is noteworthy that both stop-signals and ignore signals were equally relevant in their study, and thus required considerable processing for correct responding. How stop-signals and ignore-signals differed was that an ignore signal indicated to participants that they should keep going with the previously cued go response, whereas the stop-signal instructed engagement of a different process – the stop process. Hence auditory N1 enhancement may in fact indicate switching of attention *to engage a different process*, and not selectively attending to the stop-signal per se. This notion implies that enhanced N1 reflects engagement or triggering of the stop process, and hence may actually indicate the commencement of executive control. Using this reasoning, N1 may have been attenuated during correct Ignore trials in Dimoska and Johnstone's investigation because go response activation was on-going in response to a visual go stimulus and hence no executive engagement was necessary, whereas on stop-signal trials, stop-signal processes, revealed as a Stop-P3, were engaged. Similarly, in the current study and that of Bekker and colleagues (2005a), Stop Failure N1 may have been attenuated because executive control was not engaged in a timely fashion.

Following stop-signal N1 was a large positive deflection across the scalp previously termed stop-signal P3. This component was larger for Stops than for Stop Failures, particularly at frontal and central sites and additionally, peaked earlier during Stops

compared to Stop Failures. These findings are consistent with the results of other research groups who have reported that Stop-P3 is both larger (Bekker et al., 2005a; De Jong et al., 1990), and peaks earlier than Stop Failure-P3 (Bekker et al., 2005a; Kok et al., 2004).

Another factor distinguishing stop-signal P3s was the different cortical distribution of each component. Stop-P3 was typified by a clear central maximum, which in addition to a shorter latency than Stop Failure-P3, is suggestive of a P3a component (novelty-P3: Dien, Spencer & Donchin, 2003; Friedman, Cycowicz & Gaeta, 2001), whereas, Stop Failure-P3 had a clear parietal maximum that onset later than Stop-P3. The timing and parietal distribution of Stop Failure-P3 is indicative of a classical P3b (or target-P3: Kok et al., 2004; Ramautar et al., 2004). The difference in timing and distribution of these components suggest that each reflects either a different process, or a different set of processes (Kok et al., 2004).

Several researchers have proposed that the stopping process is characterised electrophysiologically by the Stop-P3 (De Jong et al., 1990; Kok et al., 2004), but to date, none have provided any real evidence in support of this hypothesis. Instead these authors have relied on reasoning based around the relative timing of Stop-P3s in relation to estimated SSRT to substantiate their claim. By comparison, the current study was the first to relate a direct index of inhibition processing (SSRT) to Stop-P3 measures, whereby faster SSRT was related to both larger Stop-P3 amplitudes and a shorter time difference between Stop-P3 and Stop-N1 latency measures ('Stop P3-N1 latency'). These relationships were observed at the frontal electrode Fz for both left and right hand Stops, whereas correlations between Stop P3-N1 latency and SSRT at Cz and Pz were observed for right hand Stops but not left hand Stops. The consistency of the relationships between SSRT and Stop-P3 indices at Fz suggest a crucial role for frontal structures in stopping. Indeed, when these measures were correlated with Stop > Go contrast maps for individuals participating in both fMRI and ERP sessions, a significant relationship was observed within right lateral *pars orbitalis,* suggesting a crucial role for this brain area in processing stop-signals. However, given the small sample size, this finding should be taken with caution, and moreover, it should be noted this relationship was not significant when SVC correction was applied over the whole IFG.

These findings were the result of a novel approach for assessing SSRT and ERP latency relationships: strong positive correlations were found between SSRT and Stop P3-N1 latency, for left and right hands. There were two reasons for taking this 'peak latency difference' approach. The obligatory components of auditory evoked N1, represent the extraction of information from auditory stimuli, specifically indexing activation of the auditory cortices from brain stem projections (Näätänen, 1987), and therefore reflects registration of the stop-signal into working memory. Hence, the actual act of control that is manifest as the stop-signal inhibition process, which is thought to be revealed as a Stop-P3 cannot be launched until after the onset of N1. Secondly, P3 peaks at a much later latency than the usual estimate of SSRT (e.g., De Jong et al., 1990), again confirmed in this study. Therefore, while it is wrong to say that the latency of P3 peak amplitude reflects the end of stopping process, it may contain a lot of information about SSRT variability across participants.

It follows that the stopping process itself is launched and concludes somewhere between the onset of N1 and the peak of P3. In this study it was considered that the best guess for the latency of the stopping process that is determinable from ERP data was the difference between the latency of P3 and N1peaks; this Stop P3-N1 latency was related to SSRT, whereas P3 peak latency was not. Moreover, the correlation was positive indicating that shorter SSRT was related to shorter Stop P3-N1 latencies. This is the first stop-signal study to demonstrate a relationship between an electrophysiological index of stopping to a behavioural index of stopping.

While the relationships between SSRT and Stop-P3 measures provide the first solid evidence that Stop-P3 is tightly coupled to inhibition processes, there is other evidence of response activation suppression in the data. There is a negative going component peaking about 200 ms after stop-signal onset in Stop Failure waveforms (N2) that is superimposed on Stop Failure-P3 that is not present in Stop waveforms. In their stop-signal paper, Van Boxtel and colleagues (2001) first asserted that N2 was an index of stopping, but conceded that the N2 may in fact indicate greater motor activation in Stop Failure ERPs, in which N2 amplitude was greater. If the N2 in Stop Failures is actually a motor potential, then the relative timing of Stop-P3 compared to Stop Failure-N2 suggests that Stop-P3 reflects active suppression of this motor potential. However, Stop Failure-N2 could equally likely

be related to error monitoring processes – the error negativity (Ne: Falkenstein, Hohnsbein, Hoorman, & Blanke, 1991) or error related negativity (ERN: Gehring, Goss, Coles, Meyer, & Donchin, 1993). Indeed, the timing of this component – around 200 ms after stop-signal onset – suggests that this is a plausible explanation. However, these explanations are offered cautiously as stop-signal-N2 potentials were not assessed in the current investigation.

The ERP findings reported here have important implications for stop-signal theory. The race model depicts stopping as a race between independent go processes and stop-signal processes, and implies that Stop Failures result from late activation of stop-signal processes. The current data support this notion, indicated by the difference in the timing of Stop-P3 and Stop Failure P3, but extend it by suggesting that participants 'pre-select' stopping by biasing their attention toward auditory channels prior to the stop-signal, resulting in enhanced N1 during Stops compared to Stop Failures. This idea suggests that two completely different races occur during Stops and Stop Failures.

By analogy, the difference between Stops and Stop Failures is like comparing the performance of an athlete (stop processes, stop-signal P3) in two completely different races. In one race (resulting in a Stop), the athlete is 'at the mark' in position awaiting the starting gun (attending to the stop-signal). When the starting gun fires, the athlete clearly hears the gun (indicated by N1 modulation) and is off to a good start. In another race (resulting in a Stop Failure), the athlete is not focussed on the starting gun, and consequently, is not ready when it fires (no modulation of N1); the athlete is left stranded at the starting line by the other competitor(s) with no hope of making up the lost ground. Hence the start of the race – attending to the stop-signal - may be of equal or more importance to the race itself (between the stop process and the go process) in determining the outcome.

4.4.4. Integration of fMRI and ERP findings

Despite that SSRT was strongly linked to neurophysiological activity that is thought to represent stopping in both fMRI data (BOLD response in right IFG-STN: Aron & Poldrack, 2006) and ERP data (amplitude and latency measures of Stop-P3: Bekker et al., 2005a; De Jong et al., 1990; Kok et al., 2004), it is very likely that Stop-P3 and right IFG-STN activation are unrelated. This is evident from the different (opposite) relationships

revealed between SSRT and the fMRI and ERP measures: SSRT was positively related to BOLD signal intensity within right IFG-STN, whereas SSRT was negatively related to Stop-P3 amplitude. However, formal analyses to confirm independence between Stop-P3 amplitude and the right IFG-STN network was not undertaken largely because the evidence suggests that the relationship between ERP and fMRI correlates is tenuous (Huettel et al., 2004). Nonetheless, these findings suggest that Stop-P3 is unrelated to right IFG-STN activation, which is perhaps not surprising given that no (right) lateralisation of Stop-P3 was observed. If Stop-P3 and right IFG-STN are both crucially linked to stopping, the data reported here suggest that Stop-P3 reflects a subset of processes involved in the initiation of the stop response that may or may not lead to recruitment of the right IFG-STN network, which appears only to be required when stopping is difficult. If stopping for participants with faster SSRTs was effected at a point earlier in the go response activation cycle compared to participants with slower SSRTs, then Stop-P3 may be linked to attentional processes, perhaps orienting to the stop-signal. Interestingly, the negative correlation of SSRT onto Stops > Baseline contrast maps explained BOLD signal variance within ACC and MFG/PCG, both of which are heavily involved in attentional processing, especially biasing of auditory attention (Frith & Friston, 1996) and thus larger Stop-P3s may reflect greater selectivity of attention to the stop-signal.

4.4.5. Conclusions

In conclusion, this study showed that a fronto-parietal network including right MFG, IFG, SMA and IPL is generically activated for stop-signal response inhibition, however, the proposed 'hyperdirect' stopping network, consisting of right IFG and STN, was differentially engaged depending upon the difficulty of stopping. Within right IFG, *pars opercularis* was particularly critical for difficult inhibition. Additionally, stop-signals were related to elicitation of N1 and P3 event-related potentials that were generally larger for Stops than for Stop Failures. N1 enhancement was most marked at central sites, particularly Cz, whereas Stop-P3 was larger than Stop Failure-P3 at both frontal and central sites. Also, the peak latency of Stop-P3 occurred earlier than Stop Failure-P3 consistently across all sites. Most importantly, direct evidence was found linking Stop P3 to stopping. Firstly, a strong inverse correlation was observed between SSRT and P3 peak amplitude at

Fz indicating that faster inhibitors elicit larger frontal P3s. Perhaps more telling though, was that SSRT was positively related to the temporal difference between P3 and N1 peak latencies at Fz. These behavioural-electrophysiological relationships provide the first indications that frontal regions of the brain and possibly PFC are involved in stopping.

Chapter 5: A brief introduction to schizophrenia

"Schizophrenia is arguably the worst disease affecting mankind, even AIDS not excepted."

- 1988 editorial appearing in Nature 336(10), pp95 – 96.

5.1. What is schizophrenia?

5.1.1. Introduction

Since the year of this Nature editorial, investigators have learned a great deal regarding the neuropathology of schizophrenia and its effects, but these efforts have offered little insight into the mechanisms of pathogenesis and the on-going organic and psychological deterioration seen over the course of illness in many patients. With the exception of second generation antipsychotic drugs, little has changed for individuals living with this most insidious of disorders; the disorder that has been described, perhaps without sensitivity but certainly not without basis, as 'madness'.

Schizophrenia is linked to profound disturbance in popular culture, however, what is less emphasized is the tragedy of schizophrenia disorders; those affected experience a loss of their sense of self, and many commit suicide (5-13%) and many more to attempt suicide (20-40%; Pompili et al., 2007). By comparison, the World Health Organisation (WHO) reports a suicide rate of approximately 0.01% in the whole Australian population. Hence, people with schizophrenia are at least five hundred times more likely to commit suicide than members of the general Australian population. Others affected by this disorder are the families and friends of individuals with schizophrenia who endure a vast emotional burden as they watch their loved one slowly become a stranger who is utterly dependent on others for survival (Magliano et al., 1999; Willick, 1994). These issues weigh in addition to perhaps less salient factors that include substantial social and economic impacts on the individual sufferer, their families, and national health budgets (Andlin-Sobocki & Rössler, 2005; Goeree et al., 2004; Jablensky, 2000a; Knapp, Mangalore & Simon, 2004).

5.1.2. Prevalence and incidence

The prevalence of schizophrenia is equiprobable amongst the sexes, but there is a greater incidence in male populations that contribute to a total incidence rate of around 0.015% (McGrath et al., 2004). It is well established that symptoms appear earlier in males than females, with males typically diagnosed in their late teenage years or early twenties and females diagnosed in their late twenties to early thirties (mean difference of 4-6 years; Jablensky, 2000b). National prevalence estimates of schizophrenia vary little across studies and countries, and are usually reported in the range 0.4 - 1.5%, however developed nations tend have higher prevalence rates than developing nations (Saha et al., 2004; Jablensky, 2000b), and higher prevalence is consistently observed in urban areas compared to rural areas (Barbato, 1998). Studies of regional variability by the World Health Organisation have revealed much higher prevalence rates in some isolated communities of Europe and North America, and in marginalized indigenous communities in Australia and Canada (Barbato, 1998; Warner & de Girolamo, 1995). The augmentation of prevalence in these areas has been largely attributed to out-migration of healthier individuals, and genetic isolation. However, social stress induced by exposure to western lifestyles is thought to have increased the vulnerability to psychosis of at-risk individuals (Barbato, 1998; Jablensky & Sartorius, 1975).

5.1.3. Diagnostics

Symptomatology

The wide range of clinical features displayed by patients falling within the schizophrenic spectrum was first recognized as a group of related disorders by German psychiatrist Emil Kraepelin when he differentiated psychotic patients with a good prognosis from others who exhibited a deteriorating course of illness (Pantelis, 1996). He described the condition of the former group as ‘maniacal-depressive insanity’, and the condition of the latter group as ‘dementia praecox’. The latter were clinically distinguishable by the presentation of symptoms including emotional and affective flattening, impulsive behaviour, and the absence of goal-directed behaviour. Despite delineating a range of heterogenous symptoms, Kraepelin, like his influential contemporary, the Swiss psychiatrist Eugen Bleuler (who coined the term ‘schizophrenia’ meaning ‘split-mind’),

emphasised symptoms that represent a decline in cognitive and emotional functioning as being the core features of dementia praecox or schizophrenia (Andreasen, 1997). Later thinkers, especially Karl Jaspers and Kurt Schneider, shifted the emphasis to the more salient florid psychotic symptoms including hallucinations and delusions (Andreasen, 1997).

There is currently no diagnostic test(s) for schizophrenic disorders. Instead diagnosis relies on self reported information regarding symptoms from the patients themselves (e.g., hearing of voices), and careful observation of signs of symptoms (e.g. flattened affect) by highly trained health professionals. The scope of currently recognized criteria for schizophrenic symptomatology is outlined in the fourth edition of the Diagnostic and Statistical Manual of Mental Disorders (DSM-IV; American Psychiatric Association), and the tenth edition of the WHO sponsored International Classification of Diseases (ICD-10; World Health Organization), both of which are used to guide clinical diagnoses.

The heterogeneous nature of symptoms that occur in schizophrenia often makes precise diagnosis difficult and a diagnosis is not generally given due to the presence of any one symptom but due to the presence of clusters of symptoms. The spectrum of symptoms are classified in two broad categories in DSM-IV; symptoms involving distorted cognitions are called 'positive symptoms', while symptoms related to a decline in normal cognitive, emotional and behavioural functions are termed 'negative symptoms'. Some groups have challenged this generic two factor model with the charge that it does not account well for the heterogeneity of symptoms, and proposed multi-factorial models. Noted amongst these nosologies are the three factor models of Liddle (1987) (reality distortion, disorganisation and psychomotor poverty) and Arndt et al. (1991) (delusion/hallucination dimension, disorganisation dimension, and a modified negative syndrome), and a five factor model proposed by Lindenmayer and colleagues (negative, positive, cognitive, excitement, and depression/anxiety) (Lindenmayer, Grochowski, & Hyman, 1995).

The manifestation of overt clinical symptoms usually follows either an acute trajectory, where a psychotic state ('active phase') develops over days or weeks, or symptoms develop more gradually, preceded by a protracted stage of symptom emergence ('prodromal phase'). Prodromal symptoms are negative-like symptoms and include a decline in functioning either in occupational settings, interpersonal relationships, or

personal hygiene, in addition to odd beliefs and behaviours. A full analysis of the symptoms of schizophrenia and their diagnosis is beyond the scope of this thesis (for review see Andreasen, Arndt, Alliger, Miller & Flaum, 1995), but those outlined in DSM-IV are briefly summarised below:

Positive symptoms

Positive symptoms are the dominant feature of the active phase of illness, and include delusions, hallucinations, disorganized speech and disorganized or catatonic behaviour. These symptoms fluctuate over time; they can be severe during the active phase of illness, but practically absent during residual phases.

- *Delusions* are mistaken beliefs arising from the misrepresentation of perceptions and experiences. Examples of these include: the individual believing they are being followed by the CIA (paranoid delusions); the belief that news items or song lyrics are directed at the individual with some secret/special meaning (delusions of reference); that the person is an important figure such as Jesus Christ (delusions of grandeur); that the person's thoughts have been extracted by an external agency or another's thoughts have been inserted into his or her mind or that the individual's will is being controlled by some external agency (delusions of control).
- *Hallucinations* are sensory perceptions that are outside the range of normal experience and may arise in any sensory modality, but are most often auditory. Auditory hallucinations typically take the form of voices conversing, or voices commenting on the individual's thoughts and behaviour, however some individuals experience voices telling them to perform a specific act. Hallucinatory voices may address the individual in the second person (e.g., "Get out of bed!") or third person (e.g., "He wants to get out of bed.").
- When a patient displays *disorganized speech,* he or she may display pressured speech, jump between topics in conversation, or produce answers that are unrelated or loosely related to a question asked. In severe cases speech may be completely incoherent and resemble so-called 'word salad'. The symptoms of disorganised speech are due to '*formal thought disorder*', that refers to a disruption to the normal

linkage of thoughts which manifests as disordered speech, and is unrelated to other disorders of thought such as delusions.

- *Disorganized behaviour* is present when a patient exhibits a marked decline in goal-directed behaviour and experiences difficulty performing normal life activities (e.g. meal preparation, personal hygiene). These patients often appear disheveled, or dress in an unusual way. Others display inappropriate or agitated behaviour (e.g. random shouting and swearing).
- *Catatonic behaviour* ranges from complete unawareness to unprovoked excessive activity. Generally, however, patients display a significant reduction in responsiveness to environmental stimuli, but may assume rigid postures and resist being moved, or resist instructions and attempts to be moved.

Negative Symptoms

Negative symptoms are the most disabling of symptoms in schizophrenic illnesses, and represent a decline in normal functioning. Emphasizing their enduring nature, Kraepelin saw these symptoms as a definitive feature of schizophrenia. Negative symptoms are generally resistant to medication, although second generation (atypical) antipsychotic medications are more effective in treating these symptoms than first generation drugs (Chakos, Leiberman, Hoffman, Bradford & Sheitman, 2001), but the apparent therapeutic effect of second generation antipsychotics may be due to a reduction in the severity of side effects[31] linked to atypical therapies compared to side effects arising from administration of first generation drugs (Leucht, Pitschel-Walz, Engel & Kissling, 2002; Kapur & Mamo, 2003).

- *Flattened affect* is a common symptom in schizophrenia and refers to a reduction in both emotional responsiveness and responsiveness to environmental stimuli.
- *Alogia* refers to a marked reduction in the contents of speech which is thought to derive from a curtailment of thought.
- *Avolition* refers to the inability to engage in, or persist with, goal-directed activities.

[31] Especially 'extrapyramidal side effects' - detailed below.

- *Anhedonia* refers to the inability to experience pleasure, often leading to a marked state of asociality. Patients will often withdraw from social interaction with others, even family relations, preferring a solitary existence.

Diagnosis

A diagnosis of schizophrenia is generally given when an individual displays two or more of the above symptoms that must be present most of the time for a period of at least one month. However, when delusions are sufficiently bizarre, or the individual reports hallucinations involving voices commenting on their behaviour or voices conversing (defined as first and second order hallucinations respectively), then one of these symptoms alone is sufficient for a diagnosis to be given.

The DSM-IV lists five essential diagnostic classifications for schizophrenia that are defined according to presenting symptomatology, including:

- Paranoid type - presence of delusions and hallucinations only.
- Disorganised type - presence of thought disorder and a flattened affect.
- Catatonic type - presence of salient psychomotor disturbances.
- Undifferentiated type - presence of psychotic symptoms but only when criteria for paranoid, disorganized or catatonic types are not met.
- Residual type - presence of mild positive symptoms only.

5.2. Underlying causes of schizophrenia

5.2.1. Theories

Since the time of Kraepelin, schizophrenia research has grown exponentially, but advances in knowledge regarding the pathology underpinning schizophrenia spectrum disorders have occurred slowly, leaving the mechanisms of pathogenesis equally inexplicable to contemporary thinkers as during earlier times. Throughout his life, Kraepelin believed that schizophrenia arises due to disruption of normal

neurodevelopmental processes that are affected by a chronic metabolic 'autointoxication' (Noll, 2007). Noting the age of symptom onset in most patients, he (tentatively) hypothesised that a bodily toxin is secreted from the sexual organs (gonads) into the circulatory system during sexual development that begins to poison the body, thus beginning the road to psychosis. In later years, factors aside from neurobiological causes were apportioned roles in the onset of schizophrenic psychopathology, notably psychosocial and environmental factors. Contemporary theories of schizophrenia allow for a range of causative factors in the onset of clinical symptoms, but the focus of research efforts is to understand the neurobiological mechanisms of pathogenesis and the consequent pathology that is responsible for the expression of positive and negative symptoms.

What has been well established is a primary role for genetic factors that is well illustrated by the finding that while the lifetime risk for the general population is around 1%, in approximately 48% of monozygotic twins, both twins will exhibit clinical symptoms of schizophrenia if at least one has the disorder, while in dizygotic twins, about 17% of twins will share a diagnosis if one has the disorder, which is about the same level of risk for first degree relatives (e.g., children of a parent with schizophrenia) (Gottesman, 1991). Second degree relatives (e.g., grandchildren of a grandparent with schizophrenia) have about 6% chance of developing symptoms, while 2 % of individuals with a third degree relative (e.g., first cousin of a person with schizophrenia) with a diagnosis will similarly express clinical symptoms (Gottesman, 1991). These findings have been validated by adoption studies that have shown that risk is related to the biological parents, not adoptive parents (Gottesman & Shields, 1982).

Notwithstanding these powerful links, researchers have recognized a range of causative factors in various models of pathogenesis and relapsing symptomatology of schizophrenia. Some models, most notably diathesis-stressor models (Rosenthal, 1970; Zubin & Spring, 1977), emphasise the interaction between genetic factors and environmental stressors in the emergence of symptomatology. These models suggest that a genetic loading renders an individual vulnerable to the development of psychoses, but a psychosis develops due to the interaction between the genetic abnormality and the negative influence of stressful events. One environmental factor that has been particularly influential in explaining psychotic relapses is negative *emotional expression* (EE; refers to affective

style) in families caring for a relative with schizophrenia (Leff & Vaughan, 1985, as cited in Gottesman, 1991).

Other thinkers have proposed that schizophrenia is a neurodegenerative disease stemming from either prodigious excitatory (glutamatergic) neurotransmission (Javitt & Zukin, 1991), or abnormal neural development (Harrison, 1997). Other models implicate maternally derived pathogens, such as influenza, that interact with the foetus in-utero causing abnormal neural development, and consequently a predisposition to schizophrenia (Brown et al., 2004).

While the antecedents of schizophrenia remain controversial, some consequences of this trajectory have been intensively studied. This is particularly the case for disrupted neurotransmission involving the dopaminergic and glutamatergic neurotransmitter systems, both of which are fundamental to the smooth operation of cognitive and behavioural processes. Enhanced dopaminergic activity is thought to be involved in the expression of positive symptoms (Abi-Dargham & Moore, 2003; Abi-Dargham et al., 2000; Abi-Dargham et al., 1998; Laruelle et al., 1996; Lindström et al., 1999; Meyer-Lindenberg et al., 2002; Wong et al., 1986), while attenuated glutamatergic activity is mostly associated with the expression of cognitive impairment and negative symptoms (Coyle, 2006; Goff & Coyle, 2001).

5.2.2. Neurotransmitter systems and schizophrenia

The role of dopamine in schizophrenia

The most enduring model of neuropathology in schizophrenia is 'the dopamine hypothesis of schizophrenia' first described by Carlsson and Lindqvist (1963). This model derived from observations in the 1950s of the psychotherapeutic effects of preparations containing dopamine antagonists (i.e., act by reducing dopaminergic activity) that were administered to psychotic patients; in a majority of cases, these preparations ameliorated what are now called the positive symptoms of schizophrenia (Kapur & Mamo, 2003).

Since the years of the discovery of the prototype chlorpromazine, these drugs have become known as 'antipsychotics' or 'neuroleptics', the latter meaning 'to seize the

neuron', Chlorpromazine is an antihistamine with strong tranquilising properties that effect a state of indifference without the loss of consciousness, and was first used in humans by French surgeon Henri Laborit as a surgical anesthetic. Later, other Frenchmen including, Jean Delay and Pierre Deniker, began therapeutic trials with in-patients and reported that chlorpromazine also exhibits therapeutic effects on florid psychotic symptoms in patients with schizophrenia that were concomitant with well known tranquilising effects of chlorpromazine (Kapur & Mamo, 2003).

Many years passed before researchers learned the psychotherapeutic effectiveness of these medicines lay in their ability to block (i.e., affinity for) dopamine receptors within the dopaminergic system, especially D2 dopamine receptors (Creese, Burt & Snyder, 1975; Seeman, Chau-Wong, Tedesco & Wong, 1975; Seeman & Lee, 1975). The first generation of antipsychotic medicines are known as 'typical' antipsychotics, and include: chlorpromazine, fluphenazine, haloperidol, molindone, thiothixene, thioridazine, trifluoperazine, loxapine, perphenazine, prochlorperazine, pimozide, and zuclopenthixol.

Dopaminergic pathways and antipsychotics

The dopaminergic system involves four major neural pathways, the tuberoinfundibular, nigrostriatal, mesolimbic, and mesocortical pathways, respectively, that have key roles in regulating the activity of cortical and sub-cortical brain structures. The neurochemical action of antipsychotics within these pathways is responsible for both the therapeutic effects these medicines afford, and the debilitating side effects that often come with their use.

Mesolimbic dopaminergic neurons emanate from the ventral tegmentum (or ventral tegmental area, VTA) in the basal ganglia and form a pathway that projects to the nucleus accumbens, hypothalamus, amygdala, and hippocampus. The mesolimbic pathway has a key role in reinforcement and reward learning and behaviour, in addition to a consequent role in addictive behaviours, especially those involving drugs of addiction (Montague, Hyman & Cohen, 2004; Pierce & Kumaresan, 2006). High doses and chronic use of drugs that act by elevating dopaminergic activity (dopamine agonists) within mesolimbic neurons results in symptoms that parallel those observed in schizophrenic psychoses (Angrist & Gershon, 1970). Common dopamine agonists include methylphenidate (amphetamine

derivative used in the treatment of ADHD), levodopa (a dopamine derivative used in the treatment of Parkinson's disease), amphetamines and cocaine. Enhanced dopaminergic activity within the mesolimbic pathway has been linked to the manifestation of psychotic symptoms (Abi-Dargham & Moore, 2003; Abi-Dargham et al., 2000; Laruelle et al., 1996; Lindström et al., 1999; Meyer-Lindenberg et al., 2002; Wong et al., 1986).

PET studies have been especially informative in supporting the initial hypothesis that excessive dopaminergic activity was the basis of schizophrenic symptomatology. Research over the last twenty years has indicated that, compared to healthy controls, schizophrenia patient groups display enhanced dopamine synthesis in the striatum (caudate nucleus; Wong et al., 1986), and increased concentrations of dopamine D2 receptors in striatal nuclei (caudate and putamen) and medial PFC (Lindström et al., 1999). More interestingly, Laruelle and colleagues (1996) used single photon emission tomography (SPET) to examine striatal dopaminergic activity in patient and control groups after administration of a low dose of amphetamines. Though only a low dose was administered some patients developed psychotic symptoms in the course of the experimental procedure. Striatal dopamine was also elevated in both patient and control groups, but dopamine release was over two and a half times greater in patients, and the level of dopamine release was correlated with the expression of symptoms. In support of these findings, more recent investigations have reported a link between the level of dopaminergic activity in mesolimbic neurons, especially in the striatum, and the severity of positive symptoms (Abi-Dargham & Moore, 2003; Abi-Dargham et al., 2000; Meyer-Lindenberg et al., 2002).

Researchers consider that abnormal dopaminergic activity within another primary dopaminergic pathway, the mesocortical pathway, has a crucial role in the manifestation of negative symptoms and cognitive impairments present in many patients with schizophrenia. Like mesolimbic neurons, mesocortical neurons emanate from the VTA and (dorsal) striatum, but project to wide areas of PFC, including orbital, medial, and cingulate cortices, and most notable in the account of schizophrenia, to DLPFC. In contrast to mesolimbic neuropathology, mesocortical neuropathology corresponds to hypoactivity of PFC, resulting in decreased stimulation of PFC dopaminergic D1 receptors. PFC hypoactivity is thought to be responsible for the negative symptoms (and their severity) and cognitive impairments in schizophrenia (Weinberger, 1987); negative symptoms are unlike the

(positive) symptoms that manifest in patients with subcortical lesions, but are analogous to the symptomatology of frontal patients, particularly individuals with lesions to DLPFC (Weinberger, 1987; Weinberger, Berman & Zec, 1986).

The contemporary view of dopaminergic contribution to schizophrenic symptomatology is that symptoms arise from a cortico-subcortical imbalance of dopaminergic function that is facilitated by reciprocal connections between these neural areas (Abi-dargham & Moore, 2003; Tzschentke, 2001). One function of PFC D1 dopamine receptors is to modulate striatal dopamine release; hypoactivation of this frontal system disinhibits subcortical targets of affected PFC projection neurons, resulting in enhanced striatal dopamine D2 receptor activity (Abi-dargham & Moore, 2003; Stone, Morrison & Pilowsky, 2007). These findings have led to the view that the negative symptoms and cognitive impairments ensuing from hypoactivation of the PFC dopaminergic system is primary in the emergence of schizophrenic symptomatology, and that consequent striatal dopaminergic hyperactivity is a secondary effect (Andreasen, 1999).

The tuberoinfundibular pathway projects from the arcuate nucleus in the medio-basal hypothalamus to the pituitary gland via the median eminence. Dopamine transmission through these projections modulates the release of some hormones in the anterior pituitary gland, most notably prolactin, which serves multitudinous biological roles, not the least of which is modulating homeostasis in mammals. Dopaminergic antagonism in these neurons leads to increased blood levels of prolactin ('hyperprolactinaemia') which is common in patients receiving typical antipsychotic medication, and is absent in unmedicated patients. Symptoms of hyperlactemia include galactorrhoea (spontaneous milk discharge from the breast that is unassociated with nursing), oligomenorrhoea (infrequent uterine bleeding), amenorrhoea (absence of menses in female of reproductive age), disrupted ovulation, sexual dysfunction, reduced bone mineral density and cardiovascular disease (for review see Meaney & O'Keane, 2002).

Arguably the most debilitating side effects of antipsychotic therapies arise from disruption to dopaminergic activity in nigrostriatal neurons; it is this pathway that is affected in Parkinson's Disease, the symptoms of which manifest when 80-90% of dopaminergic function is lost. Nigrostriatal neurons are part of the basal ganglia motor loop

that emanate from both the substantia nigra *pars compacta* and VTA, and project to the ventral striatum. Diminishment of dopaminergic activity within these neurons causes downstream disruption to their targets in the extrapyramidal system. Extrapyramidal neurons form part of the motor system involved in movement co-ordination, and are most common in the reticular formation of the pons and medulla. These neurons do not target spinal motor neurons as pyramidal neurons do, but instead innervate spinal neurons involved in reflexes, postural control, locomotion, and complex movements, and are in turn modulated by projections from the basal ganglia (especially nigrostriatal projections), cerebellum, vestibular nuclei and sensory cortical areas. Both acute and chronic therapy using typical antipsychotics induce extrapyramidal syndromes, including dystonia (involuntary sustained muscle spasms generally causing repetitive movements and abnormal posturing), Parkinson's symptoms, akathisia (painful feelings of inner restlessness and apathy), akinesia (difficulty initiating movement), dyskinesia (involuntary choreoathetoid and stereotyped movements such as tics), depression and cognitive impairments (Tandon & Jibson, 2002). These syndromes, collectively termed *extrapyramidal side effects* (EPS), can occur acutely or after chronic therapy and have been linked to non-compliance (Buchanan, 1992), relapse (Frances & Weiden, 1987), and an increased risk of suicide (Whitworth & Fleischhacker, 1995).

Investigators have found that EPS were due to non-selective blocking of dopamine receptor binding sites throughout the dopaminergic system. The 'good' antipsychotic action of blocking D2 receptors in mesolimbic neurons was offset by the debilitating effects of this same process on other dopaminergic pathways. Due to the presence of EPS, medications used to treat Parkinsons Disease (especially levodopa) which act by enhancing dopamine levels, in addition to anti-cholinergic medications (e.g., benztropine) which act by competitive binding at acetylcholine receptors in the central and peripheral nervous system, are prescribed to badly affected patients.

The most common EPS are dyskinesia syndromes often seen in patients who have endured chronic therapy with typical antipsychotics; due to the late onset of this syndrome, it is generically termed 'tardive dyskinesia'. While the exact causes of tardive dyskinesia are unknown, it is thought to arise from supersensitivity of dopamine receptors (especially D2 receptors) within nigrostriatal neurons.

However, one antipsychotic drug therapy, clozapine, that originally gained pre-eminence due to its ability to produce antipsychotic effects in patients who were unresponsive to other antipsychotic medications (Kane, Honigfeld, Singer, & Meltzer, 1988), was also found to induce remarkably fewer EPS than other psychotics (King & Voruganti, 2002). Administration of clozapine also led to little or no blood level prolactin increase (Kane, Cooper & Sachai, 1981), and some studies have observed a diminishment of negative symptoms (Leucht et al., 2002), though this latter finding remains controversial (Kapur & Mamo, 2003). Because of the atypical therapeutic profile of clozapine, particularly the ability to produce antipsychotic affects without EPS, it is called an 'atypical' antipsychotic. Subsequently developed atypical antipsychotics include risperidone, olanzapine, quetiapine, sertindole, ziprasidone, aripiprazole and amisulpride.

What makes atypical antipsychotics atypical is largely unknown, however there are two prominent theories. The first theory suggests the dual action of clozapine at dopamine D2 receptors and serotonin 5-HT2 receptors (clozapine has a higher affinity for 5-HT2 receptors than dopamine D2 receptors, and also acts on dopamine D1, D4, histamine H1, and muscarinic M1 receptors) underpins atypicality, however, Kapur and Mamo (2003) point out that that action at this serotonergic receptor is '…neither necessary nor sufficient for atypical activity'. A second theory posits that atypicality stems from a lower affinity of clozapine for dopamine D2 receptors, due to a faster dissociation (or 'off ') rate from the receptor, which better accounts for atypicality than 5-HT2 affinity (Kapur & Seeman, 2001). While the basis of atypicality remains controversial, it is without doubt that atypical antipsychotics are more tolerable for patients.

Recent evidence implicates a fifth dopaminergic subsystem that is potentially more important in the emergence of schizophrenia than the subsystems previously mentioned. Using an immunolabelling technique in primate (macaque monkey) and human brains, Sánchez-González and co-workers (2005) found extensive dopaminergic innervation of the thalamus in each species, particularly in discrete areas of association, limbic and motor thalamic nuclei, and the innervation of these areas was at least as concentrated as any cortical area rich in dopaminergic neurons. Subsequent retrograde labelling revealed that these neurons projected from the hypothalamus, periacqueductal grey area, ventral mesencephalon and the lateral parabrachial nucleus. This newly discovered dopaminergic

system has been termed the ‘thalamic dopaminergic system’. The relevance of this finding to schizophrenia is supported by previous neuroimaging reports of prominent thalamic abnormalities in the brains of individuals with schizophrenia (Andreasen et al., 1994; Harms et al., 2007; Konick & Friedman, 2001; Yasuno et al., 2004).

Despite the weight of evidence regarding dopaminergic dysregulation in the neuropathology of schizophrenia, clinical observations have unveiled a temporal disjunction in the efficacy of antipsychotics that has largely discredited the view that dopamine abnormality alone is responsible for schizophrenia. In particular, it has been shown that dopamine receptor occupancy occurs within hours of antipsychotic administration, while the clinical response is not observed for several days, and moreover, cessation of antipsychotic administration results in a decline of dopamine receptor occupancy within days while relapse half-life is in the order of months (Kapur & Mamo, 2003; Kapur, Zipursky, Jones, Remington & Houle, 2000; Pilowsky et al., 1993). Contemporary theories posit a central role for abnormal glutamatergic (glutamate is the primary excitatory neurotransmitter in the brain) activity in schizophrenia (Coyle, 2006; Olney, Newcomer, & Farber, 1999).

The role of glutamate in schizophrenia

A potential role for abnormal glutamatergic neurotransmission in schizophrenia was first suggested after observations of psychotomimetic effects that are induced by ingestion of NMDA receptor antagonists, particularly phencyclidine (‘PCP’ or colloquially ‘Angel Dust’) and ketamine (colloquially ‘K’ or ‘special K’), in otherwise healthy adults and patients with schizophrenia in remission (Javitt & Zukin, 1991; Stone et al., 2007). Most striking was that these effects not only elicit positive symptoms, but also negative symptoms. Therefore, the symptoms elicited resemble more closely those of schizophrenia than those produced by ingestion of dopamine agonists such as amphetamines and cocaine.

Researchers now know these effects result from blocking the normal interaction of glutamate and NMDA receptors on post-synaptic membranes of GABAergic interneurons (Farber, 2003; Olney et al., 1999). A normal function of GABAergic interneurons is to tonically inhibit the activity of their targets, which include two major excitatory pathways: a cholinergic system emanating from the basal forebrain, and the other, a glutamatergic

system emanating from the thalamus. The neurons forming these pathways innervate primary cortical neurons; activity within these cholinergic and glutamatergic pathway neurons is modulated by recurrent inhibitory collaterals that originate on the primary cortical neurons and subsequently terminate on (previously mentioned) GABAergic interneurons. Administration of NMDA antagonists disrupts the inhibitory tone of these pathways that is normally provided by GABAergic interneurons, disinhibiting excitatory cholinergic and glutamatergic projections, allowing them to hyper-stimulate their primary cortical targets that are consequently also unregulated. This hyperstimulation is thought to be responsible for the psychotomimetic effects of glutamate antagonists, and the positive symptoms observed in schizophrenic psychoses. This model (the 'NMDA receptor hypofunction hypothesis'; Olney & Farber, 1999) is seductive for reasons aside from this link: it can potentially account for both the developmental trajectory of schizophrenia and the neurodegenerative changes that accompany chronic illness.

Studies using PCP and ketamine rat models have shown that hyperactivity within the aforementioned cholinergic and glutamatergic pathways results in morphological changes to target primary neurons (Olney & Farber, 1995). These changes are reversible after brief periods of NMDA receptor blockade by atypical antipsychotics. However, chronic blockade renders irreversible neuronal changes and eventually neuronal atrophy, particularly in retrosplenial cortex and corticolimbic areas. Even after affected neurons die, hyperactive neurons continue to fire and consequently release relatively large amounts of glutamate and acetylcholine into the cerebral cortex. Olney and Farber (1999) suggest these excitotoxic processes may be responsible for the clinical deterioration, the manifestation of enduring negative symptoms, positive symptom 'burnout', and progressive cognitive decline seen in chronic schizophrenia.

The developmental aspects of NMDA hypofunction are equally interesting, and rest upon several inter-related lines of evidence. Administration of NMDA antagonists to juvenile animals does not result in excitotoxicity as it does in adult animals, and NMDA antagonists do not induce psychoses in human children as they do in adult humans. This age dependence of NMDA antagonism in eliciting psychotomimetic effects in humans, and excitotoxicity in animals, mirrors the age-at-onset profile of schizophrenia quite remarkably (Olney & Farber, 1999). This process also occurs in serotonergic and noradrenergic

neurons that provide similar inhibitory functions through glutamate-NMDA receptor interaction.

The effects outlined above of altered neurotransmission are thought to be responsible for the breakdown of normal cognitive function that is present in the onset of schizophrenia. To elucidate the functional consequences of this illness, researchers have attempted to understand neuropathology in terms of cognitive impairment.

5.3. Neuropsychological functioning in schizophrenia

5.3.1. Neuropsychological measures as diagnostic criteria

Both Kraepelin and Bleuler emphasised impairment of cognitive functioning in their descriptions of patients they diagnosed with dementia praecox and schizophrenia, respectively. Indeed Kraepelin considered that impaired cognitive abilities were characteristic of dementia praecox, particularly attention and memory functions that seemed consistently impaired (Pantelis, 1996). But after one hundred years of documenting cognitive impairment in patients with schizophrenia, current diagnostic criteria do not recognise impairment of any aspect of cognition to be a mitigating nosological factor for diagnosis or typology. However, theorists and clinicians have historically been dissatisfied with pre-eminent nosologies of schizophrenia largely because of the heterogeneity of symptom profiles of patients that has been poorly accounted for by standard diagnostic criteria. This dissatisfaction has motivated contentious debate among theorists, and led to the proposal of several noted alternative typological models for schizophrenic disorders (see Liddle, 1987; Arndt, 1991; Lindenmayer et al., 1995).

In the search for the core features of schizophrenia, researchers have turned their focus to the study of cognition with the hope of identifying endophenotypic markers for the disorders. This new paradigm of schizophrenia research has returned a more detailed picture of illness, and reconciled some thinkers to the notion that neuropsychological changes are of equal importance in the account of schizophrenia as classical symptoms, and moreover, that classical symptoms and neuropsychological changes may be vitally linked

(Pantelis, 1996). The predominant view of schizophrenia is that illness originates with dysfunction at the genetic level resulting in a 'lesion[32]' during development (Weinberger, 1987). The effect of the 'lesion' is relatively benign during early development, becoming pathologically active during later development, probably during sexual maturation, and remains active during the course of life (Noll, 2007). In some cases, the pathological effects of the 'lesion' remain relatively dormant into adulthood, but interact with internally or externally stimulated psychological stressors during the lifetime of affected individuals inducing classical symptoms. In terms of overt illness, the critical effect of this 'lesion' is disruption to the normal function of some populations of neurons, the expression of clinical symptoms (outlined earlier) and abnormal cognition. As noted earlier, there is currently no diagnostic test for schizophrenia, however there is mounting evidence that neural dysfunction is detectable via neuropsychological assessment prior to the manifestation of overt symptom manifestation, and thus neuropsychological assessment may one day be pivotal in detecting predisposition to illness, in addition to serving other clinical purposes.

However, the neuropsychological account of schizophrenia is complex, and the performance of individual patients is widely heterogeneous, with individuals falling somewhere between the normal range and dementia level impairment (Kremen et al., 2000; Kremen et al., 2004). Many investigations have failed to observe impairment that could not be explained by a decline in general IQ, or differences in task difficulty, prompting some to argue that the pattern of impairment represents a global decline in neuropsychological function rather than selective impairment of specific functions (Blanchard & Neale, 1994). But this view is not pre-eminent; in an influential meta-analysis, Heinrichs and Zakzanis (1998) found that patients with schizophrenia were most impaired on tasks probing memory, attention, language, spatial ability, motor skills and executive functions.

5.3.2. Neuropsychological impairment in schizophrenia

More recent evidence suggests that the function of several core sets of processes, involved in aspects of memory (Glahn et al., 2003; Goldman-Rakic, 1994; Riley et al., 2000; Saperstein et al., 2006; Silver, Feldman, Bilker & Gur, 2003; Cirillo & Seidman,

[32] In this context, 'lesion' refers to some localised abnormality occurring early in life that affects global development and is thus presented within quotes. This 'lesion' may be neural or non-neural.

2003;), attention (Chen & Faraone, 2000; Elvevag & Goldberg, 2000; Harris, Minassian & Perry, 2007; Liu et al., 2002) and executive functions (Chan, Chen, Cheung & Cheung, 2004; Hutton et al., 1998; Joyce et al., 2002; Pantelis et al., 1999; Riley et al., 2000) are uniquely impaired.

Well established measures of attention, memory and executive function have been successful in detecting cognitive impairment in at risk individuals (Davalos et al., 2004; Glahn et al., 2003; Mohamed, Paulsen, O'Leary, Arndt, & Andreasen, 1999; Ross et al., 2008) and prodromal patients (Lencz et al., 2006), while severe impairments have been reported in first episode patients (Hutton et al., 1998; Riley et al., 2000; Saykin et al., 1994). Fortunately, cognitive function seems to stabilize in the residual phase of illness (Hyde et al., 1994; Rund, 1998), and longitudinal studies indicate that cognitive stability is preserved over time regardless of baseline impairment or changes in positive and negative symptoms (Heaton et al., 2007; Rund, 1998). While there is no conclusive evidence linking symptoms to neuropsychological impairment, it is widely accepted that impaired cognitive functioning is an essential feature of schizophrenia (Elvevag & Goldberg, 2000; Goldman-Rakic, 1994; Heinrichs & Zachzanis, 1998; Mitchell, Elliot & Woodruff, 2001; Rund, 1998), particularly given that the degree of impairment is strongly predictive of functional outcome (Green, 1996), whereas symptoms, positive symptoms in particular, are not.

5.3.3. Executive functions, attention and memory impairments in schizophrenia

Executive functions are higher-order neuropsychological functions that enable goal-directed thought and behaviour through engagement and control of subordinate systems (Roberts & Pennington, 1996; Stuss, 2006). These functions are vital in novel situations, and entail the ability to co-ordinate activity in multiple subordinate systems simultaneously, and to flexibly interrupt and change between intentions and actions. Impairment of the executive system is increasingly recognised as a mitigating factor in the neuropsychological profiles of patients with schizophrenia (Chan et al., 2004; Chan, Chen, Cheung, Chen, & Cheung, 2006; Hutton et al., 1998; Joyce et al., 2002; Pantelis et al., 1999; Riley et al., 2000).

While executive dysfunction has become prominent in recent accounts of schizophrenia, impairment of attention was a feature highlighted by Kraepelin in his

descriptions of Dementia Praecox (Kraepelin, 1919); subsequently, many studies have demonstrated impaired capacities of attention in schizophrenia patients. Arguably the most noted aspects of attention that are impaired in schizophrenic illness are selective (Kane & Engel, 2002) and sustained attention (Chen & Faraone, 2000; Liu et al., 2002). Selective attention refers to the ability to maintain a cognitive/behavioural set while ignoring distracting stimuli that compete for allocation of attentional resources, while sustained attention refers to the ability to maintain the goals of behaviour over time (Michie et al., 2000).

Several aspects of memory are often impaired in schizophrenia patients, but most apparent are working memory (Goldman-Rakic, 1994; Perlstein, Carter, Noll & Cohen, 2001; Barch et al., 2001) and verbal declarative memory impairments (Cirillo & Seidman, 2003; Seidman et al., 2002). Working memory refers to the processes responsible for transient storage (in the order of seconds) and manipulation of information stored in separate phonological and visuospatial buffers (Baddeley, 1986). Verbal declarative memory refers to episodic memory (memory for events) and semantic memory (memory for facts) that are both aspects of long-term memory. Episodic memory in particular is impaired in schizophrenia with some consensus that there are deficits in encoding of information and possibly retrieval, but storage is probably intact (Cirillo & Seidman, 2003). It is not yet clear whether the retrieval deficits can be accounted for by problems in encoding or whether there is a separate retrieval problem. It is however acknowledged that episodic memories are encoded via conscious learning processes that are underpinned by executive processes (Cirillo & Seidman, 2003).

It is a common finding that the performance of patients with schizophrenia on tasks probing executive function, attention and working memory, parallel impairments displayed by patients with frontal lesions, but also patients with striatal lesions (e.g. Parkinson's patients) prompting theorists to suggest that schizophrenia may arise from frontal lobe dysfunction (Frith, 1992; Seidman et al., 1983; Weinberger, Aloia, Goldberg, & Berman, 1994; Weinberger, 1987), or fronto-striatal dysfunction (Elliot, McKenna, Robbins, & Sahakian, 1995; Meyer-Lindenberg et al., 2002; Pantelis et al., 1997; Robbins, 1990). These proposals are well supported by neurochemical and neurophysiological findings outlined previously that report disturbances in these areas in patients with schizophrenia

(Abi-Dargham & Moore, 2003; Abi-Dargham et al., 2000; Meyer-Lindenberg et al., 2002; Laruelle et al., 1996; Wong et al., 1986), but most notable is reduced brain activation, particularly in DLPFC that has been consistently observed in neuroimaging studies using cognitive activation paradigms (Cho, Konecky, Carter, 2006; Barch et al., 2001; Perlstein et al., 2001; Rubia et al., 2001b; Weinberger, 1987).

5.3.4. Some types of executive functions

Past and present operational definitions of executive, attention and working memory functions vary greatly. For example, Goldman-Rakic (1994) described the core function of working memory as involving '...the ability to guide behaviour by representations…", which seems to draw on all three constructs. However, more recent conceptualisations of cognition attribute guidance of thought and behaviour, and goal-directed processes generally, to the executive system (Carter, 2000; Garavan et al., 1999; Hazy et al., 2007; Nigg, 2000; Roberts & Pennington, 1996). Contemporary theories of the executive system include some aspects of attention and working memory (Baddeley, 1996; Kane & Engel, 2002; Perry et al., 2001).

Working memory processes that are functions of the executive system were recently distinguished by Perry and colleagues (2001) who proposed a two-process model of working memory that parses executive and non-executive functions. The model consists of a 'transient working memory' that is responsible for short term storage information online (in the order of seconds) and recall of information, and an 'executive working memory' that refers to processes involved when both online storage and manipulation of information is required, in addition to recall of that information. In the domain of attention, executive processes are responsible for suppressing distracting stimuli that interfere with internal representations required for correct responding (Kane & Engle, 2002). This facet of attention is called selective attention. For these reasons, past investigations of working memory, selective attention and executive function may have tapped similar, but dissociable deficits.

The definitive set of executive functions remains controversial, but is generally accepted as including multi-task co-ordination, planning/strategy formation, task-switching, performance monitoring, and inhibitory control (Carter, 2000; Garavan et al, 1999; Miyake

et al., 2000; Stuss, 2006; Roberts & Pennington, 1996), but also selective attention (Kane & Engle, 2002) and manipulation and updating of information in working memory (Baddeley, 1996; Miyake et al., 2000; Perry et al., 2001).

A crucial question regarding executive processes is whether the brain, especially PFC, acts globally in the implementation of apparently dissociable functions (Duncan & Miller, 2002), or whether discrete neural areas within PFC implement these functions in a modular fashion (Stuss, 2006; Stuss et al., 1995). Duncan and his colleagues (Duncan & Miller, 2002; Duncan & Owen, 2000) argue that PFC functionally adapts ('adaptive encoding') depending on task processing demands (Duncan & Miller, 2002), and show that among many published neuroimaging studies on diverse cognitive tasks, activation networks reported commonly include mid-dorsolateral and mid-ventrolateral PFC, in addition to dorsal anterior cingulate cortex (AAC) activation clusters (Duncan & Owen, 2000). These authors also suggest that adaptation occurs at the neuronal level, citing by example the work of Rao, Rainer and Miller (1997) who showed that during a working memory task, lateral PFC neurons in monkeys were responsive to object information about stimuli when required, but were also responsive to location information about stimuli when that was required for task performance (Duncan & Owen, 2000).

Stuss (2006) argues that the adaptation hypothesis of PFC function does not account for how functions are implemented, and that evidence from physiological research, though important, does not necessarily determine whether a particular region is necessary for a particular function rather than simply being active during the execution of a particular function. Citing evidence from his work over the past decade with lesion patients that demonstrated dissociable deficits in groups of patients with lesions to superior, left and right lateral regions of PFC which suggest fractionation of PFC function, Stuss suggests that confusion over the question of fractionation/adaptability of PFC reduces to a question of task difficulty. In this view, particular PFC regions are dedicated to particular functions in a domain-general manner rather than domain-specific manner, and other PFC regions are recruited with increases in task difficulty. Hence variations in task difficulty may lead to recruitment of additional brain regions which can produce misleading results.

From his work with lesion patients, Stuss (2006) suggests at least three dissociable functions, including an *energisation/activation* component required for response initiation

which is affected by damage to medial superior frontal cortex, a *monitoring/discrimination* component that is affected by damage to right lateral PFC, and a task-setting/selection component that is affect by damage to left lateral cortex. In healthy individuals, Miyake and colleagues (2000) demonstrated three independent functions including set-shifting, updating and monitoring, and inhibition of prepotent responses, by analysing shared variance instead of independent variance between test scores in order to identify latent factors. Further research will likely reveal more components of executive function as neuropsychological tests are refined (Stuss, 2006).

Fractionation of executive functions is vital for understanding brain function and offers the potential to develop new models of cognitive processing which will generate a slew of testable hypotheses for understanding psychopathology in schizophrenia.

5.3.5. What is probed during executive function tasks?

Executive tasks are characterised by the interaction between activation and inhibition of representations in working memory (Roberts & Pennington, 1996). Activation of relevant representations is crucial for correct responding on executive tasks but is retarded by the effect of distracting representations that usurp attentional resources and disrupt performance. To optimise performance, irrelevant representations and behavioural responses must be controlled while target representations and responses must be activated. Abilities required for control of representations in working memory and associated behavioural responses are called *cognitive and behavioural control* processes, respectively. Control processes are vital for correct responding on all executive tasks, but only crucially engaged during some traditional working memory (Perry et al., 2001) and attention tasks (Kane & Engle, 2002). Quintessential executive tasks include the Wisconsin Card Sorting Test (WCST), the Stroop Colour Word Test (Stroop), and the Antisaccade task (AS). While there are many others, these tasks are prototypical executive function tasks that probe cognitive and behavioural control functioning, and oftentimes these tasks are used as measures of executive function in neuropsychological investigations of schizophrenia. To articulate the different control functions tapped during these tasks, the tasks are outlined below.

The WCST essentially involves the presentation of stimulus cards that must be sorted according to one of three stimulus features - number, colour and form - and placed under four initial stimulus cards (e.g., cards displaying: one red triangle; two green stars; three yellow crosses; and four blue circles). Initially, participants must infer the sort (or response) rule by trial-and-error and using experimenter feedback ('correct' or 'incorrect') while maintaining possible and incorrect sort rules activated in working memory After a certain number of correct sorting trials, the sorting rule is changed, indicated only by experimenter feedback. On the subsequent trial, a sort that would have been correct if the previous sort rule applied is now incorrect. Participants must inhibit the incorrect rule and activate another on each trial until the correct sort rule is inferred. Continually sorting according to the old rule is called perseveration, or perseverative responding, and is thought to arise from a failure to inhibit the old sort rule and activate another possible sort rule in working memory and respond accordingly. Perseverative responding on WCST is often evident in schizophrenia patients, and also patients with frontal and striatal lesions. The number of perseverative responses and the number of complete 'categories', indicated by the number of sort rule changes, are recorded. Neuroimaging studies using WCST in schizophrenia patients have linked poorer performance to hypoactivation of DLPFC (Weinberger et al., 1986).

In the classic version of the Stroop task, participants must respond verbally with the ink colour of colour name words. Participants take less time to respond on trials where the ink colour and colour name word are congruent (e.g. the word 'blue' printed in blue ink) than when they are incongruent (e.g. the word 'red' printed in blue ink). Responding to the ink colour of words requires participants to attend to the colour of the stimulus and inhibit word reading which attracts attentional resources. Word reading responses are relatively automatic and strongly prepotent due to practice accrued during the normal course of life. Hence to respond correctly, i.e., name the colour, control must be exerted over the prepotent word reading response. In the literature, colour naming on the Stroop task is said to tap *interference control* (Nigg, 2000), which is important for resolving conflict between competing responses (colour naming – wording reading). Neuroimaging studies of Stroop performance in healthy participants link efficient performance in the incongruent condition to activation of ACC (Carter et al., 2000). ACC has been shown to be crucial for

interference control in other tasks tapping this function (Botvinick, Cohen & Carter, 2004, Van Veen & Carter, 2002). Schizophrenia patients often fail to inhibit the incorrect response, and correspondingly, neuroimaging studies report that correct performance in this group is characterised by reduced activation of ACC (Kerns et al., 2004), consistent with a reduced capacity to inhibit prepotent word reading responses.

In the AS, participants are required to gaze at a central fixation point while peripheral cues are presented on the horizontal plane of fixation, offset by some degree to the central point (e.g. 10°). In the prosaccade condition, participants are required to make a saccade toward the cue (an automatic orienting response – highly prepotent), while in the antisaccade condition participants are required to make a saccade in the direction opposite to cue presentation. Inhibitory control is required to inhibit the automatic prosaccade orienting response which is a form of *response inhibition*. Studies have consistently found that patients with schizophrenia make significantly more errors than healthy controls during the antisaccade condition whereby they reflexively orient toward the peripheral cue instead of generating an oppositely directed saccades (Brownstein et al., 2003; Fukushima et al., 1988; Sereno & Holzman, 1995), indicating an inability to inhibit prepotent responding. Lesion (Guitton, Buchtel, & Douglas, 1985) and neuroimaging studies (Ford, Goltz, Brown, & Everling, 2005; Matsuda et al., 2004) suggest DLPFC has a significant role, but more recent evidence indicates substantial involvement of inferior frontal cortex (Chikazoe, Konishi, Asari, Jimura & Miyashita, 2007; Chikazoe et al., 2009; Ford et al., 2005; Tu, Yang, Kuo, Hsieh & Su, 2006).

In summary, the WCST requires *inhibition of a previously learnt sorting rule* that is prepotent due to reinforcement over previous successive trials. The prepotent sorting rule interferes with performance if not controlled when the rule becomes irrelevant, and failure to do so is related to reduced activation within DLPFC. Correct responding on the Stroop requires participants to *inhibit an automatic word reading* response that will persist if not controlled. Prepotent word reading arises from many years of reading practice in literate individuals and controlling this response requires ACC activation. AS exploits an innate orienting response, which occurs automatically and is thus extremely prepotent. Hence to stop this reflexive response from commencing, inhibition must occur at the behavioural

level and has been linked to DLPFC and inferior frontal cortex activation. The control functions required for performance on WCST, Stroop and AS vary markedly, however, they share some core features.

5.3.6. Performance requirements for executive function tasks

The first and most obvious requirement for performance on any task is task set activation in working memory, which includes activation of task rules and other currently relevant representations and responses required for task performance. The performance requirements of WCST, Stroop and AS load differently on working memory capacity with minimal involvement in Stroop and AS performance and a heavy load during WCST performance. Roberts and Pennington (1996) point out that another factor differentiating executive tasks is the degree of prepotency of incorrect/irrelevant working memory representations and related responses. As outlined above, prepotency of incorrect representations and responses on these tasks arise differently: WCST prepotency accrues over trials, Stroop prepotency accrues over years, and in AS, prepotency is innate.

These differences have crucial implications for the type of control required on each task. WCST requires inhibition of irrelevant working representations therefore control is exerted on representations in working memory. This is a form of cognitive control, or *cognitive inhibition*. In Stroop performance, control is exerted on what enters working memory, and so this form of control involves *biasing of feature encoding* so that the incorrect stimulus dimension is inhibited and the correct stimulus dimension is activated in working memory. This is a form of cognitive inhibition but bears some similarity to motor control experiments investigating response conflict (Botvinick et al., 2004; Van Veen & Carter, 2002) where correct and incorrect response compete for selection. AS stimuli evoke an automatic behavioural response (orienting) that is automatically triggered in neurologically healthy individuals; in such cases, control is exerted on the orienting response by a form of *behavioural inhibition*.

Inhibition has been important in the neuropsychological account of schizophrenia, and deficits in patient groups have been reported in a wide range of inhibitory control tasks. In addition to the abovementioned impairments, inhibitory control deficits have been detected in patients with schizophrenia in tasks requiring inhibition of irrelevant memories

(Badcock, Waters, Maybery, & Michie, 2005; Waters, Badcock, Maybery, & Michie, 2005), word inhibition (Nathaniel-James, Brown & Ron, 1996) and inhibition of on-going planned behavioural responses (Badcock et al., 2002; Bellgrove et al., 2006; Davalos et al., 2004; Enticott et al., 2008; Ross et al., 2008). Planned behaviours contrast with orienting behaviours as in AS, in that planned behaviours are volitional and not reflexive as in orienting responses. This type of behavioural inhibition is also termed response inhibition and is often investigated using Go/No-go and Stop-signal paradigms.

5.4. Behavioural inhibition as a discrete impairment in schizophrenia

5.4.1. Behavioural findings

All neuropsychological tasks, including AS, require multiple integrated control functions for correct responding (Stuss, 2006), most notably working memory functions (i.e., maintaining task rules). Consequently, some authors have argued that AS deficits in schizophrenia may be explained as a generalised working memory deficit. In support of this view, many studies have reported significant correlations between working memory and AS performance in control (Roberts Jr, Hager, & Heron, 1994) and patient groups (Hutton et al., 2004). Also, neuroimaging studies suggest impairment on working memory (Barch et al., 2001; Perlstein et al., 2003) and AS (Brownstein et al., 2003) tasks may be underpinned by a common dysfunction in DLPFC, indicating a neuroanatomical basis to the link in processing deficits.

One reason that response inhibition deficits may not have been dissociable from working memory deficits in the past may lie in the performance requirements of tasks used for study (Miyake et al., 2000; Stuss, 2006). Paradigms used to assess a common function should load similarly on the function under investigation, and not load significantly on other functions required for performance of a comparison paradigm(s). Hence for a comparison of response inhibition and working memory abilities, response inhibition demands should be similar (i.e. similar response prepotency) on response inhibition tasks and have low working memory requirements, whereas working memory paradigms should load heavily on working memory requirements and have minimal response inhibition

requirements. Breaches of these conditions may explain experimental findings that suggest strong relationships between tasks purported to tap different functions, and also apparent contradictory findings.

This explanation is supported by the findings of a recent study. Donohoe and colleagues (2006) tested the hypothesis that behavioural inhibition deficits in schizophrenia patients, measured via AS performance, could be accounted for by another behavioural inhibition measure rather than by working memory or sustained selective attention performance and thus provide evidence of a uniquely impaired inhibition mechanism. Patients (only) were assessed on AS, a spatial working memory measure (SWM, the Spatial Working Memory Task from CANTAB), a verbal working memory task (VWM - the Wechsler Letter Number Sequencing Task), a sustained selective attention task (the distractibility CPT – the distractibility version of the Continuous Performance Task), and a Go/No-go task (the XY task identical to Garavan et al., 1999) that involved highly prepotent responses indicated by a large percentage of errors of commission on No-go trials. Multiple regression analyses were used to find the best predictor(s) of AS performance after controlling for age. Go/No-go performance was the best predictor when entered first, accounting for 25% of the variance, while SWM, VWM and CPT performance (entered in that order) explained 8.4%, 0% and 9.1%, respectively, implicating an overlap of processing requirements on these tasks and AS performance. However, Go/No-go performance was strongest predictor and was still significant when entered last in the regression model. These results suggest a strong relationship between the processing requirements of Go/No-go performance and the processing requirements for AS performance, thus indicating a common impairment that affects performance similarly on these tasks, and is distinct from impairments of selective attention and working memory.

Furthermore, the use of tasks that do not effectively tap the process under investigation (e.g. response inhibition) may lead to contradictory and equivocal findings (Stuss, 2006). This problem was apparent in a recent study by Thoma and colleagues (2007) who used a range of executive tasks to investigate the effect of co-morbid drug use in schizophrenia. Five cohorts were studied including four groups of patients and non-psychiatric controls who either had a co-morbid substance use disorder or did not, and a fifth group were individuals with depression. Tasks used included a Stroop variant to test

interference control, a Go/No task to assess response inhibition, the Trails Making Test (TMT) to test attention shifting, and an object alteration task to test visuo-spatial set-shifting. The authors used these tasks specifically because they are thought to tap the ability to inhibit prepotent response tendencies which is impaired in both schizophrenia and substance abuse groups. The crucial hypotheses were that substance abuse and schizophrenia groups would be impaired, with co-morbid patients displaying the greatest deficit. Interestingly, only the group of schizophrenia patients were impaired on the tasks, while co-morbid patients performed similarly to controls. Go/No-go task impairment was small and limited to slower RTs with no increase in errors of commission. However, in an analysis of only male subjects (conducted to rule out between group gender bias), co-morbid patients made significantly more errors of commission and, large impairments were observed in Stroop interference costs, TMT attentional set-shifting costs and reaction times on the object alteration task, the latter indicating impaired visuo-spatial set-shifting. While impairment across the tasks was obvious in schizophrenia patients, ceiling and floor effects apparent in the Go/No-go results suggest the task used did not effectively tap inhibitory processing. In contrast, the Go/No-go variant used by Donohoe and colleagues (2006) involved highly prepotent responses resulting in high numbers of commission errors on No-go trials. Therefore, the Go/No-go task used by Thoma and colleagues (2007) may be an ineffective tool for differentiating individuals or groups in response inhibition even if impairment is present, and therefore may not be as useful as other Go/No-go variants and response inhibition paradigms to probe response inhibition.

5.4.2. Further evidence for response inhibition impairments in schizophrenia

Historically, response inhibition research had not figured quite so prominently as other forms of inhibitory control in the neuropsychological account of schizophrenia, with the exception of studies using AS, but over the last decade researchers have increasingly begun to use Go/No-go paradigms in behavioural (Donohoe et al., 2006; Thoma et al., 2007) and neuroimaging and electrophysiological studies (Arce et al., 2006; Ford et al., 2004; Kaladjian, 2007; Kiehl, Smith, Hare & Liddle, 2001; Perlstein, Dixit, Carter, Noll, & Cohen, 2003; Rubia et al., 2001b; Weisbrod, Kiefer, Marzinzik, & Spitzer, 2000), while some groups have utilized stop-signal paradigms in purely behavioural studies (Badcock et

al., 2002; Bellgrove et al., 2006; Davalos et al., 2004; Enticott, et al., 2008; Ross et al., 2008). The relative paucity of response inhibition studies in schizophrenia, compared to WCST for example, is surprising given that it is well know that these tasks engage fronto-striatal-thalamic circuitry including pathways that are thought to be compromised in schizophrenia, and thought to have a significant role in the emergent psychopathology of the disorder. The techniques of cognitive neuroscience are perfectly suited to the study of impaired executive functioning in schizophrenia. Indices of *in vivo* brain function derived through functional neuroimaging (e.g., fMRI), and electroencephalographic (ERPs, EEG) methods have enabled researchers to isolate dysfunctional neurocircuitry, and to investigate relationships between brain function and task performance.

5.4.3. Go/No-go evidence

A few research groups have investigated No-go inhibition in schizophrenia using physiological indices including ERPs (Ford et al., 2004; Kiehl, Smith, Hare & Liddle, 2001; Weisbrod et al., 2000) and fMRI (Arce et al., 2006; Ford et al., 2004; Rubia et al., 2001b). Both auditory (Weisbrod et al., 2000) and visual (Ford et al., 2004; Kiehl et al., 2000) paradigms have been employed in the study of No-go inhibition in schizophrenia. A sequence of N1, N2 and P3 components are usually elicited in these paradigms, but group differences are usually observed in the P3 latency range. N2 differences are sometimes reported, but these will not be reviewed here as they are not routinely observed during stopping (see Experiment 2; Bekker et al., 2005; Dimoska et al., 2008) which is the focus of this thesis.

5.4.4. ERP evidence

The first group to study No-go inhibition in schizophrenia patients using ERPs was Weisbrod et al. (2000) who used an auditory Go/No-go paradigm. Stimuli were frequent (p = .8) and infrequent (p = .2) tones that instructed alternative response styles in separate Go and No-go tasks. For the Go task, infrequent tones instructed a button press response and the frequent tone were ignored, while in the No-go condition frequent tones instructed a button press response and infrequent tones were ignored. Go-P3 amplitudes in schizophrenia patients were comparable to that of controls, but No-go-P3 amplitudes were

reduced in the patient group. Interestingly, patient Go-P3s were larger than No-go-P3s at centro-parietal electrodes whereas the reverse was true for controls. At fronto-central sites, both groups exhibited larger No-go-P3s than Go-P3s, but controls produced No-go-P3s that were larger in the left hemisphere than Go-P3s. Analyses of error rates indicated that patients performed similarly to controls in Go trials but made significantly more errors of commission on No-go trials indicating an impaired ability to inhibit prepotent responses. Additionally, analysis of perceptual sensitivity scores showed that patients could discriminate Go stimuli at a comparable level to controls, but were significantly impaired in their capacity to discriminate No-go stimuli.

Around the same time, Kiehl and colleagues (2000) investigated response inhibition in schizophrenia patients[33] using a visual Go/No-go paradigm where stimuli were arrows pointing either up or down (Go or No-go, counterbalanced across participants) presented equi-probably. In contrast to the findings of Weisbrod and colleagues (2000), Go-P3s amplitudes were larger than No-go-P3s in healthy controls, but no difference between these potentials was observed in patients with schizophrenia. Additionally, much larger P3s were observed in the right hemisphere in healthy controls for Go and No-go trials, whereas no lateralization was observed in the patient group. There were no RT differences between groups, but patients with schizophrenia made significantly more errors of commission than healthy controls.

Ford and colleagues (2004) also investigated response inhibition using a visual Go/No-go paradigm, but employed both ERPs and fMRI to understand the temporal and spatial dynamics of No-go inhibition processes. The paradigm included a simple RT Go task a trial type probabilities of No-go = .12 and Go = .88. Behavioural analyses revealed the patient group made significantly more errors, but the pattern of errors differed from controls. Control group errors were largely errors of commission, while patients made significantly more errors of omission, suggesting that patients failed to establish a prepotent response bias. In ERP analyses, no effects were observed for N1 or N2 potentials, but No-go-P3 peaks were larger and onset later for No-go compared to Go stimuli. The amplitude of Go-P3s was non-significantly larger in patients, while the amplitude of No-go-P3s was

[33]Participants in this study were all incarcerated prisoners. Groups were schizophrenia patients, psychopaths and non-psychopaths. The review here focuses on the differences between the schizophrenia patients and the non-psychopaths (termed healthy controls here).

non-significantly larger in controls. However, the difference in amplitude between Go and No-go potentials was significantly larger in controls compared to patients. Analysis of P3 peak latencies showed that these potentials peaked significantly later in patients compared to controls, and the difference between Go and No-go-P3 peaks was marginally larger for controls compared to patients. These findings show that the amplitude and latency differences for patient Go and No-go P3s are substantially less than the same differences in controls.

In combination, the findings of Ford et al. (2004), Weisbrod et al. (2000) and Keihl et al. (2000), show that patients with schizophrenia process Go and No-go stimuli differently to controls. Notably, for healthy individuals, P3s elicited by Go and No-go stimuli are quite different, whereas in patients these potentials are more comparable. In particular, patients with schizophrenia exhibit abnormal No-go P3s and have more trouble inhibiting prepotent responses. Noting that the P3 is thought to reflect context updating (Donchin & Coles, 1988), whereby larger P3s are elicited when the context of a stimulus changes (e.g., larger No-go compared to go P3s), Ford and colleagues (2004) suggest that patients do not use the context of the paradigm (i.e., most stimuli are go stimuli) to establish a prepotent response bias, but instead processed each stimulus in a comparable manner. Hence Go and No-go events were of comparable novelty for patients whereas No-go stimuli were more novel for controls due to less frequent presentation. It follows that Go responding was more effortful in patients compared to controls.

5.4.5. Neuroimaging evidence

Ford and colleagues investigated this effect of more effortful Go processing in patients in event-related fMRI data by computing Go > No-go contrast maps. Corresponding to their ERP P3 findings, the patient group exhibited more activated voxels than controls when groups were assessed separately, and when group maps were contrasted, patients revealed significantly greater activation in the somatosensory and sensorimotor (M1) cortices, ACC, DLPFC, striatum and insula areas compared to controls, while at the same threshold for the reverse contrast, no voxels were more activated in controls compared to patients. Ford and colleagues interpreted these findings as further evidence of more effortful Go processing in patients with schizophrenia.

Control group activation for the No-go > Go contrast was right dominant and included bilateral inferior frontal gyri (IFG), middle frontal gyri (MFG), medial frontal gyri, superior frontal gyri (SFG), anterior cingulate cortex (ACC), precentral gyrus, posterior cingulate gyrus, inferior parietal lobe (IPL), superior temporal gyrus (STG), middle temporal gyrus (MTG), precuneus, globus pallidus (GP), putamen, caudate and insula, and interestingly, right subthalamic nucleus (STN) activation was also reported. Patients activated a similar network, though substantially fewer voxels were activated. These differences were consistent with Ford's ERP findings reviewed above, and interpreted as further evidence that patients process Go and No-go stimuli in a comparable manner, whereas controls exhibit greater processing in response of No-go stimuli. When the groups were compared, it was found that patients activated no area greater than controls, while the controls > patients contrast revealed significant differences (thresholding was $p < .01$, 6 contiguous voxels) within widespread areas, particularly bilateral medial frontal, cingulate, temporal and parietal areas, in addition to bilateral SFG and left MFG (corresponding to DLPFC). Subcortical differences were observed in bilateral striatal and right thalamic nuclei, but not in STN. These findings were largely interpreted as reflecting more effortful No-go processing in controls.

In an exploratory analysis, ERP (reported above) and fMRI data were integrated by correlating parameter estimate images for No-go trials (β images) with P3 peak amplitudes. In controls, P3 amplitudes were significantly positively correlated with bilateral regions of MFG (predominately right lateral), ACC, caudate nuclei and right IPL. In patients, only ACC activation correlated with No-go P3 amplitudes, prompting the authors to suggest that the No-go P3 is linked to ACC activation and moreover, that the No-go-P3 may reflect the detection of response conflict and that patients have an impaired ability to recruit MFG (corresponding to DLPFC, especially right lateral), IPL and striatum for No-go performance.

In the first neuroimaging investigation of response inhibition in schizophrenia, Rubia and colleagues (2001b) scanned participants during performance of a Go/No-go paradigm and a stop task (stop task discussed below with stop task experiment) using epoch based designs and analyses. Stimuli were airplanes pointing to the right (70%) or left (30%); during Go blocks, participants made a right hand button response to all stimuli, and

during No-go blocks, left pointing arrows instructed no response. There were no significant differences in behavioural performance data between groups. In controls No-go performance was linked to significant activation in left pre/post central gyrus, right SMA, left IPL, left precuneus, posterior cingulate, bilateral IFG, left MFG, ACC and left middle temporal lobe, whereas patients activated bilateral superior parietal cortex, posterior cingulate, and the right inferior temporal lobe. The only activation difference between the groups was greater BOLD signal intensity in left lateral ACC in controls.

Arce and colleagues (2006) also investigated No-go inhibition in patients with schizophrenia, but used an implicit cuing paradigm in an epoch based fMRI design. The majority of trials were Go trials (75%) instructed by three different stimuli and the remainder were No-go trials instructed by only one stimulus. However, most No-go trials (86%) were preceded by the same Go stimulus on each presentation, hence that Go stimulus served as an implicit cue that a No-go trial was next. It follows that participants could learn when a No-go trial was about to be presented, hence the load on inhibitory control was low. Corresponding to the findings of Rubia and colleagues (2001b) the between group contrast of No-go > Go revealed reduced BOLD signal intensity within left lateral DLPFC and ACC in patients compared to controls.

While the above studies have highlighted dysfunction in ACC and DLPFC, other studies suggest dysfunction within inferior frontal cortex of patient groups. In a recent Go/No-go fMRI study using an event-related fMRI design, Kaladjian and colleagues (2007) enhanced response prepotency by presenting a series of warning cues over a 5 sec period prior to presentation of each stimulus. In the crucial comparison, No-go > Go, controls activated a network that included bilateral IFG and IPL, left SFG and MFG. Patient group activation included bilateral MFG and left SFG. In contrast to the findings of both Rubia et al. (2001b) and Arce et al. (2006) the only activation that separated the groups was BOLD reductions within rIFG in the patient group.

The studies of Weisbrod et al. (2000), Kiehl et al. (2000), Rubia et al (2001b), Arce et al (2006) and Ford et al (2004) demonstrate several key aspects of performance in patient groups on response inhibition tasks. Firstly, patients are less sensitive to the difference between inhibition and response stimuli than healthy controls, and do not establish a prepotent response tendency as controls do. This is evident by a lack of activity modulation

between conditions, whereby No-go-P3 and Go-P3 amplitudes are similar in patients but No-go amplitudes are larger in controls. This is also evident in neuroimaging data showing that patients exhibit greater activation during Go trials than healthy controls but reduced No-go activation, especially within left DLPFC ACC. However, the data reported by Kaladjian and colleagues (2007) suggest that more prepotent response inhibition requirements may tap dysfunction in right IFG. This latter study is interesting given that right IFG is crucial for response inhibition in stop-signal tasks (Aron et al., 2003a; Aron & Poldrack, 2006; Experiments 1 & 2; Reiger et al., 2003), which load more heavily on response inhibition than Go/No-go tasks. Rubia and colleagues (2001a) suggest that No-go inhibition loads more heavily on task selection processes (selection of a non-response). These findings raise the possibility that tasks loading heavily on the requirement for response inhibition may probe response inhibition processes more selectively and thereby tap a unique impairment in patients with schizophrenia. Indeed, at the recent CNTRICS (Cognitive Neuroscience Treatment Research to Improve Cognition in Schizophrenia) meeting, the stop-signal task was recommended for studying behavioural control in schizophrenia groups (Barch, Braver, Carter, Poldrack & Robbins, 2009).

5.5. Stop-signal evidence

5.5.1. Studies of stop-signal inhibition

At the time of writing, there had been two related investigations of children at-risk of developing schizophrenia (Davalos et al., 2004; Ross et al, 2008) and three studies with patients with a diagnosis of schizophrenia (Badcock et al., 2002; Bellgrove et al., 2006; Enticott et al., 2008) that have used standard stop-signal paradigms (i.e., using the procedures outlined by Logan & Cowan, 1984), in addition to one highly cited neuroimaging study by Rubia and colleagues (2001b) who used a general stop task.

5.5.2. Stopping in at-risk groups

A genetic basis for schizophrenia is well established (Gottesman, 1991; Gottesman & Shields, 1982; Weinberger et al., 2001), hence researchers often study children who have

not been diagnosed with schizophrenia but whose parents have such a diagnosis in order to probe a predisposition to schizophrenia. This may be performed by comparing children with at least one parent with schizophrenia (i.e., children at-risk) to children whose parents are not diagnosed with schizophrenia. To this end, researchers have attempted to establish whether at-risk children display neuropsychological impairment, and whether any detected impairment is specific to a subset of processes, or generalise to a range of cognitive processes. One research group has investigated whether stop-signal performance can statistically distinguish at-risk children from control children (Davalos et al., 2004; Ross et al., 2008).

In an initial study, Ross and colleagues compared the performance of children who had at least one parent with schizophrenia (*at-risk* group, N = 51) to a matched control group (N = 51) on a range of neuropsychological tasks (Davalos et al., 2004), and subsequently studied a subsample of the initial at-risk cohort (N = 25) who were still within the age-range of the initial cohort (6-16 years) after a follow-up period of an average of 2.6 years (Ross et al., 2008). In the initial investigation, participants were tested on emotional perception, verbal abilities, visuo-spatial skills, working memory and stop-signal task[34] performance. At-risk children were impaired on verbal skills and working memory tasks, but were most impaired in stopping whereby at-risk children exhibited significantly slower SSRTs.

At follow-up, the at-risk subsample and a newly recruited control group (N = 82) were tested on the neuropsychological tasks for which the initial at-risk cohort exhibited impairment, which included the counting span task, the sentence span task and the stop-signal task (Ross et al., 2008). The impairments were maintained but did not worsen, indicated by similar effect sizes between testing sessions, suggesting that at-risk children develop along a similar trajectory to normal children despite neuropsychological impairment. Interestingly, SSRT for the at-risk subsample was highly correlated between testing sessions ($r = .74$, $p < .001$) whereas working memory indices were less correlated between sessions (counting span scores: $r = .41$, $p = .04$; sentence span scores: $r = .11$, $p = .61$), suggesting that SSRT is a more stable measure than working memory indices. A

[34] In both studies, the stop-signal task utilised a tracking algorithm to set stop-signal delays such that inhibition success was maintained at 50%.

striking feature of individual subject data in the follow-up study was from a high-risk participant who became psychotic between the initial session and follow up. This participants' SSRT slowed markedly from the first to the second session – worsening by almost four standard deviations. This participant was the only one to display such a vast change over the period on any task.

These studies highlight the utility of stop-signal procedures outlined by Logan and Cowan (1984) in detecting neuropsychological impairment in children with a genetic predisposition to schizophrenia in non-clinical children, and that stopping performance may be a more sensitive measure of neuropsychological impairment in schizophrenia groups than working memory and verbal skill indices.

5.5.3. Stopping in patients with a diagnosis of schizophrenia

In the first study to use the stop-signal procedures articulated by Logan and Cowan (1984; Logan, 1994) as a tool for schizophrenia research, Badcock and colleagues (2002) employed a variant where six stop-signal delays were set relative to a participants' mean reaction time (MRT: MRT – 0 ms, MRT – 100 ms… MRT – 500 ms), thereby affording estimates of SSRT and inhibition functions. Groups compared were healthy controls (N = 34), patients with schizophrenia (N = 19) and a psychosis comparison group (N = 15), most of whom were diagnosed with bipolar disorder) who did not differ on age, years of education, or intellectual performance. Despite substantial differences in group SSRT (schizophrenia group = 258 (78) ms; psychosis comparison group = 271 (81) ms; control group = 227 (44) ms), the groups were not statistically distinguishable, however both patient groups exhibited significantly flatter inhibition functions compared to healthy controls. Since GoRT was more variable in the patient cohorts than controls, a ZRFT transformation was applied to inhibition functions to account for the effect this variability had on inhibition function slopes (Logan, 1994). After ZRFT correction, only the schizophrenia patient group exhibited significantly flatter slopes than the control groups which did not differ. The authors considered this finding may represent either a difference in the variability of cohort SSRTs, or inhibition processes were triggered less often. To resolve this, the coefficient of variation (CV = SD of SSRT/mean SSRT), which provides a measure of the variability in SSRT within each group, was calculated. The groups did not

vary significantly in CV of SSRT, suggesting the flatter slope of patient inhibition functions was due to a deficit in triggering stopping processes.

These findings were challenged by Enticott and colleagues (2008) who also employed a range of stop-signal delays set relative to mean reaction time (MRT) in their investigation of stopping in schizophrenia patients. However, the manner of setting stop-signal delays differed in this study in that stop-signal delays were proportions of MRT: stop-signals were set at 20%, 40%, 60% and 80% of MRT. This protocol is thought to account for inter-subject variability in MRT (Carter et al., 2003). In contrast to Badcock et al (2002), patients had significantly slower SSRT compared to matched controls, and moreover, the slopes of inhibition functions were flatter before but not after ZRFT correction.

In a more recent investigation, Bellgrove and colleagues (2006) studied stopping performance in patients with Early Onset Schizophrenia (EOS; morbidity presenting before 19 y.o.), which is characterized by neurodevelopmental delay. This cohort was sub-divided into paranoid EOS or undifferentiated EOS subtypes according to DSM-IV criteria. Notably, the undifferentiated group exhibited greater negative symptomatology. A single staircase tracking algorithm was used to set stop-signal delays that converged on a 50% inhibition criterion. Using a mixed model ANOVA on SSRTs, Bellgrove observed a significant interaction between group and response hand, and post-hoc tests showed that left hand SSRT was significantly slower for the undifferentiated EOS subgroup than both the paranoid patient subgroup and control group. Furthermore, the undifferentiated group showed a significant difference between left and right SSRTs (left > right), which was not observed in the paranoid subgroup or controls. No significant between group differences were observed for right hand SSRT. The results indicate an impaired inhibition processing specific to inhibition of left hand responses in EOS patients with negative symptoms.

5.5.4. Neuroimaging evidence

Only one neuroimaging investigation of stopping in schizophrenia has been published (Rubia et al., 2001b), however the paradigm used for study was not based on the procedures recommended by Logan (1994). The paradigm involved a simple RT Go task and a single stop-signal delay of 250 ms. Generic stop activation in controls was revealed in

bilateral ACC and IFG, in addition to right cerebellum, while patients activated right lateral IFG, IPL, precentral gyrus, thalamus, putamen, ACC and cerebellar cortex. Patients exhibited diminished activation in left lateral ACC and SFG compared to controls, but showed significantly more activation in bilateral dorsomedial and ventrolateral thalamus, right putamen and right precentral gyrus/insula. However, the behavioural findings in this study were quite anomalous with other reports in that the patient group mean reaction time was much faster than for the control group on the Go task (controls = 605 ms, patients = 533 ms), suggesting that controls strategically slowed Go responding to facilitate inhibition success, hence the neuroimaging findings may be spurious.

The behavioural findings using the stop-signal task to probe response inhibition in patients with schizophrenia have consistently revealed impairment, although the nature of impairment has differed, namely, impaired speed of processing (Bellgrove et al., 2006; Enticott et al., 2008), and impaired triggering of stopping processes (Badcock et al., 2002). Additionally, the data reported suggest that this task may be used to detect impairment in children at risk of developing schizophrenia (Davalos et al., 2004; Ross et al., 2008). To date no physiological studies using the stop-signal task have been conducted in patients with schizophrenia. The following chapter details a thorough investigation of stopping in patients with schizophrenia using behavioural, ERP and fMRI methods.

Chapter 6: Experiment 3

6.1. Introduction

Research over the last 25 years has led to the view that impaired neuropsychological functioning is a core feature of schizophrenia (Elvegag & Goldberg., 2000; Kremen et al., 2000; Reichenberg & Harvey, 2007). Of the impairments identified, those pertaining to the executive system ('executive functions') are among those most consistently reported (Reichenberg & Harvey, 2007). These functions are largely reliant upon the integrity of the frontal lobes, which are compromised in schizophrenia, and it has been suggested that dysfunction within the executive system may underpin other neuropsychological impairments observed in schizophrenia patients (Shallice, Burgess & Frith, 1991). A key focus of current neuropsychological research involves fractionation of the executive system into component functions, and moreover, discerning how these map onto frontally mediated networks. The evidence so far derived from neurologically healthy individuals indicates that a crucial function of the executive system is the capacity to inhibit prepotent responses (Miyake et al., 2000), which is commonly termed response inhibition. Arguably the most useful paradigm for studying response inhibition is the stop-signal paradigm (Logan & Cowan, 1984), which is advantageous because it affords indices of response inhibition, notably the speed of response inhibition (the stop-signal reaction time, SSRT) that are not estimable using other paradigms. Research efforts using the stop-signal paradigm (Logan & Cowan, 1984) have consistently reported stopping impairments in patients with schizophrenia (Badcock et al., 2002; Bellgrove et al., 2006; Enticott et al., 2008) and in those at risk of developing schizophrenia (Davalos et al., 2004) which are maintained over time (Ross et al., 2008). To date, no studies have attempted to elucidate the neural basis of these deficits, to which the current investigation is aimed by way of ERP and fMRI techniques.

Research with the stop-signal paradigm indicate that patients with schizophrenia exhibit impaired stop-signal task performance, but that the specific deficit may be contingent upon symptomatology within the group tested (see Bellgrove et al., 2006). In general, the data reported suggest that stopping is slowed in these groups (Bellgrove et al.,

2006; Enticott et al., 2008), and in those at risk (Davalos et al., 2004; Ross et al., 2008), but also that patients with schizophrenia may be impaired in their capacity to trigger stopping processes (Badcock et al., 2002).

Only one neuroimaging study has investigated stopping performance in schizophrenia patients, that conducted by Rubia and colleagues (2001b), who reported that compared to healthy controls, BOLD activation in patients was reduced in left DLPFC, but enhanced in thalamic and striatal nuclei. However for that study, a non-standard stop-signal paradigm was used that included a single fixed stop-signal delay (SSD; see Chapter 5). FMRI investigations of no-go inhibition in schizophrenia patients have typically reported inhibition contrasts indicating that patients exhibit reduced BOLD activation within distributed networks (Arce et al., 2006; Ford et al., 2004; Rubia et al., 2001b), and one study found a unique reduction in right IFG (Kaladjian et al., 2007).

There is now substantial evidence that stopping requires engagement of a right IFG-STN network, within which the level of activation is influenced by SSRT (Aron & Poldrack, 2006; Aron et al., 2007a) and inhibition difficulty (Experiment 2). In the light of these findings, and reports that SSRT is slowed in patients with schizophrenia, the evidence suggests that patients with schizophrenia have an impaired capacity to activate the right IFG-STN network required for stopping. Hence it was hypothesized that stop related activation in a patient group would exhibit reduced activation compared to controls within this network.

To date, there have been no electrophysiological investigations of stop-signal inhibition in patients with schizophrenia. The few ERP investigations of no-go response inhibition in schizophrenia have consistently reported No-go P3 abnormalities in patients compared to controls (Ford et al., 2004; Kiehl et al., 2000; Weisbrod et al., 2000). However, it is clear that Stop-P3s are quite unique, given the peak latency of these potentials occurs substantially earlier (200 – 300 ms: Bekker et al., 2005a: Experiment 2) than a typical auditory[35] evoked P3 (300 – 450 ms: Comerchero & Polich, 1999), whereas No-go P3s peak substantially later (400 – 500 ms: Ford et al., 2004; Kiehl et al., 2000; Weisbrod et al., 2000) closer to the range of a typical P3 of the stimulus modality used (Comerchero & Polich, 1999). Since the Stop-P3 is thought to reflect the stopping process,

[35] Stop-signals are usually auditory tones, with which the current investigation is consistent.

and that SSRT is slowed in schizophrenia, it was hypothesized that Stop-P3s in patients with schizophrenia would exhibit a later P3 peak latency than healthy controls.

Relationships between SSRT and BOLD/ERP indices of stopping were also investigated in this study. Given the fMRI findings of Experiment 2, it was critical that stopping performance be matched in terms of inhibition difficulty across patients and healthy controls, thus an adaptive approach was employed for setting stop-signal delays, set at chance level stopping for each participant. To this end, inhibition probability was matched both within and between patient and control groups. Hence for the neuroimaging aspect of this experiment, it was also hypothesized that faster SSRT would be related to greater BOLD response within the right IFG-STN network. Note that this hypothesis is the opposite of that forwarded for Experiment 2 where inhibition difficulty varied between participants and predicted activation in the right IFG-STN network.

Hypotheses regarding relationships between P3 amplitudes and peak latencies (at least the difference between P3 and N1 peak latencies), and SSRT were less certain. In Experiment 2, participants with faster SSRT exhibited larger P3 peak amplitudes and a shorter Stop-N1 and Stop-P3 peak-to-peak latency difference than their colleagues with slower SSRT. However, it was the latter who exhibited the greatest activation in right IFG-STN, whereas the former exhibited little to no response in that network. Hence Stop-P3s probably do not reflect the stopping process per se, but the capacity to trigger the stop response, i.e., processes that precede right IFG-STN engagement, but are nonetheless a feature of the stopping act. Indeed, the dissociation between Stop-P3 amplitude measures and activation in right IFG-STN noted in Experiment 2 may be a crucial insight into the two-mechanism theory of response (central and peripheral mechanisms) inhibition proposed by De Jong and colleagues (1990). Thus, the correlations between SSRT and Stop-P3s may have been paradigm driven.

6.2. Method

6.2.1. Research overview

There were three sessions: a practice session, an fMRI session and an ERP session. The practice session consisted of an interview to determine suitability for participation and practice on the stop-signal paradigm. During experimental sessions, participants responded to stop-signal paradigm stimuli whilst undergoing fMRI scanning and EEG recordings.

Exclusion criteria for control participants were a personal or family history of psychological or psychiatric disorders, a personal history of neurological disorders, brain injury or current substance abuse, claustrophobia sufferer, and having ferromagnetic objects within or on the body. This information was obtained from potential participants by self-report. Exclusion criteria for patient participants were the same except that a personal or family history of psychological or psychiatric disorders did not warrant exclusion from the study. Patient diagnoses were made using the Diagnostic Interview for Psychosis (DIP; Castle et al., 2006). Current symptomatology of patients was assessed using the Scale for the Assessment of Positive Symptoms (SAPS; Andreasen & Olsen, 1984) and the Scale for the Assessment of Negative Symptoms (SANS; Andreasen & Olsen, 1982) during the practice session, and checked for change prior to the commencement of subsequent experimental sessions. Self reported information was obtained from patients regarding their current medication intake, and from all participants regarding their level of education.

The project was approved by the Human Research Ethics Committee of the University of Newcastle, and the Hunter Area Research Ethics Committee. Written and informed consent was obtained from all participants according to the Helsinki declaration.

6.2.2. Participants

Because of the difficulty posed in recruitment of suitable patient volunteers for this experiment, in addition to limited funds for scanning related costs, patients were recruited first and control participants were recruited subsequently with controls selected on the basis of closely matching the age, gender and education level of patients.

Fourteen right-handed individuals with a diagnosis of schizophrenia were recruited from the Schizophrenia Research Institute (SRI) volunteer register, and from a group of

individuals who reside in supported housing provided by the Richmond Fellowship. Of these volunteers, one withdrew prior to the experimental session, while two others had difficulty performing the task and were thus unsuitable for participation. A fourth individual was excluded as he had ferrous metals lodged in his skin. The final group of ten individuals participated in all aspects of the experiment.

Fourteen right handed controls were recruited from the University of Newcastle campus and the local community. However some of these individuals did not participate in all sessions, although at least thirteen subjects participated in each experimental session. Due to data quality issues (head motion and signal drop out artifacts), the final control sample was only ten subjects in the fMRI session matched to patients for age, gender and years of education, and thirteen in the ERP session. These thirteen controls did not differ significantly from patients in age, education and gender. Demographic data of patient and control groups are reported in the results for fMRI and ERP sessions separately.

Patient medication details and symptom ratings

Medication details for the patient group are presented in Table 6.01 and symptom ratings in Table 6.02. One patient was taking a combination of amisulpride and risperidone, and another was taking a combination of amisulpride, risperidone, aripiprazole in addition to lithium carbonate. A third patient was taking a combination of amisulpride and quetiapine, while a fourth took daily dosages of aripiprazole, quetiapine, venlafaxine and thyroxin. All other patients were taking a single medication except for one patient who had been unmedicated for 3-4 years.

Table 6.01

Antipsychotic medication summary for the patient group

Medication type	Number of patients
amisulpride (Solian)	5
risperidone (Risperidal)	2
quetiapine (Serequel)	3
olanzapine (Zyprexa)	1
aripiprazole (Abilify)	2
fluanxol (Flupentixol)	1
no medication	1

Table 6.02

Mean ratings (with standard deviations in parentheses) on SAPS and SANS sub-scales, total global scores for the patient group

SAPS		SANS	
Measure	Score	Measure	Score
Hallucinations	5.1 (6.5)	Negative Affect	9.3 (9.9)
Delusions	14.5 (6.5)	Alogia	2.5 (2.7)
Bizarre behaviour	3.1 (3.9)	Avolition	7.5 (5.4)
Thought disorder	4.1 (5.2)	Anhedonia	8.5 (4.6)
		Attention	2.3 (2.6)
Total SAPS	27.0 (23.0)	Total SANS	30.1 (17.4)
Global SAPS	5.8 (4.0)	Global SANS	8.6 (4.5)

6.2.3. Tasks and stimuli

Go stimuli were the letter O, indicating a left hand response, and the letter X, indicating a right hand response. The stop-signal was a (1000 Hz, 50 ms, 85 dB, square wave tones with 5 ms rise and fall time with a 40 ms plateau) presented on 25% of all trials, and instructed participants to suppress the response indicated by the Go stimulus on that trial. These stimuli were presented in blocks of 224 trials lasting 7m 28 s at a constant inter-trial interval of 2000 ms. Stop-signals occurred pseudo-randomly on 56 trials within each block, 28 preceded by an O and 28 preceded by an X; blocks were sub-divided into four equivalent sub-blocks[36] and Stop-signals (14 per sub-block, 7 trials for each hand) were randomized within each sub-block separately to avoid clustering of stop-signal trials.

On-going across sub-blocks was a single tracking algorithm that was used to adjust stop-signal delay for left and right hands (separately), and to ensure a 50% inhibition rate for left and right hand stop-signal task trials (Levitt, 1970). Sampling inhibition performance at PI = .5 facilitates the most stable estimate of SSRT compared to other methods (Band et al., 2003); central estimates are derived from the median of the correct

[36] There was no gap between sub-blocks, hence participants were not aware of this manipulation experiencing stimulus presentation sequence as a continuous block of trials.

Go RT distribution and are relatively insensitive to violations of the assumptions of the race model (Band et al., 2003). To achieve this, the algorithm increased stop-signal delay by 50 ms after each Stop and decreased stop-signal delay by 50 ms after each Stop Failure. Identical algorithms have been successfully deployed in previous stop-signal experiments (e.g., van den Wilderberg, van der Molen, & Logan, 2002). In each practice session, an initial stop-signal delay of 200 ms was set at the beginning of testing. The mean stop-signal delay estimated for successfully inhibited stop-signal task trials during this session was recorded and later served as the initial stop-signal delay during fMRI and ERP sessions.

Blocks were preceded by a 5 s countdown and a sequence of seven practice Go trials presented at a constant inter-trial interval of 2000 ms. The countdown was intended to focus participant's attention to the task, while practice Go trials were included to give participants an opportunity to get settled in responding to the stimuli, and to avoid movement-related artifacts that sometimes occur at the beginning of a scanning run. The duration of the gap separating the onset of the last practice Go stimulus and the commencement of the experimental block was 5000 ms, allowing the HRF associated with these practice trials to settle. Due to a programming error, Go stimuli for no-signal trials were not presented with equal probability; more right-hand Go trials were presented (see trial type proportions analysis in results). This error varied in severity across participants, but a right hand Go stimuli bias was consistent and analyses showed no difference between the groups in the degree of bias in either the fMRI or ERP study. While this error limits interpretation of the data, it does not detract from the major findings of the study.

Prior to practice and experimental sessions, participants were instructed that speed and accuracy of responding on the primary task were of equal importance to successful inhibition. It was explained that the paradigm was such that performance would necessarily include many stopping errors (i.e. Stop Failures), and that when this occurred they should not slow Go responses in order to facilitate inhibition. During this pre-test period of each session, participants were given approximately two minutes pre-practice responding on the tasks, then performed two blocks of the paradigm. The mean stop-signal delay estimated from these latter blocks (resulting in approximately PI = .5) during the practice session was used as a seed for fMRI and ERP sessions for each participant. Two blocks of data were

recorded during fMRI sessions, while four blocks were acquired during EEG recording sessions.

Stimulus presentation

The method of stimulus presentation was identical to that used in the previous experiment (outlined in chapter 2).

6.2.4. Behavioural variables

Median correct Go RT (GoRT), median Stop Failure RT (SFRT), mean stop-signal delay for successful inhibition trials[37] (SSD), and PI were calculated for left and right hands separately. Also calculated were the numbers of left and right hand correct Go trials, incorrect Go trials, and missed Go trials (the sum of incorrect and missed Go trials). GoRT and SFRT estimates were entered into a Hand x Event type x Group ANOVA, where Event Type consisted of GoRT and SFRT. Error trial numbers were entered into a Group x Hand x Error type (incorrect Go/missed Go) ANOVA. As the groups were matched (numbers, age, gender and years of education) in the fMRI session, behavioural analyses were conducted treating Group as both a between subjects factor and matched-pair factor for behavioural data for that session.

As for the previous experiment, an analysis was undertaken to investigate the RT slowing prior to Stops that was reported by Vink and colleagues (2005). Therefore, in a separate analysis, RTs that preceded (pre-) and followed (post-) left and right hand correct Go trials, Stops, and Stop Failures were extracted separately. As there were very few incorrect Go trials, these events were not included in this analysis. Median Go RTs preceding and following each of these event-types were determined and entered into multi-factorial ANOVAs with factors of Time (pre-, post-) x Hand (left, right) x Event type (Go, Stops, Stop Failures) x Group ANOVA. In separate analyses, the factor Time was dropped, and the ANOVA rerun for pre- and post RT estimates separately.

[37] Stop Failure SSD was always 50 ms longer than Stop SSD owing to the 50 ms step size that was used in the adaptive procedure.

SSRT estimation was based on corrected PIs using the procedure described by Tannock and colleagues (1995) that adjusts PI according to the number of missed Go trials recorded. SSRT was analysed in a Hand (left, right) x Group ANOVA.

6.2.5. fMRI data

MR image acquisition

Magnetic resonance images were acquired using a Siemens Vision 1.5 T whole-body MR scanner equipped with a Siemens quadrature head coil. Prior to all experimental runs a magnetization prepared rapid acquisition gradient echo (MPRAGE) sequence (TR = 9.7 ms, TE = 4 ms, flip angle = 12°, 224 x 256 matrix, FoV = 250 mm, voxel size = 0.98 mm^3) was used to acquire a 176 slice, high-resolution T1-weighted anatomical image for later registration into standardised stereotactic space (MNI). During stimulus presentation, 130 whole brain EPI images (TR = 3.839, TE = 70 ms, flip angle = 90°, FoV = 256 mm, 64 x 64 matrix, voxel size = 4 mm^3) were acquired during each stimulus presentation block. Individual images were acquired as 32 interleaved slices (no gap) beginning at the top of the head and positioned oblique to the anterior-posterior commissural line, maximizing brain volume imaged (including cerebellum).

MR image pre-processing

Initially, bad slices present in individual volumes were identified and repaired using image artifact repair tools ('ArtRepair'; Mazaika et al., 2007) that identify and replace aberrant slices with corrected slices estimated (using interpolation algorithms) from slices in surrounding images. Further image pre-processing and subsequent statistical analyses were performed using SPM2 (Wellcome Department of Neurology, London). The first 6 images from each imaging run were associated with the countdown and practice Go trials, and were thus discarded. Differences in EPI slice acquisition timing were corrected using the central slice as a reference. Image time series were then realigned[38] to the first EPI image and a mean realigned EPI image was created. Each participant's T1 image was co-

[38] Uwarping was not used in this protocol as per Experiment 2. It was at first attempted but produced deformed output images in one patient participant. For this reason a standard affine transformation was performed to correct for head motion artifacts.

registered to the mean EPI image and normalized to the T1 template provided with SPM2. The parameters from this transformation were then applied to all EPI images. Accuracy of registration between functional and structural data was assessed by visual inspection of the overlay of individual subject's mean EPI and T1 image. Normalised EPIs were then smoothed with an 8 mm FWHM. Artifact repair tools (Mazaika et al., 2007) were then used to identify and replace outlier volumes with volumes estimated via interpolation algorithms. This process identifies volumes that are extreme outliers (e.g. 100 x mean volume intensity), but is insensitive to less variant images (e.g. 10 x mean volume intensity). Therefore a final process was undertaken to identify 'badscans'.

Identifying 'bad scans'

To further reduce the effect of residual motion-related BOLD variance, individual image data sets were investigated using a time-series diagnostic tool ('tsdiffana'; Matthew Brett, MRC CBU: http://imaging.mri-cbu.cam.ac.uk/imaging/DataDiagnostics) to identify aberrant images. This tool was used to calculate and output an array (in MATLAB) specifying the variance between successive images calculated as the mean of squared differences in BOLD signal intensity of corresponding voxels in successive volumes divided by the mean of all voxels in all tested volumes. Variances that were three standard deviations from the mean were identified using a simple MATLAB script. Subsequently, volumes causing the variability were identified and their intensities compared to adjacent volumes were checked using MRIcro. The positions of these volumes in the time series were compared to a plot of realignment parameters and volumes whose intensity difference was related to movement were identified and termed 'bad scans'. This was done for each scanning run separately. To regress out the effect of bad scans in first level modeling, a vector was constructed for each scanning run with a '1' coding bad scans and immediately adjacent volumes, and a '0' coding all other volumes, and modeled for affected participants.

Modeling: First level analyses

Time-series data were first smoothed with a 60 s high-pass filter then modeled with regressors predicting BOLD signal variance related to Stops, Stop Failures and correct Go

events, for left and right hand events separately. Each predictor was estimated by first fitting a convolved canonical HRF and its temporal derivative (Josephs et al., 1997) to the onset of Os and Xs for correct Go events, and to the onset of tones for Stops and Stop Failures. Incorrect Go trials, missed Go trials and correct inhibition trials preceded by a missed Go trial were modelled as a single nuisance variable. The motion parameters derived during realignment were included as covariates of no interest in the model to account for BOLD signal correlated head motion. A final covariate of no interest was the 'bad scans' vector described above that functioned to regress out any large motion related effects in the time series. The contrasts of most interests from this model were, for left and right hands separately, Stops > Go, and Stop Failures > Go.

Modeling: Second level analyses

Group results were initially derived for each group separately by entering individual subject contrast maps into random effects one sample t-tests for each contrast of interest, i.e., Stops > Go, Go > Stops, Stop Failures > Go, Stops > Stop Failures, Stop Failures > Stops, and Go > Baseline (tables not reported for this last contrast for either group). Matched-samples t-tests (matched on age and gender) were used to investigate differences in brain activation between the patient and control groups for contrasts of interest, i.e., Stops > Go, Stop Failures > Go, and Go > Baseline.

To ensure that only areas above threshold in each group contrast were considered for between-group t-tests, masks were created for each group contrast and then combined into a single mask image. To perform this, group one sample t-tests were individually threshold at $p < .05$ and 5 contiguous voxels, and a mask defining all above threshold voxels made for each contrast (three) for each group (six in total). Respective contrast masks for each group were then combined using an 'OR' operator in SPM2 ('imcalc' function). During the application of thresholds for between group tests, the contrast appropriate mask was applied to the data so that only voxels that were above threshold in the individual group contrasts could be considered for analysis in between-group tests. Simple correlation models were set up (for each group) which investigated between subject BOLD signal variance explained by SSRT combined over hands.

In addition, in order to replicate an analysis performed by Ford et al. (2004) with Go/No-go paradigm fMRI data, the number of activated voxels surviving a threshold of $p < .05$ and 10 activated voxels in the Go > Stop contrast were calculated from each group contrast.

Small volume correction (SVC) analyses

Regions of interest were identified using the Automated Anatomical Labeling maps (AAL; Tzourio-Mazoyer et al., 2002). These were the right hemisphere IFG (combined *pars triangularis*, *pars opercularis* and *pars orbitalis*), MFG, pre-SMA, putamen, globus pallidus (internal and external capsules not delineated) and thalamus. The right rSTN ROI was informed by Aron and Poldrack (2006), and identical to that used in Experiment 2. These ROIs were used as a priori small volumes for SVC analyses by first converting them to images using marsbar software (Brett et al., 2002a). Group activation maps were threshold at $p < .01$ (0 contiguous voxels) and the corrections applied.

6.2.5. ERP data

EEG data recording

The EEG was recorded using a Quik-cap from 30 scalp electrodes positioned according to the 10/20 system (M1, M2, Oz, Pz, P4, CP4, P8, C4, TP8, T8, P7, P3, CP3, CPz, Cz, FC4, FT8, TP7, C3, FCz, Fz, F4, F8, T7, FT7, FC3, F3, FP2, F7, FP1) and referenced to a nose electrode. Vertical and horizontal electro-oculograms (EOG) were recorded via electrodes positioned above and below the left eye, and on the outer canthi of each eye, respectively. EEG and EOG were continuously sampled at 500Hz/channel on a Synamps system (Neuroscan) with a band-pass of 0.01-30Hz using a 50Hz notch filter and gain of $2x10^4$.

ERP data preprocessing

Preprocessing of EEG data was performed using Scan 4.3. First, raw EEG time series were inspected for sections of EEG contaminated with channel saturation or noise, which were blocked out and excluded from further analysis. Vertical eyeblink artifacts were corrected in the continuous EEG files using the algorithm developed by Semslitch et al. (1986) as implemented in Neuroscan software.

ERP trial averaging

ERP averages were created for Stops and Stop Failures by locking events to the onset of tones for these trials, and Go event averages were created by locking events to the onset of correct Go trials only. All averages were created by extracting 1000 ms epochs around the onset of crucial stimuli (-200 ms to 800 ms). This procedure was followed for left and right hand averages separately for each event type.

ADJAR correction and Group averaging procedure for stop-signal group average waveforms

Stop and Stop Failure ERPs were corrected for Go response overlap using the ADJAR procedures described for experiment 2. Consequent corrected waveforms were baseline corrected over the pre-stimulus interval (-200 - 0ms) using Scan software (see Figure 6.09 for graphic display of correction waves at Cz) .Group averages were then created from these ADJAR and baseline corrected waveforms (see Figure 6.09, Figure 6.10 and Figure 6.11) separately for Stops and Stop Failures.

Component measures analyses for Go, Stop and Stop Failure waveforms

In house software was used to extract maximum and minimum ERP component latencies and amplitudes within a time-window specified by the user, in addition to mean amplitudes across a specified window at selected lateral and midline sites located over frontal, central and parietal areas as per Experiment 2. Appropriate windows were determined by visual inspection of the grand average waveforms for each event-type (Go events, Stops and Stop Failures) and are detailed in the results. For all analyses, Greenhouse-Geisser corrected p-values are reported.

To further investigate the findings of Experiment 2 where it was found that SSRT predicted Stop-P3 amplitude and the latency difference between Stop-P3 and Stop-N1 ('Stop P3-N1 latency'), peak amplitude and latency measures (Stop-N1 and Stop-P3), in addition to Stop P3-N1 latency, were, for each hand, entered into a correlation matrix with left and right hand SSRT.

Integration of fMRI and ERP data

Latency and amplitude measures of Stop-N1, Stop-P3 and the Stop P3-N1 latency were correlated with Stops > Go contrast maps and explored in an SVC analysis using *a priori* ROIs outlined previously. Additionally, the mean of a potential identified in the N2 latency range in Stop Failure ERPs for both groups was correlated with Stop Failure > Go contrast maps for each group separately, testing for a negative relationship. This data was (post-hoc) explored by application of an ACC ROI constructed from AAL maps in an SVC analysis.

6.3. Results

6.3.1. Trial type proportions for fMRI and ERP sessions

Due to a programming error as noted earlier, most participants were presented more right hand Go trials ('X' only) than left hand Go trials ('O' only), but were presented equal numbers of left and right hand stop-signal trials (56 each hand), as intended. Consequently, the probability that a trial beginning with an O would be a stop-signal trial was increased, and the probability that a trial beginning with and X would be a stop-signal trial was decreased. Fortunately this error was consistent across patient and control groups and across fMRI and ERP sessions. However its effects were investigated by entering the proportions of stop-signal and Go trial types (see Table 6.03) into separate 2-way ANOVAs

with Hand (left or right) as the within-subjects factor and Group (patient or control) as the between subjects factor.

Table 6.03

Mean numbers and proportions (with standard deviations in parentheses) of trial types by experimental session

Variable*	Controls		Patients	
	total	range	total	Range
fMRI session				
no. left go trials	159 (8.4)	144 – 171	159 (6.6)	147 – 171
no. right go trials	177 (8.4)	165 - 192	177 (6.6)	165 – 189
P(O)	.47 (.03)	.43 -.51	.47 (.02)	.44 -.51
P(X)	.53 (.03)	.49 -.57	.53 (.02)	.49 -.56
P(left SST)	.26 (.01)	.25 -.28	.26 (.01)	.25 -.28
P(right SST)	.24 (.01)	.23 -.25	.24 (.01)	.23 -.25
no. left Stop trials	56 (0)	N/A	56 (0)	N/A
no. right Stop trials	56 (0)	N/A	56 (0)	N/A
ERP session				
no. left go trials	316 (11)	296 - 340	313 (12)	295 – 337
no. right go trials	356 (11)	332 - 376	359 (12)	335 – 377
P(O)	.47 (.02)	.44 -.51	.47 (.02)	.44 -.50
P(X)	.53 (.02)	.49 - .56	.53 (.02)	.50 -.56
P(left SST)	.26 (.01)	.25 -.27	.26 (.01)	.25 -.28
P(right SST)	.24 (.01)	.23 -.25	.24 (.01)	.23 -.25
no. left Stop trials	112 (0)	N/A	112 (0)	N/A
no. right Stop trials	112 (0)	N/A	112 (0)	N/A

*P(O) = probability of a left hand go trial among all go trials (no.left go trials/no. left stop-signal trials); P(X) = probability of a right hand go trial among all go trials; P(left SST) = probability of a left hand stop-signal task trial; P(right SST) = probability of a right hand stop-signal task trial (no.right go trials/no. right stop-signal trials).

Go trial proportions were computed by separately dividing the number of left and right Go trials by the total number of Go trials. Stop-signal trial proportions were

determined by dividing the number of left and right stop-signal trials by the number of their respective Go trial homologues. As expected, there were more right hand Go trials than left hand Go trials, revealed by a significant effect of Hand for both the fMRI, $F(1,18) = 29.98$, $p < .001$, and ERP sessions, $F(1,21) = 80.18$, $p < .001$. Importantly however, there was no effect of Group and no Hand X Group interaction in either session. Similarly, stop-signal trial type analyses revealed a significantly higher proportion of left hand trials that were stop-signal trials than right hand trials that were stop-signal trials shown by an effect of Hand in fMRI, $F(1,18) = 29.80$, $p < .001$, and ERP sessions, $F(1,21) = 79.63$, $p < .001$. These analyses likewise found no effect of Group and no Group X Hand interaction.

To validate matched-sample fMRI analyses, fMRI trial type proportions were also entered into a matched samples Hand x Group ANOVA. This analysis also found a significant effect of Hand, $F(1,9) = 26.91$, $p = .001$, but no effect of group, and no Group X Hand interaction.

6.3.2. fMRI session

6.3.2.1. Age, gender and education

Participants were matched for gender (three females and seven males in each group), and a matched-samples t-test (two-tailed) found no difference in the ages of Patients (M = 35.9, SD = 7.7) and matched Controls (M = 35.1, SD = 8.5), $t(9) = -.63$, *ns*. Years of education also did not differ between the Control (M = 17.5, SD = 1.4) and Patient (M = 16.3, SD = 2.9) groups, $t(9) = 1.41$, *ns*.

6.3.2.2. Behavioural data analyses

RT data and errors from the fMRI session (see Table 6.04) were examined using Group X Hand X Condition ANOVAs. Matched samples analyses were primarily used in fMRI session analyses, but independent samples ANOVAs were also run in order to verify findings and to be compatible with ERP session analyses where only independent samples analyses were used. For RT analyses, Conditions were GoRT and stop-failure RT (SFRT), while for Go error analyses, Conditions were errors of commission (incorrect Go trials) and errors of omission (missed Go trials). Analysis of SSD measures were conducted using a

Hand x Event type x Group ANOVA, while SSRT measures were assessed using a Hand x Group ANOVA model.

RT data

Analyses of RT data (see Table 6.04) revealed main effects for Condition, $F(1,9) = 59.19$, $p < .001$, and Hand, $F(1,9) = 21.69$, $p = .001$, while Group approached significance, $F(1,9) = 4.06$, $p = .075$. This analysis showed that control group Go responses tended to be faster than those of patients, right hand RTs were significantly faster than left hand RTs, and SFRTs were faster than GoRTs. No Hand x Group interaction was observed. When Group was treated as a between-subjects factor, a significant main effect of Group was revealed, $F(1,18) = 5.56$, $p = .03$, and in agreement with the matched samples analysis, strong main effects of Hand, $F(1,18) = 13.14$, $p = .002$, and Condition, $F(1,18) = 65.01$, $p < .001$, were observed while no interactions were found.

SSRT and SSD analyses

Stop-signal delay and SSRT were entered into separate Group X Hand ANOVAs. In a matched samples ANOVA, no significant main effects or interactions were found in SSRT analyses despite large group mean differences in SSRT. However, when the data were analysed as a between group design, the group effect approached significance, $F(1,18) = 4.18$, $p = .056$. Inspection of individual subject data suggested that this non-significant finding was largely driven by one participant in the patient group who had extremely fast estimated SSRTs (left = 122 ms, right = 172 ms, combined = 144 ms). For this reason, the participant with the fastest combined SSRT in each group was dropped from the analysis and the between subjects ANOVA re-run. In this analysis, the effect of Group was substantial, $F(1,16) = 5.91$, $p = .027$. To test whether generalized slowing could account for this effect, left and right hand GoRT were added as covariates to the model. ANCOVA analyses confirmed the previous result, indeed the effect was increased, $F(1,14) = 6.80$, $p = .021$. SSD analyses also revealed no significant main effects or interactions, but there was a trend for Hand to be significant, $F(1,9) = 4.64$, $p = .060$, indicating that SSDs tended to be shorter on right hand trials, which is not surprising given that right hand GoRT was faster in each group.

Table 6.04

Left and right hand fMRI session behavioural data for patient and control groups

Variable*	Controls		Patients	
	left	right	left	right
GoRT (ms)	464 (66)	450 (70)	574 (135)	553 (121)
SFRT (ms)	429 (59)	409 (54)	522 (126)	503 (115)
no. correct go (Go)	151 (12)	171 (12)	149 (10)	165 (16)
no. incorrect go	3 (4)	3 (4)	3 (3)	4 (5)
no. missed go	4 (8)	4 (10)	7 (6)	9 (16)
correct Go (%)	96 (6)	96 (6)	94 (4)	93 (8)
missed Go (%)	2 (6)	2 (6)	5 (4)	5 (9)
incorrect Go (%)	2 (2)	2 (3)	2 (2)	2 (3)
Go errors (%)	4 (6)	4 (6)	6 (4)	7 (8)
missed Go/Go errors (%)†	18 (39)	32 (36)	60 (37)	50 (38)
incorrect Go/Go errors (%)†	52 (51)	68 (36)	20 (22)	50 (38)
Mean PI	.51 (.02)	.51 (.03)	.50 (.07)	.48 (.08)
mean cPI	.50 (.02)	.50 (.02)	.48 (.08)	.45 (.09)
mean SSD	240 (78)	223 (65)	295 (181)	274 (175)
SSRT	223 (40)	227 (31)	284 (102)	291 (98)

†The percentages reported are mean percentages that were calculated by dividing the number of each go error type (separately) and dividing by the sum of all go errors, and multiplying the quotient by 100. The figures do not sum to 100 percent because some participants made no errors thereby reducing the mean.

*Median Go reaction time = GoRT; Median Stop Failure reaction time = SFRT; probability of inhibition = PI; corrected PI = cPI; stop-signal delay = SSD; stop-signal reaction time = SSRT.

Errors

The numbers of Go trial errors of commission and errors of omission were entered into a Group X Hand X Type of error ANOVA. No effects were observed, indicating that patient accuracy was equivalent to that of controls.

Pre and post-event RT analyses

Data extracted for pre- and post- event RTs (medians; see Table 6.05) were entered into a Hand x Event type x Time x Group ANOVA, where Event type factor included Go, Stop and Stop Failure levels and the factor Time pre- and post- event RTs.

Table 6.05

Patient and control group median pre and post event RTs for left and right hands

Event	Controls		Patients	
	Pre	Post	Pre	Post
Left				
Go	457 (69)	454 (64)	554 (127)	557 (136)
Stop Failures	443 (62)	462 (72)	548 (132)	576 (148)
Stops	451 (60)	458 (75)	571 (129)	576 (122)
Right				
Go	450 (63)	449 (64)	558 (128)	552 (129)
Stop Failures	444(62)	461 (70)	536 (112)	552 (140)
Stops	459 (72)	452 (71)	568 (138)	559 (110)

Despite that Go and Stop trial RT differences were on average approximately 2 ms, whereas Stop Failure RT differences were approximately 20 ms, an Event type x Time interaction only approached significance, $F(1.873,33.716) = 2.935$, $p = .070$, indicating that the differences between pre and post RTs surround Stop Failures were generally larger than those surrounding Go and Stop trials, but not significantly so. However, a main effect of Event type, $F(1.995, 35.911) = 3.52$, $p = .040$, demonstrated that events surrounding Stops were significantly slower than for other events. Group was also significant, $F(1,18) = 5.51$, $p = .031$, with patient RTs overall being slower than control RTs but there were no interactions between Group and Time or Event type.

In separate analyses, pre- and post- event RTs were analysed in Hand x Event type x Group ANOVAs. In pre- event RT analysis, a main effect of Event type was observed, $F(1.65,29.66) = 13.02$, $p < .001$, signalling that pre- Stop Failure event RTs (493 ms) were significantly faster than pre- event Go RTs (505 ms) and Stop RTs (513 ms). As expected, there was a main effect of Group, $F(1,18) = 5.51$, $p = .030$, confirming that control pre-event RTs were significantly faster than patient pre- event RTs, but there were no Group x Event type interaction. In post- event RT analyses, a main effect of Hand was observed, $F(1,18) = 7.29$, $p = .015$, indicating that right hand post event RTs were significantly faster than left hand post- event RTs, in line with RT/SFRT analyses. Additionally, a main effect

of Group was observed, $F(1,18) = 5.41$, $p = .032$, confirming that control post- event RTs were significantly faster than patient post- event RTs. Planned comparisons between pre-Stop RTs and pre Stop Failure RTs using paired samples t-tests were significant for both the left hand, $t(20) = 2.56$, $p = .019$, and right hand, $t(20) = 3.40$, $p = .003$. In an identical analysis for post-event RTs, no effects were observed.

Paired t-test comparisons of pre-event with post-event RTs for each event-type confirmed that Go RTs following Stop Failures were significantly slower. Go RTs following Stops were not slowed.

Relationships between behavioural variables and symptom profiles

Total SAPS and total SANS scores were entered into a correlation matrix with SSRT, GoRT and for each hand, in addition to age. No relationships were observed.

6.3.2.3. fMRI data

Go > Baseline: one-sample t-tests

Though not of particular interest, Go related activation was initially assessed for each group by contrasting Go trials against the implicit baseline (see Figure 6.01). This was performed to check that left hand Go trials activated right primary motor cortex (M1) and that right hand Go trials activated left M1, which, in addition to premotor areas, especially SMA, was observed.

Go > Baseline: Matched sample t-tests

In the comparison Controls > Patients, differences were limited to the left thalamus and posterior cingulate/precuneus areas, whereas in the reverse contrast, Patients > Controls, the differences observed were more extensive, including right MFG and anterior cerebellar cortex (see Table 6.06, and Figure 6.01).

Table 6.06

Brain areas surviving thresholding from matched samples t-tests, Controls > Patients and Patients > Controls, in a comparison of Go > Baseline contrast maps (thresholding was $p < .01$, and 10 contiguous voxels)

Brain Area*	BA	Cluster Size	T-score	MNI Coords
Patients > Controls				
Right hemisphere				
Cerebellum (anterior)	-	16	7.32	24 -40 -36
Cerebellum (anterior)	-		4.63	16 -40 -32
MFG	9/46	6	6.46	40 24 28
MFG	10	4	4.88	40 40 12
Controls > Patients				
Left hemisphere				
Thalamus	-	9	4.17	-8 -4 12
Posterior cingulate/precuneus		1	3.21	-4 -52 28

* MFG = middle frontal gyrus

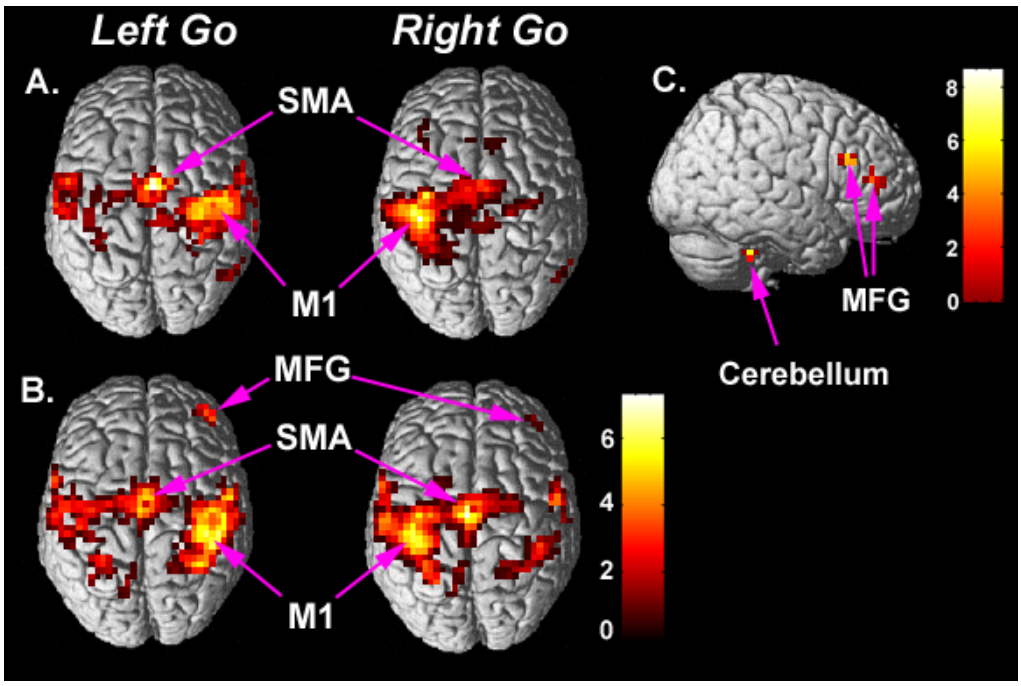

Figure 6.01. Go > Baseline contrasts (right is right). A. shows SMA and M1 activation for left and right hand contrasts in controls (thresholding was $p < .05$, and 10 contiguous voxels). B. Shows SMA and M1 activation for left and right hand contrasts in patients (thresholding was $p < .05$, and 10 contiguous voxels). C. shows between group patients > controls activation for the contrast of left and right hand combined within each group (thresholding was $p < .01$, and 10 contiguous voxels).

Stops > Go contrast: One sample t-tests

In the contrast of most interest for this experiment, Stops > Go, controls exhibited significant BOLD activation peaks within an anticipated network of fronto-parietal and temporal cortical areas, but crucially, significant activation was detected within predicted nuclei of the basal ganglia. Predictably, there was widespread activation observed within bilateral temporal cortex, especially STG that is particularly engaged during the processing of tones during stop-signal trials. Aside from these areas, the inhibition network activated in controls was predominantly located in right lateralized frontal cortical structures, including IFG and MFG, SFG, medial SFG including preSMA and SMA, and also ACC. Significant BOLD responses were also observed within right parietal cortex including IPL and the cuneus. Right basal ganglia activation included the ventrolateral nucleus of the thalamus, and also STN. Left hemisphere activation included IFG, MFG, insula cortex, the cuneus, and ventrolateral nucleus of the thalamus.

Table 6.07

Control group activation for Stops > Go contrast (thresholding was p < .01, and 10 contiguous voxels)

Brain Area*	BA	No. Voxels	t - score	MNI Co-ords
Right hemisphere				
MFG/IFG	9/44	213	8.65	40 12 28
IFG/insula	47/44/45		7.99	40 20 -8
MFG	9/46		5.83	44 20 32
STG	22	101	6.76	56 -28 4
STG	41		4.83	44 -32 4
STG	22		4.45	56 -48 12
SFG	10	48	6.59	28 52 20
MFG	46		4.68	40 44 12
SPL	7	28	5.51	36 -60 52
IPL	40		4.42	40 -52 52
Cuneus	18		3.65	4 -84 16
Cuneus	18		3.17	0 -88 8
Thalamus	-	21	4.72	12 -16 4
GP/STN	-		3.97	16 -8 -4
MFG/PCG	6	18	4.68	36 -4 52
MFG/PCG	6		3.82	32 4 52
IPL	40	29	4.07	52 -40 32
ACC	32	12	4.05	8 24 32
SFG	6	18	3.85	28 -8 72
SFG	6		3.71	16 4 72
Left Hemisphere				
IFG	47	102	7.35	-32 20 0
Insula	13		6.12	-40 12 8
Insula	13		5.08	-44 12 0
STG	42	132	6.82	-64 -32 8
STG	22		5.58	-60 -44 16
TTG	41		5.02	-40 -36 12
MFG	9	16	4.89	-44 32 32
MFG	9		3.35	-52 24 36
MFG	9		3.16	-36 44 32
Cuneus	18	19	4.76	-8 -80 20
Thalamus (vln)	-	12	4.05	-12 -8 8

*MFG = middle frontal gyrus; IFG = inferior frontal gyrus; STG = superior temporal gyrus; SFG = superior frontal gyrus; SPL = superior parietal lobe; IPL = inferior parietal lobe; GP = globus pallidus; STN = subthalamic nucleus; PCG = precentral gyrus; ACC = anterior cingulate gyrus; TTG = transverse temporal gyrus.

Table 6.08

Patient group activation for Stops > Go contrast (thresholding was p < .01, and 10 contiguous voxels)

Brain Area*	BA	No. Voxels	t - score	MNI Co-ords
Right hemisphere				
SMG	40	34	5.27	60 -48 36
IPL	40		5.13	64 -36 36
MTG	21	36	5.06	64 -4 -8
IFG	47		4.62	44 20 -16
STG	38		3.53	60 8 -12
ACC	32	19	5.04	8 32 24
STG	42	14	4.89	64 -24 8
Left hemisphere				
IPL	40	53	8.31	-56 -44 28
IPL	40		6.99	-56 -44 40
IPL	40		3.65	-52 -48 52
Insula	13	31	5.20	-40 16 0
Insula	13		4.96	-40 8 -12
STG	38		3.58	-44 16 -12
ACC	24		3.91	-4 32 20
MTG	39	21	4.99	-44 -60 4
MTG	21		3.64	-60 -60 4

*SMG = supramarginal gyrus; IPL = inferior parietal lobe; MTG = middle temporal gyrus; IFG = inferior frontal gyrus; STG = superior temporal gyrus; ACC = anterior cingulate gyrus.

Patient group activation in general was reduced compared to controls, but the network of activated areas overlapped that of controls mostly in cortical areas. At the same thresholding (p < .01, 10 contiguous voxels), bilateral activation was observed within ACC, the parietal lobe (IPL and supramarginal gyrus) and temporal cortex (STG and MTG). Right lateralized clusters were observed within IFG, while left lateralized clusters were observed within the insula.

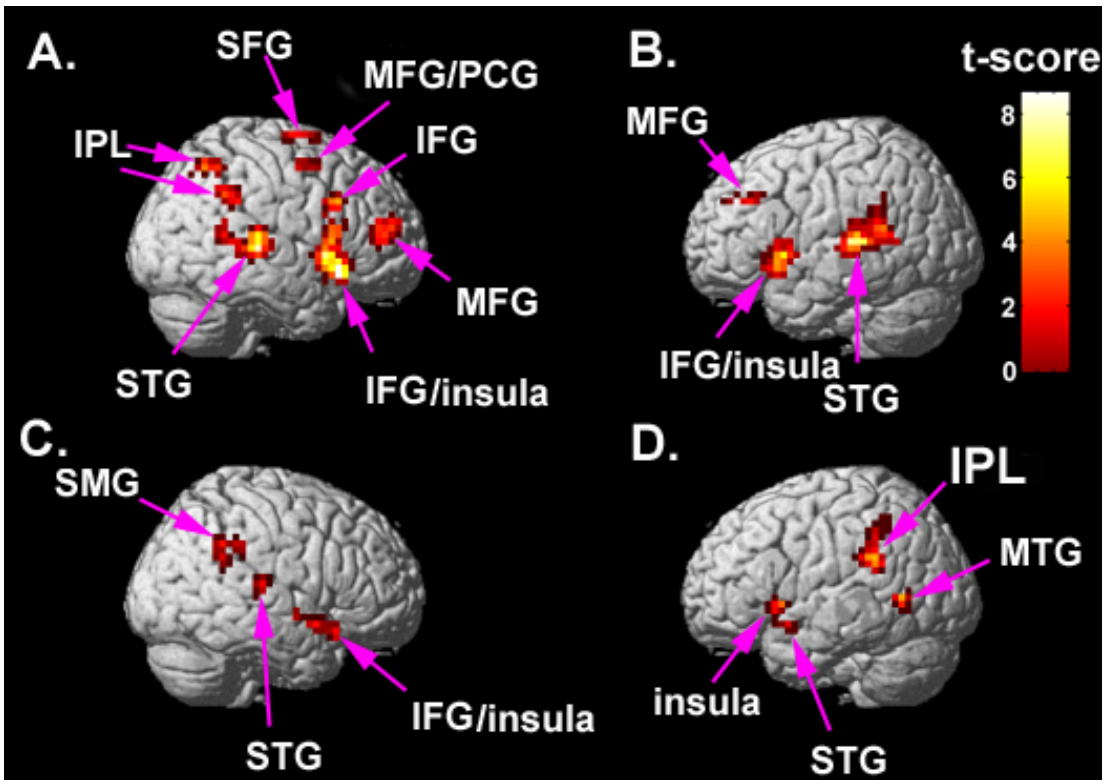

Figure 6.02. Cortical activation for Stops > Go in control and patient groups (thresholding was p < .01, and 10 contiguous voxels) with t-score bar shown on top right (right is right). Top panel shows right hemisphere (A.) and left hemisphere (B.) activation for controls. The bottom panel shows right hemisphere (C.) and left hemisphere (D.) activation for patients.

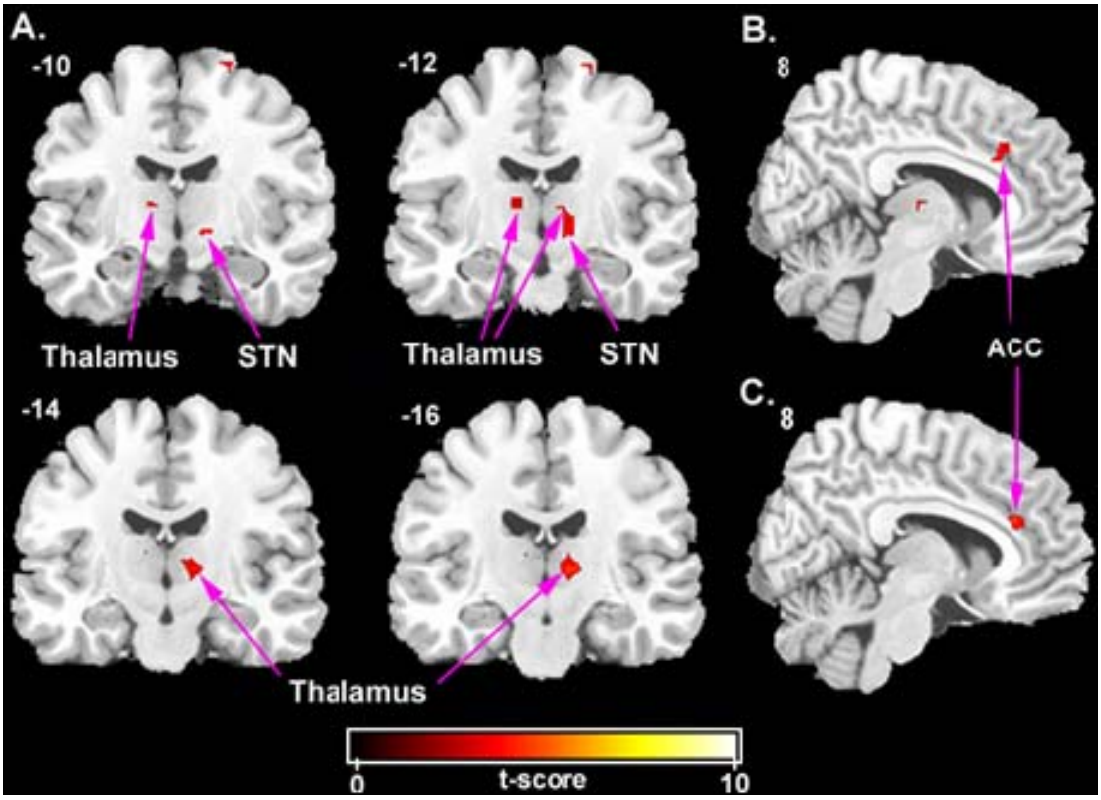

Figure 6.03. Subcortical and anterior cingulate (ACC) activation revealed in Stops > Go (thresholding was p < .01, and 10 contiguous voxels) with t-score bar shown at bottom (right is right). A. depicts thalamic and subthalamic nucleus (STN) activation for controls (numbers refer to MNI y-coordinates); B. ACC activation for controls (numbers refer to MNI x-coordinates); C. ACC activation for patients (numbers refer to MNI x-coordinates).

Matched samples t-tests of Stop > Go contrast

In a matched-samples t-test, controls were found to have significantly greater activation than patients in predominantly right lateralised brain areas including IFG, MFG, thalamus and STN (see Table 6.09, Figure 6.04). Additional activation was observed in right insula, IPL, SPL, precuneus and the paracentral lobule, while significant left lateralized activation was seen within the thalamus and globus pallidus (GP).

Table 6.09

Areas surviving thresholding in a matched-samples t-test contrast testing differences in Stop > Go related activation for Controls > Patients

Brain Area*	BA	No. Voxels	t - score	MNI Co-ords
Right hemisphere				
STN/SN	-	18	6.51	16 -16 -4
Thalamus	-		5.76	12 -20 0
MFG	9	14	6.13	32 12 28
MFG	9		4.98	48 20 32
IFG	44	35	6.07	48 16 12
Insula	13		3.77	36 24 20
Paracentral lobule	5	4	4.58	8 -40 60
SPL	7	3	3.73	28 -60 40
SPL	7	11	3.66	36 -64 52
IPL	40	2	3.49	36 -48 56
Precuneus	7	2	2.95	8 -72 32
Left hemisphere				
GP/STN	-	20	5.97	-16 -4 8
GP	-		3.42	-20 -12 -4

*STN = subthalamic nucleus; SN = substantia nigra; MFG = middle frontal gyrus; IFG = inferior frontal gyrus; SPL = superior parietal lobule; IPL = inferior parietal lobule; GP = globus pallidus.

SVCs were applied across the a priori ROIs for this contrast. The IFG contained both cluster and voxel corrected activation which was located within pars opercularis, and likewise, STN and thalamus ROIs contained significant activations at both the cluster and voxel levels, though it must be conceded that the same voxel was significant in both ROIs (MNI cords: 12 -20 0). The peak STN voxel reported in Table 6.09 corresponded to a voxel that was adjacent to the STN ROI.

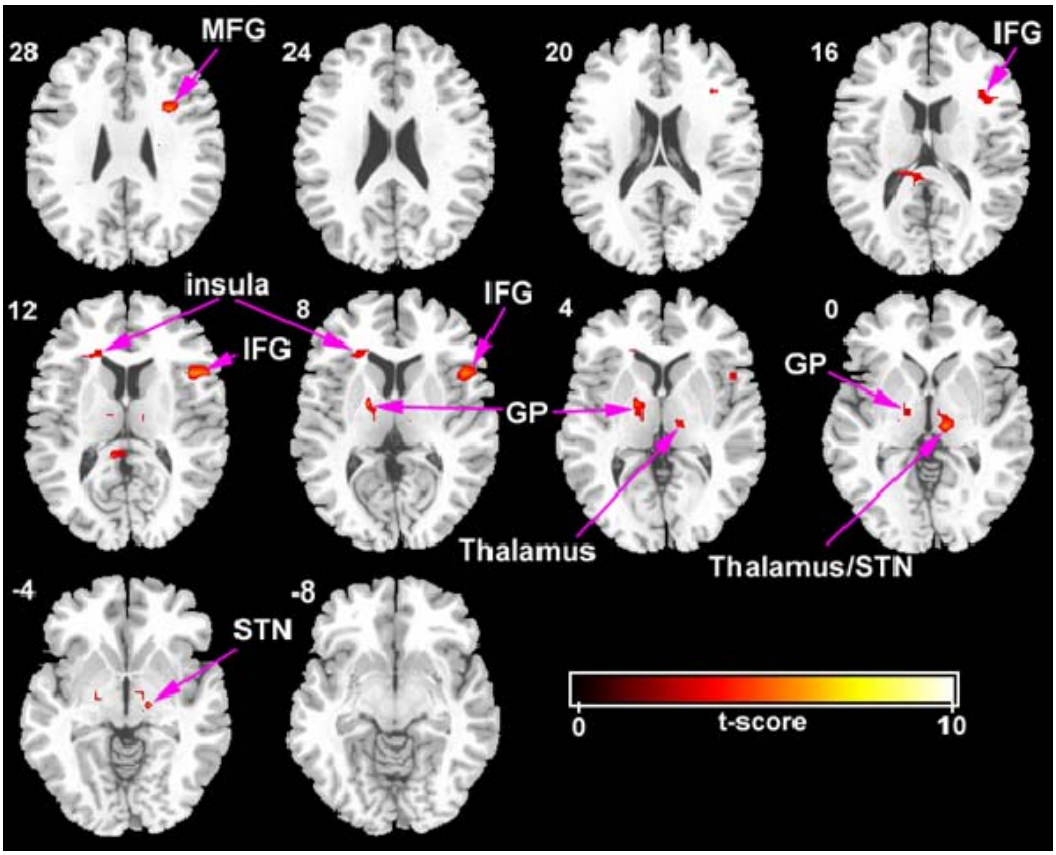

Figure 6.04. Prefrontal and subcortical areas revealing greater activation in the controls > patients contrast above threshold activation ($p < .01$, and 10 contiguous voxels; right is right).

No significant activation was observed at the same thresholding in the reverse contrast, Patients > Controls, hence a more liberal thresholding criteria ($p < .05$, 10 contiguous voxels) was applied to the data. At this level, significant activation was observed bilaterally in ACC, while right hemisphere activity was seen within portions of the precuneus and anterior STG (see Table 6.10 and Figure 6.05). In the left hemisphere, significant peaks were observed within cerebellar tonsil, MTG, and MFG.

Table 6.10

Areas surviving thresholding in a matched-samples t-test contrast testing differences in Stop > Go related activation for Patients > Controls

Brain Area*	BA	No. Voxels	t - score	MNI Co-ords
Right hemisphere				
ACC	24	18	3.62	4 32 20
Precuneus	9	4	2.95	8 -80 44
STG (anterior)	38	1	2.13	48 16 -20
STG (anterior)	38	2	1.94	48 8 -16
Left hemisphere				
Cerebellar tonsil	-	7	4.87	-16 -32 -44
MTG	39	12	3.30	-44 -60 4
MFG	9	4	2.61	-24 36 28
ACC	32	1	2.32	-16 36 20

*ACC = anterior cingulate cortex; STG = superior temporal gyrus; MTG = middle temporal gyrus; MFG = middle frontal gyrus.

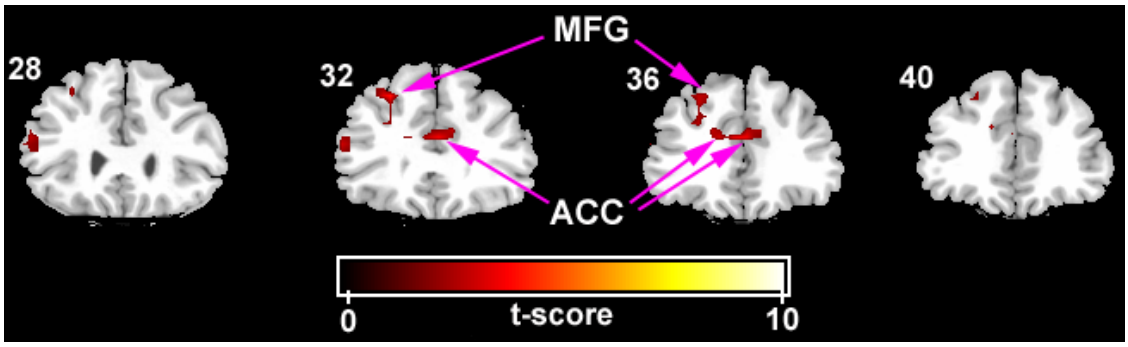

Figure 6.05. PFC activation surviving threshold39 (p < .05, 10 contiguous) when Stops > Go contrasts were compared for patients > controls.

[39] Some residual activation can be observed in the left IFG, however, this cluster was not present when the combined group mask was applied. As such, it was not reported in the tabled summary for this contrast.

Number of activated voxels in Go > Stops and Stops > Go contrasts for patient and controls groups

In an attempt to replicate the analysis performed by Ford et al. (2004), the contrasts, Stop > Go and Go > Stop were threshold at $p < .05$ and 5 contiguous voxels, and the resulting number of activated voxels was determined from the SPM2 output (see Table 6.11).

Table 6.11

Total voxels surviving thresholding (at $p < .05$, 5 contiguous voxels) for left, right and combined Go > Stops and Stops > Go contrasts for patient and control groups

	Left	Right	Collapsed
Go > Stop			
Controls	1619	1067	1639
Patients	1761	1731	2618
Controls - Patients	-142	- 664	- 979
Stop > Go			
Controls	2690	1465	2621
Patients	1113	602	1000
Controls - Patients	1577	863	1621

Controls elicited a greater number of activated voxels during Stops > Go compared to their Go > Stop contrast and the patient group Stop > Go contrast. However, more above threshold activation was present in the patient group Go > Stops contrast compared to the control group Go > Stop contrast, and also the patient group Stop > Go contrast. While not a formal analysis, these observations underscore the heightened level of Go related activation present in the patient group neuroimaging data, that was already indicated in the group comparisons of Go > Baseline contrasts where the patient group elicited greater PFC activation than controls (see Table 6.11).

Stop Failures > Go: One sample t-tests

This contrast revealed quite different activation patterns for patient and control groups. Control group activation (see Table 6.12, Figure 6.06) included bilateral activation

of the cerebellum, STG, and at the ACC/preSMA boundary, while right hemisphere BOLD peaks included rostral (BA10) and caudal (BA6) portions of MFG, extensively in IFG, the cuneus, substantia nigra, and parahippocampal gyrus. Left lateralized activation was limited to the lingual gyrus and precuneus.

Table 6.12

Control group activation for Stop Failures > Go one sample t-test ($p < .01$, and 10 voxels)

Brain Area*	BA	No. Voxels	t - score	MNI Co-ords
Right hemisphere				
MFG	6	14	7.79	48 8 52
IPL	40	135	6.79	68 -32 24
STG	41		6.22	60 -20 4
STG	22		5.33	56 -4 -4
Cuneus	18		5.00	0 -92 4
IFG	44	146	6.08	52 12 4
IFG	47		5.97	44 20 -8
IFG	47		5.66	36 20 -12
PreSMA /FEF	6/8	74	5.71	4 16 56
PreSMA	6		5.66	4 8 60
ACC/preSMA	32		5.42	0 4 48
SN	-	21	5.65	8 -24 -12
Parahippocampal gyrus	27		4.94	12 -36 -4
MFG	10	23	4.82	28 48 24
Cerebellar culmen	-	16	4.15	16 -64 -12
ACC	24		3.37	0 20 28
Left Hemisphere				
Cerebellar declive	-	53	6.18	-16 -68 -16
Lingual Gyrus	18		3.90	-12 -76 -8
STG	13	208	5.81	-56 -44 20
STG	21		5.27	-44 -16 -16
STG	22		5.20	-52 4 0
Precuneus	7	13	5.20	-12 -80 40
ACC	32	13	3.56	-8 24 32

*MFG = middle frontal gyrus; IPL = inferior parietal lobe; STG = superior temporal gyrus; IFG = inferior frontal gyrus; SFG = superior frontal gyrus; FEF = frontal eye fields; PreSMA = pre-supplementary motor area; SN = substantia nigra; ACC = anterior cingulate gyrus.

Patient group activation (see Table 6.13, Figure 6.06) was noticeably greater in height and extent, and included activation within bilateral MFG, IFG (extended in insula bilaterally and also into PCG on the right), ACC, STG and the supramarginal gyrus. Additional right lateralized activation was observed within the cerebellar cortex (tonsil and declive areas), lingual gyrus, and very substantial putamen activation. Other left hemisphere activation included MTG, SFG/MFG, the red nucleus/SN STN/SN and thalamus.

Table 6.13

Patient group activation for Stop Failures > Go one-sample t-test ($p < .01$, and 10 voxels)

Brain Area*	BA	No. Voxels	t - score	MNI Co-ords
Right hemisphere				
Putamen (ln)	-	528	9.94	28 -24 0
STG	38		8.63	44 12 -12
IFG/insula	47		8.57	40 20 0
MFG	9	91	6.12	36 32 36
ACC	32		5.93	16 20 40
ACC	32		5.17	12 16 32
Supramarginal gyrus	40	25	5.75	56 -44 36
Cerebellar tonsil	-	11	5.68	32 -56 -52
STG	22	33	5.07	56 -52 8
STG	22		4.23	64 -48 20
Lingual gyrus	30	16	4.76	20 -40 -4
Cerebellar declive	-	10	4.24	8 -64 -28
Left Hemisphere				
IFG	13	475	10.33	-44 0 12
IFG	44		9.94	-48 8 12
IFG	13		9.00	-40 4 -8
MTG	19	70	7.00	-44 -64 12
MTG	39		5.97	-48 -60 4
STG	42	98	5.63	-64 -32 12
STG	13		5.16	-44 -48 20
Supramarginal gyrus	40		4.58	-52 -48 28
Red nucleus/SN	-	47	4.80	-8 -28 -8
SN/STN	-		4.57	-8 -20 -12
Thalamus	-		4.30	-8 -16 0
MFG	10	34	4.35	-36 44 24
SFG/MFG	9		3.87	-36 36 32

Brain Area*	BA	No. Voxels	t - score	MNI Co-ords
ACC	32	35	4.27	-20 28 24
ACC	32		4.07	-20 16 28
ACC	32		3.19	-8 28 32
MFG	10	13	3.63	-28 52 0
MFG			3.32	-24 44 4

*STG = superior temporal gyrus; IFG = inferior frontal gyrus; MFG = middle frontal gyrus; ACC = anterior cingulate cortex; MTG = middle temporal gyrus; SN = substantia nigra; STN = subthalamic nucleus; SFG = superior frontal gyrus.

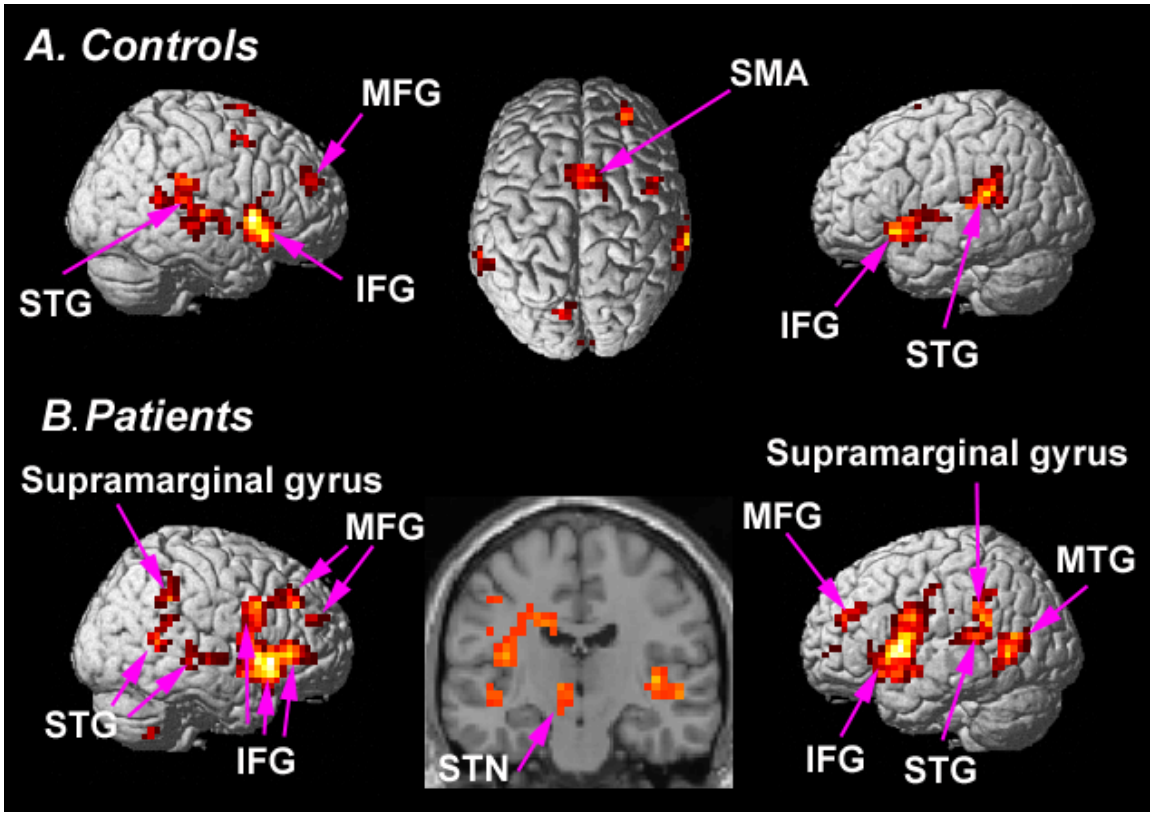

Figure 6.06. Stop Failures > Go within group activation for (A) controls (top panel views: right hemisphere cortex, superior cortical surface, and left hemisphere cortex), and (B) patients (bottom panel views: right hemisphere cortex, axial slice emphasizing STN activation, and left hemisphere cortex). All thresholding was ($p < .01$, and 10 contiguous voxels).

Matched sample t-tests

Matched samples t-tests revealed significantly greater control group activation only within the medial precuneus. For this reason a more liberal thresholding criteria ($p < .05$, 10 contiguous voxels; threshold masking was applied as in other matched samples t-tests) was used for both patients > controls and controls > patients contrasts. At this level, additional activation in the Controls > Patients matched samples t-test was observed within preSMA and ACC, in addition to right hemisphere lingual gyrus and cerebellar declive.

Table 6.14

Areas surviving thresholding in a matched-samples t-test contrast testing differences in Stop Failures > Go related activation for Controls > Patients.

Brain Area*	BA	No. Voxels	t - score	MNI Co-ords
Right hemisphere				
preSMA	6	16	3.65	4 4 52
Lingual gyrus	19	8	3.21	16 -64 -4
Cerebellar declive	-		2.16	16 -68 -16
Left hemisphere				
ACC/preSMA/SMA	24		3.22	-8 0 48
Precuneus	7	9	3.17	-8 -80 44
Precuneus	7		3.02	-4 -72 48

*preSMA = presupplementary motor area; ACC = anterior cingulate cortex; SMA = supplementary motor area.

In the reverse contrast, Patients > Controls, significant peaks were observed in widespread cortical and subcortical brain areas (see Table 6.15). This activation was far more extensive than was present in control group data (see Table 6.14). Activated areas included bilateral portions of IFG, MFG, PCG, the claustrum and insula, while right lateralized activation was limited to the putamen. Left hemisphere activation was more extensive including peaks within PCG, ACC and mid-cingulate, MTG, STG, supramarginal gyrus (SMG) and the caudate.

Table 6.15

Areas surviving thresholding in a matched-samples t-test contrast testing differences in Stop Failures > Go related activation for Patients > Controls

Brain Area*	BA	No. Voxels	t - score	MNI Co-ords
Right hemisphere				
IFG	45	24	5.56	56 32 8
IFG	46		4	40 36 8
IFG	47		3.74	40 36 0
MFG	9	16	5.33	32 32 32
Putamen	-	9	5.2	28 -20 0
Claustrum	-		4.88	28 -24 12
IFG/PCG	44	7	4.99	48 0 12
Claustrum	-	6	4.76	24 24 -4
MFG	9	18	4.14	48 12 28
IFG	9		3.79	44 8 32
Claustrum	-	6	4.01	32 4 12
Claustrum	-		3.19	36 0 8
Insula	13	4	3.7	40 -4 0
Insula	13	1	2.93	40 4 0
Left hemisphere				
IFG/PCG	44	90	9.39	-48 8 12
PCG	6		6.67	-52 -4 20
IFG	9		6.28	-48 4 32
PCG	6		5.09	-44 -8 36
PostCG	2		4.14	-44 -24 28
IFG	45		3.93	-52 16 4
ACC	32	22	5.28	-16 20 24
ACC	32		4.37	-20 16 32
Cingulate gyrus	24	12	4.66	-24 -12 36
MTG	37	24	4.37	-48 -60 0
Claustrum	-	4	4.13	-24 20 8
Claustrum	-	7	3.68	-32 -16 16
Insula	13		3.17	-32 -24 24
SMG	40	6	3.26	-44 -44 32
STG	13		3.26	-44 -48 24
MFG	10	4	3.19	-24 44 0
Caudate	-	1	3.11	-12 -16 28
MFG	10	1	2.89	-28 44 12

*IFG = inferior frontal gyrus; MFG = middle frontal gyrus; PCG = precentral gyrus; PostCG = post central gyrus; ACC = anterior cingulate cortex; SMG = supramarginal gyrus; STG = superior temporal gyrus.

For control group data only, a paired samples t-test of Stop > Go and Stop Failures > Go was performed to compare with the findings of Experiment 2. Stop > Stop Failure data are presented in Table 6.16, and Stop Failure > Stop data are presented in Table 6.17.

What is most noticeable in the graphical output of the Stop > Stop Failures contrast is extensive activation of left PFC, which includes clusters in IFG and SFG/FEF, but most extensively within MFG. Slightly posterior to these regions was activation in the claustrum and uncus. Bilateral cortical activation was observed in PostCG and inferior parietal areas, while the left hemisphere had additional activation within SPL. Other right hemisphere activation clusters were found in the fusiform gyrus and MTG. Another striking feature of this contrast is substantial sub-cortical activation, which is bilateral within striatal areas (caudate and putamen), and also the thalamus.

Table 6.16

Control group activation for a repeated-measures t-test contrast of (Stops > Go) > (Stop Failures > Go; $p < .01$, and 10 voxels)

Brain Area*	BA	No. Voxels	t - score	MNI Co-ords
Right hemisphere				
Claustrum	-	15	6.69	36 -16 -8
Putamen	-		4.80	28 -20 4
Thalamus	-		4.03	16 -20 4
Caudate	-	24	6.6	16 4 24
Caudate	-		4.73	16 -8 28
Caudate	-		3.29	24 -16 32
PostCG	4	16	5.22	16 -28 68
SFG	6		4.57	24 -12 72
IPL	40	10	4.35	48 -72 40
Angular gyrus	39		3.64	52 -72 32
GP/STN	-	27	4.26	16 -8 -4
Caudate	-		3.72	12 16 0
Putamen	-		3.66	24 4 0
Thalamus	-	13	4.13	0 -20 20
Thalamus	-		3.83	8 -20 16
Uncus	20	15	4.04	32 -4 -36
Fusiform gyrus	20		3.91	48 -4 -28
MTG	21		3.41	40 -4 -32

Brain Area*	BA	No. Voxels	t - score	MNI Co-ords
Left hemisphere				
SPL	7	21	6.01	-32 -76 44
Thalamus	-	13	5.80	-12 -12 12
Caudate	-		3.42	-4 0 16
Putamen	-	18	5.70	-32 -22 -4
Parahippocampal gyrus	36		3.48	-36 -32 -12
PCG/IFG	6	103	5.38	-44 0 32
MFG	8		5.26	-44 8 48
MFG	9		4.92	-52 8 40
MFG	10	50	5.22	-32 56 8
MFG	10		4.48	-28 64 16
IFG	46		3.74	-48 48 4
IPL	40	35	4.95	-52 -56 48
SPL	40		4.44	-36 -60 56
IPL	7		4.35	-56 -56 36

*PostCG = posterior cingulate gyrus; SFRG = superior frontal gyrus; IPL = inferior parietal lobe; GP = globus pallidus; STN = subthalamic nucleus; MTG = middle temporal gyrus; SPL = superior parietal lobe; PCG = precentral gyrus; MFG = middle frontal gyrus; FEF = frontal eye fields; IFG = inferior frontal gyrus.

In the reverse contrast, Stop Failure > Stop, activation was limited to right cuneus and cerebellar cortex (declive) and left hemisphere activation in MOG at the fusiform and lingual gyri bordering the cerebellum.

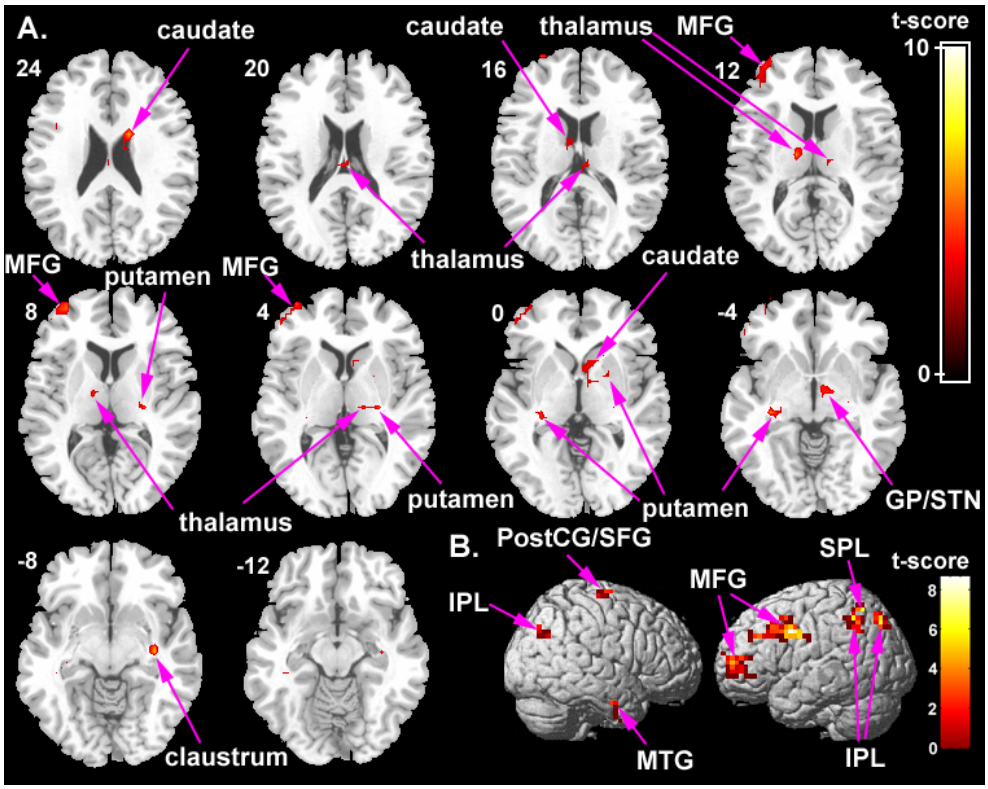

Figure 6.07. Control group activation shown by axial slices through the cortex for the Stops > Stop Failure contrast (thresholding was p < .01, 10 contiguous voxels). A. is focused on subcortical activation, including caudate, thalamus, putamen, claustrum, and globus pallidus/subthalamic nucleus (GP/STN).

Table 6.17

Control group activation for a repeated-measures t-test contrast of (Stop Failures > Go) > (Stops > Go; p < .01, and 10 voxels)

Brain Area*	BA	No. Voxels	t - score	MNI Co-ords
Right hemisphere				
Cuneus		15	4.59	16 -84 36
Cerebellar declive		10	4.33	20 -68 -16
Left hemisphere				
Fusiform gyrus	19	68	7.68	-20 -68 -16
Lingual gyrus\cerebellar declive	18		7.33	-20 -76 -20
Fusiform gyrus\cerebellar declive			4.53	-28 -60 -20
MOG	19	13	4.86	-48 -80 4

*MOG = middle occipital gyrus.

Simple correlation: SSRT and Stops > Go

The correlation between SSRT and Stops > Go in controls was of special interest given the results of Experiment 2 where it was found that SSRT was positively correlated with activation in right IFG and STN. However, in that study, SSRT predicted inhibition difficulty (inhibition difficulty ratio = SSRT/(GoRT – SSD)) whereby participants with longer SSRT had a reduced capacity to stop, whereas in the current investigation inhibition difficulty was identical for all participants. SSRT from the combined left and right hand data was correlated with Stop > Go contrast maps. Of most interest was the negative correlation (see Table 6.18). As anticipated, in controls, SSRT predicted activation in right IFG, and also at the SFG/preSMA boundary. Left IFG (*pars opercularis* and *pars triangularis*) activation was also predicted by SSRT, but was more extensive and extended into PCG. Left hemisphere relationships were also observed with SFG activation, ACC, and STS. STN activation was not predicted by SSRT. When the positive-tail of the correlation was assessed, SSRT did not predict activation in either IFG or STN.

Table 6.18

Control group t-maps arising from the negative correlation of SSRT with Stops > Go contrast maps (thresholding was $p < .01$ and 10 contiguous voxels)

Brain Area*	BA	No. Voxels	t - score	MNI Co-ords
Right hemisphere				
SFG/preSMA	6	21	8.43	16 16 52
IFG	46	17	5.30	48 44 8
IFG	47	10	3.76	48 12 0
Left Hemisphere				
SFG	6	15	4.74	-24 40 36
IFG	46	19	4.73	-48 44 8
STG/Insula	22/13	24	4.67	-48 0 4
ACC	32	11	4.61	-16 4 44
IFG/PCG	9	17	4.15	-52 8 36
STG	42	10	4.10	-60 -32 16

*SFG = superior frontal gyrus; preSMA = anterior supplementary motor area; IFG = inferior frontal gyrus; STG = superior temporal gyrus; ACC = anterior cingulate; PCG = precentral gyrus.

When the same analyses were performed for patient SSRT (combined over hands) and Stops > Go contrast maps and the negative correlation tested, SSRT was found to predict BOLD signal variance within right IFG and SFG, but also right IPL and thalamus. Left hemisphere clusters were revealed within the caudate (cluster was contiguous with right thalamus) and SFG.

Table 6.19

Patient group t-maps arising from the correlation of SSRT with Stops > Go contrast maps (thresholding was $p < .01$ and 10 contiguous voxels)

Brain Area*	BA	No. Voxels	t - score	MNI Co-ords
Right hemisphere				
IPL	40	16	10.93	56 -44 52
IPL	40		3.61	50 -40 40
Thalamus	-	50	6.49	4 -4 0
IFG	47	16	5.49	40 16 -4
IFG	47		4.12	56 16 -4
SFG	10	15	3.77	28 56 16
SFG	10		3.49	28 48 16
Left hemisphere				
Caudate	-		4.04	-12 12 16
Caudate	-		3.92	-12 -4 16
SFG	9	15	3.77	-32 48 32

*IPL = inferior parietal lobe; IFG = inferior frontal gyrus; SFG = superior frontal gyrus.

SVCs were applied to control group Stop > Go, Stop > Stop Failure and correlation maps as outlined in the method. No significant voxels were revealed for the correlation with SSRT, hence these data are not included below.

Table 6.20

SVC analyses for control group Stops > Go and Stop Failures > Go contrast t-maps

Brain Area	t-score	FWE	MNI coords
Stops > Go			
IFG	8.65†	.003	40 12 28
	6.57†	.013	40 24 -8
Pars opercularis	8.65†	.001	40 12 28
	4.90†	-	48 12 0
Pars triangularis	5.73	.030	40 12 24
Pars Orbitalis	6.57†	.008	40 24 -8
MFG	6.59†	.028	28 52 20
preSMA	-	-	-
Putamen	-	-	-
Pallidum	-	-	-
Thalamus	4.72†	-	12 -16 4
STN	3.81†	.037	12 -12 -4
Stop Failures > Go			
IFG	6.08†	.048	56 12 4
Pars opercularis	6.08†	.014	56 12 4
Pars triangularis	-	-	-
Pars Orbitalis	5.23†	.044	48 20 -8
MFG	7.79	-	48 8 52
	4.82†	-	28 48 24
preSMA	5.71†	.020	4 16 56
Putamen	-	-	-
Pallidum	-	-	-
Thalamus	-	-	-
STN	-	-	-

†Indicates cluster correction
IFG = inferior frontal gyrus; MFG = middle frontal gyrus; preSMA = pre-supplementary motor area; STN = subthalamic nucleus.

When SVCs were applied to Stops > Go, *pars opercularis*, *pars triangularis* and *pars orbitalis* all contained FWE corrected voxel peaks, but significant clusters were observed only within *pars opercularis* and *pars orbitalis.* STN and MFG ROIs also contained both clusters and peaks that survived multiple comparisons correction, while the

thalamic ROI contained a significant cluster. No significant effects were observed within the PreSMA ROI.

In the Stop failures > Go contrast, MFG, preSMA, *pars orbitalis* and *pars opercularis* activations were significant both at the voxel and cluster levels. No other ROIs showed significant effects.

6.3.3. ERP session

6.3.3.1. Age and education

Independent samples t-tests (two-tailed) were used to assess differences between Control and Patient group ages and years of education. No difference was observed between the ages of the Patient (M = 35.9 yrs, SD = 7.7 yrs) and Control (M = 32.8 yrs, SD = 8.0 yrs) groups, t(21) = -.95, *ns*. Years of education also did not differ between the Control (M = 17.8, SD = 1.5) and Patient (M = 16.3, SD = 2.9) groups, t(21) = 1.60, *ns*.

Table 6.21

ERP session behavioural data (hand-wise) for patients and control groups

Variable*	Controls		Patients	
	left	right	left	right
GoRT (ms)	472 (69)	457 (71)	520 (100)	500 (103)
SFRT (ms)	438 (66)	407 (73)	473 (95)	457 (97)
no. correct go (Go)	304 (17)	346 (12)	286 (23)	339 (21)
no. incorrect go	7 (9)	8 (8)	12 (10)	12 (11)
no. missed go	3 (3)	3 (4)	15 (16)	8 (12)
correct Go (%)	96 (3)	97 (3)	92 (6)	95 (4)
missed Go (%)	1 (1)	1 (1)	5 (5)	2 (3)
incorrect Go (%)	2 (3)	2 (2)	4 (3)	3 (3)
Go errors (%)	3 (3)	3 (3)	8 (6)	5 (4)
missed Go / Go errors (%)	39 (6)	29 (31)	47 (30)	33 (32)
incorrect Go / Go errors (%)	61 (36)	71 (31)	53 (30)	67 (32)
Mean PI	.50 (.02)	.50 (.02)	.49 (.02)	.48 (.02)
mean cPI	.50 (.02)	.49 (.02)	.46 (.04)	.47 (.03)
mean SSD	285 (83)	261 (80)	270 (142)	240 (149)
SSRT	186 (25)	195 (21)	258 (71)	266 (70)

*Median Go reaction time = GoRT; Median Stop Failure reaction time = SFRT; probability of inhibition = PI; corrected PI = cPI; stop-signal delay = SSD; stop-signal reaction time = SSRT.

6.3.3.2. Behavioural data analyses

It should be noted that because the ERP session was twice as long as the fMRI session, behavioural results were based on more trials and therefore, might be expected to exhibit more stable estimates of effects than the fMRI data.

RT data

RT analyses largely mirrored those from the fMRI session results. There were significant main effects of Hand, $F(1,21) = 98.90$, $p = .001$, and Condition, $F(1,21) = 13.35$, $p < .001$, indicating that right hand RTs were faster than left hand homologues, and that SFRT was faster than GoRT, respectively. No other effects or trends were observed.

Error analyses

These analyses were conducted on the number of errors in a Group x Hand x Type of error (levels incorrect go and missed go). There were significant main effects of Group, $F(1,21) = 4.918$, $p = .038$, and Hand, $F(1,21) = 6.067$, $p = .022$, that were moderated by a Hand x Group interaction, $F(1,21) = 5.062$, $p = .035$, but no effect of Type of error (missed Go or IncorrectGo) was observed. These data show that most errors were made on left hand go trials, and that patients made significantly more errors than controls, particularly for left hand go trials. A marginal Group X Hand X Type of error interaction, $F(1,21) = 4.163$, $p = .054$, showed that the difference between the number of incorrect go trials compared to missed go trials was generally greater for right hand compared to left hand go trials.

SSD and SSRT

SSD (for Stops) and SSRT were entered into separate 2X2 ANOVAs, with Hand as a within subjects factor, and Group a between subjects factor. The groups did not differ in SSD required for successful inhibition, $F(1,21) = .19$, *ns*, but a large effect of Hand was observed, $F(1,21) = 13.63$, $p = .001$, indicating that participants required shorter delays for right hand stopping. SSRT analyses revealed that patients had significantly longer SSRTs than controls, $F(1,21) = 12.49$, $p = .002$; no Hand X Group interaction was observed. For consistency with fMRI session analyses, GoRTs were added to the model. The ANCOVA further confirmed the ANOVA result, again with a larger effect, $F(1,19) = 18.38$, $p < .001$.

Group GoRT and SSRT measures were entered into separate correlation matrices. No relationships were observed for patient group data, but control group GoRT and SSRT revealed a significant relationship for the left hand, but oddly, this was an inverse relationship, $r = -.613$, $p = .013$. A scatterplot of this data indicated that one outlier was driving this correlation. When that participant was removed, the relationship was no longer significant, $r = -.372$, ns.

Relationships between behavioural variables and symptom profiles

Total SAPS and total SANS scores were entered into a correlation matrix with SSRT, GoRT and for each hand, in addition to age. It was predicted that patients with more negative symptoms would exhibit slower SSRT and GoRT. No relationship was observed between SSRT and symptom scores, however, strong relationships were observed between Total SANS scores and GoRT for the left hand, $\rho = .770$, $p = .005$, and right hand, $\rho = .624$, $p = .027$. No relationships were observed between behavioural variables and positive symptoms.

Pre and post event RTs differences

Paralleling fMRI session analyses, a Group X Hand X Event type X Time ANOVA revealed a significant effect of Event type, $F(1.782,37.431) = 3.67$, $p = .040$. Additionally, a significant Event type X Time interaction, $F(1.930,40.529) = 3.27$, $p = .050$ was observed. Group was not significant – nor were any interactions with group (see Table 6.22).

Pre- and post- event RTs were analysed separately in Hand x Event type x Group ANOVA models. In the pre-event analysis, there was a significant effect of Event type, $F(1.3.25,27.83) = 13.34$, $p < .001$. No other effects or interactions were observed. Planned comparisons between pre-Stop RTs, pre-Stop Failure RTs and pre-Go RTs were conducted using repeated measures t-tests (two-tailed), for left and right hands separately (FWE = .05/3 = .017, for each hand). This analysis demonstrated that both left and right hand pre-Stop RTs were significantly slower than pre-Stop Failure RTs, $t(22) = 2.89$, $p = .009$, $t(22) = 4.48$, $p < .001$, respectively. Additionally, for the right hand only, pre-Stop RTs were significantly slower than pre-Go RTs $t(22) = 3.25$, $p = .004$, and pre-Stop Failure RTs were

significantly faster than pre-Go RTs, t(22) = -3.01, p = .006. When post-event RTs were analysed no significant effects or interactions were observed.

Table 6.22

Control and patient group pre and post event RTs for left and right hand events

Event	Controls		Patients	
	Pre	Post	Pre	Post
Left				
Go	456 (68)	457 (66)	505 (97)	497 (106)
Stop Failures	455 (67)	456 (68)	488 (98)	505 (95)
Stops	461 (72)	464 (62)	507 (109)	501 (94)
Right				
Go	459 (70)	458 (73)	504 (101)	499 (105)
Stop Failures	453 (70)	458 (65)	489 (98)	511 (93)
Stops	473 (71)	456 (67)	509 (108)	510 (93)

Pair-wise comparisons were conducted between pre and post event RTs for each event type using paired samples t-tests, firstly for the groups combined, and subsequently for the groups separately.

When the groups were combined, no effects were significant, but RT differences approached significance for right Stop Failure, t(22) = -1.925, p = .067, and right Stops, t(22) = 1.814, p = .083. These effects indicate a general slowing of GoRT after a right Stop Failure, and conversely, some speeding up of GoRT after a right Stop.

When the groups were assessed separately, no effects were observed for patients (all p > .1), but significant speeding of GoRT was detected after right Stops in controls, t(12) = 3.837, p = .002.

6.3.3.3. Go stimulus ERP analyses

Left and right hand Go ERPs (see Figure 6.08) for both patient and control groups began with a brief positive going wave, P1, that was prominent at central sites (C3, Cz and C4) and Pz in both patients and control groups, followed by a prominent N1 at lateral

parietal and central sites. N1 was temporally extended in control group data, particularly at Cz, probably due to the overlap of a later larger N2 component in controls. Following N2, a large positive deflection can be observed across the scalp, maximal at Pz and appears to be larger in controls compared to patients. In controls, this component is broadly distributed across the scalp, although larger at parietal sites, consistent with the scalp topography of the P3b component (Comerchero & Polich, 1999).

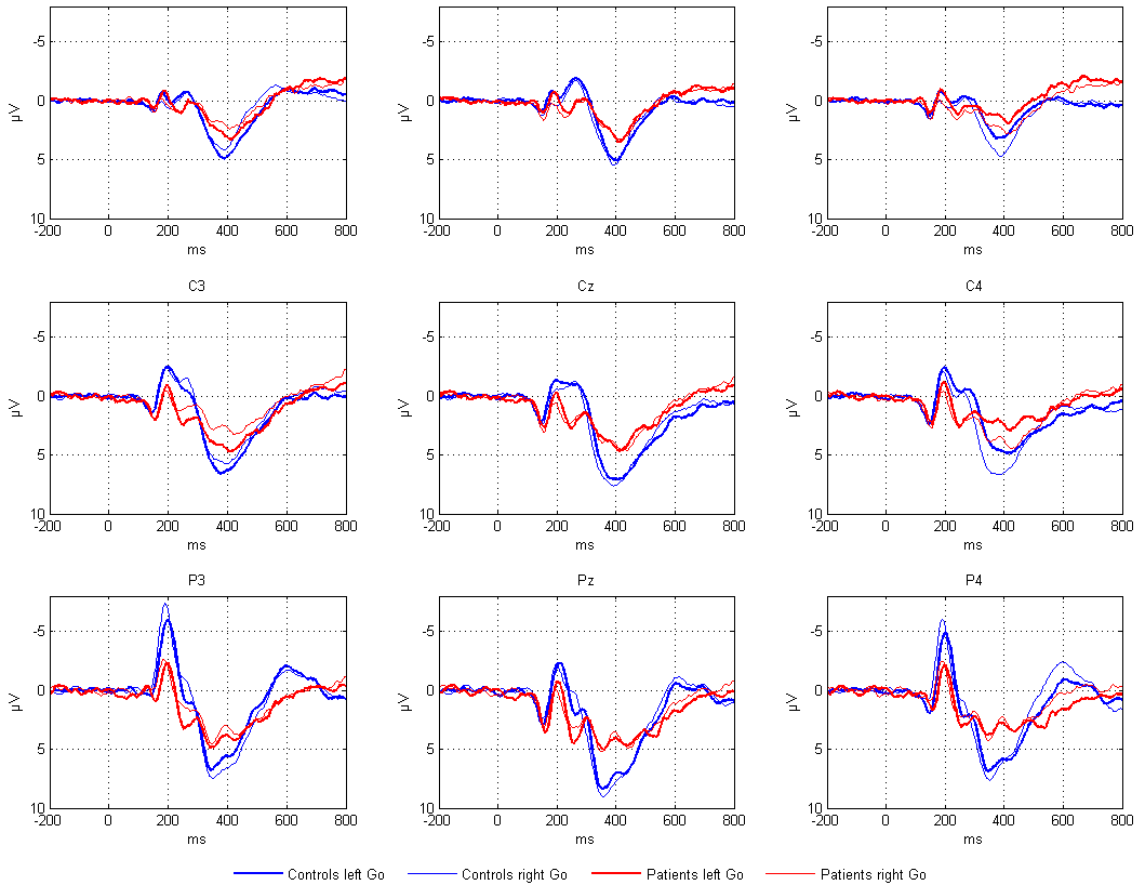

Figure 6.08. Left and right hand correct grand average Go ERPs for control and patient groups.

The P3 is followed by a late, slow negativity that is most salient in control data at parietal sites and in patients at frontal sites. Group differences in the peak latencies and

amplitudes of N1 and P3 components at sites where these components were maximal were assessed as well as the scalp topography of both components by measuring mean amplitudes around the respective peaks in the grand average waveforms. No attempt was made to measure N2 because of the difficulties in distinguishing N2 peaks in individual participant waveforms and apparent overlap with preceding and following components.

Go-N1 data

N1 was largest at site P3, peaking at approximately 190-200 ms and appeared to be substantially larger in controls than in the patient group. Additionally, in the control group data N1 appears to be substantially larger during right hand Go trials (an 'X') than during left hand Go trials (an 'O'). To examine these group and hand effects on N1, the amplitude and latency of N1 peaks in individual subject data were extracted across a 140 – 230 ms post Go stimulus onset time window; peaks could be identified in the data from nine patients and eleven controls in these analyses. In a subsequent analysis, mean amplitudes extracted across a 170-220 ms post stimulus time window were examined in order to determine scalp topography effects.

Table 6.23

Group means at parietal sites P3 and P4 for Go-N1 peak amplitude and latency (controls = 11, patients = 9), and for mean Go-N1 amplitude (controls = 13, patients = 10)

	Left hand		Right hand	
	Controls	Patients	Controls	Patients
Peak latency				
P3	192 (18)	192 (18)	190 (12)	185 (17)
P4	201 (13)	194 (19)	190 (10)	189 (16)
Peak amplitude				
P3	-7.6 (1.9)	-3.7 (5.0)	-8.6 (2.8)	-3.8 (5.1)
P4	-7.4 (3.1)	-3.2 (3.3)	-7.9 (3.7)	-3.1 (3.2)
Mean amplitude				
P3	-4.9 (2.5)	-1.4 (4.3)	-5.9 (2.6)	-1.7 (4.5)
P4	-3.6 (3.6)	-1.1 (2.7)	-4.5 (3.6)	-1.4 (2.9)

Peak Go-N1 amplitude and latency analyses

The visual N1 peak latency and amplitude measures from lateral parietal sites (P3/P4) and were entered into a Hand x Hemisphere x Group ANOVAs where the factor Hemisphere coded the parietal site that was ipsilateral and contralateral to response hand.

Parietal sites: Go-N1 peak amplitude

Peak amplitude analyses revealed main effects of Group, $F(1,18) = 9.445$, $p = .007$, and Hemisphere, $F(1,18) = 4.640$, $p = .045$. The Group effect was underpinned by a mean difference of 4.5 μV in control and patient group in the visually evoked N1 (larger in controls), while the effect of Hemisphere showed that N1 amplitudes were slightly larger at sites contralateral to response hand.

Parietal sites: Go-N1 peak latency

When Go-N1 latency data were analysed, the main effect of Hand was significant, $F(1,18) = 12.234$, $p = .003$, indicating that N1 peaked much earlier for right hand Go trials compared to left hand Go trials, with a mean difference of approximately 6.4 ms. No other effects were observed.

Mean Go-N1 amplitude analysis

To analyse the scalp topography of N1, mean amplitude estimates at F3, Fz, F4, C3, Cz, C4, P3, Pz and P4 were entered into a Hand x AP x Laterality x Group ANOVA, where AP coded frontal, central and parietal sites, Laterality coded sites ipsilateral to response hand, midline and sites contralateral to response hand.

Scalp topography analysis: mean Go-N1 amplitudes

Main effects of Laterality, $F(1.060,22.268) = 25.012$, $p < .001$, and AP, $F(1.320,27.726) = 13.935$, $p < .001$, confirmed that Go-N1 was larger at sites lateral to response hand compared to those at the midline, and larger at parietal sites compared to fronto-central sites. Moderating these effects, an AP x Laterality interaction, $F(1.132,23.780) = 29.444$, $p < .001$, demonstrated that the difference between mean Go-N1 amplitudes at sites lateral to response hand and midline sites was greatest at parietal sites.

While no effect of Hand was observed, a Hand x AP interaction, $F(1.254,26.326) = 21.648$, $p < .001$, and a marginal Hand x AP x Laterality interaction, $F(1.258,26.413) = 3.727$, $p = .056$, showed that right hand Go-N1 amplitudes were significantly larger than left hand homologues at parietal sites compared to midline and fronto-central site differences, and that these differences were larger at sites contralateral to response hand..

Finally, the overall Group effect was marginal, $F(1,21) = 4.286$, $p = .051$, but a Group x AP interaction, $F(1.320,27.726) = 4.960$, $p = .026$, revealed that group Go-N1 mean amplitude differences (controls > patients) were substantially larger at parietal sites compared to fronto-central sites.

Peak Go-P3 amplitude and latency analyses

At parietal sites only, Go-P3 peak amplitudes and latencies were extracted over the time window 300 – 550 ms post Go stimulus onset, and mean Go-P3 amplitudes were extracted in the window 310-410 ms. Peak data were identifiable in the data of only seven patients and all thirteen controls. In an initial analysis, data from the sites P3, Pz, and P4 were assessed using a Hand x Laterality x Group ANOVA models, for peak amplitude and latency data in addition to mean amplitude data. In these models, Hand had levels left and right hand, and Laterality comprised midline sites, and sites ipsilateral and contralateral to response hand. Group distinguished patients from controls. In a subsequent scalp topography analysis using mean Go_p3 amplitudes, data from frontal (F3, Fz and F4), central (C3, Cz, C4) and parietal (P3, Pz, P4) electrodes were analyzed, in a Group x Hand x Laterality x AP ANOVA, where AP (Anterior-Posterior extent) denoted frontal, central and parietal electrode sites.

Parietal sites: Go-P3 peak amplitude

The effect of Group only approached significance, $F(1,18) = 3.472$, $p = .079$, despite that control group Go-P3 amplitudes (10.0 μV) were much larger than for patients (6.5 μV). However, the effect of Laterality, $F(1.471,26.475) = 15.159$, $p < .001$, which confirmed that midline Go-P3s were significantly larger than homologues at sites lateral to response hand, interacted with Group (Group x Laterality interaction), $F(1.471,26.475) = 5.869$, $p = .013$, indicating that differences between patient and control group amplitudes

was significantly less at sites contralateral to response hand compared to midlines sites and sites ipsilateral to response hand.

Parietal sites: Go-P3 peak latency

Interestingly, patients group (374 ms) mean Go-P3s were faster than controls (393 ms), but the main effect of Group was not significant, $F(1,18) = 1.100$, $p = .308$. Only the effect of Laterality was significant, $F(1.620,29.160) = 4.336$, $p = .029$, whereby midline Go-P3s were slower than at sites ipsilateral and contralateral to response hand.

Scalp topography analysis: mean Go-P3 amplitudes

Quite large group differences were also evident in these data (patients = 2.9 μV, controls = 5.1 μV), but again only marginal significance was revealed in the effect of Group, $F(1,21) = 4.155$, $p = .054$. Additionally, main effects of Laterality, $F(1.421,29.832) = 22.955$, $p < .001$, and AP, $F(1.378,28.934) = 22.738$, $p < .001$, showed that mean Go-P3 amplitudes were significantly reduced at sites contralateral to response hand and significantly reduced at frontal sites compared to central and parietal sites, respectively. These factors interacted (Laterality x AP interaction), $F(2.226,46.748) = 9.088$, $p < .001$, showing that the difference between mean Go-P3 amplitudes at frontal sites (smaller) compared to central and parietal sites (larger) at the midline was significantly larger than the same differences at sites lateral to response hand.

6.3.3.4. Stop and Stop Failure ADJAR correction waveforms

The ADJAR method (Woldorff et al., 1993) was employed to account for overlapping Go response activation in stop-signal ERPs (see Figure 6.09 for a comparison of uncorrected and corrected stop-signal waveforms at Cz for patients and controls). This method was first used in a stop-signal experiment by Bekker and colleagues (2005a), and was shown to be effective in removing preceding Go ERP response in Experiment 2. To reiterate from Experiment 2 (Chapter 4), the principal effects of the application of ADJAR procedures for stop-signal ERPs is that N1 amplitudes are increased, and P3 amplitudes are reduced, and baselines are flattened (Bekker et al., 2005a). These effects can be seen in Figure 6.09, where uncorrected and corrected stop-signal waveforms at Cz can be visually

compared. In comparison with the correction (averaged convolution) waves for Experiment 2 (see Chapter 4, Figure 4.10), it is notable that the correction waves for controls in this experiment are substantially smaller. This is explained by comparing the visual-evoked Go P3s from the previous experiment (see Chapter 4, Figure 4.10) with those elicited in this experiment (see Figure 6.08). Go P3s in this experiment are much smaller in amplitude (in controls) than those elicited Experiment 2 and it is these late positive potentials that are the primary source of contaminating overlap in auditory evoked stop-signal ERPs (Bekker et al., 2005a).

It is also notable that, as in Experiment 2, the largest potential in the Stop correction wave peaks at around 200 ms after stop-signal onset, but somewhat earlier for the Stop Failure correction wave (see Figure 6.09). This noticeable difference in the peak potential between stop-signal correction waves was not evident in Experiment 2. This can be understood by comparing the difference in SSD for Stops and Stop Failures for Experiment 2 (15 ms difference) and the current experiment (50 ms difference). The large SSD difference in the current experiment was enforced by the step-size, but was not in the previous experiment. This means that, relative to the Go ERP, Stop Failure ERPs commence 50 ms later than Stop ERPs, hence the overlapping Go potentials that are removed from Stop Failure ERPs should appear to onset closer to the stop-signal than in Stop ERPs.

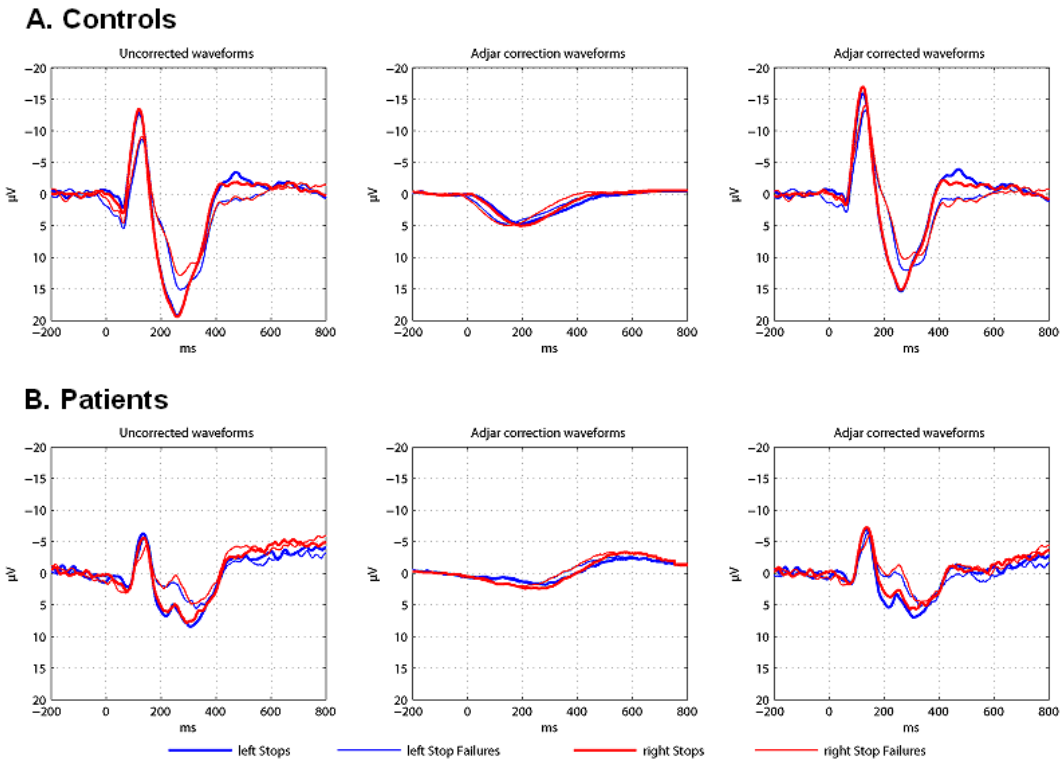

Figure 6.09. Outcome from ADJAR correction procedure at Cz for (A) left hand, and (B) right hand, Stop and Stop Failure grand average ERP waveforms for control and patient groups.

Bekker et al. (2005a) and Woldorff et al. (1993) refer to another consequence of employing ADJAR procedures – flattening of corrected stop-signal locked ERP baselines. Inspection of baseline period activity in corrected stop-signal ERPs, the 200 ms period preceding time zero, presented in Figure 6.09, indicate that such flattening has indeed occurred, although it is more marked in patients.

6.3.3.5. Stop-signal ERP analyses

As seen in Figure 6.10 and Figure 6.11, left and right hand Stop waveform morphologies for Stops and Stop Failures largely paralleled one another within both control and patient groups. These stop-signal waveforms reveal a large auditory evoked N1 that, at Cz in controls, appears have both larger amplitude (left: Stop = -15.9 μV; Stop Failure = -13.2 μV; right: Stop = -17.0 μV, Stop Failure = -13.9 μV) and with an earlier peak latency

(left: Stop = 124 ms, Stop Failure = 132 ms, right Stop = 122 ms, Stop Failure = 134 ms) compared to patient stop-signal N1 peak amplitudes (left: Stop = -7.0 μV, Stop Failure = -6.6; right: Stop = -7.2 μV, Stop Failure = -6.3) and latencies (left: Stop = 136 ms, Stop Failure to 144 ms; right Stop = 138 ms, Stop Failure = 150 ms). Stop-signal N1 was followed by a large positive component which we will identify here as P3a given its scalp topography in controls, namely, larger fronto-centrally than parietally and relatively early peak latency (250-310 ms). Control data for these potentials (Stop-P3 and Stop Failure-P3) also reveal larger amplitudes (left: Stop = 15.4 μV, Stop Failure = 12.1 μV; right: Stop = 15.2 μV, Stop Failure = 10.3 μV) and earlier peak latencies (left: Stop = 260 ms, Stop Failure = 284 ms; right: Stop = 260 ms, Stop Failure = 276 ms) compared to patient stop-signal P3 amplitudes (left: Stop = 7.1 μV, Stop Failure = 5.3 μV; right: Stop = 5.7 μV, Stop Failure = 4.5 μV) and latencies (left: Stop = 306 ms, Stop Failure = 330 ms; right: Stop = 294 ms, Stop Failure = 334 ms).

Patients also exhibit a second negative going component that we identify here as N2 that peaks at approximately 260 ms in patients. Controls do not exhibit a clearly defined N2 although a notch in the positive going arm of the P3 is evident in control waveforms at an earlier latency. Within-group differences between Stop and Stop Failure waveforms are visually salient, as are between group differences across hands and event types. Group Stop Failure waveforms share the gross morphological features of respective group Stop waveforms, but in controls, Stop Failure ERP components appear to be smaller in amplitude and peak later than Stop homologues. This observation does not appear to hold true for patient Stop and Stop Failure waveforms. However, in patients N1 peak latencies in Stop Failure waveforms appear to be later than during Stops. However the latencies of later N2 and P3 components appear to be invariant across event types whereas later components in control group data appear to be slower with smaller amplitudes in Stop Failure waveforms compared to Stop waveforms.

While displaying similar gross morphological features, especially N1, and P3 components (see Figure 6.10 and Figure 6.11), patient and control groups also elicited a small early positive component that peaked earlier in controls (controls at approximately 50 ms and patients at 70-100 ms), but had a larger amplitude in patients, particularly at parietal

sites. This component was not further analysed because the primary focus of stop-signal experiments has traditionally been on N1 and P3 potentials. What follows is an in depth analysis of effects on N1 and P3 latency and amplitude measures.

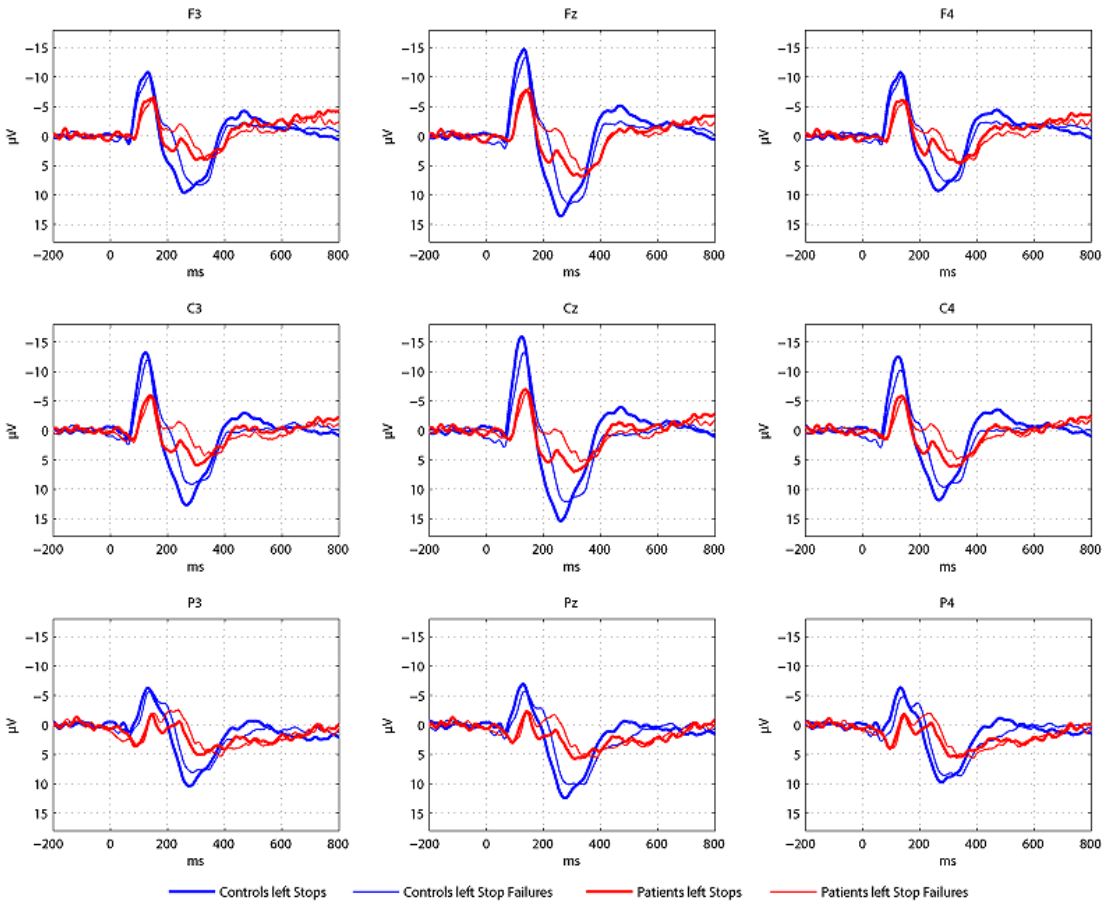

Figure 6.10. Left hand ADJAR corrected Stop and Stop Failure grand average ERP waveforms for control and patient groups.

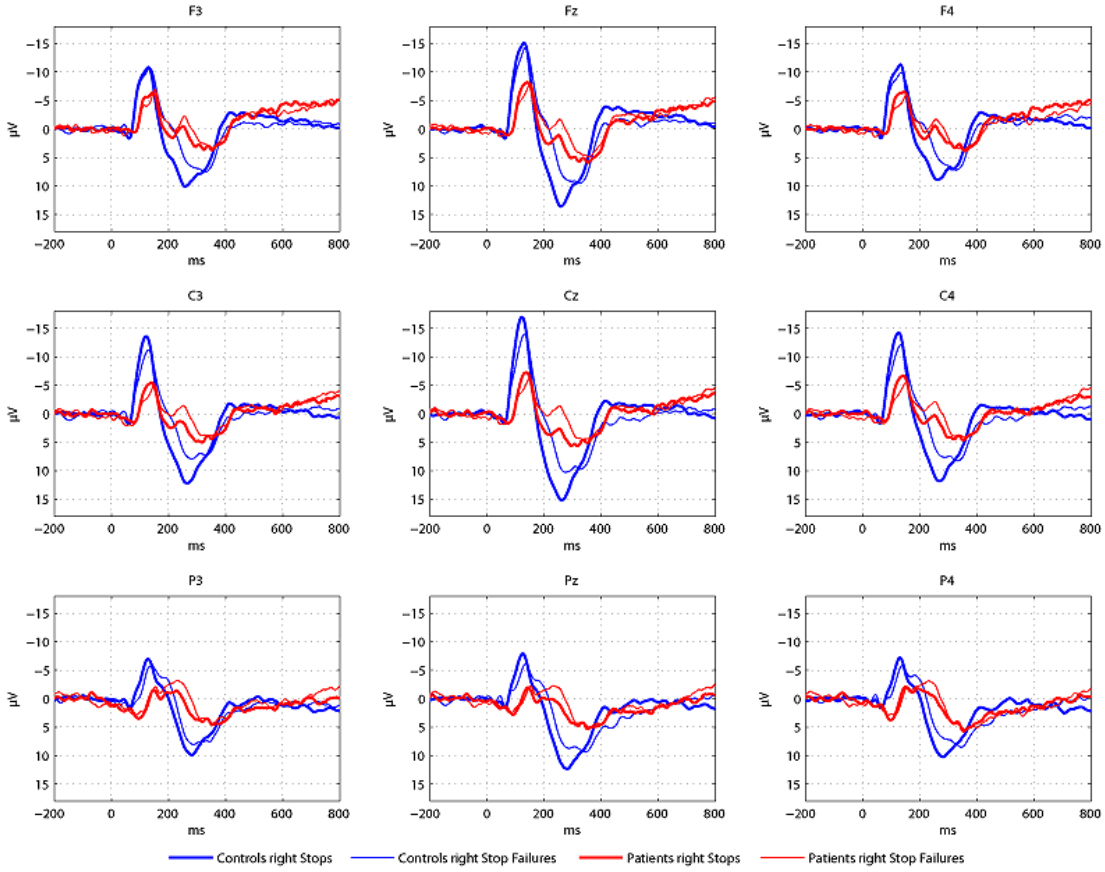

Figure 6.11. Right hand ADJAR corrected Stop and Stop Failure grand average waveforms for control and patient groups.

Auditory evoked N1: average waveform analyses

The auditory N1 was evident as a sharp negative deflection that was broadly distributed across the scalp but appears larger at Cz as is generally observed (Näätänen & Picton, 1987). To assess these apparent differences in N1 features, peak amplitude and latency measures were extracted across the time window 50 – 175 ms post stop-signal onset. In an initial analysis, only Cz measures were considered in a Group (controls and patients) x Hand (left and right) x Event type (Stops and Stop Failures) ANOVA. In a subsequent analysis, a larger model was used that incorporated three frontal electrodes (F3, Fz, and F4) and three central electrodes (C3, Cz and C4) that resulted in a Group x Hand x Event type x AP X Laterality: AP represented an anterior-posterior factor (distinguishing frontal from central sites) and Laterality which comprised levels ipsilateral, midline and

contralateral sites relative to response hand. Two controls were excluded from the analysis at Cz (controls: N = 11; patients: N = 10), and for the larger model one patients was also excluded (controls: N = 11; patients: N = 9); participant exclusion was necessary because N1 waves were superimposed upon later components rendering effective N1 identification within the specified latency range impossible at some electrodes for some participants. No attempt was made to measure N1 at parietal sites as it could not be reliably measured in patients in particular.

Stop-signal N1 peak latency and amplitude measures: At Cz only

Peak latencies of left and right hand Stops and Stop Failures at Cz (comprising the factor Inhibition type) were entered into a Hand x Inhibition x Group repeated measures ANOVA. The effect of Group was almost significant, $F(1,20) = 3.803$, $p = .065$, indicating that stop-signal N1 latencies elicited at Cz tended to be shorter in controls compared to patients, underpinned by an 11 ms group mean N1 latency difference (controls = 126 ms, patients = 137 ms).

Analysis of stop-signal amplitude measures at Cz revealed a significant effect of Inhibition, $F(1,20) = 5.256$, $p = .033$, confirming that Stop-N1 was significantly larger than Stop Failure-N1, and a main effect of Group, $F(1,20) = 16.740$, $p = .001$, confirmed that N1 elicited by stop-signals in the control group (-17.3 μV) was much larger than in the patient group (-8.5 μV). A Group X Hand x Inhibition type interaction was almost significant, $F(1,20) = 3.925$, $p = .062$, due to the difference between Stop-N1 and Stop Failure-N1 being greater for controls compared to patients for left hand events compared to right hand events. Indeed stopping had no apparent modulation of N1 for left hand events in patients (< +.1 μV), whereas the effect was present for right hand events in patients (-1.4 μV), and for both left hand (-3.8 μV) and right hand (-2.7 μV) in controls).

Stop-signal N1 peak amplitude and latency measures: Across fronto-central sites

In a more detailed analysis, stop-signal N1 amplitude and latency measures were entered into separate factorial ANOVAs that included factors AP (Anterior-Posterior: levels frontal and central), and Laterality (with levels midline, ipsilateral and contralateral to

response hand). These were Group x Inhibition x AP x Laterality ANOVAs that included eleven controls and nine patients for analysis.

In the analysis of amplitude measures, a main effect of Laterality, $F(1.145,22.900) = 50.980$, $p < .001$, and a Laterality x AP interaction, $F(1.330,26.590) = 8.249$, $p = .004$, showed that stop-signal amplitudes were significantly larger at midline sites compared to sites ipsilateral and contralateral to response hand, and that this difference was greater at central sites compared to frontal sites, respectively. Main effects of Inhibition or AP were not observed, however, Inhibition x AP, $F(1,20) = 13.590$, $p = .001$, and Inhibition x Laterality x AP, $F(1.837,36.734) = 6.023$, $p = .007$, interactions indicated that Stop-N1 was significantly larger than Stop Failure-N1 at central compared to frontal sites, and that this enhancement was significantly larger at midline sites, i.e., Stop-N1 and Stop Failure-N1 amplitude differences were significantly larger at Cz compared to other sites analysed.

As indicated by visual inspection, there was a main effect of Group, $F(1,20) = 12.045$, $p = .002$, confirming that stop-signal N1 amplitudes were significantly reduced in patients (-8.2 μV) compared to controls (-14.5 μV). More interesting were Group x Laterality, $F(1.145,22.900) = 11.738$, $p = .002$, and Group x AP, $F(1,20) = 7.940$, $p = .011$, interactions showing that group differences were significantly larger at midline compared to sites lateral to response hand, and larger at central compared to frontal sites, respectively. But most interesting was a Group x Inhibition x AP interaction, $F(1,20) = 4.735$, $p = .042$, which revealed that the difference between Stop-N1 and Stop Failure-N1 amplitudes was significantly larger for controls compared to patients at central sites compared to frontal sites. Also revealing was a marginal Group x Hand x Inhibition x Laterality interaction, $F(1.823,36.458) = 3.207$, $p = .056$. Though not quite reaching significance, this interaction showed that the difference between Stop-N1 and Stop Failure-N1 at midline sites in controls compared to patients was greater for left hand stop-signals compared to right hand homologues. There were two main reasons for this: firstly, in patients, Stop-N1 amplitude was little different to Stop Failure-N1 amplitude (in fact measured Stop-N1 was slightly smaller), and secondly, in controls, modulation of stop-signal N1 was greater for left hand stop-signal task trials than for right hand stop-signal task trials.

A final group effect was observed in a marginal Group x Hand x AP interaction, $F(1,20) = 4.623$, $p = .044$, which showed that stop-signal N1 differences were larger at

central compared to frontal sites and that these group differences were significantly larger for right compared to left hands, respectively. These group effects were underpinned by a reversal of stop-signal N1 amplitudes in the patient group compared to the control group: control amplitudes are larger at central sites compared to frontal sites, whereas in patients, frontal amplitudes are larger than central site amplitudes.

When latency measures were analysed, the effect of Group did not approach significance despite substantial latency differences between controls (128 ms) and patients (136 ms), however, a main effect of Inhibition was observed, $F(1,20) = 5.994$, $p = .024$, indicating that Stop-N1 (129 ms) was significantly faster than Stop Failure-N1 (135 ms). Additionally, an Inhibition x Laterality interaction, $F(1.845,36.904) = 3.813$, $p = .034$, showed that the latency difference between Stop-N1 and Stop Failure-N1 was significantly less at sites ipsilateral to response hand compared to homologues at midline sites and sites contralateral to response hand.

Inter-relationships between N1 measures, age and symptomatology

Peak amplitude and latency measures for patient Stop-N1 and Stop Failure-N1 at Fz and Cz were entered into a correlation matrix with age, Total SAPS and Total SANS scores (two-tailed tests). Age bore no relationship with any measure and no relationships were observed between amplitude measures and symptom scores, however, a very interesting pattern of correlations between total symptom scores and latency measures was observed. While no relationships were observed between Stop Failure-N1 latency measures, Total SANS scores were strongly correlated with left hand Stop-N1 latency at Fz, $\rho = .713$, $p = .021$. A scatterplot of the relationship between SANS scores and N1 latency measures revealed a bivariate outlier in each plot (see Figure 6.12). Inspection of the raw data revealed that the outlying data points were from the data of the same participant, hence this participant was dropped from the analysis, and the correlation rerun.

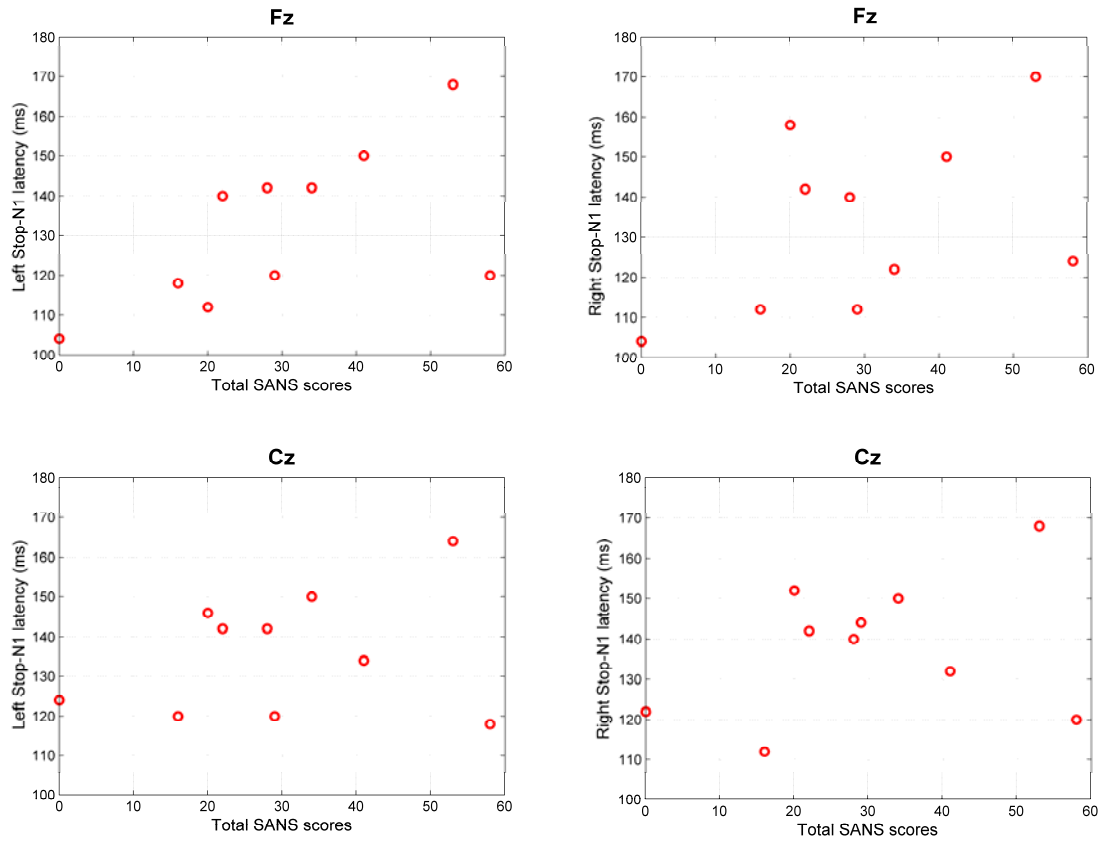

Figure 6.12. Scatterplots of Stop-N1 latency and total SANS scores for left and right hands at Fz (top panel) and Cz (bottom panel). The top panel depicts the (separate) relationships between left hand (on left) and right hand (on right) Stop-N1 at Fz and total SANS scores, while the bottom panel depicts the same relationships at Cz. A consistent bivariate outlier is observable in the bottom right hand of each plot (total SANS score = 58).

Removal of this outlier resulted in a tight coupling of SANS scores and N1 latency, $\rho = .921$, $p < .001$, and though not significant, moderate to strong correlations were observed between SANS scores and left hand Stop-N1 latency[40] at Cz, $\rho = .496$, $p = .175$, and right hand Stop-N1 latency at Fz, , $\rho = .550$, $p = .125$, and Cz, , $\rho = .569$, $p = .110$. Left and right hand Stop-N1 latencies were averaged at Fz and Cz and correlated with Total

[40] Pearson's correlations between Total SANS scores and left Stop-N1 latency were: Fz, r = .899, p = .001; Cz, r = ,647, p = .060, and for right Stop-N1 latency: Fz, r = .688, p = .041; Cz, r = .672, p = .672, p = .047.

SANS scores, resulting in Spearman's correlations[41] at Fz of $\rho = .745$, $p = .021$, and at Cz of, $\rho = .600$, $p = .088$.

Mean N2 amplitude measures

As N2 peaks were largest at midline electrodes, mean amplitudes were calculated for Stops and Stop Failures across the range of this component (150 – 300 ms) at midline Fz, Cz and Pz. Confirming the visual evidence (Figures 6.10 and 6.11), mean N2 amplitudes were more negative for Stop Failures (0.9 μV) compared to Stops (4.5 μV), $F(1,21) = 44.84$, $p < .001$, and more negative for patients (0.6 μV) compared to controls (4.9 μV), $F(1,21) = 8.52$, $p = .008$.

P3 peak amplitude and latency measures

Peak latency and amplitude measures for Stops and Stop Failures were extracted over a 180-600 ms time window at midline electrodes (Fz, Cz) only as peaks at Pz from many participants could not be identified witin the window, resulting in a substantial loss of data for analysis. Data from each participant were included only if P3 peaks from both electrodes included in the analysis fell within this window. These data were analysed in a Group x Inhibition x AP x Hand ANOVA, where Group had levels patients and controls, Inhibition had levels Stops and Stop Failures, AP had levels frontal and central, and Hand had levels left and right. In a subsequent scalp topography analysis, mean amplitudes measured over a 150 – 400 ms interval from electrodes, F3, Fz, F4, C3, Cz, C4, P3, Pz and P4 were analysed in a Group x Laterality x AP x Inhibition x Hand ANOVA model; Laterality had levels left, midline and right hemisphere electrode sites, and AP comprised and additional level – parietal electrode sites.

Latency measures

A main effect of Inhibition was observed, $F(1,17) = 6.019$, $p = .025$ for P3 peak latency, confirming that Stop-P3s peaked significantly earlier than Stop Failure-P3s (see Table 6.24), and a large main effect of Group, $F(1,17) = 18.074$, $p = .001$, demonstrated

[41] Pearson's correlations between Total SANS scores and Stop-N1 latency at Fz was, $r = .854$, $p = .003$, and at Cz was, $r = .697$, $p = .037$.

that stop-signal P3s peaked significantly later in patients compared to controls. Perhaps most interesting was a strong Group x Inhibition x AP interaction, $F(1,17) = 8.492$, $p = .010$, which indicated that the pattern of latency differences between Stop-P3 and Stop Failure-P3 peaks differed markedly at Fz and Cz between the groups: in patients the difference between the peak latencies of Stop and Stop Failure P3s was non-existent (0 ms) at Fz compared with a very large difference at the same site in controls (44 ms), whereas at Cz the difference was substantial in both patients (25 ms) and controls (34 ms). Finally, a Group x Hand x AP interaction, $F(1,17) = 5.728$, $p = .028$, suggested that the difference between left and right hand stop-signal P3 peak latencies was significantly larger at Fz in but little difference at Cz in patients or at either site in controls.

Table 6.24

Group mean stop-signal P3 peak latency measures (in milliseconds, ms) for control (N = 12) and patient (N = 7) groups used in fronto-central midline electrode analysis. Standard deviations are in parentheses

	Left Hand		Right Hand	
	Patients	Controls	Patients	Controls
Stops				
Fz	356 (63)	259 (30)	312 (56)	259 (27)
Cz	324 (85)	261 (21)	311 (58)	254 (25)
Stop Failures				
Fz	352 (88)	298 (31)	314 (50)	310 (30)
Cz	352 (94)	293 (42)	333 (64)	290 (45)

Peak amplitude analyses

Main effects of Group, $F(1,17) = 6.838$, $p = .018$, and AP, $F(1,17) = 4.582$, $p = .047$, confirmed that controls elicited larger stop-signal P3s than patients, and that overall, these potentials were largest centrally. While no other significant effects were observed, a weak trend revealed for Inhibition, $F(1,17) = 3.210$, $p = .091$, indicated a tendency for Stop-P3 amplitudes to be larger than Stop Failure-P3s.

Table 6.25

Group mean stop-signal P3 peak amplitude measures (in microvolts, μV) for control (N = 12) and patient (N = 7) groups used in fronto-central midline electrode analysis. Standard deviations are in parentheses

	Left hand		Right hand	
	Patients	Controls	Patients	Controls
Stops				
Fz	9.9 (3.0)	15.0 (7.4)	8.4 (3.4)	15.2 (5.7)
Cz	10.7 (4.0)	17.1 (8.6)	8.9 (4.9)	17.1 (7.4)
Stop Failures				
Fz	8.5 (3.0)	14.9 (6.1)	7.4 (4.3)	12.3 (4.4)
Cz	9.5 (2.7)	16.0 (6.7)	7.9 (3.5)	14.2 (7.1)

Mean amplitudes: Scalp topography analysis (Group x Hand x Inhibition x AP x Laterality ANOVA)

Importantly, the main effects observed in this analysis were comparable to those observed in Experiment 2, in particular, a main effect of Inhibition, $F(1,21) = 14.740$, $p = .001$, showed that Stop-P3 mean amplitudes were significantly larger than Stop Failure-P3 amplitudes. Similarly, main effects of AP, $F(1.391,29.212) = 5.079$, $p = .022$, and Laterality, $F(1.487,31.222) = 38.955$, $< .001$, showed that midline stop-signal P3 amplitudes were significantly larger than homologues at sites lateral to response hand, and that stop-signal P3 amplitudes at central sites were significantly larger than homologues at frontal and parietal sites, respectively.

An Inhibition x Laterality interaction, $F(1.722,32.411) = 6.847$, $p = .006$, showed that the difference between Stop-P3s and Stop Failure-P3s were significantly larger at central sites compared to the same differences at sites lateral to response hand, and additionally, an Inhibition x AP interaction approach significance, $F(1.212,25.446) = 3.544$, $p = .064$, suggested these same differences tended to be smaller at parietal sites compared to frontal and central sites. Other interactions included Hand x Inhibition x Laterality,

F(1.590,33.386) = 3.878, p = .039, and Hand x Laterality x AP, F(1.946,40.858) = 4.869, p = .013.

But of most interest were effects distinguishing patients from controls. Two effects were observed including a main effect of Group, F(1,21) = 6.088, p = .022, which showed that stop-signal P3 amplitudes were significantly smaller in patients compared to controls, and a Laterality x Group interaction, F(1.487,31.222) = 4.460, p = .018, which showed that the group effect was significantly larger at midline sites compared to those lateral to response hand.

Relationship between stop-signal P3 measures and symptomatology

Patient stop-signal P3 amplitude and latency measures were entered into a correlation matrix with Total SAPS and Total SANS scores. No reliable relationships were observed.

Relationships between SSRT and ERP amplitude and latency measures

In Experiment 2, strong relationships were observed between SSRT and Stop-P3 peak amplitudes, and also between SSRT and the difference between peak Stop-N1 and Stop-P3 latency (P3-N1 latency). This was explored in the current experiment by determining pooled within-group correlations for these measures at Cz and Fz with left hand SSRT, right hand SSRT and an average of handwise SSRT measures for those participants where consistent peaks could be observed (13 controls and 8 patients; N = 21). Additionally, pooled correlations for Stop-N1 amplitudes, Stop-N1 and Stop-P3 latencies were entered into the correlation matrix to explore whether this adaptive paradigm elicited any relationships which were not observed in Experiment 2. While in each instance, there was no significant difference between the respective correlations in the two groups, thus justifying pooling, no significant pooled correlations with SSRT measures were observed for any of the ERPs measures.

Relationships between ERP measures and Stops>Go contrasts

To examine associations between fMRI and ERP data in controls, amplitude and latency measures of Stop-N1 and Stop-P3 were correlated with Stops>Go contrast images

for individuals who participated in both sessions. The resultant t-map was threshold at p<.05 and 15 contiguous-voxels and SVC corrections were applied over right *pars opercularis* and STN ROIs. No significant activation survived. The same procedure was adopted to examine any association in patients between larger (more negative) Stop-N2 amplitude and Stop>Go contrast images. No significant activation survived. Finally, for patient and controls groups separately, mean N2 amplitudes were correlated with Stop Failures > Go contrast maps to examine the possibility of relationships between mean N2 amplitudes and ACC activation. An SVC approach was taken whereby an ACC ROI was constructed from the AAL probability maps and applied to thresholded maps (p<.05 and 15 contiguous-voxels). To this end, the negative correlation was examined, testing for greater Stop Failure N2 negativity. No significant voxels were observed for either group.

6.3.4. Between session behavioural analyses

To investigate the consistency of behavioural indices, an analysis of GoRT and SSRT (separately) was run for subjects participating in each session using Session (ERP and fMRI sessions) x Hand repeated measures ANOVAs; nine controls and ten patients who completed both sessions. For GoRT data, there was a main effect of Hand, $F(1,17) = 18.71$, $p = p < .001$, indicating that right hand GoRT was significantly faster than left hand GoRT across sessions, while the main effect of Group was only marginally significant, $F(1,17) = 4.10$, $p = .059$. Additionally, there was a Group x Session interaction, $F(1,17) = 5.91$, $p = .026$, revealing that the difference in patient GoRTs between sessions was significantly greater than that for controls. Interestingly, patients responded more slowly in the fMRI session (563 ms) than the ERP session (510 ms), whereas control ERP session GoRTs (458 ms) were slower than fMRI session GoRTs (445 ms). There was no main effect of Session overall. When between session effects were investigated for SSRT data, again there was no effect of Session, but the effect of Group was significant, $F(1,17) = 7.52$, $p = .014$, confirming that controls had significantly faster stopping processes than patients. It should be noted that this analysis included the patient participant who exhibited exceptionally fast SSRTs in the fMRI session.

Finally, left and right hand GoRT and SSRT measures for each session were submitted to a correlation matrix. All measures by hand were significantly correlated: left

hand GoRT, r = .820, p < .001, right hand GoRT, r = .797, p < .001, Left hand SSRT, r = .415, p = .039, right hand SSRT, r = .497, p = .015.

6.4. Discussion

6.4.1. Overview

This study was concerned with understanding the neural basis of stop-signal inhibition performance in adult patients with schizophrenia, in whom previous behavioural studies have reported impaired stop processing (Badcock, et al., 2002; Bellgrove et al., 2006; Enticott et al., 2008). To this end, high functioning out-patients with a diagnosis of schizophrenia and healthy controls that were matched for age, gender and years of education, were compared on behavioural, BOLD fMRI, and electrophysiological measures recorded during performance of a stop-signal paradigm. Given the results of Experiment 2, which showed that inhibition difficulty influences BOLD signal intensity within the right lateral IFG-STN network thought to underpin stopping (Aron & Poldrack, 2006; Aron et al., 2007a; Aron et al., 2007b), it was vital that the difficulty of control was held constant between individuals, and moreover, between groups. To achieve this, stop-signal delays (SSDs) were set using a performance tracking algorithm that maintained stopping probability at approximately chance level for all participants. This means that the inhibition difficulty ratio as defined in the previous experimental chapter (Chapter 4) was equal to one for all participants.

There were several important findings. Firstly, analysis of behavioural data from both sessions showed that the speed of inhibition processes (stop-signal reaction time, SSRT) estimated in patients was significantly slower than SSRT estimated for controls, whereas go task reaction time (GoRT) did not differ significantly between the groups (although there was a trend for patients to have slower GoRTs in the fMRI session). The main differences in BOLD activity observed when the control group inhibition contrast was compared to that for patients, was in the right IFG (*pars opercularis*)-STN network that is thought to be responsible for stop-signal inhibition (Aron & Poldrack, 2006). Interestingly,

when between group comparisons were performed for Go > Baseline contrast maps, patients revealed significantly greater activation within right lateral DLPFC and cerebellar cortex compared to controls. Analysis of amplitude measures of ERPs elicited by go and stop-signal stimuli showed that N1 and P3 potentials for both go and stop-signal stimuli were smaller in patients compared to controls, although Go-P3 group differences were marginal. Analysis of the peak latencies of these potentials revealed a similar pattern of results whereby no difference was found between patients and controls in the latency of Go-N1 and Go-P3, whereas stop-signal P3s peaked substantially later in patients and stop-signal N1s were also slower, but only marginally so, and only at the vertex. Consistent with Experiment 2, the N2 mean amplitudes for Stop Failures were larger than for Stops, but interestingly, not only were N2 potentials observed in all patient stop-signal waveforms, but mean stop-signal N2 amplitudes were larger for patients compared to controls.

6.4.2. Behavioural Data

SSRT

The main behavioural finding of this experiment was that SSRT was significantly slower in patients with schizophrenia compared to healthy matched controls, which was consistent across two experimental sessions and could not be accounted for by differences in GoRT for either session. The slowed stopping speed revealed in this patient group, which consisted of high functioning out-patients, parallels the processing deficit reported by other research groups who have assessed this form of behavioural control in adults with schizophrenia (Enticott et al., 2008), teenagers with early onset schizophrenia exhibiting mostly negative symptoms (Bellgrove et al., 2006), and children at risk of developing schizophrenia (Davalos et al., 2004; Ross et al., 2008). It is significant that SSRT was consistently slower in patients with schizophrenia compared to matched controls, particularly when considering that GoRT, while longer in patients, was not consistently[42] slower. This latter finding is unusual given that patients normally exhibit slower reaction times (Nuechterlein, 1977), but may be explained by the small number comprising the patient sample, each of whom were very high functioning. Nonetheless, these findings

[42] In the fMRI session, patients were slower when patients and controls were treated as independent groups, but not in a matched samples analysis. For the ERP session, which contained twice as many trials as the fMRI session, no group effect was found in an independent groups analysis.

provide further evidence that stop and go processes are independent functions, and that among these functions, patients with schizophrenia are uniquely impaired in stopping performance.

While most investigations of stopping in schizophrenia have reported slower SSRT in patient groups, it has not been a universal finding. Badcock and colleagues (2002) found that while adult patients had a reduced capacity to trigger stopping processes, evident as flatter inhibition functions, SSRT was not significantly different to controls despite substantial group mean differences (31 ms). Bellgrove and colleagues (2006) found no stopping deficit in a paranoid group with early onset schizophrenia (EOS), but did find that another EOS group exhibiting predominantly negative symptoms, had slower left hand SSRT than the paranoid group and healthy controls. Bellgrove found no difference between patients and controls when all EOS patients were considered as a single group, but when diagnostic subtype was included as a group factor in an ANOVA model, the impairment was revealed. Hence the discriminating factor for SSRT impairment may be the dominant symptom clusters exhibited by patient groups, negative symptoms in particular. No evidence supporting this hypothesis however was revealed in the current investigation, as no relationship was observed between patient SSRT for either hand and symptoms assessed using SAPS and SANS. However, the participating group comprised high functioning out patients and numbered only ten members.

There is a reason that may explain why Badcock and colleagues (2002) found no significant difference between patients and controls in their study, stemming from a combination of the protocol employed for setting SSDs, in addition to the method used for SSRT calculation. To outline this argument, race model theory must be revisited. Like go RT, SSRT is thought to vary from trial-to-trial (Logan & Cowan, 1984), such that if SSRT were measurable on a trial-to-trial basis, then SSRTs recorded over an experiment would produce a distribution of latencies. If a hypothetical experiment is considered where SSDs are set such that stopping is successful 50% of the time for each participant, by the race model, only the fastest of SSRTs (left of SSRT distribution median) can successfully inhibit the slowest of Go responses (right of Go RT distribution median). As SSD increases for an individual, estimated SSRT decreases (Logan & Cowan, 1984; Logan, 1994), implying that as SSD increases, only the fastest SSRTs are successful because on-going go

activation is closer to the point of execution hence slower SSRTs 'lose' the race. If Stops were separated into a long SSD and short SSD conditions, long SSD Stops would have a resultant SSRT that is faster than that estimated for the short SSD condition. This means that trial-wise SSRTs arising from long SSD Stops are sampled from a smaller portion of the SSRT distribution compared to the portion of the SSRT distribution from which shorter SSD Stops are sampled. The long SSD SSRT distribution portion is in fact a sub-sample of the portion of the SSRT distribution from which short SSD SSRTs arise, but the means of these portions are different.

It should also be noted that for an individual, trials with longer SSDs compared to trials with shorter SSDs involve more difficult inhibition (inhibition difficulty = SSRT/(GoRT-SSD)). From the discussion outlined above, this implies that more difficult inhibition is linked to faster SSRT compared to SSRT necessary for easier inhibition. This has important implications for studies comparing SSRT between groups where stop-signals are set relative to Go RT such as Badcock and colleagues (2002). If the groups being compared truly have different SSRTs, then setting stop-signal delays relative to Go RT necessitates that inhibition difficulty will be different for the groups. Hence SSRT for the participants comprising each group will be estimated from different portions of their respective Go RT distributions: SSRT estimates for participants in the slow SSRT group will be derived from a smaller proportion of the SSRT distribution than for participants comprising the fast SSRT group. The upshot of this situation is that individual SSRT and hence group mean SSRT estimated in the slow SSRT group will faster than the individual/group SSRT that would have been estimated if inhibition difficulty is the same as for the fast SSRT group. This may lead to incorrect conclusions about the nature of group differences.

This situation may have arisen in the study of Badcock and colleagues (2002) who compared patients with schizophrenia to healthy controls (and a psychosis comparison group, but only schizophrenia patients and healthy controls are relevant to this discussion). In the study, a range of SSDs were used such that the onsets of stop-signals were set relative to median Go RT (GoRT[43]; as per Experiment 2). Hence SSD varied between individuals due to GoRT differences. The SSRT distributions of schizophrenia patients and

[43] In the Badcock et al. (2002) paper, GoRT was termed MRT (median reaction time).

controls were not distinguishable statistically, but the patient group on the average did have longer SSRT (group mean difference = 31 ms), hence inhibition difficulty was different for the groups. If inhibition difficulty was matched across individuals and groups, SSRT for the schizophrenia patient group may have been slower and hence a larger effect size may have been observed leading to a significant difference between group SSRTs.

This leads us to the second issue: the method used to estimate SSRT was the 'averaging method', where SSRT is estimated at each delay and then averaged (Band et al., 2003). Due to the SSD protocol Badcock et al. (2002) employed, which ensured that a smaller proportion of patient SSRTs were sampled (the faster proportion) compared to the proportion sampled for healthy controls, an artificially fast estimate of patient SSRT was estimated compared to that estimated for healthy controls and may have led to Badcock's null finding. This may have been avoided by calculating SSRT from the median of the inhibition function, which essentially entails subtracting the SSD at the median of the inhibition function from median GoRT (Band et al., 2003).

Overall, the literature regarding stopping in schizophrenia suggests that patients have slow SSRT, and consistent with the recommendations of the CNTRICS breakout group (Barch et al., 2009), combined they present a compelling case for a rigorous investigation of stopping capacity in patients with schizophrenia. However, future studies should note the findings of Bellgrove and colleagues (2005) which indicate that patient study groups comprised of participants exhibiting heterogeneous symptom profiles may likewise exhibit SSRTs that overlap the normal range, despite a large difference between patient and control group mean SSRTs. The finings of Bellgrove et al. (2005) further suggest that mean SSRT of patient groups comprised of participants with homogenous symptom profiles may be more stable resulting in a significant or non-significant difference compared to healthy controls, contingent upon dominant symptomatology. It follows that a larger study would likely benefit from assessing patients from diverse sub-groups of patients with homogeneous symptom clusters characterizing each sub-group, enabling an assessment of specific link between stopping difficulties and schizophrenia subtypes.

Pre and post event RTs

Analysis of pre and post event RTs showed that compared to Stop Failures, Stops were linked to slower responding on the preceding trial, which was a consistent finding in both patient and control groups. This replicated the finding from Experiment 2, however, in that study, pre-Stop RTs were slower than both pre-Stop Failure RTs and pre-GoRTs, which did not differ in latency, whereas in the current experiment, pre-Stop Failure RTs were faster than both pre-Stop RTs and pre-Go RTs, while the latter two trial types did not differ. A qualitative comparison of these findings suggests that in the current experiment, Go trial responding may have been slowed generally, and that Stop Failures resulted from relatively fast response activation processing on those trials, whereas in Experiment 2, slowed responding was specifically related to facilitation of Stops and Stop Failures may have been incurred when participants failed to implement this strategy.

The reason for these disparate findings is not clear, but could be related to the different paradigm variants used in these experiments. In Experiment 2, SSDs were fixed relative to GoRT across participants although varied over a 100 ms range, whereas in the current experiment SSDs were set adaptively varying by 50 ms between successive trials. Hence in Experiment 2, two successive stop-signal trials may have SSDs that varied by 100 ms, whereas in the current experiment, successive stop-signal trials varied only by 50 ms, at least for trials of the same hand. Given that SSRT was around 200 ms for both studies, a 50 ms potential difference in subsequent SSDs (100 ms compared to 50 ms for Experiments 2 and 3 respectively) may have invoked a different response strategy. An additional potentially influential factor is that in the previous experiment, all stop-signal trials were followed by a go trial, whereas in the current experiment, stop-signal trials could be successive. These differences raise the possibility that in the current experiment participants may have adopted a (Go) response strategy that was in general slower than the strategy adopted by participants in Experiment 2, which would suggest that paradigm variants may induce markedly different response strategies in participants.

6.4.3. fMRI data

Stopping data

Control group data for the Stops > Go contrast revealed an anticipated network: predominantly right lateral activation pattern including IFG, MFG, IPL, the thalamus and STN/GPi. This pattern of activation foci was almost identical to that observed by Aron and Poldrack (2006) in their comparison of Stops > Go and overlaps with the activation pattern revealed when Stop blocks were compared to Passive epochs in Experiment 1, and thus provides further evidence that this network underpins stopping.

When SSRT was correlated with inhibition contrast maps (Stops > Go) for controls, negative relationships were observed in right IFG and preSMA but not STN. SSRT predicted IFG related BOLD signal variance in *pars opercularis and pars triangularis*, however, left IFG relationships were more extensive. In patients with schizophrenia, faster SSRT also predicted larger BOLD signal responses within right IFG, specifically *pars opercularis* and *pars orbitalis*, in addition to right IPL and sub-cortically within right thalamic and left caudate nuclei. This finding supports previous evidence linking faster SSRT to larger BOLD signal responses in right IFG (Aron & Poldrack, 2006; Experiment 1) and preSMA (Aron & Poldrack, 2006), but failed to replicate similar linkage between SSRT and STN as reported by Aron and Poldrack (2006).

There is some evidence suggesting that the role of STN in stopping may be more crucially linked to triggering stopping processes and not predicted by faster SSRT (Eagle et al., 2008), which is consistent with the lack of relationship between STN and SSRT in the current experiment. However the sample size used to relate SSRT to STN activity in the current experiment was quite small which may have hindered the detection of any relationship. It should be noted that in Experiment 2, SSRT predicted inhibition difficulty and given that some participants inhibited most of the time (faster SSRT, low difficulty) while other inhibition less often (slower SSRT, high difficulty), slower SSRT loaded more heavily on triggering stopping processes compared to faster SSRT.

The main finding from the neuroimaging aspect of this experiment was that patients with schizophrenia exhibited regional reductions in BOLD signal intensity compared to controls in the right lateral brain areas thought to underpin stopping, most notably within the right IFG (*pars opercularis*)-STN network, but also right MFG and parietal areas, in

addition to left lateral globus pallidus merging into left STN. This suggests that impulsive behaviour exhibited by patients with schizophrenia, categorized neuropsychologically by slowed SSRT (Enticott et al., 2008), may stem from an inability to recruit the brain circuitry required to suppress on-going behavioral activation. While it may be argued that patients would be expected to exhibit *less* activation than controls, there are several aspects of this work that point to the contrary. Firstly, the patient group exhibited greater activation than controls in the Go > Baseline contrast, notably within mid-dorsolateral portions of right MFG, which probably accounts for the BOLD differences between groups when Stops > Go contrasts were compared. Secondly, a summary of activated voxels in the Go > Stops contrasts (albeit at a low threshold, $p < .05$) indicated that patients activated more during 'going' compared to stopping, which was consistent when assessing the data for this contrast for either the left hand, the right hand, or collapsed across both hands. Whereas in the reverse contrast, Stops > Go, controls consistently activated more than patients who exhibited very little activation at the thresholds applied ($p < .01$ and 10 contiguous voxels). Finally, the patient group exhibited substantially more activation in the Stop Failures > Go contrast than did controls, including left STN suggesting these individuals could activate these subcortical nuclei. Hence, although patients exhibited reduced activation compared to controls in the Stops > Go contrast, they exhibited greater activation in other contrasts, thereby discounting the notion that patients would be expected to exhibit reduced activation during stopping. What was most evident in the differences observed for the Stops > Go contrast was that the patient group did not activate the anticipated network including right IFG (*pars opercularis*)–STN. This finding is particularly notable given the finding that SSRT, which has been linked to activation in an IFG-STN network (Aron & Poldrack 2006), was slowed in the patient group compared to controls. The neuroimaging results of Experiment 2 suggested that right IFG-STN activation may actually depend on the difficulty of inhibition posed by an experimental paradigm; in the current investigation inhibition difficulty was matched across participants by setting SSD adaptively from trial-to-trial. That patients did not activate the fast acting right IFG-STN network during stopping suggests that fast inhibition process were not in operation in this group. This indicates that once Go processes are launched by patients they cannot be stopped, whereas in controls, after the launch of Go processes stopping can be effected via recruitment of the

right IFG-STN network. This further suggests that a processing bottleneck is present in patients that is not present in controls: once Go processes reach the bottleneck, the response cannot be stopped. This could be investigated by comparing electromyographic recording of response-related muscle groups in both patients and controls during stop-signal task performance. De Jong and colleagues (1990) showed that healthy participants can inhibit responses even after EMG onset; if the hypothesis outlined above is correct, presumably patients with schizophrenia would not be able to do so.

While the current data indicate that slowed SSRT in patients with schizophrenia may be linked to an inability to recruit the right IFG-STN 'hyperdirect' stopping network, it imparts no knowledge regarding the biological underpinnings of the impairment. This network does however map onto the mesocortical dopaminergic pathways that are known to be dysfunctional in schizophrenia, and is thought to stem from down-regulation of NMDA receptors on GABAergic thalamic and PFC interneurons which diminishes control over output neurons (Javitt, 2009; Olney & Farber, 1995; Stone et al., 2007).

In controls, the contrast comparing Stop and Stop Failure related activity (repeated measures t-test, (Stops > Go) > (Stop Failure > Go)) revealed substantial striatal activation, including foci within bilateral caudate and putamen nuclei. This was similar to the finding from Experiment 2 where Stops were directly compared to Stop Failures (Stops > Stop Failures). In the previous experiment the argument was made that such striatal activation represented Go trial slowing to facilitate stopping which corresponded to slower responding on trials preceding Stops compared to Stop Failures, which was confirmed in the present experiment.

Go data

The Go > Baseline contrasts showed that both groups activated SMA and M1 contralateral to response hand, which is consistent with other reports (Aron & Poldrack, 2006), but interestingly, patients with schizophrenia exhibited larger BOLD responses in right MFG and right cerebellar cortex compared to controls. While the reason for this fronto-cerebellar enhancement in patients with schizophrenia is unclear, these brain structures have been strongly linked to functions required for correct go task responding.

Cerebellar cortex is heavily involved in controlled execution of motor (Ivry, 2000), and also attentional functions (Gottwald et al, 2003). It should be noted that in Experiment 1, task blocks requiring response inhibition (STOP blocks) were linked to greater cerebellar activation, albeit left cerebellum, compared to essentially identical blocks that required only go task responses (GO blocks). Go responding was much slower in STOP blocks compared to GO blocks indicating greater control over response execution. Right DLPFC has been linked to cognitive control functions including decision making (Fleck et al., 2006; Knoch et al., 2006) and response selection (Bunge et al., 2002; Rowe et al., 2000) which are also required for correct go responding. In combination these data suggest that patients with schizophrenia exert greater control over responding on go trials compared to healthy control participants. Ford and colleagues (2004) arrived at similar conclusions. They suggested that during Go/No-go paradigm performance, patients with schizophrenia do not establish a go trial prepotency but make a deliberate choice whether or not to respond on each trial. The data reported here suggest this 'deliberate' response style may be underpinned by a right lateral MFG-cerebellar network.

6.4.4. ERP data

ADJAR efficacy

The correction procedures developed by Worldorff (1993) were, as in Experiment 2, very effective at removing over-lapping go response activation in stop-signal waveforms. This is observable in flattened pre-stimulus baselines, in addition to enhanced N1 and reduced P3 in stop-signal waveforms for both patient and controls groups. The amplitude of the potential removed from stop-signal waveforms was smaller in this experiment (for controls) compared to that removed in Experiment 2. There are two reasons for this, relating to both amplitude and temporal characteristics of go and stop-signal waveforms, respectively. Firstly, for reasons that are unclear, Go-P3 potentials, which are the main potential removed by ADJAR procedures (Bekker et al., 2005a), had a smaller amplitude in the current experiment compared to Experiment 2. Hence there was less corruption of stop-signal waveforms in terms of amplitude. Secondly, group mean SSD was substantially longer in the current experiment compared to Experiment 2 resulting in a later onset of stop-signal potentials relative to the go stimulus, while the latency of Go-P3 was

approximately the same, hence the temporal overlap of go-related potentials in stop-signal waveforms was substantially less in the current experiment compared to Experiment 2. This latter point was particularly evident in patient waveforms where the overlapping Go ERP potential removed was very small.

Go and stop-signal waveforms

The brain potentials of most interest in this experiment were auditory evoked stop-signal N1 and P3 potentials. However visual N1 and P3 potentials elicited by Go stimuli were also considered and will be discussed in the following primarily to illustrate stop-signal ERP findings. The scalp topography of Go and stop-signal N1 and P3 potentials were as expected, largely paralleling those observed in Experiment 2. Auditory evoked stop-signal N1 revealed a fronto-central distribution, maximal at the vertex (Cz), while visual evoked Go-N1 revealed a centro-parietal distribution, largest at lateral parietal electrodes. P3s evoked by stop-signal and go stimuli were enhanced at midline compared to lateral electrodes, but differed in topography: Go-P3s displayed a centro-parietal distribution, maximal at Pz, whereas stop-signal P3s were by comparison more fronto-centrally distributed, and maximal at the vertex (frontal and parietal amplitudes were comparable). These differences were largely consistent across the groups, and indicate markedly different processing requirements during go and stop-signal trials, namely the parietal distribution of Go-P3s resemble that of a 'target' P3, usually termed P3b, whereas stop-signal P3s were, by comparison, fronto-centrally distributed, consistent with the 'novelty' P3, or P3a (Katayama & Polich, 1998) and comparable to No-go-P3s (Falkenstein, Hoormann, & Hohnsbein, 1999).

Analysis of amplitude measures for each component revealed reductions in patients compared to controls, but what was most revealing was that the peak latencies of both stop-signal N1 and P3 potentials were later in patients, whereas no latency differences were observed between the groups for Go-N1 or Go-P3. These findings mirror the reaction time data whereby SSRT was significantly slower in patients whereas GoRT was not. Additionally, stop-signal N1 amplitudes were modulated by stopping success in controls, in that Stop-N1 was larger than Stop Failure-N1, but no modulation of stop-signal N1 was present in the patient data. A further finding worth noting was that the latency of Stop-N1

was linked to the expression of more negative symptoms in patients, for left hand stop-signal trials in particular.

N1 findings

Reduced auditory evoked N1 amplitudes are often observed in patients with schizophrenia, which has led to consideration of this potential as a possible trait marker for schizophrenia (Ahvenien et al., 2006), however the impairment is primarily observed at inter-stimulus intervals greater than one second (Rosburg et al., 2008; Shelley, Silipo, & Javitt, 1999). The current findings are consistent with these observations given that the shortest interval between successive stop-signal presentations in the current experiment was approximately two seconds.

Auditory N1 is thought to be generated by a network of neural areas including the structures in the superior temporal lobe, in addition to frontal and motor cortical areas (Näätänen & Picton, 1987), but no direct linkage has been determined between the functional impairment and the structural integrity of these structures in patient groups (Egan et al., 1994; Donnell et al., 1993; Rosburg et al., 2008). Nonetheless, a recent meta-analysis of voxel-based morphometry studies showed that medial and superior temporal lobe structures are the most affected cortical regions in schizophrenia (Honea, Crow, Passingham & MacKay, 2005), the latter being critically involved in N1 generation (Näätänen & Picton, 1987). Additionally, a recent investigation of the relationship between grey matter volume and 'mismatch negativity' (MMN[44]), in patients with schizophrenia reported that MMN reduction in patients was related to reduced grey matter volumes in frontal (motor and associative regions) and temporal lobe areas, the latter including bilateral Heschel's and superior temporal gyri (Rasser et al., 2009). Crucially, MMN is thought to be generated by brain regions that overlap with those generating the obligatory N1 component (Näätänen & Picton, 1987). Indeed some have argued that MMN is a latency- and amplitude-modulated expression of the auditory N1 response (May & Tiitinen, in press).

[44] MMN is a difference waveform indexing the difference in automatic electrophysiological responses between frequently presented 'standard' tones and rarely presented 'deviant' tones (Näätänen & Picton, 1987).

Stop-signal N1 modulation

A further interesting finding was that patients exhibited impaired modulation of stop-signal N1 potentials contingent upon inhibition success, especially during left hand (non-dominant hand) stop-signal trials, whereas Stop-N1 was consistently larger than Stop Failure-N1 in controls. Modulation of stop-signal N1 amplitudes, first reported by Bekker and colleagues (2005a) and confirmed in Experiment 2, has only been observed in stop-signal ERP investigations that have employed ADJAR correction procedures to remove overlapping potentials elicited by go stimuli on stop-signal trials. Citing previous work demonstrating auditory N1 enhancement during a selective attention condition compared to an ignore condition (Hillyard et al., 1973), Bekker proposed that modulation of stop-signal N1 stems from selectively attending to auditory channels during Stops and a failure to selectively attend to the stop-signals on Stop Failure trials. Hence the data concerning patients with schizophrenia reported here suggest a failure of auditory selective attention processes, which are well documented in schizophrenia (Michie, Fox, Ward, Catts, & McConaghy, 1990a; Michie, Bearpark, Crawford, & Glue, 1990b; Rosburg et al., 2008; Ward et al., 1991; Wood et al., 2006).

Investigations of selective attention in schizophrenia have shown processing during the earliest stages, linked to a mid-latency positive potential termed P1, are intact, whereas subsequent processing related to N1 and P3 components, is impaired (Hackley, Worldorff, & Hillyard, 1990; Mathalon, Heinks, & Ford, 2004). Mathalon and co-workers (2004) have proposed three possibilities to explain this impairment in schizophrenia by referring to compromise in and/or between two fronto-temporal circuits. Firstly, they suggest that a subset of fronto-temporal pathways, those which underpin the initial biasing of attention to relevant stimuli is intact (P1 related), but those involving N1 generation are impaired. Secondly, that both subsets are intact, but that connectivity between these pathway subsets is impaired, and finally, that both are intact and the impairment stems from dysfunction within auditory cortex.

In the current experiment, P1 effects were not examined. However the stop-signal waveforms presented here do not suggest any consistent amplitude differences between patients and controls in the P1 latency range at least at fronto-central sites (if anything, P1 is larger in patients at parietal sites), but the data reported here show quite clearly that stop-

signal N1 potentials are much smaller in the patient group, and may even peak at a longer latency than for controls which is of particular note given that no latency differences were observed in Go-N1 peak latency. This suggests that engagement of the processes involved in generating stop-signal N1 are impaired in schizophrenia, hence patients may have particular trouble decoupling attention from one stimulus modality and re-engaging attention in another modality.

However, there are at least two factors to consider before concluding that modulation of stop-signal N1 is due solely to selective attention processes. Firstly, stop-signals are equally relevant during Stops as during Stop Failures, the latter resulting from faster go response activation processes, demonstrable by faster Stop Failure RT. This implies that selection processing must *precede* the onset of the stop-signal, which is suggested by slowed RTs on the trial preceding Stops compared to the trials preceding Stop Failures. A second factor is that in controls, Stop-N1 enhancement is substantially greater at Cz compared to Fz, which was also the case in Experiment 2. Previous research suggests that selective attention effects on auditory ERPs around the N1 latency are observed at both frontal and central electrode sites (Hansen & Hillyard, 1980), but N1 modulation observed in the current study was primarily observed centrally. This seems to imply that Stop Failure-N1 is suppressed at central sites, but where could such suppression occur?

Some evidence is provided by a PET study by Frith and Friston (1996) who investigated selective attention in healthy volunteers. Participants were presented with concurrent streams of auditory and visual stimuli at varying presentation rates, in which participants were required to respond to target stimuli during PET scanning. Using an ANOVA (attention modality/visual x presentation rate) model, this team found that greater attention to tones (attention x presentation rate interaction) was linked only to greater rCBF in the right thalamus, but not auditory cortex, indicating that the thalamus is critical for selective attention to auditory stimuli. Comparably, a recent fMRI study reported greater BOLD signal intensity within bilateral thalamic nuclei in the attend condition (target tones) compared to the ignore condition (standard tones) of an auditory selective attention task (Morey et al., 2008). These findings suggest that thalamic nuclei have a crucial role in selective attention.

However, the thalamus also has a crucial role in response execution, given that it is thalamo-cortical output to motor cortex that controls motor output (Alexander & Crutcher, 1990). At this point it should be noted that in the aforementioned study of Frith and Friston (1996), the main effect of attention to auditory stimuli was revealed in lateral pre-motor cortex (BA 6), suggesting recruitment of the motor system during auditory attention, and thus may share common motor circuitry with Stop Failure motor output. It is obvious that Stop Failures involve greater motor activity than Stops, hence it possible that motor activation may gate frontally mediated selective attention processes at the level of the thalamus, hence suppressing Stop Failure-N1 at Cz.

Corresponding to the results of Frith and Friston (1996) and Morey et al. (2008), the imaging data from the current study revealed greater BOLD activation in the bilateral thalami for the comparison of Stops to Stop Failures (contrast was (Stops > Go) > (Stop Failures > Go)) and Stops > Go contrast, but not Stop Failures > Go contrast in controls, whereas no thalamus activation was observed for these contrasts in patients, though some activation was observed in the left thalamus of patients in Stop Failures > Go contrast. Additionally, when control group Stop > Go contrast was compared to that for patients, the BOLD contrast estimate was significantly greater in the right thalamus (controls > patients). These observations support the speculative proposal that the thalamus has a significant role in selective attention during normal stopping, and that patients with schizophrenia, who reveal impaired stop-signal N1 modulation during Stops compared to Stop Failures, do not to activate the thalamus. This finding corresponds to the study of Morey et al., (2008) outlined previously, who reported significantly greater thalamic activation, especially in the right thalamus, in controls compared to patients with schizophrenia during selective attention. The observations reported here, though speculative, are consistent with a large body of evidence linking schizophrenia spectrum disorders to thalamic abnormalities including synaptic degeneration (Blennow et al., 2000) and neuronal loss (Popken et al., 2000), reduced glucose metabolism (Hazlett et al., 2004), neurochemical abnormalities (Watis et al., 2008; Yoo et al., 2008), low resting state BOLD signal intensity (Welsh, Chen & Taylor, 2008) and reductions in grey matter volume (Andreasen et al., 1994; Csernansky et al., 2004; Konick & Friedman, 2001; Lang et al., 2006). Further research must be conducted before any firm links can be made, but the data

reported here suggest the stop-signal paradigm may be a prime tool for studying selective attention deficits in patients with schizophrenia.

N1 Latency

A surprising finding was that latencies of stop-signal N1 peaked later in patients compared to controls at the vertex (Cz), though only marginally so, indicating slowed auditory processing in schizophrenia. More surprising was that the latency of Stop-N1, particularly for the left hand at Fz, was related to negative symptoms as indexed by SANS symptoms scores in the patient group, whereby longer latencies were related to greater overall negative symptomatology. No relationship was observed for Stop Failure-N1 at any electrode. Tenuous links between auditory N1 latency and SANS scores have been reported previously (Bougerol, Benraaiss & Scotto, 1997), but the linearity of the relationships observed in the current experiment was striking.

While an explanation for these findings can only be speculative here, it should be noted that the attention requirements of the stop-signal task are substantially different to traditional selective attention tasks such as dichotic listening paradigms that are commonly used to index selective attention effects on auditory N1 and related potentials. These selective attention tasks generally require participants to attend to a single stream of stimuli amongst multiple streams and respond to or count only specific (target) stimuli within that stream. In contrast, the traditional stop-signal task requires participants to respond to a go response stimulus and concurrently switch attention to an auditory stop-signal during activation of go responses. It is certainly possible that dysfunction within thalamic nuclei may not only attenuate stop-signal N1 amplitude, but also slow processing in patients with schizophrenia resulting in an N1 peak delay. As stated previously, thalamic abnormalities have been strongly linked to schizophrenia, but additionally, there is some evidence linking thalamic dysfunction and irregularity to negative symptoms in schizophrenia (Lang et al., 2006; Yoshihara et al., 2008).

P3 findings

The findings resulting from analyses of stop-signal and go P3 amplitude and latency measures correspond with the electrophysiological literature on schizophrenia whereby P3s

elicited by auditory stimuli (stop-signals) in patients exhibited marked differences to controls whereas only marginal differences in P3s evoked by visual go stimuli were found between the groups (Ford, 1999). Critical among these findings were that patient stop-signal P3 amplitudes were smaller than for controls, but more interestingly, the peak latency of these potentials occurred later in patients compared to controls. In contrast, control Go-P3 amplitudes were marginally larger than for patients across the scalp and significantly larger only at midline sites, however the peak latency of Go-P3s did not differ between patients and controls; in fact patient Go-P3s peaked slightly earlier than did control Go-P3s, though not significantly so. Hence P3 amplitude reduction in patients was a general finding, though the impairment in auditory evoked stop-signal P3s was most marked, whereas impaired timing of P3s was specific to stop-signal events. It is noteworthy that the dissociation between go and stop-signal P3 timing differences between the groups paralleled the behavioural findings whereby no significant differences were observed in GoRT whereas SSRT was significantly slower in patients compared to controls.

While no statistical comparisons were made between stop-signal and Go-P3s, these qualitative observations are important when comparing these components between groups and for comparison to the findings of studies that have previously investigated No-go inhibition in patients with schizophrenia (Ford et al., 2004; Keihl et al., 2000; Weisbrod et al., 2000). In all these studies, patients also exhibited reduced No-go-P3 amplitudes in both visual (Ford et al., 2004; Kiehl et al., 2000) and auditory (Weisbrod et al., 2000) go/no-go paradigms. Only Ford and colleagues specifically analysed P3 latency data, reported delayed P3s in patients, but this was mostly due to later Go-P3s in patients, whereas No-go-P3s were largely invariant between the groups.

Perhaps more relevant to the current investigation is that of Weisbrod et al. (2000) who used auditory go and no-go stimuli. Despite that no latency analyses were reported, the waveforms presented in the paper do not suggest any No-go-P3 latency differences between patient and control groups, whereas in the current study, between group differences were salient (see Figures 7.10 and 7.11). Additionally, the No-go-P3 peaks visible in Weisbrods' figure appear to peak much later (in the range of 350-400 ms) than for auditory evoked Stop-P3s observed here for either group, which probably indicates differential processing No-go and stop-signal stimuli between the studies.

Impaired P3 is arguably the most robust finding in the schizophrenia literature (Ford, 1999), particularly in the case of auditory evoked P3s. Many studies have reported that auditory evoked P3s are more impaired than visual evoked P3s in schizophrenia patients (Duncan, 1988; Pfefferbaum, Ford, White, & Roth, 1989). Additionally, visual evoked P3 is modulated by medication and clinical status whereas auditory evoked P3 is independent of these factors (Duncan, 1988; Pfefferbaum et al., 1989; Mathalon, Ford & Pfefferbaum, 2000) and degenerates with illness duration (Mathalon, Ford, Rosenbloom, & Pfefferbaum, 2000; van der Stelt, Frye, Lieberman, & Belger, 2004). These findings have lead to the hypotheses that visual and auditory evoked P3s may be state and trait markers of schizophrenia, respectively, however it has been argued that the usefulness of P3 in this regard may be limited to ruling out a diagnosis of schizophrenia (Ford et al., 1992).

While reduced P3 amplitudes are most consistently reported, longer P3 latencies in patients are not common (Michie et al., 1990b; Mathalon et al., 2004; Pfefferbaum et al., 1989). Indeed it is the longer latency of the patient group in this study that is of critical importance, given the very fast nature of stop-signal P3s, particularly Stop-P3s. Critically, no difference (0 ms) was observed between Stop-P3 and Stop Failure-P3s in patients at Fz whereas the difference in controls at Fz was large (44 ms), and large for both groups at Cz (patients = 25 ms, controls = 34 ms); a Stop and Stop Failure P3 latency dissociation was also observed Experiment 2. This dissociation observed in the current study for patient and control stop-signal P3 peak latencies is particularly notable given the results of Experiment 2 where SSRT was linked to processing at Fz by strong correlations between SSRT and Stop-P3 amplitudes, but more pertinently by a strong correlation between SSRT and the difference in peak latency between Stop-N1 and Stop-P3. Although not replicated in the current experiment, these correlations suggest that frontal processes are crucially linked to the timing of stop related activation, and the dissociation in the timing of Stop-P3 and Stop Failure-P3 observed here and previously (Bekker et al., 2005a; Kok et al., 2004; Ramataur et al., 2004; Experiment 2) suggests that slowed engagement of frontal processes leads to a Stop Failure. The lack of peak latency differences between Stop-P3 and Stop Failure-P3 at Fz in patients with schizophrenia suggest that the timing of frontal activation in patients does not predict stopping success, whereas it does in controls.

N2 findings

Patient and control stop-signal waveforms were also distinguishable by clear morphological differences observable in the group average waveforms: patients exhibited a large negative deflection superimposed on stops-signal P3s that peaked approximately 250 ms after stop-signal onset. Based on the latency of this component it is identified here as stop-signal N2 (van Boxtel et al., 2001; Ramautar et al., 2004; Dimoska et al., 2006). This potential is clearly observeable only in Stop Failure waveforms of controls but was consistently observed across the scalp in both Stop and Stop Failure waveforms of patients, though appears to be more negative in patient Stop Failure waveforms. In control group stop-signal waveforms, no clear N2 is apparent, but a notch beginning just before 200 ms after stop-signal onset is observable in the positive going arm of control group Stop Failure waveforms. Control group Stop waveforms also reveal a small negative inflection at approximately the same latency, which is most prominent at lateral frontal sites. Analyses of the mean amplitudes across the range of this potential confirmed that stop-signal N2 was larger (i.e., more negative) for Stop Failures than for Stops, and moreover, was larger for patients compared to controls. It is uncertain what cognitive operation(s) this potential reflects, and no analyses were conducted to investigate them further, but the polarity and latency are commensurate with N2, which is commonly linked to conflict processing (Donkers & von Boxtel., 2004; Stahl & Gibbons, 2007), that is thought to be subserved by ACC (Botvinick et al., 2004, Carter et al., 2000; Van Veen & Carter, 2002). Most interestingly the patient group exhibited this negativity not only in Stop Failure waveforms, but also in Stop waveforms raising the intriguing possibility that patients experienced greater conflict during stopping compared to controls. This possibility is supported by the neuroimaging data that showed that patients had a greater reliance on ACC for stopping, though no correspondence between ERP measures and brain activation in ACC could be ascertained.

The key outcomes from this experiment, derived from behavioural, electrophysiological and functional BOLD imaging measures, demonstrated several aspects of impaired functioning during stop-signal performance in patients with schizophrenia. Most notable was an impaired capacity to exert efficient control over behaviour which has

been demonstrated in previous experiments employing the stop-signal paradigm to investigate response inhibition in schizophrenia. Behavioural analyses showed that the speed of inhibition processes, SSRT, was consistently slower in patients with schizophrenia compared to controls. Commensurate with this behavioural manifestation, an electrophysiological index that most stop-signal researchers consider to reflect the stopping process, the Stop-P3 potential, was slower and reduced in amplitude in the patient group. Neuroimaging data suggested that slowed stopping in the patient group derived from an inability to recruit the right lateral IFG-STN network which is thought to enable fast inhibition. While patients did activate ventral aspects of right IFG, corresponding to *pars orbitalis* (BA47), this group did not activate *pars opercularis* (BA44) that previous lesion (Aron et al., 2003a) and neuroimaging reports (Aron & Poldrack, 2006; Aron et al., 2007a) have indicated is required for efficient control of responding during stop-signal task performance. Instead patients engaged a network including ACC for successful inhibition which is often found to be engaged for No-go inhibition and resolution of response conflict (Botvinick et al., 2004), but not stopping. In combination, these behavioural, ERP and fMRI findings suggests that slower processing of stops-signals results in greater conflict between Go response activation processes and Stop response inhibition processes.

Chapter 7: Discussion and Conclusions

7.1 Introduction

The principal aim of this thesis was to investigate the neural basis of response inhibition using the stop-signal paradigm in healthy individuals (Logan & Cowan, 1984), and secondly, to elucidate the neural basis of stopping impairments that have been reported in behavioural studies of patients with schizophrenia (Badcock et al., 2002; Bellgrove et al., 2006; Enticott et al., 2008) and children at risk of developing schizophrenia (Davalos et al., 2004; Ross et al., 2008). These aims were pursued using behavioural, epoch-based and event-related fMRI, and event-related potential (ERP) EEG methods. FMRI and ERPs were chosen as investigative tools for the complementary spatial and temporal information regarding the neural basis of cognitive processes afforded by these techniques, respectively. There were several key findings.

7.2 Key findings

In each of the three fMRI studies conducted, stop-signal inhibition was linked to BOLD activation in right lateral IFG and STN of healthy individuals confirming the findings of previous studies reporting involvement of these brain areas in stopping (Aron et al., 2003a; Aron & Poldrack, 2006; Aron et al., 2007a; Chambers et al., 2006; Chambers et al., 2007; Eagle et al., 2008; Rieger et al., 2003; Rubia et al., 2003). In two of these studies, Experiment 1 and Experiment 3 (see Chapters 3 and 6), a tracking algorithm was employed that operationalised stopping probability at the level of chance, ensuring that stopping task difficulty was equated across participants. For these studies, right IFG and STN activation was consistently observed across participants revealed by random effects group t-tests on stop related contrast images, and additionally, faster SSRT predicted BOLD enhancement in right IFG, linking the speed of inhibition processing to activation of that area, that is, BOLD measures were *negatively* correlated with SSRT. Conversely, IFG activation in the group random effects t-tests for the stopping contrast in Experiment 2 (see Chapter 4) was minimal and STN activation was absent, whereas right MFG (merging into IFG) dominated the frontal activation pattern for the group contrast. However, SSRT was strongly predictive of the BOLD response in both right IFG and STN, but in contrast to the findings

of Aron and colleagues (2003a/2006/2007a) and Experiments 1 and 3 of this thesis, these BOLD measures were *positively* correlated with SSRT. This finding was predicted, based on a task difficulty manipulation where task (inhibition) difficulty varied between participants as a function of individual SSRT: SSRT was a proxy for inhibition difficulty, indicating that task difficulty may determine both the degree and nature of right IFG-STN engagement.

ERP data recorded from healthy participants in Experiment 2 and Experiment 3 revealed marked differences in both the amplitude and latency of Stop compared to Stop Failure ERPs. Compared to Stop Failures, Stops revealed enhancement of auditory-evoked stop-signal N1 and P3 potentials, and additionally, the peak latency of Stop-P3s occurred much earlier than for Stop Failure-P3s. In Experiment 2, there was evidence linking SSRT to latency and amplitude measures of Stop-P3 but this was not confirmed in Experiment 3, suggesting the relationships observed were due to paradigmatic differences. A final observation based on visual inspection of the ERPs was that stop-signal N2, a proposed electrophysiological substrate of the stopping process (van Boxtel et al., 2001), was not observed in Stops but was present in Stop Failure ERPs, thereby supporting the proposal that N2 does not reflect response inhibition (Donkers & van Boxtel, 2004).

When patients with a diagnosis of schizophrenia were compared to healthy controls that were matched for age, gender and years of education, SSRT was significantly slower in the patient group confirming previous reports[45] of this behavioural deficit in schizophrenia patients (Bellgrove et al., 2006; Enticott et al., 2008). Correspondingly, the right IFG-STN network was uniquely underactivated in patients, suggesting that these participants did not engage the putative stopping mechanism (Aron & Poldrack, 2006). Analysis of electrophysiological data showed that the amplitudes of stop-signal N1 and P3 potentials elicited in patients were smaller compared to controls, and patients exhibited little or no amplitude modulation of stop-signal N1, whereas in controls the amplitude of Stop-N1 was substantially larger than of Stop Failure-N1. Analysis of stop-signal P3 peak latencies showed an interesting dissociation between the groups: in controls Stop-P3s peaked earlier than Stop Failure-P3s at frontal and central electrodes, whereas the latencies of these

[45] Badcock et al. (2002) found no significant difference between patients with schizophrenia and controls on SSRT despite that the groups differed on this measure by 31 ms, which for reasons outlined in Chapter 6 may have been an underestimate of the true difference between the groups.

potentials did not differ in patients at frontal electrodes (Fz). Finally, the peak latency of stop-signal N1 potentials was marginally longer in patients compared to controls, a difference that may have been partly explained by the presence of negative symptoms in patients: a greater number of negative symptoms measured using SANS was linked to a longer peak latency of Stop-N1, especially for left (non-dominant) hand Stop potentials.

7.3 Neuroimaging data

Involvement of the right IFG (*pars opercularis*) and STN 'hyperdirect' network, that has been proposed as the neural substrate of stopping (Aron & Poldrack, 2006), was related to stop-signal inhibition in each of the three neuroimaging experiments detailed in this thesis. In the first experiment[46] (see Chapter 3), enhanced BOLD signal intensity was observed in the stopping network when blocks requiring stopping (Stop blocks) were compared to blocks where participants were required only to passively view the stimuli presented (Passive blocks). But when Stop blocks were compared to Go blocks, which required only go responses (tones were presented but ignored), right IFG activation was limited to *pars orbitalis*, and STN activation was not observed.

The reason for non-observance of the *pars opercularis*-STN network in the Stop > Go block contrast is unclear, but may be due to the epoch-based design which is insensitive to phasic changes in BOLD signal intensity, or due to the presence of response selection requirements in both Stop and Go blocks that were not present in Passive blocks. A role for STN in response selection has been revealed in rodent lesion models (for review see Tan, et al., 2006). Response selection processes would be particularly relevant for go trials preceded by a go trial that instructed opposite response mapping to the current trial, and presumably, there would be greater demand on these processes on go trials from Go blocks of the first experiment due to the faster GoRT[47] observed in Go blocks compared to Stop blocks (Stop blocks: GoRT = 483 ms, Go blocks: GoRT = 425 ms). While STN activity was not above threshold in Go blocks, it may have been substantial enough to suppress

[46] This finding was not expanded upon in that chapter, which was submitted for publication to Human Brain Mapping (rejected after review), as involvement of STN in stopping had not previously been indicated in the literature.

[47] In Chapter 3 GoRTs for Stop blocks were described as Stop/no-signal trials and for Go blocks they were divided into Go/no-signal (425 ms) and Go/signal (426 ms) trials, where for the latter, the tone ('signal') was ignored.

significance in the Stop > Go block contrast. Nonetheless, IFG activation, albeit within *pars orbitalis*, was observed in the Stop > Go contrast and was inversely correlated with SSRT in line with previous reports linking IFG to SSRT (Aron et al., 2003a; Aron & Poldrack, 2006; Aron et al., 2007a; Rieger et al., 2003).

The second experiment – a combined event-related fMRI and ERP (electrophysiological data detailed below) experiment – introduced a novel conceptualization of task (inhibition) difficulty posed by different stop-signal paradigm variants. The model of inhibition difficulty proposes that the time given to inhibit a response impacts on the probability with which a participant will successfully inhibit, contingent upon individual SSRT. To vary inhibition difficulty between participants, the time given to inhibit was kept approximately constant across individuals by setting stop-signal onsets relative to median Go reaction time (GoRT), resulting in a negative and essentially collinear correlation between SSRT and PI (note that in the adaptive paradigm of Experiment 3, SSRT and PI are unrelated). This relationship was observed in the behavioural data of both experimental (fMRI and ERP) sessions and taken as definitive evidence that task difficulty in stop-signal experiments is best described by the SSRT/(GoRT – SSD) ratio. The traditional parameter of stopping difficulty, stop-signal delay, does not convey any real information about stopping difficulty for a given stop-signal trial or paradigm variant other than the obvious: that longer stop-signal delays are in general linked to more difficult stopping.

The neuroimaging findings from Experiment 2 provided insights into the role of the putative right IFG (*pars opercularis*)-STN stopping network. Activation in the stopping network was not observed in the group random effects t-test of Stops > Baseline (essentially Stops compared to the mean of Go related activity). Instead the group frontal activation pattern was dominated by mid-dorsolateral portions of PFC (MFG merging into *pars triangularis* of IFG), which is commonly linked to No-go inhibition (Kawashima et al., 1996; Watanabe et al., 2002; Zheng et al., 2008; de Zubicaray et al., 2000). However, the correlation of SSRT onto Stops > Baseline contrast maps was strongly predictive of BOLD signal intensity within the right *pars opercularis*-STN (a positive relationship), indicating that participants for whom the stop-signal task was increasingly difficult (low inhibition difficulty ratio) activity in the stopping network was substantial. This points to a

dissociation in frontal activity for stopping, whereby stopping generically engages mid-dorsolateral portions of PFC (MFG merging into *pars triangularis* of IFG), whereas increasing stopping difficulty requires engagement of the right IFG (*pars opercularis*)-STN network. Mid-DLPFC is also thought to have roles in decision making (Fleck et al., 2005; Knoch et al., 2006) and response selection (Bunge et al., 2002; Rowe et al., 2000), processes that are also important in no-go and stop-signal trials. Indeed it has been suggested that these processes map more directly onto the response control requirements for no-go tasks than do response inhibition processes (Rubia et al., 2001a), thus it follows that decision making/response selection processes may be generically activated for stopping, as suggested by all experiments in this thesis, but is the primary process for trials of low inhibition difficulty.

In the third experiment, also a combined event-related fMRI and ERP (electrophysiological data detailed below) study, inhibition difficulty was kept equal for each participant by adaptively setting stop-signal onsets such that PI converged on chance level stopping. When Stop events were compared to Go events in psychiatrically healthy participants, BOLD activity was generically observed in the right IFG (*pars opercularis*)-STN network indicating that this network underpinned stopping, thereby confirming the findings of Experiment 1 and Aron and colleagues (2006/2007a) who also observed a corresponding activation pattern in a Stop > Go contrast derived from a similarly designed study. However, SSRT was predictive of activation in right IFG (*pars opercularis* and *pars triangularis*), but not STN, which conflicts with the findings of Aron and colleagues (2006/2007a) who found that the BOLD response in both structures was predicted by SSRT. Nonetheless, other researchers, namely Eagle and colleagues (2008), found no effect of STN lesions on SSRT in rodent lesion models, and no relationship between STN integrity and SSRT, but STN lesions impaired the capacity of rodents to trigger stopping process, revealed by flatter inhibition functions. In contrast, grey matter lesions to rodent orbitofrontal cortex (OFC) slowed SSRT, and OFC integrity was related to SSRT, prompting Eagle to tentatively suggest that OFC in rodents may be a homologue of human IFG. This pattern of results largely corresponds to the findings of Experiment 3 in healthy participants (see Chapter 6).

What is most important to note from these experiments is that for Experiments 1 and 3, task difficulty was high for all participants, tapping stopping probability at approximately chance level, (PI = .5). This manipulation resulted in generic activation of the right IFG (pars opercularis)-STN stopping network, whereas in Experiment 2, where PI ranged from .17-.85, the stopping network was only significantly engaged by participants with lower PI (slower SSRT). In combination, these findings suggest that the right IFG (pars opercularis)-STN stopping network is only engaged when stopping is difficult, but when inhibition difficulty is primarily a function of the speed of inhibition (rather than controlled by adaptive setting of stop-signal delay (as per Aron and Poldrack, 2006, and Experiments 1 & 3), a different role of the *pars opercularis*-STN network becomes evident.

A final observation worth noting was that the BOLD activation patterns resulting from comparison of Stops > Stop Failures for both Experiment 2 and Experiment 3 in (healthy individuals) revealed enhanced activation within striatal nuclei, which corresponded to the findings of Aron and Poldrack (2006) and Vink and colleagues (2005). This was linked to slowed Go responding, as Vink et al. (2005) observed, suggesting engagement of the cortical-basal ganglia 'indirect' pathway for control of response activation (Alexander & Crutcher, 1990; Temel et al., 2005). These findings in combination with aforementioned role of right IFG-STN in stopping, suggests that the 'indirect' pathway that includes striatal nuclei (and possibly SMA: Vink et al., 2005) implement executive control in the form of a response slowing strategy (Logan, 1994) while the right IFG-STN 'hyperdirect' pathway is engaged when response inhibition is urgent, i.e., after the launch of response activation and/or execution processes. These data thereby support the notion of central and peripheral controls mechanisms, respectively, proposed by De Jong and colleagues (1990).

7.4 Electrophysiological data

In both Experiment 2 and Experiment 3, the scalp potentials elicited by stop-signals for both Stops and Stop Failures included a sequence of N1 and P3 potentials; Stop Failure ERPs on the basis of visual inspection in addition exhibited an N2 intervening N1 and P3 peak potentials. The ADJAR correction procedure (Woldorff, 1993) was used to remove overlapping activity elicited by preceding go stimuli on stop-signal trials as performed by

Bekker and colleagues (2005). Consistent with Bekker, it was found that ADJAR flattened baselines, enhanced stop-signal N1 potentials and attenuated stop-signal P3 potentials, thereby supporting the utility of these procedures in stop-signal experiments. Additionally, it was found, in healthy participants, that the amplitude of Stop-N1 was larger than for Stop Failure-N1, and also that Stop-P3 was both larger and peaked earlier than Stop Failure-P3.

Several authors have proposed that Stop-P3 is the electrophysiological substrate of the stopping process (De Jong et al., 1990; Kok et al., 2004), but this argument is based purely on the observation that the timing of Stop-P3 peak latency approximately corresponded to SSRT. No direct link between SSRT and Stop-P3 latency has previously been demonstrated. In support of this hypothesis, Experiment 2 revealed links between Stop-P3 measures and SSRT; SSRT predicted both the peak amplitude of Stop-P3 and also the latency difference between Stop-N1 and Stop-P3 peak latencies (Stop P3-N1 latency). To this end, faster SSRT was related to both larger Stop-P3 amplitudes – an inverse correlation - and a shorter Stop P3-N1 latency difference – a positive correlation. It should be noted that *larger Stop-P3 amplitudes did not indicate more difficult inhibition*. However, neither of these relationships was detected in Experiment 3 where inhibition difficulty was equivalent across participants suggesting that the relationships observed in Experiment 2 were paradigm driven. Hence Stop-P3s do not index stopping. But what process or set of processes could account for the apparent modulation of Stop-P3?

One explanation involves the *relative attentional resource allocation* afforded by the timing of the stop-signal relative to anticipated response time (GoRT). For this hypothetical account it must be understood that in Experiment 2, where SSRT was linked to Stop-P3, the time given for response inhibition was kept *absolutely equal* for each participant such that PI was primarily a function of individual SSRT. Whereas in Experiment 3 SSRT was not linked to Stop-P3, and the time given for stopping was *relatively equal* in that this time was equal to SSRT for each participant, hence PI was approximately equal, converging on .5. Assuming that when PI = .5 for each participant[48], the point in the motor hierarchy that stopping processes are effective is similarly identical, then different PIs indicate different sites of response inhibition: higher PIs (faster SSRT) indicate response inhibition at a stage of response activation that is higher in the motor

[48] This explanation assumes that motor activation processes and their timing are similar across individuals.

hierarchy (e.g., response selection/planning stage) whereas lower PI (slower SSRT) suggests that inhibition is effective at a lower stage in the motor hierarchy – closer to response execution. It follows that on an equivalent stop-signal trial (e.g., GoRT – 255 ms) the processing requirements, and hence attentional resources consumed, were less for fast SSRT participants compared to slow SSRT participants for whom response activation processes were comparatively well advanced when stopping processes were effective. Thus participants with faster SSRT had more attentional resources that could be allocated to processing the stop-signal enabling faster switching of attention to and processing of the stop-signal, thus eliciting a Stop-P3 of both larger amplitude and an earlier peak. By contrast, the attentional bias built into Experiment 2 was not present in Experiment 3 where the relative amount of attentional resources that could be allocated for processing of the stop-signal by each participant was equal, thus yielding no relationships between Stop-P3 amplitude and SSRT.

7.5 Stopping in patients with schizophrenia

Experiment 3 compared stop-signal inhibition performance of schizophrenia patients to a matched control group on behavioural, fMRI and ERP indices. The main behavioural finding was that SSRT was slower in patients compared to controls, which is consistent with previous behavioural reports (Bellgrove et al., 2006; Enticott et al., 2008). Most interesting however, was that the right IFG (*pars opercularis*)-STN network that is thought to underpin stopping was uniquely underactivated in the patient group compared to controls. Moreover, patients revealed very little BOLD activation in the Stops > Go contrast, whereas Stop Failures > Go and Go > Baseline activation for this group was substantial. Particularly noteworthy was the between-group comparison of Go > Baseline which revealed significantly greater activation in a right lateral MFG and cerebellar network in patients compared to controls, which was interpreted as indicating enhanced response selection and attentional processing in patients during Go trials. Ford and colleagues (2004) have suggested that enhanced Go related activation in patients with schizophrenia indicates that these individuals make a deliberate choice to respond or not on each Go trial that is concomitant with a reduced tendency to build up a prepotent response style.

Analyses of ERP data revealed stop-signal N1 and P3 related processing impairments in patients with schizophrenia. Overall the amplitude of auditory evoked stop-signal N1 was significantly reduced in patients compared to controls, and no modulation of stop-signal N1 during Stops compared to Stop Failures was observed in patients whereas this effect was strong in controls, suggesting an impaired capacity for stimulus selection in patients. Additionally, the peak latency of stop-signal N1 occurred (non-significantly) later in patients compared to controls, indicating impaired speed of sensory registration of the stop-signal in patients. This marginal effect was in part explained by negative symptoms in patients, whereby the number of negative symptoms (measured by SANS) was correlated with Stop-N1 at fronto-central electrodes, especially for (non-dominant) left hand Stops at Fz indicated slowed auditory processing.

Stop-signal P3s in the patient group had both smaller amplitudes and peaked at longer latencies than for controls. Most interestingly, no latency difference was observed between Stop-P3 and Stop Failure-P3 at Fz in patients whereas a large difference was observed for controls, indicating that the timing of the stop-signal did not affect the outcome of the race between stop-signal and go processes in patients.

In combination, these findings were interpreted as indicating a processing bottleneck that manifests quite early during stop-signal trials in patients that is not present in controls. This impairment begins with an impaired ability to selectively attend to the stop-signal (combined with perhaps delayed registration of the auditory stop signal) implying that patients with schizophrenia have to detect the stop-signal prior to the launch of go response activation processes in order to stop; if go response activation processes are launched they cannot be stopped and go on to completion. Hence stopping in patients involves simply not engaging response activation processes whereas healthy individuals can simultaneously activate both response activation (go) processes and response inhibition (stop) processes with the utility of a fast response inhibition mechanism, namely the right IFG-STN network which can inhibit on-going response at any stage of response execution (De Jong et al., 1990).

These findings affirm the evolving thesis that impaired neuropsychological functioning is an essential feature of schizophrenia (Elvevag & Goldberg, 2000; Goldman-Rakic, 1994; Heinrichs & Zachzanis, 1998; Mitchell, Elliot & Woodruff, 2001; Rund,

1998), and moreover that dysfunction within the executive system may be a key facet of this impairment (Chen et al., 2003; Hutton et al., 1998; Joyce et al., 2002; Pantelis et al., 1999; Riley et al., 2000). In particular the data reported suggest widespread impairments of inhibitory control functions in patients with schizophrenia, extending to an impaired capacity to selectively attend to relevant, salient environmental stimuli, in addition to an impaired capacity to stop behavioural activation after it has begun. These impairments could impact heavily on the capacity of patients to control attention and behaviour on a moment-by-moment basis and thus impair their ability to operate effectively in changing environments.

The cognitive impairments in patients with schizophrenia detailed in this thesis are linked to dysfunction within fronto-basal ganglia pathways, mapping onto the mesocortical system that is known to be dysfunctional in schizophrenia. At the cellular level, impaired frontal cognitive function is thought to arise from reduced NMDA receptor activity on GABAergic interneurons within frontal and basal ganglia (especially thalamic) structures (Olney & Faber, 1995; Stone et al., 2007). The cognitive impairments and psychiatric symptoms observed in schizophrenia patients are reliably observed in otherwise healthy individuals after administration of NMDA antagonists such as phencyclidine and ketamine (Stone et al., 2007). Hence the stop-signal paradigm may be a crucial tool for studying fronto-basal ganglia functioning in schizophrenia patients and in healthy individuals under pharmacological challenge.

7.6 How this thesis has added to the literature

The experiments conducted for this thesis have confirmed the findings from previous stop-signal inhibition experiments, but more importantly, have added significantly to the general and clinical literatures on stopping. Indeed, the findings detailed herein are the first to investigate stopping via a combination of behavioural, fMRI and ERP methods, and the first to report neurophysiological stop-signal data in patients with schizophrenia.

The findings strongly support the model of a right lateral IFG and STN network proposed to underpin stopping (Aron & Poldrack, 2006), and confirmed the usefulness of ADJAR methods for revealing the link between stopping and stop-signal N1 and P3 ERP modulation. The findings have furthered the general understanding of stop-signal inhibition

by introducing a model of stopping difficulty and demonstrated the impact of stopping difficulty operationalised in paradigm variants can potential have on brain activation patterns reported in neuroimaging studies in addition to differential modulation of brain potentials elicited in auditory evoked stop-signal ERP studies. Finally, this work has indicated that the neural basis of stopping impairments in patients with schizophrenia lies in their inability to recruit the putative right IFG-STN stopping mechanism.

The major contribution to the general stop-signal literature is the model of inhibition difficulty described in Chapter 4 (inhibition difficulty = SSRT/(GoRT – SSD)), which offers a standardized measure for assessing stop-signal task difficulty; this work has several important implications. At the most basic level, the model imparts an *a priori* method of estimating the relative difficulty of response inhibition in a given situation (trial), given SSRT and GoRT, whereas previously greater inhibition difficulty has only been realised *a posteriori* by the observation that PI is reduced as stop-signal delay increases (Logan, 1994). The facility of inhibition difficulty estimation also enables a comparison of the relative task difficulty between individuals, and perhaps more importantly, between groups. In Chapter 6, the critical importance of matching groups on inhibition difficulty was articulated; briefly, it was described how the outcome of group SSRT comparisons may be spurious when the groups experience a difference in inhibition difficulty, stemming from the commonly observed phenomena that, within an individual, SSRT is faster when inhibition difficulty is greater, i.e., SSRT is faster at longer stop-signal delays (Logan, 1994). It follows that a group experiencing greater overall inhibition difficulty may have a relatively low (fast) estimation of SSRT compared to a group experiencing relatively easy inhibition difficulty yielding a high (slow) estimation of SSRT. Hence, the difference in inhibition difficulty should be controlled for either by matching groups on inhibition difficulty, or by controlling for group differences in inhibition difficulty. This is most problematic for SSRT estimation in experiments employing either fixed delays due to the inherent differences in inhibition difficulty between individuals and hence groups in such designs.

A comparison of the results of Experiment 2 and Experiment 3 highlight the impact of inhibition difficulty operationalised in neurophysiological experiments. In Experiment 2 it was shown that greater inhibition difficulty affected the network activated for stopping:

stopping generically required activation of a right DLPFC dominated network irrespective of task difficulty, whereas more difficult stopping was linked to increasing BOLD signal intensity within right IFG (*pars opercularis*)-STN. By comparison, in the control group data for Experiment 3, participants were matched for inhibition difficulty and right IFG (*pars opercularis*)-STN activation was generically observed. Additionally, it was found that the stop-signal task difficulty manipulation affected the amplitude and latency of auditory evoked stop-signal potentials, whereas in Experiment 3, participants were matched for inhibition difficulty, and no relationships were observed between stop-signal potentials and SSRT. While each of these findings needs replication, they suggest that inhibition difficulty impacts markedly upon neuronal activation between subjects and offers some explanation as to why different response inhibition activation maps are reported when different paradigms and paradigm variants are used for studying response inhibition.

Additionally, these findings provide strong support for the notion of a fractionated executive vis-à-vis PFC, whereby fractionated executive processes (Miyake et al., 2000; Stuss, 2006) are thought to map onto discrete areas of PFC (Miyake et al., 2000; Shallice, 2002; Stuss, 2006; Stuss, Shallice, Alexander & Picton, 1995),and correspond directly to the assertion of Stuss (2006), who proposed that increasing task difficulty requires recruitment of additional processes and hence brain areas for correct performance on the same cognitive task. Of particular significance are the results of Experiment 2 where stopping difficulty affected frontal and basal ganglia activation.

Finally, the model of inhibition difficulty suggests a method of mapping the point in the cycle of response activation process that response inhibition is effected for different stop-signal delays for an individual. The variation in inhibition difficulty that is predictable by this model corresponds to inhibiting responses before they are launched (when SSD = 0) until after they are launched (SSD = GoRT) and the data suggest that different networks are engaged depending upon the difficulty of inhibition. This suggests a method of mapping the point in the response activation cycle that response inhibition is effective.

7.7 Limitations of studies

Despite the consistency of the findings of the experiments overall, the rather low number of participants in each study clearly warrants some caution in drawing firm

conclusions. Additionally, all experiments involved the use of auditory stop-signals, which may hinder the generality of the findings, hence comparable investigations using visual stop-signals must be employed; this is a problem with most other stopping investigations (e.g., Aron & Poldrack, 2006), with the exception of Rubia et al. (2003) who used visual stimuli for both go and stop-signal stimuli. This may have particular relevance for Experiment 3 as the auditory system in patients with schizophrenia is known to be dysfunctional (Duncan, 1988; Michie, 2001, Umbricht & Krjles, 2005; Näätänen & Kahkönen, 2009).

A major drawback of Experiment 1 is that the design was epoch based with which it is impossible to assess phasic (trial-by-trial) neural responses which are necessary for the purposes of directly assessing stopping activity. Additionally, the epoch-based analysis necessarily included Stop Failures during Stop blocks, contaminating these blocks with error related activity, however, this was somewhat circumvented by the increased go trial error rate for Go blocks compared to Stop blocks.

The second experiment was limited in some respects by not modeling Go trials. This approach was taken in order to negate problems in modeling trial by trial SSD differences involved in the SSD setting protocol used in that study. It is well known that BOLD responses summate linearly until a point of saturation hence the average of this remained very high due to the small interstimulus interval (mean = 1.5s) and the high frequency of responding which occurred on almost all go trials and also for Stop Failures. Another factor limiting the conclusions of this study was that more difficult stopping was not assessed within-subjects. This was not performed largely because many subjects inhibited with low probability across all SSDs, making such an analysis impossible for these participants.

The third experiment was limited principally by a programming error that resulted in more right handed go trials than left hand go trials, however this error did not differ between groups leaving the main findings intact. Additionally, this design was not optimized for detecting BOLD responses between stop-signal trials and go trials, i.e., by using a variable intertrial interval. This manipulation was not included because it was considered that such a design may make the task more difficult for the patient group, hence a predictable sequence of intertrial intervals (all 2 seconds) was used. These trials were

modeled separately for left and right hands to introduce a source of jitter to aid detection of unique BOLD responses for each trial type.

7.8 Future directions

The outcomes from the studies conducted for this thesis have prompted several future experiments. Obviously, the outcomes from Experiment 2 where a model of stopping difficulty was proposed, and evidence linking more difficult inhibition to enhanced activity within the putative 'hyperdirect' right IFG (pars opercularis) – STN stopping network was detailed, needs further investigation. This is particularly important given the results of Aron and Poldrack (2006) who linked faster SSRT to activation in this same network, whereas in Experiment 2, the difficulty manipulation meant that slower SSRT predicted enhanced activation in the network. Ethical clearance has been granted for a high field fMRI study with twenty participants comparing brain activation across participants performing two stop-signal paradigm variants: one using an adaptive stop-signal delay as per Experiment 3 where inhibition difficulty will be equated across participants and another using fixed stop-signal delays as per Experiment 2 where inhibition difficulty will be contingent upon individual SSRT. A further aspect of these studies will be a go trial manipulation aimed at investigating the role of STN in response selection, as indicated by studies with rodent lesion models (Baunez et al., 2001; Tan et al., 2006). If this manipulation successfully activates STN in healthy participants, the paradigm will be applied to patients with schizophrenia to investigate the generality of STN dysfunction in patients.

Another study planned (ethical permission application submitted) will focus on the role of different PFC areas in the elicitation of stop-signal ERPs. This will be assessed by recording ERPs during performance of a stop-signal paradigm after application of repetitive TMS (rTMS) to specific brain areas in healthy participants. Comparable investigations have previously been conducted by Chambers and colleagues (2006/2007), but scalp ERPs and the electromyogram (EMG) from response finger muscles will be simultaneously recorded enabling a thorough study of brain-behaviour relationships in stopping. A corresponding study is proposed in patients with schizophrenia, only without rTMS application; stopping will be assessed while recording ERP and EMG activity to investigate whether patients

with schizophrenia can stop go responses even as response finger muscles are active as observed by De Jong and colleagues (1990/1995) and van Boxtel and colleagues (2001).

A further TMS study planned involves the use of single pulse TMS (spTMS) where the timing of stimulation will be varied about the onset of stop-signals to identify the temporal dynamics of right IFG during stopping.

Use of the stop-signal paradigm for investigating executive control in schizophrenia has recently been advocated by the CNTRICS breakout group (Barch et al., 2009). To this end, the studies outlined above are aimed at furthering the understanding of the neural networks responsible for executive control in healthy participants and also for impaired processing in schizophrenia. In particular, studies using healthy participants under pharmacological challenge with NMDA antagonists as a model for schizophrenia using behavioural, ERP, MRI and EMG indices of stopping could prove invaluable in furthering the understanding of the schizophrenic brain, as suggested by Javitt (2009). This stop-signal paradigm may be of particular utility for such investigation given the consistency of impairments observed in schizophrenia. Magnetic resonance spectroscopy (MRS) could also be an invaluable tool for assessing PFC function during stop-signal task performance.

References

Abi-Dargham, A., Gil, R., Krystal, J., Baldwin, R. M., Seibyl, J. P., Bowers, M., et al. (1998). Increased striatal dopamine transmission in schizophrenia: confirmation in a second cohort. *American Journal of Psychiatry, 155*(6), pp 761-767.

Abi-dargham, A., & Moore, H. (2003). Prefrontal DA transmission at D1 receptors and the pathology of schizophrenia. *Neuroscientist, 9*(5), pp 404-416.

Abi-Dargham, A., Rodenhiser, J., Printz, D., Zea-Ponce, Y., Gil, R., Kegeles, L. S., et al. (2000). Increased baseline occupancy of D2 receptors by dopamine in schizophrenia. *Proceedings of the National Academy of Sciences of the United States of America, 97*(14), pp 8104-8109.

Ahveninen, J., Jääskeläinen, I. P., Osipova, D., Huttunen, M. O., Ilmoniemi, R. J., Kaprio, J., et al. (2006). Inherited auditory-cortical dysfunction in twin pairs discordant for schizophrenia. *Biological Psychiatry, 60*(6), pp 612-620.

Alexander, G. E., & Crutcher, M. D. (1990). Functional architecture of basal ganglia circuits: Neural substrates of parallel processing. *Trends in Neurosciences, 13*(7), pp 266-271.

Alexander, G. E., DeLong, M. R., & Strick, P. L. (1986). Parallel organization of functionally segregated circuits linking basal ganglia and cortex. *Annual Review of Neuroscience, 9*(1), pp 357-381.

American Psychiatric Association. (1994). *Diagnostic and Statistical Manual of Mental Disorders, Fourth Edition*. Washington, DC: American Psychiatric Association.

Andlin-Sobocki, P., & Rössler, W. (2005). Cost of psychotic disorders in Europe. *European Journal of Neurology, 12*(SUPPL. 1), pp 74-77.

Andreasen, N., Arndt, S., Swayze, V., 2nd, Cizadlo, T., Flaum, M., O'Leary, D., et al. (1994). Thalamic abnormalities in schizophrenia visualized through magnetic resonance image averaging. *Science, 266*(5183), pp 294-298.

Andreasen, N. C. (1982). Negative symptoms in schizophrenia. Definition and reliability. *Archives of General Psychiatry, 39*(7), pp 784-788.

Andreasen, N. C. (1997). The evolving concept of schizophrenia: From Kraepelin to the present and future. *Schizophrenia Research, 28*(2-3), pp 105-109.

Andreasen, N. C. (1999). Understanding the causes of schizophrenia. *New England Journal of Medicine, 340*(8), pp 645-647.

Andreasen, N. C. (1999). A unitary model of schizophrenia. Bleuler's 'fragmented phrene' as schizencephaly. *Archives of General Psychiatry, 56*(9), pp 781-787.

Andreasen, N. C., Arndt, S., Alliger, R., Miller, D., & Flaum, M. (1995). Symptoms of schizophrenia: methods, meanings, and mechanisms. *Archives of General Psychiatry, 52*(5), pp 341-351.

Andreasen, N. C., & Olsen, S. (1982). Negative v positive schizophrenia: Definition and validation. *Archives of General Psychiatry, 39*(7), pp 789-794.

Angrist, B. M., & Gershon, S. (1970). The phenomenology of experimentally induced amphetamine psychosis - preliminary observations. *Biological Psychiatry, 2*(2), pp 95-107.

Arce, E., Leland, D. S., Miller, D. A., Simmons, A. N., Winternheimer, K. C., & Paulus, M. P. (2006). Individuals with schizophrenia present hypo- and hyperactivation during implicit cueing in an inhibitory task. *NeuroImage, 32*(2), pp 704-713.

Arndt, S., Alliger, R., & Andreasen, N. (1991). The distinction of positive and negative symptoms. The failure of a two- dimensional model. *The British Journal of Psychiatry, 158*(3), pp 317-322.

Aron, A. R. (2007). The neural basis of inhibition in cognitive control. *Neuroscientist, 13*(3), pp 214-228.

Aron, A. R., Behrens, T. E., Smith, S., Frank, M. J., & Poldrack, R. A. (2007a). Triangulating a cognitive control network using diffusion-weighted magnetic resonance imaging (MRI) and functional MRI. *Journal of Neuroscience, 27*(14), pp 3743-3752.

Aron, A. R., Dowson, J. H., Sahakian, B. J., & Robbins, T. W. (2003b). Methylphenidate improves response inhibition in adults with attention-deficit/hyperactivity disorder. *Biological Psychiatry, 54*(12), pp 1465-1468.

Aron, A. R., Durston, S., Eagle, D. M., Logan, G. D., Stinear, C. M., & Stuphorn, V. (2007b). Converging evidence for a fronto-basal-ganglia network for inhibitory control of action and cognition. *Journal of Neuroscience, 27*(44), pp 11860-11864.

Aron, A. R., Fletcher, P. C., Bullmore, E. T., Sahakian, B. J., & Robbins, T. W. (2003a). Stop-signal inhibition disrupted by damage to right inferior frontal gyrus in humans. *Nature Neuroscience, 6*(2), pp 115-116.

Aron, A. R., Fletcher, P. C., Bullmore, E. T., Sahakian, B. J., & Robbins, T. W. (2003c). Stop-signal inhibition disrupted by damage to right inferior frontal gyrus in humans. *Nature Neuroscience, 6*(12), pp 1329-1329.

Aron, A. R., Monsell, S., Sahakian, B. J., & Robbins, T. W. (2004a). A componential

analysis of task-switching deficits associated with lesions of left and right frontal cortex. *Brain, 127*(7), pp 1561-1573.

Aron, A. R., & Poldrack, R. A. (2006). Cortical and subcortical contributions to stop signal response inhibition: Role of the subthalamic nucleus. *Journal of Neuroscience, 26*(9), pp 2424-2433.

Aron, A. R., Robbins, T. W., & Poldrack, R. A. (2004b). Inhibition and the right inferior frontal cortex. *Trends in Cognitive Sciences, 8*(4), pp 170-177.

Badcock, J. C., Michie, P. T., Johnson, L., & Combrinck, J. (2002). Acts of control in schizophrenia: dissociating the components of inhibition. *Psychological Medicine, 32*(02), pp 287-297.

Badcock, J. C., Waters, F. A. V., Maybery, M. T., & Michie, P. T. (2005). Auditory hallucinations: Failure to inhibit irrelevant memories. *Cognitive Neuropsychiatry, 10*(2), pp 125-136.

Baddeley, A. (1996). Exploring the central executive. *The Quarterly Journal of Experimental Psychology A, 49*, pp 5-28.

Baddeley, A. (2003). Working memory: looking back and looking forward. *Nature Reviews Neuroscience, 4*(10), pp 829-839.

Baddeley, A. D. (1986). *Working memory*. London: Oxford University Press.

Ball, T., Schreiber, A., Feige, B., Wagner, M., Lucking, C. H., & Kristeva-Feige, R. (1999). The role of higher-order motor areas in voluntary movement as revealed by high-resolution EEG and fMRI. *NeuroImage, 10*(6), pp 682-694.

Band, G. P. H., & van Boxtel, G. J. M. (1999). Inhibitory motor control in stop paradigms: review and reinterpretation of neural mechanisms. *Acta Psychologica, 101*(2-3), pp 179-211.

Band, G. P. H., van der Molen, M. W., & Logan, G. D. (2003). Horse-race model simulations of the stop-signal procedure. *Acta Psychologica, 112*(2), pp 105-142.

Barbato, A. (1998). *Nations for mental health: Schizophrenia and public health*. Geneva: World Health Organisation Division of Mental Health and Prevention of Substance Abuse (MSA).

Barch, D. M., Braver, T. S., Carter, C. S., Poldrack, R. A., & Robbins, T. W. (2009). CNTRICS final task selection: Executive control. *Schizophrenia Bulletin, 35*(1), pp 115-135.

Barch, D. M., Carter, C. S., Braver, T. S., Sabb, F. W., MacDonald III, A., Noll, D. C., et al. (2001). Selective deficits in prefrontal cortex function in medication-naive

patients with schizophrenia. *Archives of General Psychiatry, 58*(3), pp 280-288.

Baunez, C., Humby, T., Eagle, D. M., Ryan, L. J., Dunnett, S. B., & Robbins, T. W. (2001). Effects of STN lesions on simple vs choice reaction time tasks in the rat: preserved motor readiness, but impaired response selection. *European Journal of Neuroscience, 13*(8), pp 1609-1616.

Bekker, E. M., Kenemans, J. L., Hoeksma, M. R., Talsma, D., & Verbaten, M. N. (2005a). The pure electrophysiology of stopping. *International Journal of Psychophysiology, 55*(2), pp 191-198.

Bekker, E. M., Kenemans, J. L., & Verbaten, M. N. (2004). Electrophysiological correlates of attention, inhibition, sensitivity and bias in a continuous performance task. *Clinical Neurophysiology, 115*(9), pp 2001-2013.

Bekker, E. M., Overtoom, C. C., Kenemans, J. L., Kooij, J. J., De Noord, I., Buitelaar, J. K., et al. (2005b). Stopping and changing in adults with ADHD. *Psychological Medicine, 35*(06), pp 807-816.

Bellgrove, M. A., Chambers, C. D., Vance, A., Hall, N., Karamitsios, M., & Bradshaw, J. L. (2006). Lateralized deficit of response inhibition in early-onset schizophrenia. *Psychological Medicine, 36*(4), pp 495-505.

Benazzouz, A., Gross, C., Féger, J., Boraud, T., & Bioulac, B. (1993). Reversal of rigidity and improvement in motor performance by subthalamic high-frequency stimulation in MPTP-treated monkeys. *European Journal of Neuroscience, 5*(4), pp 382-389.

Bjorklund, D. F., & Harnishfeger, K. K. (1990). The resources construct in cognitive development: Diverse sources of evidence and a theory of inefficient inhibition. *Developmental Review, 1*, pp 48-71.

Blackwood, N., Ffytche, D., Simmons, A., Bentall, R., Murray, R., & Howard, R. (2004). The cerebellum and decision making under uncertainty. *Cognitive Brain Research, 20*(1), pp 46-53.

Blakemore, S. J., Frith, C. D., & Wolpert, D. M. (2001). The cerebellum is involved in predicting the sensory consequences of action. *NeuroReport, 12*(9), 1879-1884.

Blanchard, J., & Neale, J. (1994). The neuropsychological signature of schizophrenia: generalized or differential deficit? *American Journal of Psychiatry, 151*(1), pp 40-48.

Blennow, K., Bogdanovic, N., Heilig, M., Grenfeldt, B., Karlsson, I., & Davidsson, P. (2000). Reduction of the synaptic protein rab3a in the thalamus and connecting brain regions in post-mortem schizophrenic brains. *Journal of Neural Transmission, 107*(8-9), pp 1085-1097.

Boehler, C. N., Münte, T. F., Krebs, R. M., Heinze, H. J., Schoenfeld, M. A., & Hopf, J. M. (2009). Sensory MEG responses predict successful and failed inhibition in a stop-signal task. *Cerebral Cortex, 19*(1), pp 134-145.

Booth, J. R., Burman, D. D., Meyer, J. R., Lei, Z., Trommer, B. L., Davenport, N. D., et al. (2005). Larger deficits in brain networks for response inhibition than for visual selective attention in attention deficit hyperactivity disorder (ADHD). *Journal of Child Psychology and Psychiatry, 46*(1), pp 94-111.

Botvinick, M. M., Cohen, J. D., & Carter, C. S. (2004). Conflict monitoring and anterior cingulate cortex: an update. *Trends in Cognitive Sciences, 8*(12), pp 539-546.

Boucher, L., Palmeri, T. J., Logan, G. D., & Schall, J. D. (2007). Inhibitory control in mind and brain: An interactive race model of countermanding saccades. *Psychological Review, 114*(2), pp 376-397.

Bougerol, T., Benraiss, A., & Scotto, J. C. (1997). Correlations between standard auditory evoked potentials and symptomatology in a group of 50 schizophrenic patients. *European Psychiatry, 12*(8), pp 387-394.

Brett, M, Anton, J-L, Valabregue, R, Poline, J-B (2002a): Region of interest analysis using an SPM toolbox [abstract]. Presented at the 8th International Conference on Functional Mapping of the Human Brain, June 2-6, 2002, Sendai, Japan. Available on CD-ROM in NeuroImage 16, No 2, abstract 497.

Brett M, Johnsrude IS, Owen AM (2002b): The problem of functional localization in the human brain. *Nature Reviews Neuroscience,* 3(3): pp 243-249.

Brown, A. S., Begg, M. D., Gravenstein, S., Schaefer, C. A., Wyatt, R. J., Bresnahan, M., et al. (2004). Serologic evidence of prenatal influenza in the etiology of schizophrenia. *Archives of General Psychiatry, 61*(8), pp 774-780.

Brown, V. J., & Robbins, T. W. (1991). Simple and choice reaction time performance following unilateral striatal dopamine depletion in the rat. Impaired motor readiness but preserved response preparation. *Brain, 114*(1 B), pp 513-525.

Brownstein, J., Krastoshevsky, O., McCollum, C., Kundamal, S., Matthysse, S., Holzman, P. S., et al. (2003). Antisaccade performance is abnormal in schizophrenia patients but not in their biological relatives. *Schizophrenia Research, 63*(1-2), pp 13-25.

Buchanan, A. (1992). A two-year prospective study of treatment compliance in patients with schizophrenia. *Psychological Medicine, 22*(3), pp 787-797.

Bunge, S. A., Hazeltine, E., Scanlon, M. D., Rosen, A. C., & Gabrieli, J. D. E. (2002). Dissociable contributions of prefrontal and parietal cortices to response selection. *NeuroImage, 17*(3), pp 1562-1571.

Bunge, S. A., & Wright, S. B. (2007). Neurodevelopmental changes in working memory and cognitive control. *Current Opinion in Neurobiology, 17*(2), pp 243-250.

Burle, B., Vidal, F., Tandonnet, C., & Hasbroucq, T. (2004). Physiological evidence for response inhibition in choice reaction time tasks. *Brain and Cognition, 56*(2), pp 153-164.

Carlsson, A., & Lindqvist, M. (1963). Effect of chlorpromazine or haloperidol on formation of 3-methoxytyramine and normetanephrine in mouse brain. *Acta Pharmacologica Et Toxicologica, 20*(2), pp 140-144.

Carter, C. (2000). Images in neuroscience. Cognition: executive function. *American Journal of Psychiatry, 157*(1), pp 3.

Carter, C. S., Braver, T. S., Barch, D. M., Botvinick, M. M., Noll, D., & Cohen, J. D. (1998). Anterior cingulate cortex, error detection, and the online monitoring of performance. *Science, 280*(5364), pp 747.

Carter, C. S., Macdonald, A. M., Botvinick, M., Ross, L. L., Stenger, V. A., Noll, D., et al. (2000). Parsing executive processes: Strategic vs. evaluative functions of the anterior cingulate cortex. *Proceedings of the National Academy of Sciences of the United States of America, 97*(4), pp 1944-1948.

Casey, B. J., Durston, S., & Fossella, J. A. (2001). Evidence for a mechanistic model of cognitive control. *Clinical Neuroscience Research, 1*(4), pp 267-282.

Casey, B. J., Epstein, J. N., Buhle, J., Liston, C., Davidson, M. C., Tonev, S. T., et al. (2007). Frontostriatal connectivity and iIts role in cognitive control in parent-child dyads with ADHD. *American Journal of Psychiatry, 164*(11), pp 1729-1736.

Casey, B. J., Tottenham, N., Liston, C., & Durston, S. (2005). Imaging the developing brain: what have we learned about cognitive development? *Trends in Cognitive Sciences, 9*(3), pp 104-110.

Castle, D. J., Jablensky, A., McGrath, J. J., Carr, V., Morgan, V., Waterreus, A., et al. (2006). The diagnostic interview for psychoses (DIP): Development, reliability and applications. *Psychological Medicine, 36*(1), pp 69-80.

Chakos, M., Lieberman, J., Hoffman, E., Bradford, D., & Sheitman, B. (2001). Effectiveness of second-generation antipsychotics in patients with treatment-resistant schizophrenia: A review and meta-analysis of randomized trials. *American Journal of Psychiatry, 158*(4), pp 518-526.

Chamberlain, S. R., Fineberg, N. A., Menzies, L. A., Blackwell, A. D., Bullmore, E. T., Robbins, T. W., et al. (2007). Impaired cognitive flexibility and motor inhibition in unaffected first-degree relatives of patients with obsessive-compulsive disorder. *American Journal of Psychiatry, 164*(2), pp 335-338.

Chambers, C. D., Bellgrove, M. A., Gould, I. C., English, T., Garavan, H., McNaught, E., et al. (2007). Dissociable mechanisms of cognitive control in prefrontal and premotor cortex. *Journal of Neurophysiology, 98*(6), pp 3638-3647.

Chambers, C. D., Bellgrove, M. A., Stokes, M. G., Henderson, T. R., Garavan, H., Robertson, I. H., et al. (2006). Executive "brake failure" following deactivation of human frontal lobe. *Journal of Cognitive Neuroscience, 18*(3), pp 444-455.

Chan, R. C. K., Chen, E. Y. H., Cheung, E. F. C., Chen, R. Y. L., & Cheung, H. K. (2006). The components of executive functioning in a cohort of patients with chronic schizophrenia: A multiple single-case study design. *Schizophrenia Research, 81*(2-3), pp 173-189.

Chan, R. C. K., Chen, E. Y. H., Cheung, E. F. C., & Cheung, H. K. (2004). Executive dysfunctions in schizophrenia. *European Archives of Psychiatry and Clinical Neuroscience, 254*(4), pp 256-262.

Chen, Q., Andersen, A. H., Zhang, Z., Ovadia, A., Cass, W. A., Gash, D. M., et al. (1999). Functional MRI of Basal Ganglia Responsiveness to Levodopa in Parkinsonian Rhesus Monkeys. *Experimental Neurology, 158*(1), pp 63-75.

Chen, W. J., & Faraone, S. V. (2000). Sustained attention deficits as markers of genetic susceptibility to schizophrenia. *American Journal of Medical Genetics - Seminars in Medical Genetics, 97*(1), pp 52-57.

Chikazoe, J., Jimura, K., Asari, T., Yamashita, K.-i., Morimoto, H., Hirose, S., et al. (2009). Functional dissociation in right inferior frontal cortex during performance of Go/No-Go task. *Cerebral Cortex, 19*(1), pp 146-152.

Chikazoe, J., Konishi, S., Asari, T., Jimura, K., & Miyashita, Y. (2007). Activation of right inferior frontal gyrus during response inhibition across response modalities. *Journal of Cognitive Neuroscience, 19*(1), pp 69-80.

Cho, R. Y., Konecky, R. O., & Carter, C. S. (2006). Impairments in frontal cortical δ synchrony and cognitive control in schizophrenia. *Proceedings of the National Academy of Sciences, 103*(52), pp 19878-19883.

Cirillo, M. A., & Seidman, L. J. (2003). Verbal declarative memory dysfunction in schizophrenia: From clinical assessment to genetics and brain mechanisms. *Neuropsychology Review, 13*(2), pp 43-77.

Colonius, H. (1990). A note on the stop-signal paradigm, or how to observe the unobservable. *Psychological Review, 97*(2), pp 309-312.

Comerchero, M. D., & Polich, J. (1999). P3a and P3b from typical auditory and visual stimuli. *Clinical Neurophysiology, 110*(1), pp 24-30.

Cooper, J. A., Sagar, H. J., Tidswell, P., & Jordan, N. (1994). Slowed central processing in simple and go/no-go reaction time tasks in Parkinson's disease. *Brain, 117*(3), pp 517-529.

Coull, J. T. (2004). fMRI studies of temporal attention: Allocating attention within, or towards, time. *Cognitive Brain Research, 21*(2), pp 216-226.

Coyle, J. (2006). Glutamate and schizophrenia: Beyond the dopamine hypothesis. *Cellular and Molecular Neurobiology, 26*(4), pp 363-382.

Creese, I., Burt, D. R., & Snyder, S. H. (1976). Dopamine receptor binding predicts clinical and pharmacological potencies of antischizophrenic drugs. *Science, 192*(4238), pp 481-483.

Csernansky, J. G., Schindler, M. K., Splinter, N. R., Wang, L., Gado, M., Selemon, L. D., et al. (2004). Abnormalities of thalamic volume and shape in schizophrenia. *American Journal of Psychiatry, 161*(5), pp 896-902.

Davalos, D. B., Compagnon, N., Heinlein, S., & Ross, R. G. (2004). Neuropsychological deficits in children associated with increased familial risk for schizophrenia. *Schizophrenia Research, 67*(2-3), pp 123-130.

De Jong, R., Coles, M. G., Logan, G. D., & Gratton, G. (1990). In search of the point of no return: The control of response processes. *Journal of Experimental Psychology: Human Perception and Performance, 16*(1), pp 164-182.

De Jong, R., Coles, M. G. H., & Logan, G. D. (1995). Strategies and mechanisms in nonselective and selective inhibitory motor control. *Journal of Experimental Psychology: Human Perception and Performance, 21*(3), pp 498-511.

De Zubicaray, G. I., Andrew, C., Zelaya, F. O., Williams, S. C. R., & Dumanoir, C. (2000). Motor response suppression and the prepotent tendency to respond: A parametric fMRI study. *Neuropsychologia, 38*(9), pp 1280-1291.

Deiber, M. P., Ibanez, V., Sadato, N., & Hallett, M. (1996). Cerebral structures participating in motor preparation in humans: A positron emission tomography study. *Journal of Neurophysiology, 75*(1), pp 233-247.

Deiber, M. P., Passingham, R. E., Colebatch, J. G., Friston, K. J., Nixon, P. D., & Frackowiak, R. S. J. (1991). Cortical areas and the selection of movement: A study with positron emission tomography. *Experimental Brain Research, 84*(2), pp 393-402.

Dien, J., Spencer, K. M., & Donchin, E. (2003). Localization of the event-related potential novelty response as defined by principal components analysis. *Cognitive Brain Research, 17*(3), pp 637-650.

Dillon, D. G., & Pizzagalli, D. A. (2007). Inhibition of action, thought, and emotion: A selective neurobiological review. *Applied and Preventive Psychology, 12*(3), pp 99-114.

Dimitrov, M., Nakic, M., Elpern-Waxman, J., Granetz, J., O'Grady, J., Phipps, M., et al. (2003). Inhibitory attentional control in patients with frontal lobe damage. *Brain and Cognition, 52*(2), pp 258-270.

Dimoska, A., & Johnstone, S. J. (2008). Effects of varying stop-signal probability on ERPs in the stop-signal task: Do they reflect variations in inhibitory processing or simply novelty effects? *Biological Psychology, 77*(3), pp 324-336.

Dimoska, A., Johnstone, S. J., & Barry, R. J. (2006). The auditory-evoked N2 and P3 components in the stop-signal task: Indices of inhibition, response-conflict or error-detection? *Brain and Cognition, 62*(2), pp 98-112.

Dimoska, A., Johnstone, S. J., Barry, R. J., & Clarke, A. R. (2003). Inhibitory motor control in children with attention-deficit/hyperactivity disorder: event-related potentials in the stop-signal paradigm. *Biological Psychiatry, 54*(12), pp 1345-1354.

Donchin, E., & Coles, M. G. H. (1998). Context updating and the P300. *Behavioral and Brain Sciences, 21*(01), pp 152-154.

Donders, F. C. (1969). Over de snelheid van psychische processen [On the speed of mental processes]. (W. G. Koster, Trans.). In W. G. Koster (Ed.), *Attention and performance II* (pp. 412-431). Amsterdam: North Holland.

Donkers, F. C. L., & van Boxtel, G. J. M. (2004). The N2 in go/no-go tasks reflects conflict monitoring not response inhibition. *Brain and Cognition, 56*(2), pp 165-176.

Donnell, B. F. O., Shenton, M. E., McCarley, R. W., Faux, S. F., Smith, R. S., Salisbury, D. F., et al. (1993). The auditory N2 component in schizophrenia: Relationship to MRI temporal lobe gray matter and to other ERP abnormalities. *Biological Psychiatry, 34*(1), pp 26-40.

Donohoe, G., Reilly, R., Clarke, S., Meredith, S., Green, B., Morris, D., et al. (2006). Do antisaccade deficits in schizophrenia provide evidence of a specific inhibitory function? *Journal of the International Neuropsychological Society, 12*(06), pp 901-906.

Duncan, C. C. (1988). Event-related brain potentials: A window on information processing in schizophrenia. *Schizophrenia Bulletin, 14*(2), pp 199-203.

Duncan, J., Emslie, H., Williams, P., Johnson, R., & Freer, C. (1996). Intelligence and the frontal lobe: The organization of goal-directed behavior. *Cognitive Psychology, 30*(3), pp 257-303.

Duncan, J., & Miller, E. K. (2002). Cognitive focus through adaptive neural encoding in the primate prefrontal cortex. In D. T. Stuss & R. T. Knight (Eds.), *Principles of Frontal Lobe Function* (pp. 278-291). New York: Oxford University Press.

Duncan, J., & Owen, A. M. (2000). Common regions of the human frontal lobe recruited by diverse cognitive demands. *Trends in Neurosciences, 23*(10), pp 475-483.

Durston, S., Thomas, K. M., Worden, M. S., Yang, Y., & Casey, B. J. (2002). The effect of preceding context on inhibition: An event-related fMRI study. *NeuroImage, 16*(2), pp 449-453.

Eagle, D. M., Baunez, C., Hutcheson, D. M., Lehmann, O., Shah, A. P., & Robbins, T. W. (2008). Stop-signal reaction-time task performance: Role of prefrontal cortex and subthalamic nucleus. *Cerebral Cortex, 18*(1), pp 178-188.

Eagle, D. M., & Robbins, T. W. (2003a). Inhibitory control in rats performing a stop-Signal reaction-time task: Effects of lesions of the medial striatum and d-amphetamine. *Behavioral Neuroscience, 117*(6), pp 1302-1317.

Eagle, D. M., & Robbins, T. W. (2003b). Lesions of the medial prefrontal cortex or nucleus accumbens core do not impair inhibitory control in rats performing a stop-signal reaction time task. *Behavioural Brain Research, 146*(1-2), pp 131-144.

Egan, M. F., Duncan, C. C., Suddath, R. L., Kirch, D. G., Mirsky, A. F., & Wyatt, R. J. (1994). Event-related potential abnormalities correlate with structural brain alterations and clinical features in patients with chronic schizophrenia. *Schizophrenia Research, 11*(3), pp 259-271.

Elliott, R., McKenna, P. J., Robbins, T. W., & Sahakian, B. J. (1995). Neuropsychological evidence for frontostriatal dysfunction in schizophrenia. *Psychological Medicine, 25*(3), pp 619-630.

Elvevag, B., & Goldberg, T. E. (2000). Cognitive impairment in schizophrenia is the core of the disorder. *Critical Reviews in Neurobiology, 14*(1), pp 1-21.

Enticott, P. G., Ogloff, J. R. P., & Bradshaw, J. L. (2008). Response inhibition and impulsivity in schizophrenia. *Psychiatry Research, 157*(1-3), pp 251-254.

Falkenstein, M., Hohnsbein, J., Hoormann, J., & Blanke, L. (1991). Effects of crossmodal divided attention on late ERP components. II. Error processing in choice reaction tasks. *Electroencephalography and Clinical Neurophysiology, 78*(6), pp 447-455.

Falkenstein, M., Hoormann, J., & Hohnsbein, J. (1999). ERP components in Go/Nogo tasks and their relation to inhibition. *Acta Psychologica, 101*(2-3), pp 267-291.

Farber, N. B. (2003). The NMDA Receptor Hypofunction Model of Psychosis, *Annals of the New York Academy of Sciences,* 1003, pp 119-130.

Fassbender, C., Murphy, K., Foxe, J. J., Wylie, G. R., Javitt, D. C., Robertson, I. H., et al. (2004). A topography of executive functions and their interactions revealed by functional magnetic resonance imaging. *Cognitive Brain Research, 20*(2), 132-143.

Fiehler, K., Ullsperger, M., & Von Cramon, D. Y. (2004). Neural correlates of error detection and error correction: Is there a common neuroanatomical substrate? *European Journal of Neuroscience, 19*(11), pp 3081-3087.

Fleck, M. S., Daselaar, S. M., Dobbins, I. G., & Cabeza, R. (2006). Role of prefrontal and anterior cingulate regions in decision-making processes shared by memory and nonmemory tasks. *Cerebral Cortex, 16*(11), pp 1623-1630.

Folstein, J. R., & Van Petten, C. (2008). Influence of cognitive control and mismatch on the N2 component of the ERP: A review. *Psychophysiology, 45*(1), pp 152-170.

Ford, J. M. (1999). Schizophrenia: The broken P300 and beyond. *Psychophysiology, 36*(6), pp 667-682.

Ford, J. M., Gray, M., Whitfield, S. L., Turken, U., Glover, G., et al. (2004). Acquiring and Inhibiting Prepotent Responses in Schizophrenia: Event-Related Brain Potentials and Functional Magnetic Resonance Imaging. *Archives of General Psychiatry, 61*(2), pp 119-129.

Ford, J. M., Mathalon, D. H., Marsh, L., Faustman, W. O., Harris, D., Hoff, A. L., et al. (1999). P300 amplitude is related to clinical state in severely and moderately ill patients with schizophrenia. *Biological Psychiatry, 46*(1), pp 94-101.

Ford, J. M., Mathalon, D. H., Whitfield, S., Faustman, W. O., & Roth, W. T. (2002). Reduced communication between frontal and temporal lobes during talking in schizophrenia. *Biological Psychiatry, 51*(6), pp 485-492.

Ford, J. M., Pfefferbaum, A., & Roth, W. (1992). P3 and schizophrenia. *Annals of the New York Academy of Sciences, 658*, pp 146-162.

Ford, K. A., Goltz, H. C., Brown, M. R. G., & Everling, S. (2005). Neural processes associated with antisaccade task performance investigated with event-related fMRI. *Journal of Neurophysiology, 94*(1), pp 429-440.

Forstmann, B. U., Jahfari, S., Scholte, H. S., Wolfensteller, U., van den Wildenberg, W. P. M., & Ridderinkhof, K. R. (2008). Function and Structure of the Right Inferior Frontal Cortex Predict Individual Differences in Response Inhibition: A Model-Based Approach. *J. Neurosci., 28*(39), 9790-9796.

Frances, A., & Weiden, P. (1987). Promoting compliance with outpatient drug treatment. *Hospital and Community Psychiatry, 38*(11), pp 1158-1160.

Friedman, D., Cycowicz, Y. M., & Gaeta, H. (2001). The novelty P3: an event-related brain potential (ERP) sign of the brain's evaluation of novelty. *Neuroscience & Biobehavioral Reviews, 25*(4), pp 355-373.

Friston, K. J. (1997). Testing for anatomically specified regional effects. *Human Brain Mapping, 5*(2), pp 133-136.

Frith, C. D. (1992). *The Cognitive Neuropsychology of Schizophrenia* Hove: Lawrence Erlbaum.

Frith, C. D., & Friston, K. J. (1996). The role of the thalamus in "Top Down" modulation of attention to sound. *NeuroImage, 4*, pp 210-215.

Fukushima, J., Fukushima, K., Chiba, T., Tanaka, S., Yamashita, I., & Kato, M. (1988). Disturbances of voluntary control of saccadic eye movements in schizophrenia patients. *Biological Psychiatry, 23*, pp 670-677.

Fuster, J. M. (1997). *The Prefrontal Cortex: Anatomy, Physiology, and Neuropsychology*. Philadelphia: Lippincott-Raven.

Fuster, J. M. (2000). Executive frontal functions. *Experimental Brain Research, 133*(1), pp 66-70.

Garavan, H., Ross, T. J., Kaufman, J., & Stein, E. A. (2003). A midline dissociation between error-processing and response-conflict monitoring. *NeuroImage, 20*(2), pp 1132-1139.

Garavan, H., Ross, T. J., Li, S. J., & Stein, E. A. (2000). A parametric manipulation of central executive functioning. *Cerebral Cortex, 10*(6), pp 585-592.

Garavan, H., Ross, T. J., Murphy, K., Roche, R. A. P., & Stein, E. A. (2002). Dissociable executive functions in the dynamic control of behavior: Inhibition, error detection, and correction. *NeuroImage, 17*(4), pp 1820-1829.

Garavan, H., Ross, T. J., & Stein, E. A. (1999). Right hemispheric dominance of inhibitory control: An event-related functional MRI study. *Proceedings of the National Academy of Sciences of the United States of America, 96*(14), pp 8301-8306.

Gauggel, S., Rieger, M., & Feghoff, T.-A. (2004). Inhibition of ongoing responses in patients with Parkinson's disease. *J Neurol Neurosurg Psychiatry, 75*(4), pp 539-544.

Gehring, W. J., Goss, B., Coles, M. G. H., Meyer, D. E., & Donchin, E. (1993). A neural system for error detection and compensation. *Psychological Science, 4*(6), pp 385-390.

Glahn, D. C., Therman, S., Manninen, M., Huttunen, M., Kaprio, J., Lönnqvist, J., et al.

(2003). Spatial working memory as an endophenotype for schizophrenia. *Biological Psychiatry, 53*(7), pp 624-626.

Goeree, R., Farahati, F., Burke, N., Blackhouse, G., O'Reilly, D., Pyne, J., et al. (2005). The economic burden of schizophrenia in Canada in 2004. *Current Medical Research and Opinion, 21*(12), pp 2017-2028.

Goff, D. C., & Coyle, J. T. (2001). The emerging role of glutamate in the pathophysiology and treatment of schizophrenia. *American Journal of Psychiatry, 158*(9), pp 1367-1377.

Goldman-Rakic, P. (1994). Working memory dysfunction in schizophrenia. *Journal of Neuropsychiatry and Clinical Neurosciences, 6*(4), pp 348-357.

Gottesman, I. I. (1991). *Schizophrenia Genesis: The Origin of Madness*. New York: Freeman.

Gottesman, I. I., & Shields, J. (1982). *Schizophrenia: The Epigenetic Puzzle*. Cambridge: Cambridge University Press.

Gottwald, B., Mihajlovic, Z., Wilde, B., & Mehdorn, H. M. (2003). Does the cerebellum contribute to specific aspects of attention? *Neuropsychologia, 41*(11), pp 1452-1460.

Green, M. (1996). What are the functional consequences of neurocognitive deficits in schizophrenia? *American Journal of Psychiatry, 153*(3), pp 321-330.

Guitton, D., Buchtel, H., & Douglas, R. (1985). Frontal lobe lesions in man cause difficulties in suppressing reflexive glances and in generating goal-directed saccades. *Experimental Brain Research, 58*(3), pp 455-472.

Hackley, S. A., Woldorff, M., & Hillyard, S. A. (1990). Cross-modal selective attention effects on retinal, myogenic, brainstem, and cerebral evoked potentials. *Psychophysiology, 27*(2), pp 195-208.

Hansen, J. C., & Hillyard, S. A. (1980). Endogenous brain potentials associated with selective auditory attention. *Electroencephalography and Clinical Neurophysiology, 49*(3-4), pp 277-290.

Harms, M. P., Wang, L., Mamah, D., Barch, D. M., Thompson, P. A., & Csernansky, J. G. (2007). Thalamic shape abnormalities in individuals with schizophrenia and their nonpsychotic siblings. *Journal of Neuroscience, 27*(50), pp 13835-13842.

Harnishfeger, K. K. (1995). The development of cognitive inhibition: Theories, definitions, and research evidence. In F. N. Dempster & C. J. Brainerd (Eds.), *Interference and Inhibition in Cognition* (pp. 175-205). San Diego: Academic Press.

Harnishfeger, K. K., & Bjorklund, D. F. (1993). The ontogeny of inhibition mechanisms: A renewed approach to cognitive development. In M. L. Howe & R. Pasak (Eds.), *Emerging Themes in Cognitive Development: Vol. 1. Foundations* (pp. 28-49). New York: Springer-Verlag.

Harris, J. G., Minassian, A., & Perry, W. (2007). Stability of attention deficits in schizophrenia. *Schizophrenia Research, 91*(1-3), pp 107-111.

Harrison, P. J. (1997). Schizophrenia: A disorder of neurodevelopment? *Current Opinion in Neurobiology, 7*(2), pp 285-289.

Hazlett, E. A., Buchsbaum, M. S., Kemether, E., Bloom, R., Platholi, J., Brickman, A. M., et al. (2004). Abnormal glucose metabolism in the mediodorsal nucleus of the thalamus in schizophrenia. *American Journal of Psychiatry, 161*(2), pp 305-314.

Hazy, T. E., Frank, M. J., & O'Reilly, R. C. (2007). Towards an executive without a homunculus: Computational models of the prefrontal cortex/basal ganglia system. *Philosophical Transactions of the Royal Society B: Biological Sciences, 362*(1485), pp 1601-1613.

Heaton, R. K., Gladsjo, J. A., Palmer, B. W., Kuck, J., Marcotte, T. D., & Jeste, D. V. (2001). Stability and course of neuropsychological deficits in schizophrenia. *Archives of General Psychiatry, 58*(1), pp 24-32.

Heinrichs, R. W., & Zakzanis, K. K. (1998). Neurocognitive deficit in schizophrenia: A quantitative review of the evidence. *Neuropsychology, 12*(3), pp 426-445.

Hester, R., Fassbender, C., & Garavan, H. (2004). Individual differences in error processing: A review and reanalysis of three event-related fMRI studies using the GO/NOGO task. *Cerebral Cortex, 14*(9), pp 986-994.

Hillyard, S. A., Hink, R. F., Schwent, V. L., & Picton, T. W. (1973). Electrical signs of selective attention in the human brain. *Science, 182*(4108), pp 177-180.

Honea, R., Crow, T. J., Passingham, D., & Mackay, C. E. (2005). Regional deficits in brain volume in schizophrenia: A meta-analysis of voxel-based morphometry studies. *American Journal of Psychiatry, 162*(12), pp 2233-2245.

Huettel, S. A., McKeown, M. J., Song, A. W., Hart, S., Spencer, D. D., Allison, T., et al. (2004). Linking hemodynamic and electrophysiological measures of brain activity: evidence from functional MRI and intracranial field potentials. *Cerebral Cortex, 14*(2), pp 165-173.

Humberstone, M., Clare, S., Hykin, J., Morris, P. G., & Sawle, G. V. (1997). The roles of pre-SMA and SMA-proper in motor initiation and decision making; Studies using 'event related' fMRI. *NeuroImage, 5*(4 PART II).

Hutton, S. B., Huddy, V., Barnes, T. R. E., Robbins, T. W., Crawford, T. J., Kennard, C., et al. (2004). The relationship between antisaccades, smooth pursuit, and executive dysfunction in first-episode schizophrenia. *Biological Psychiatry, 56*(8), pp 553-559.

Hutton, S. B., Puri, B. K., Duncan, L.-J., Robbins, T. W., Barnes, T. R. E., & Joyce, E. M. (1998). Executive function in first-episode schizophrenia. *Psychological Medicine, 28*(02), pp 463-473.

Hyde, T., Nawroz, S., Goldberg, T., Bigelow, L., Strong, D., Ostrem, J., et al. (1994). Is there cognitive decline in schizophrenia? A cross-sectional study. *The British Journal of Psychiatry, 164*(4), pp 494-500.

Ivry, R. (2000). Exploring the role of the cerebellum in sensory anticipation and timing: Commentary on Tesche and Karhu. *Human Brain Mapping, 9*(3), pp 115-118.

Jablensky, A. (2000a). Epidemiology of schizophrenia: The global burden of disease and disability. *European Archives of Psychiatry and Clinical Neuroscience, 250*(6), pp 274-285.

Jablensky, A. (2000b). Prevalence and incidence of schizophrenia spectrum disorders: Implications for prevention. *Australian and New Zealand Journal of Psychiatry, 34*(SUPPL. 1), S26-S34.

Jablensky, A., & Sartorius, N. (1975). Culture and schizophrenia. *Psychological Medicine, 5*(2), pp 113-124.

Javitt, D. C. (2009). When doors of perception close: Bottom-up models of disrupted cognition in schizophrenia, *Annual Review of Clinical Psychology* (Vol. 5, pp. 249-275).

Javitt, D. C., & Zukin, S. R. (1991). Recent advances in the phencyclidine model of schizophrenia. *American Journal of Psychiatry, 148*(10), 1301-1308.

Josephs, O., Turner, R., & Friston, K. (1997). Event-related fMRI. *Human Brain Mapping, 5*(4), pp 243-248.

Joyce, E. M., Hutton, S. B., Mutsatsa, S., Gibbins, H., Webb, E., Paul, S., et al. (2002). Executive dysfunction in first-episode schizophrenia and relationship to duration of untreated psychosis: the West London Study. *The British Journal of Psychiatry, 181*(43), s38-44.

Jurado, M., & Rosselli, M. (2007). The elusive nature of executive functions: A review of our current understanding. *Neuropsychology Review, 17*(3), pp 213-233.

Kaladjian, A., Jeanningros, R., Azorin, J.-M., Grimault, S., Anton, J.-L., & Mazzola-Pomietto, P. (2007). Blunted activation in right ventrolateral prefrontal cortex

during motor response inhibition in schizophrenia. *Schizophrenia Research, 97*(1-3), pp 184-193.

Kane, J. M., Cooper, T. B., & Sachai, E. J. (1981). Clozapine: Plasma levels and prolactin response. *Psychopharmacology, 73*(2), pp 184-187.

Kane, J. M., Honigfeld, G., Singer, J., & Meltzer, H. (1988). Clozapine in treatment-resistant schizophrenics. *Psychopharmacology Bulletin, 24*(1), pp 62-67.

Kane, M. J., & Engle, R. W. (2002). The role of prefrontal cortex in working-memory capacity, executive attention, and general fluid intelligence: An individual-differences perspective. *Psychonomic Bulletin & Review, 9*(4), pp 637-671.

Kapur, S., & Mamo, D. (2003). Half a century of antipsychotics and still a central role for dopamine D2 receptors. *Progress in Neuro-Psychopharmacology and Biological Psychiatry, 27*(7), pp 1081-1090.

Kapur, S., & Seeman, P. (2001). Does fast dissociation from the dopamine D2 receptor explain the action of atypical antipsychotics?: A new hypothesis. *American Journal of Psychiatry, 158*(3), pp 360-369.

Kapur, S., Zipursky, R., Jones, C., Remington, G., & Houle, S. (2000). Relationship between dopamine D2 occupancy, clinical response, and side effects: A double-blind PET study of first-episode schizophrenia. *American Journal of Psychiatry, 157*(4), pp 514-520.

Katayama, J., & Polich, J. (1998). Stimulus context determines P3a and P3b. *Psychophysiology, 35*, pp 23-33.

Kawashima, R., Satoh, K., Itoh, H., Ono, S., Furumoto, S., Gotoh, R., et al. (1996). Functional anatomy of GO/NO-GO discrimination and response selection - A PET study in man. *Brain Research, 728*(1), pp 79-89.

Kerns, J. G., Cohen, J. D., MacDonald, A. W., III, Cho, R. Y., Stenger, V. A., & Carter, C. S. (2004). Anterior cingulate conflict monitoring and adjustments in control. *Science, 303*(5660), pp 1023-1026.

Kiehl, K. A., Smith, A. M., Hare, R. D., & Liddle, P. F. (2000). An event-related potential investigation of response inhibition in schizophrenia and psychopathy. *Biological Psychiatry, 48*(3), pp 210-221.

King, C., & Voruganti, L. N. P. (2002). What's in a name? The evolution of the nomenclature of antipsychotic drugs. *Journal of Psychiatry and Neuroscience, 27*(3), pp 168-175.

Knapp, M., Mangalore, R., & Simon, J. (2004). The global costs of schizophrenia. *Schizophrenia Bulletin, 30*(2), 279-293.

Knoch, D., Pascual-Leone, A., Meyer, K., Treyer, V., & Fehr, E. (2006). Diminishing reciprocal fairness by disrupting the right prefrontal cortex. *Science, 314*(5800), pp 829-832.

Kok, A., Ramautar, J. R., Ruiter, M. B. D., Band, G. P. H., & Ridderinkhof, K. R. (2004). ERP components associated with successful and unsuccessful stopping in a stop-signal task. *Psychophysiology, 41*(1), pp 9-20.

Konick, L. C., & Friedman, L. (2001). Meta-analysis of thalamic size in schizophrenia. *Biological Psychiatry, 49*(1), pp 28-38.

Kraepelin, E. (1919). *Dementia Praecox and Paraphrenia*. Endinburgh: E&S Livingstone.

Kraft, E., Loichinger, W., Diepers, M., Lule, D., Schwarz, J., Ludolph, A. C., et al. (2009). Levodopa-induced striatal activation in Parkinson's disease: A functional MRI study. *Parkinsonism & Related Disorders, 15*(8), pp 558-563.

Kremen, W. S., Seidman, L. J., Faraone, S. V., Toomey, R., & Tsuang, M. T. (2000). The paradox of normal neuropsychological function in schizophrenia. *Journal of Abnormal Psychology, 109*(4), pp 743-752.

Kremen, W. S., Seidman, L. J., Faraone, S. V., Toomey, R., & Tsuang, M. T. (2004). Heterogeneity of schizophrenia: a study of individual neuropsychological profiles. *Schizophrenia Research, 71*(2-3), pp 307-321.

Laming, D. R. J. (1968). *Information theory of choice-reaction times*. Oxford: Academic Press.

Lancaster, J. L., Woldorff, M. G., Parsons, L. M., Liotti, M., Freitas, C. S., Rainey, L., et al. (2000). Automated Talairach Atlas labels for functional brain mapping. *Human Brain Mapping, 10*(3), pp 120-131.

Lang, D. J., Khorram, B., Goghari, V. M., Kopala, L. C., Vandorpe, R. A., Rui, Q., et al. (2006). Reduced anterior internal capsule and thalamic volumes in first-episode psychosis. *Schizophrenia Research, 87*(1-3), pp 89-99.

Laruelle, M., Abi-Dargham, A., Van Dyck, C. H., Gil, R., D'Souza, C. D., Erdos, J., et al. (1996). Single photon emission computerized tomography imaging of amphetamine-induced dopamine release in drug-free schizophrenic subjects. *Proceedings of the National Academy of Sciences of the United States of America, 93*(17), pp 9235-9240.

Leff, J., & Vaughn, C. (1986). First episodes of schizophrenia. *The British Journal of Psychiatry; the Journal of Mental Sscience, 148*, pp 215-216.

Lencz, T., Smith, C. W., McLaughlin, D., Auther, A., Nakayama, E., Hovey, L., et al.

(2006). Generalized and specific neurocognitive deficits in prodromal schizophrenia. *Biological Psychiatry, 59*(9), pp 863-871.

Leucht, S., Pitschel-Walz, G., Engel, R. R., & Kissling, W. (2002). Amisulpride, an unusual "atypical" antipsychotic: A meta-analysis of randomized controlled trials. *American Journal of Psychiatry, 159*(2), pp 180-190.

Lévesque, M., & Parent, A. (2005). The striatofugal fiber system in primates: A reevaluation of its organization based on single-axon tracing studies. *Proceedings of the National Academy of Sciences of the United States of America, 102*(33), pp 11888-11893.

Levitt, H. (1971). Transformed up-down methods in psychoacoustics. *The Journal of the Acoustical Society of America, 49*(2B), pp 467-477.

Li, C.-s. R., Huang, C., Yan, P., Paliwal, P., Constable, R. T., & Sinha, R. (2008). Neural correlates of post-error slowing during a stop signal task: A functional magnetic resonance imaging study. *Journal of Cognitive Neuroscience, 20*(6), pp 1021-1029.

Liddle, P. (1987). The symptoms of chronic schizophrenia. A re-examination of the positive- negative dichotomy. *The British Journal of Psychiatry, 151*(2), 145-151.

Liddle, P. F., Kiehl, K. A., & Smith, A. M. (2001). Event-related fMRI study of response inhibition. *Human Brain Mapping, 12*(2), pp 100-109.

Limousin, P., Krack, P., Pollak, P., Benazzouz, A., Ardouin, C., Hoffmann, D., et al. (1998). Electrical stimulation of the subthalamic nucleus in advanced Parkinson's Disease. *New England Journal of Medicine, 339*(16), pp 1105-1111.

Limousin, P., Pollak, P., Benazzouz, A., Hoffmann, D., Broussolle, E., Perret, J. E., et al. (1995). Bilateral subthalamic nucleus stimulation for severe Parkinson's Disease. *Movement Disorders, 10*(5), pp 672-674.

Lindenmayer, J. P., Grochowski, S., & Hyman, R. B. (1995). Five factor model of schizophrenia: replication across samples. *Schizophrenia Research, 14*, pp 229-234.

Lindström, L. H., Gefvert, O., Hagberg, G., Lundberg, T., Bergström, M., Hartvig, P., et al. (1999). Increased dopamine synthesis rate in medial prefrontal cortex and striatum in schizophrenia indicated by -([beta]-11C) DOPA and PET. *Biological Psychiatry, 46*(5), pp 681-688.

Liston, C., Watts, R., Tottenham, N., Davidson, M. C., Niogi, S., Ulug, A. M., et al. (2006). Frontostriatal microstructure modulates efficient recruitment of cognitive control. *Cerebral Cortex, 16*(4), pp 553-560.

Liu, S. K., Chiu, C.-H., Chang, C.-J., Hwang, T.-J., Hwu, H.-G., & Chen, W. J. (2002). Deficits in sustained attention in schizophrenia and affective disorders: Stable versus state-dependent markers. *American Journal of Psychiatry, 159*(6), pp 975-

982.

Logan, G. D. (1994). On the ability to inhibit thought and action: A users guide to the stop-signal paradigm. In T. H. Dagenbach & T. H. Carr (Eds.), *Inhibitory Processes in Attention, Memory, and Language* (pp. 189-239). San Diego: Academic Press.

Logan, G. D., & Burkell, J. (1986). Dependence and independence in responding to double stimulation. A comparison of stop, change, and dual-task paradigms. *Journal of Experimental Psychology: Human Perception and Performance, 12*(4), pp 549-563.

Logan, G. D., & Cowan, W. B. (1984). On the ability to inhibit thought and action: A theory of an act of control. *Psychological Review, 91*(3), pp 295-327.

Logan, G. D., Cowan, W. B., & Davis, K. A. (1984). On the ability to inhibit simple and choice reaction time responses: A model and a method. *Journal of Experimental Psychology: Human Perception and Performance, 10*(2), pp 276-291.

Logan, G. D., Schachar, R. J., & Tannock, R. (1997). Impulsivity and inhibitory control. *Psychological Science, 8*(1), pp 60-64.

MacDonald III, A. W., Cohen, J. D., Andrew Stenger, V., & Carter, C. S. (2000). Dissociating the role of the dorsolateral prefrontal and anterior cingulate cortex in cognitive control. *Science, 288*(5472), pp 1835-1838.

MacLeod, C. M., Dodd, M. D., Sheard, E. D., Wilson, D. E., & Bibi, U. (2003). In opposition to inhibition, *Psychology of Learning and Motivation - Advances in Research and Theory* (Vol. 43, pp. 163-214).

Magliano, L., Fadden, G., Fiorillo, A., Malangone, C., Sorrentino, D., Robinson, A., et al. (1999). Family burden and coping strategies in schizophrenia: Are key relatives really different to other relatives? *Acta Psychiatrica Scandinavica, 99*(1), pp 10-15.

Maguire, R. P., Broerse, A., De Jong, B. M., Cornelissen, F. W., Meiners, L. C., Leenders, K. L., et al. (2003). Evidence of enhancement of spatial attention during inhibition of a visuo-motor response. *NeuroImage, 20*(2), pp 1339-1345.

Mathalon, D. H., Ford, J. M., & Pfefferbaum, A. (2000). Trait and state aspects of p300 amplitude reduction in schizophrenia: a retrospective longitudinal study. *Biological Psychiatry, 47*(5), pp 434-449.

Mathalon, D. H., Ford, J. M., Rosenbloom, M., & Pfefferbaum, A. (2000). P300 reduction and prolongation with illness duration in schizophrenia. *Biological Psychiatry, 47*(5), pp 413-427.

Mathalon, D. H., Heinks, T., & Ford, J. M. (2004). Selective attention in schizophrenia: sparing and loss of executive control. *American Journal of Psychiatry, 161*(5), pp 872-881.

Matsuda, T., Matsuura, M., Ohkubo, T., Ohkubo, H., Matsushima, E., Inoue, K., et al. (2004). Functional MRI mapping of brain activation during visually guided saccades and antisaccades: cortical and subcortical networks. *Psychiatry Research: Neuroimaging, 131*(2), pp 147-155.

Matsuzaka, Y., Aizawa, H., & Tanji, J. (1992). A motor area rostral to the supplementary motor area (presupplementary motor area) in the monkey: Neuronal activity during a learned motor task. *Journal of Neurophysiology, 68*(3), pp 653-662.

Mattingley, J. B., Husain, M., Rorden, C., Kennard, C., & Driver, J. (1998). Motor role of human inferior parietal lobe revealed in unilateral neglect patients. *Nature, 392*(6672), pp 179-182.

May, P. J. C., & Tiitinen, H. (2009). Mismatch negativity (MMN), the deviance-elicited auditory deflection, explained. *Psychophysiology, (in press*).

Mayr, U., Diedrichsen, J. r., Ivry, R., & Keele, S. W. (2006). Dissociating task-set selection from task-set inhibition in the prefrontal cortex. *Journal of Cognitive Neuroscience, 18*(1), pp 14-21.

Mazaika P, Whitfield-Gabrieli S, Reiss A., & Glover, G. (2007). Artifact repair for fMRI data from high motion clinical subjects. Poster presented at: 13th Annual Meeting of the Organization for Human Brain Mapping; Chicago, IL. Hum Brain Mapp Conf.

McGrath, J., Saha, S., Welham, J., El Saadi, O., MacCauley, C., & Chant, D. (2004). A systematic review of the incidence of schizophrenia: The distribution of rates and the influence of sex, urbanicity, migrant status and methodology. *BMC Medicine, 2*.

Meaney, A. M., & O'Keane, V. (2002). Prolactin and schizophrenia: Clinical consequences of hyperprolactinaemia. *Life Sciences, 71*(9), pp 979-992.

Menon, V., Adleman, N. E., White, C. D., Glover, G. H., & Reiss, A. L. (2001). Error-related brain activation during a Go/NoGo response inhibition task. *Human Brain Mapping, 12*(3), pp 131-143.

Menzies, L., Achard, S., Chamberlain, S. R., Fineberg, N., Chen, C. H., Del Campo, N., et al. (2007). Neurocognitive endophenotypes of obsessive-compulsive disorder. *Brain, 130*(12), pp 3223-3236.

Meyer-Lindenberg, A., Miletich, R. S., Kohn, P. D., Esposito, G., Carson, R. E., Quarantelli, M., et al. (2002). Reduced prefrontal activity predicts exaggerated striatal dopaminergic function in schizophrenia. *Nature Neuroscience, 5*(3), pp 267-271.

Michie, P. T. (2001). What has MMN revealed about the auditory system in schizophrenia? *International Journal of Psychophysiology, 42*(2), pp 177-194.

Michie, P. T., Fox, A. M., Ward, P. B., Catts, S. V., & McConaghy, N. (1990a). Event-related potential indices of selective attention and cortical lateralization in schizophrenia. *Psychophysiology, 27*(2), pp 209-227.

Michie, P. T., Bearpark, H. M., Crawford, J. M., & Glue, L. C. (1990b). The nature of selective attention effects on auditory event-related potentials. *Biological Psychology, 30*(3), pp 219-250.

Michie, P. T., Kent, A., Stienstra, R., Castine, R., Johnston, J., Dedman, K., et al. (2000). Phenotypic markers as risk factors in schizophrenia: neurocognitive functions. *Australian and New Zealand Journal of Psychiatry, 34*((Suppl.)), S74-S85.

Middleton, F. A., & Strick, P. L. (1994). Anatomical evidence for cerebellar and basal ganglia involvement in higher cognitive function. *Science, 266*(5184), pp 458-461.

Miller, E. K., & Cohen, J. D. (2001). An integrative theory of prefrontal cortex function. *Annual Review of Neuroscience, 24*(1), pp 167-202.

Mink, J. W. (1996). The basal ganglia: Focussed selection and inhibition of competing motor programs. *Progress in Neurobiology, 50*(4), pp 381-425.

Mitchell, R. L. C., Elliott, R., & Woodruff, P. W. R. (2001). fMRI and cognitive dysfunction in schizophrenia. *Trends in Cognitive Sciences, 5*(2), pp 71-81.

Miyake, A., Friedman, N. P., Emerson, M. J., Witzki, A. H., Howerter, A., & Wager, T. D. (2000). The unity and diversity of executive functions and their contributions to complex "frontal lobe" tasks: A latent variable analysis. *Cognitive Psychology, 41*(1), pp 49-100.

Mohamed, S., Paulsen, J. S., O'Leary, D., Arndt, S., & Andreasen, N. (1999). Generalized cognitive deficits in schizophrenia: A study of first-episode patients. *Archives of General Psychiatry, 56*(8), pp 749-754.

Montague, P. R., Hyman, S. E., & Cohen, J. D. (2004). Computational roles for dopamine in behavioural control. *Nature, 431*(7010), pp 760-767.

Morey, R. A., Mitchell, T. V., Inan, S., Lieberman, J. A., & Belger, A. (2008). Neural correlates of automatic and controlled auditory processing in schizophrenia. *Journal of Neuropsychiatry and Clinical Neurosciences, 20*(4), pp 419-430.

Mostofsky, S. H., Schafer, J. G. B., Abrams, M. T., Goldberg, M. C., Flower, A. A., Boyce, A., et al. (2003). FMRI evidence that the neural basis of response inhibition is task-dependent. *Cognitive Brain Research, 17*(2), pp 419-430.

Näätänen, R. (1982). Processing negativity: An evoked-potential reflection. *Psychological Bulletin, 92*(3), pp 605-640.

Näätänen, R., & Kähkönen, S. (2009). Central auditory dysfunction in schizophrenia as revealed by the mismatch negativity (MMN) and its magnetic equivalent MMNm: A review. *International Journal of Neuropsychopharmacology, 12*(1), pp 125-135.

Näätänen, R., & Michie, P. T. (1979). Early selective-attention effects on the evoked potential: A critical review and reinterpretation. *Biological Psychology, 8*(2), pp 81-136.

Näätänen, R., & Picton, T. (1987). The N1 wave of the human electric and magnetic response to sound: A review and an analysis of the component structure. *Psychophysiology, 24*(4), pp 375-425.

Nambu, A., Takada, M., Inase, M., & Tokuno, H. (1996). Dual somatotopical representations in the primate subthalamic nucleus: evidence for ordered but reversed body-map transformations from the primary motor cortex and the supplementary motor area. *Journal of Neuroscience, 16*(8), pp 2671-2683.

Nambu, A., Tokuno, H., & Takada, M. (2002). Functional significance of the cortico-subthalamo-pallidal `hyperdirect' pathway. *Neuroscience Research, 43*(2), pp 111-117.

Nathaniel-James, D. A., Brown, R., & Ron, M. A. (1996). Memory impairment in schizophrenia: Its' relationship to executive function. *Schizophrenia Research, 21*(2), pp 85-96.

Nathaniel-James, D. A., Fletcher, P., & Frith, C. D. (1997). The functional anatomy of verbal initiation and suppression using the Hayling Test. *Neuropsychologia, 35*, pp 559-566.

Nichols, T. E., & Holmes, A. P. (2002). Nonparametric permutation tests for functional neuroimaging: A primer with examples. *Human Brain Mapping, 15*(1), pp 1-25.

Nigg, J. T. (2000). On inhibition/disinhibition in developmental psychopathology: Views from cognitive and personality psychology and a working inhibition taxonomy. *Psychological Bulletin, 126*(2), pp 220-246.

Noll, R. (2007). Kraepelin's `lost biological psychiatry'? Autointoxication, organotherapy and surgery for dementia praecox. *History of Psychiatry, 18*(3), pp 301-320.

Norman, D. A., & Shallice, T. (1986). Attention to action: Willed and automatic control of behaviour. In R. J. Davidson, G. E. Schwartz & D. Shapiro (Eds.), *Consciousness and Self-Regulation: Advances in Research and Theory.* (Vol. 4, pp. 1-18). New York: Plenum Press.

Nuechterlein, K. H. (1977). Reaction time and attention in schizophrenia: A critical evaluation of the data and theories. *Schizophrenia Bulletin, 3*(3), pp 373-428.

Nuechterlein, K. H., Barch, D. M., Gold, J. M., Goldberg, T. E., Green, M. F., & Heaton, R. K. (2004). Identification of separable cognitive factors in schizophrenia. *Schizophrenia Research, 72*(1), pp 29-39.

Ollman, R. T. (1973). Simple reactions with random countermanding of the 'go' signal. In S. Kornblum (Ed), *Attention and Performance* (4th ed., pp. 571-581). New York: Academic Press.

Olney, J. W., & Farber, N. B. (1995). Glutamate receptor dysfunction and schizophrenia. *Archives of General Psychiatry, 52*(12), pp 998-1007.

Olney, J. W., Newcomer, J. W., & Farber, N. B. (1999). NMDA receptor hypofunction model of schizophrenia. *Journal of Psychiatric Research, 33*(6), pp 523-533.

Oosterlaan, J., Logan, G. D., & Sergeant, J. A. (1998). Response inhibition in AD/HD, CD, comorbid AD/HD+CD, anxious, and control children: A meta-analysis of studies with the stop task. *Journal of Child Psychology and Psychiatry, 39*(3), pp 411-425.

Overtoom, C. C. E., Kenemans, J. L., Verbaten, M. N., Kemner, C., van der Molen, M. W., van Engeland, H., et al. (2002). Inhibition in children with attention-deficit/hyperactivity disorder: a psychophysiological study of the stop task. *Biological Psychiatry, 51*(8), pp 668-676.

Pantelis, C. (1996). Overview: Towards a neuropsychology of schizophrenia. In C. Pantelis, H. E. Nelson & T. R. E. Barnes (Eds.), *Schizophrenia: A neuropsychological perspective* (pp. 3-18). New York: John Wiley & Sons.

Pantelis, C., Barber, F. Z., Barnes, T. R. E., Nelson, H. E., Owen, A. M., & Robbins, T. W. (1999). Comparison of set-shifting ability in patients with chronic schizophrenia and frontal lobe damage. *Schizophrenia Research, 37*(3), pp 251-270.

Pantelis, C., Barnes, T. R. E., Nelson, H. E., Tanner, S., Weatherley, L., Owen, A. M., et al. (1997). Frontal-striatal cognitive deficits in patients with chronic schizophrenia. *Brain, 120*(10), pp 1823-1843.

Pantelis, C., Velakoulis, D., McGorry, P. D., Wood, S. J., Suckling, J., Phillips, L. J., et al. (2003). Neuroanatomical abnormalities before and after onset of psychosis: a cross-sectional and longitudinal MRI comparison. *The Lancet, 361*(9354), pp 281-288.

Perlstein, W. M., Carter, C. S., Noll, D. C., & Cohen, J. D. (2001). Relation of prefrontal cortex dysfunction to working memory and symptoms in schizophrenia. *American Journal of Psychiatry, 158*(7), pp 1105-1113.

Perlstein, W. M., Dixit, N. K., Carter, C. S., Noll, D. C., & Cohen, J. D. (2003). Prefrontal cortex dysfunction mediates deficits in working memory and prepotent responding in schizophrenia. *Biological Psychiatry, 53*(1), pp 25-38.

Perry, W., Heaton, R. K., Potterat, E., Roebuck, T., Minassian, A., & Braff, D. L. (2001). Working memory in schizophrenia: Transient "online" storage versus executive functioning. *Schizophrenia Bulletin, 27*(1), pp 157-176.

Pfefferbaum, A., Ford, J. M., White, P. M., & Roth, W. T. (1989). P3 in schizophrenia is affected by stimulus modality, response requirements, medication status, and negative symptoms. *Archives of General Psychiatry, 46*(11), pp 1035-1044.

Pierce, R. C., & Kumaresan, V. (2006). The mesolimbic dopamine system: The final common pathway for the reinforcing effect of drugs of abuse? *Neuroscience & Biobehavioral Reviews, 30*(2), pp 215-238.

Pilowsky, L. S., Costa, D. C., Ell, P. J., Murray, R. M., Verhoeff, N. P., & Kerwin, R. W. (1993). Antipsychotic medication, D2 dopamine receptor blockade and clinical response: a 123I IBZM SPET(single photon emission tomography) study. *Psychological Medicine, 23*(3), pp 791-797.

Pliszka, S. R., Liotti, M., & Woldorff, M. G. (2000). Inhibitory control in children with attention-deficit/hyperactivity disorder: event-related potentials identify the processing component and timing of an impaired right-frontal response-inhibition mechanism. *Biological Psychiatry, 48*(3), pp 238-246.

Pompili, M., Amador, X. F., Girardi, P., Harkavy-Friedman, J., Harrow, M., Kaplan, K., et al. (2007). Suicide risk in schizophrenia: Learning from the past to change the future. *Annals of General Psychiatry, 6*, pp10.

Popken, G. J., Bunney Jr, W. E., Potkin, S. G., & Jones, E. G. (2000). Subnucleus-specific loss of neurons in medial thalamus of schizophrenics. *Proceedings of the National Academy of Sciences of the United States of America, 97*(16), pp 9276-9280.

Posner, M. I., & Petersen, S. E. (1990). The attention system of the human brain. *Annual Review of Neuroscience, 13*, pp 25-42.

Ramautar, J. R., Kok, A., & Ridderinkhof, K. R. (2004). Effects of stop-signal probability in the stop-signal paradigm: The N2/P3 complex further validated. *Brain and Cognition, 56*(2), pp 234-252.

Rao, S. C., & Rainer, G. (1997). Integration of what and where in the primate prefrontal cortex. *Science, 276*(5313), pp 821.

Rasser, P. E., Schall, U., Todd, J., Michie, P. T., Ward, P. B., Johnston, P., et al. (2009). Gray matter deficits, mismatch negativity, and outcomes in schizophrenia. *Schizophrenia Bulletin*, (in press).

Reichenberg, A., & Harvey, P. D. (2007). Neuropsychological impairments in schizophrenia: Integration of performance-based and brain imaging findings.

Psychological Bulletin, 133(5), pp 833-858.

Rieger, M., Gauggel, S., & Burmeister, K. (2003). Inhibition of ongoing responses following frontal, nonfrontal, and basal ganglia lesions. *Neuropsychology, 17*(2), pp 272-282.

Riley, E. M., McGovern, D., Mockler, D., Doku, V. C. K., ÓCeallaigh, S., Fannon, D. G., et al. (2000). Neuropsychological functioning in first-episode psychosis -- evidence of specific deficits. *Schizophrenia Research, 43*(1), pp 47-55.

Ring, H. A., & Serra-Mestres, J. (2002). Neuropsychiatry of the basal ganglia. *Journal of Neurology Neurosurgery and Psychiatry, 72*(1), pp 12-21.

Robbins, T. W. (1990). The case for frontostriatal dysfunction in schizophrenia. *Schizophrenia Bulletin, 16*(3), pp 391-402.

Roberts, R. J., & Pennington, B. F. (1996). An interactive framework for examining prefrontal cognitive processes. *Developmental Neuropsychology, 12*(1), pp 105.

Roberts Jr, R. J., Hager, L. D., & Heron, C. (1994). Prefrontal cognitive processes: Working memory and inhibition in the antisaccade task. *Journal of Experimental Psychology: General, 123*(4), pp 374-393.

Rogers, R. D., & Monsell, S. (1995). Costs of a predictible switch between simple cognitive tasks. *Journal of Experimental Psychology: General, 124*(2), 207-231.

Rosburg, T., Boutros, N. N., & Ford, J. M. (2008). Reduced auditory evoked potential component N100 in schizophrenia - A critical review. *Psychiatry Research, 161*(3), pp 259-274.

Rosenthal, D. (1970). *Genetic theory and abnormal behaviour.* New York: McGraw Hill.

Roskies, A. L., Fiez, J. A., Balota, D. A., Raichle, M. E., & Petersen, S. E. (2001). Task-dependent modulation of regions in the left Inferior frontal cortex during semantic processing. *Journal of Cognitive Neuroscience, 13*(6), pp 829-843.

Ross, R. G., Wagner, B., Heinlein, S., & Zerbe, G. O. (2008). The stability of inhibitory and working memory deficits in children and adolescents Wwho are children of parents with schizophrenia. *Schizophrenia Bulletin, 34*(1), pp 47-51.

Rowe, J. B., Toni, I., Josephs, O., Frackowiak, R. S. J., & Passingham, R. E. (2000). The prefrontal cortex: Response selection or maintenance within working memory? *Science, 288*(5471), pp 1656.

Rubia, K., Russell, T., Bullmore, E. T., Soni, W., Brammer, M. J., Simmons, A., et al. (2001b). An fMRI study of reduced left prefrontal activation in schizophrenia during normal inhibitory function. *Schizophrenia Research, 52*(1-2), pp 47-55.

Rubia, K., Russell, T., Overmeyer, S., Brammer, M. J., Bullmore, E. T., Sharma, T., et al. (2001a). Mapping motor inhibition: Conjunctive brain activations across different versions of Go/No-Go and stop tasks. *NeuroImage, 13*(2), pp 250-261.

Rubia, K., Smith, A. B., Brammer, M. J., & Taylor, E. (2003). Right inferior prefrontal cortex mediates response inhibition while mesial prefrontal cortex is responsible for error detection. *NeuroImage, 20*(1), pp 351-358.

Rund, B. R. (1998). A Review of longitudinal studies of cognitive functions in schizophrenia patients. *Schizophrenia Bulletin, 24*(3), pp 425-435.

Sánchez-González, M. Ã., Garcá-a-Cabezas, M. Ã., Rico, B., & Cavada, C. (2005). The primate thalamus is a key target for brain dopamine. *Journal of Neuroscience, 25*(26), pp 6076-6083.

Saha, S., Chant, D., Welham, J., & McGrath, J. (2005). A systematic review of the prevalence of schizophrenia. *PLoS Medicine, 2*(5), pp 0413-0433.

Saperstein, A. M., Fuller, R. L., Avila, M. T., Adami, H., McMahon, R. P., Thaker, G. K., et al. (2006). Spatial working memory as a cognitive endophenotype of schizophrenia: Assessing risk for pathophysiological dysfunction. *Schizophrenia Bulletin, 32*(3), pp 498-506.

Saykin, A. J., Shtasel, D. L., Gur, R. E., Kester, D. B., Mozley, L. H., Stafiniak, P., et al. (1994). Neuropsychological deficits in neuroleptic naive patients with first-episode schizophrenia. *Archives of General Psychiatry, 51*(2), pp 124-131.

Schachar, R., & Logan, G. D. (1990). Impulsivity and inhibitory control in normal development and childhood psychopathology. *Developmental Psychology, 26*(5), pp 710-720.

Schachar, R., Tannock, R., Marriott, M., & Logan, G. (1995). Deficient inhibitory control in attention deficit hyperactivity disorder. *Journal of Abnormal Child Psychology, 23*(4), pp 411-437.

Scheres, A., Oosterlaan, J., Swanson, J., Morein-Zamir, S., Meiran, N., Schut, H., et al. (2003). The effect of methylphenidate on three forms of response inhibition in boys with AD/HD. *Journal of Abnormal Child Psychology, 31*(1), pp 105-120.

Schneider, W., & Shiffrin, R. M. (1977). Controlled and automatic human information processing: I. Detection, search, and attention. *Psychological Review, 84*(1), pp 1-66.

Schwent, V. L., & Hillyard, S. A. (1975). Evoked potential correlates of selective attention with multi channel auditory inputs. *Electroencephalography and Clinical Neurophysiology, 38*(2), pp 131-138.

Seeman, P., Chau Wong, M., Tedesco, J., & Wong, K. (1975). Brain receptors for antipsychotic drugs and dopamine: direct binding assays. *Proceedings of the National Academy of Sciences of the United States of America, 72*(11), pp 4376-4380.

Seeman, P., & Lee, T. (1975). Antipsychotic drugs: direct correlation between clinical potency and presynaptic action on dopamine neurons. *Science, 188*(4194), pp 1217-1219.

Seidman, L. J. (1983). Schizophrenia and brain dysfunction: An integration of recent neurodiagnostic findings. *Psychological Bulletin, 94*(2), pp 195-238.

Seidman, L. J., Kremen, W. S., Koren, D., Faraone, S. V., Goldstein, J. M., & Tsuang, M. T. (2002). A comparative profile analysis of neuropsychological functioning in patients with schizophrenia and bipolar psychoses. *Schizophrenia Research, 53*(1-2), pp 31-44.

Semlitsch, H. V., Anderer, P., Schuster, P., & Presslich, O. (1986). A solution for reliable and valid reduction of ocular artifacts, applied to the P300 ERP. *Psychophysiology, 23*(6), pp 695-703.

Sereno, A. B., & Holzman, P. S. (1995). Antisaccades and smooth pursuit eye movements in schizophrenia. *Biological Psychiatry, 37*(6), pp 394-401.

Shallice, T. (1982). Specific impairments of planning. *Philosophical Transactions of the Royal Society B: Biological Sciences, 298*(1089), pp 199-209.

Shallice, T. (1988). *From neuropsychology to mental structure*. New York: Cambridge University Press.

Shallice, T. (2002). Fractionation of the supervisory system. In D. T. Stuss & R. T. Knight (Eds.), *Principles of Frontal Lobe Function* (pp. 261-277). New York: Oxford University Press.

Shallice, T., Burgess, P. W., & Frith, C. D. (1991). Can the neuropsychological case-study approach be applied to schizophrenia? *Psychological Medicine, 21*(3), pp 661-673.

Shelley, A.-M., Silipo, G., & Javitt, D. C. (1999). Diminished responsiveness of ERPs in schizophrenic subjects to changes in auditory stimulation parameters: implications for theories of cortical dysfunction. *Schizophrenia Research, 37*(1), pp 65-79.

Shiffrin, R. M., & Schneider, W. (1977). Controlled and automatic human information processing: II. Perceptual learning, automatic attending and a general theory. *Psychological Review, 84*(2), pp 127-190.

Silver, H., Feldman, P., Bilker, W., & Gur, R. C. (2003). Working memory deficit as a core neuropsychological dysfunction in schizophrenia. *American Journal of Psychiatry,*

160(10), pp 1809-1816.

Smith, A., Taylor, E., Lidzba, K., & Rubia, K. (2003). A right hemispheric frontocerebellar network for time discrimination of several hundreds of milliseconds. *NeuroImage, 20*(1), pp 344-350.

Smith, E. E., & Jonides, J. (1999). Storage and executive processes in the frontal lobes. *Science, 283*(5408), pp 1657.

Sokolov, E. N., Nezlina, N. I., Polyanskii, V. B., & Evtikhin, D. V. (2002). The orientating reflex: The "targeting reaction" and "searchlight of attention". *Neuroscience and Behavioral Physiology, 32*(4), pp 347-362.

Stahl, J., & Gibbons, H. (2007). Dynamics of response-conflict monitoring and individual differences in response control and behavioral control: An electrophysiological investigation using a stop-signal task. *Clinical Neurophysiology, 118*(3), pp 581-596.

Stone, J. M., Morrison, P. D., & Pilowsky, L. S. (2007). Glutamate and dopamine dysregulation in schizophrenia - A synthesis and selective review. *Journal of Psychopharmacology, 21*(4), pp 440-452.

Stuss, D. T. (2006). Frontal lobes and attention: Processes and networks, fractionation and integration. *Journal of the International Neuropsychological Society, 12*(02), pp 261-271.

Stuss, D. T., & Alexander, M. P. (2007). Is there a dysexecutive syndrome? *Philosophical Transactions of the Royal Society B: Biological Sciences, 362*(1481), pp 901-915.

Stuss, D. T., Shallice, T., Alexander, M. P., & Picton, T. W. (1995). A multidisciplinary approach to anterior attentional functions. *Annals of the New York Academy of Sciences, 769*(Structure and Functions of the Human Prefrontal Cortex), pp 191-212.

Talairach, J., & Tournoux, P. (1988). *Co-planar Stereotaxic Atlas of the Human Brain*. Stuttgart: Thieme.

Tamada, T., Miyauchi, S., Imamizu, H., Yoshioka, T., & Kawato, M. (1999). Cerebro-cerebellar functional connectivity revealed by the laterality index in tool-use learning. *NeuroReport, 10*(2), pp 325-331.

Tan, S. K. H., Temel, Y., Blokland, A., Steinbusch, H. W. M., & Visser-Vandewalle, V. (2006). The subthalamic nucleus: From response selection to execution. *Journal of Chemical Neuroanatomy, 31*(3), pp 155-161.

Tandon, R., & Jibson, M. D. (2002). Extrapyramidal side effects of antipsychotic treatment: scope of problem and impact on outcome. *Annals of Clinical Psychiatry, 14*(2), pp

123-129.

Tannock, R., Schachar, R., & Logan, G. (1995). Methylphenidate and cognitive flexibility: Dissociated dose effects in hyperactive children. *Journal of Abnormal Child Psychology, 23*(2), pp 235-266.

Taylor, S. F., Kornblum, S., Lauber, E. J., Minoshima, S., & Koeppe, R. A. (1997). Isolation of specific interference processing in the stroop task: PET activation studies. *NeuroImage, 6*(2), pp 81-92.

Tedroff, J., Pedersen, M., Aquilonius, S. M., Hartvig, P., Jacobsson, G., & Långström, B. (1996). Levodopa-induced changes in synaptic dopamine in patients with Parkinson's disease as measured by [11C]raclopride displacement and PET. *Neurology, 46*(5), pp 1430-1436.

Tedroff, J. M. (1997). The neuroregulatory properties of L-DOPA. A review of the evidence and potential role in the treatment of Parkinson's disease. *Reviews in the Neurosciences, 8*(3-4), pp 195-204.

Temel, Y., Blokland, A., Steinbusch, H. W. M., & Visser-Vandewalle, V. (2005). The functional role of the subthalamic nucleus in cognitive and limbic circuits. *Progress in Neurobiology, 76*(6), pp 393-413.

Tesche, C. D., & Karhu, J. J. T. (2000). Anticipatory cerebellar responses during somatosensory omission in man. *Human Brain Mapping, 9*(3), pp 119-142.

Thoma, P., Wiebel, B., & Daum, I. (2007). Response inhibition and cognitive flexibility in schizophrenia with and without comorbid substance use disorder. *Schizophrenia Research, 92*(1-3), pp 168-180.

Tu, P. C., Yang, T. H., Kuo, W. J., Hsieh, J. C., & Su, T. P. (2006). Neural correlates of antisaccade deficits in schizophrenia, an fMRI study. *Journal of Psychiatric Research, 40*(7), pp 606-612.

Tzourio-Mazoyer, N., Landeau, B., Papathanassiou, D., Crivello, F., Etard, O., Delcroix, N., et al. (2002). Automated anatomical labeling of activations in SPM using a macroscopic anatomical parcellation of the MNI MRI single-subject brain. *NeuroImage, 15*(1), pp 273-289.

Tzschentke, T. M. (2001). Pharmacology and behavioral pharmacology of the mesocortical dopamine system. *Progress in Neurobiology, 63*(3), pp 241-320.

Ullsperger, M., & Von Cramon, D. Y. (2001). Subprocesses of performance monitoring: A dissociation of error processing and response competition revealed by event-related fMRI and ERPs. *NeuroImage, 14*(6), pp 1387-1401.

Umbricht, D., & Krljesb, S. (2005). Mismatch negativity in schizophrenia: A meta-

analysis. *Schizophrenia Research, 76*(1), pp 1-23.

van Boxtel, G. J. M., van der Molen, M. W., Jennings, J. R., & Brunia, C. H. M. (2001). A psychophysiological analysis of inhibitory motor control in the stop-signal paradigm. *Biological Psychology, 58*(3), pp 229-262.

van den Wildenberg, W. P. M., van Boxtel, G. J. M., van der Molen, M. W., Bosch, D. A., Speelman, J. D., & Brunia, C. H. M. (2006). Stimulation of the subthalamic region facilitates the selection and inhibition of motor responses in Parkinson's Disease. *Journal of Cognitive Neuroscience, 18*(4), pp 626-636.

van den Wildenberg, W. P. M., van der Molen, M. W., & Logan, G. D. (2002). Reduced response readiness delays stop signal inhibition. *Acta Psychologica, 111*(2), pp 155-169.

van der Stelt, O., Frye, J., Lieberman, J. A., & Belger, A. (2004). Impaired P3 generation reflects high-level and progressive neurocognitive dysfunction in schizophrenia. *Archives of General Psychiatry, 61*(3), pp 237-248.

van Veen, V., & Carter, C. S. (2002). The anterior cingulate as a conflict monitor: fMRI and ERP studies. *Physiology & Behavior, 77*(4-5), pp 477-482.

Verbruggen, F., & Logan, G. D. (2008). Response inhibition in the stop-signal paradigm. *Trends in Cognitive Sciences, 12*(11), pp 418-424.

Vink, M., Kahn, R. S., Raemaekers, M., Heuvel, M. v. d., Boersma, M., & Ramsey, N. F. (2005). Function of striatum beyond inhibition and execution of motor responses. *Human Brain Mapping, 25*(3), pp 336-344.

Ward, P., Catts, S., Fox, A., Michie, P., & McConaghy, N. (1991). Auditory selective attention and event-related potentials in schizophrenia. *The British Journal of Psychiatry, 158*(4), pp 534-539.

Warner, R. & de Girolamo, G. (1995). *Epidemiology of Mental Disorders and Psychosocial Problems: Schizophrenia*. Geneva, World Health Organisation.

Watanabe, J., Sugiura, M., Sato, K., Sato, Y., Maeda, Y., Matsue, Y., et al. (2002). The human prefrontal and parietal association cortices are involved in NO-GO performances: An event-related fMRI study. *NeuroImage, 17*(3), pp 1207-1216.

Waters, F. A. V., Badcock, J. C., Maybery, M. T., & Michie, P. T. (2003). Inhibition in schizophrenia: association with auditory hallucinations. *Schizophrenia Research, 62*(3), pp 275-280.

Watis, L., Chen, S. H., Chua, H. C., Chong, S. A., & Sim, K. (2008). Glutamatergic abnormalities of the thalamus in schizophrenia: A systematic review. *Journal of Neural Transmission, 115*(3), pp 493-511.

Weinberger, D. R. (1987). Implications of normal brain development for the pathogenesis of schizophrenia. *Archives of General Psychiatry, 44*(7), pp 660-669.

Weinberger, D. R., Aloia, M. S., Goldberg, T. E., & Berman, K. F. (1994). The frontal lobes and schizophrenia. *Journal of Neuropsychiatry and Clinical Neurosciences, 6*(4), pp 419-427.

Weinberger, D. R., Berman, K. F., & Zec, R. F. (1986). Physiologic dysfunction of dorsolateral prefrontal cortex in schizophrenia. I. Regional cerebral blood flow evidence. *Archives of General Psychiatry, 43*(2), pp 114-124.

Weinberger, D. R., Egan, M. F., Bertolino, A., Callicott, J. H., Mattay, V. S., Lipska, B. K., et al. (2001). Prefrontal neurons and the genetics of schizophrenia. *Biological Psychiatry, 50*(11), pp 825-844.

Weisbrod, M., Kiefer, M., Marzinzik, F., & Spitzer, M. (2000). Executive control is disturbed in schizophrenia: evidence from event-related potentials in a Go/NoGo task. *Biological Psychiatry, 47*(1), pp 51-60.

Welsh, R. C., Chen, A. C., & Taylor, S. F. (2008). Low-frequency BOLD fluctuations demonstrate altered thalamocortical connectivity in schizophrenia. *Schizophrenia Bulletin*, (in press).

Whitworth, A. B., & Fleischhacker, W. W. (1995). Adverse effects of antipsychotic drugs. *International Clinical Psychopharmacology, 9*(SUPPL. 5), pp21-27.

Williams, B. R., Ponesse, J. S., Schachar, R. J., Logan, G. D., & Tannock, R. (1999). Development of inhibitory control across the life span. *Developmental Psychology, 35*(1), pp 205-213.

Willick, M. S. (1994). A parents perspective - mourning without end. In N. C. Andreasen (Ed.), *Schizophrenia: From Mind to Molecule* (pp. 5-19). Washington: American Psychiatric Press.

Woldorff, M. G. (1993). Distortion of ERP averages due to overlap from temporally adjacent ERPs: Analysis and correction. *Psychophysiology, 30*(1), pp 98-119.

Wölwer, W., & Gaebel, W. (2002). Impaired Trail-Making Test-B performance in patients with acute schizophrenia is related to inefficient sequencing of planning and acting. *Journal of Psychiatric Research, 36*(6), pp 407-416.

Wong, D. F., Wagner Jr, H. N., & Tune, L. E. (1986). Positron emission tomography reveals elevated D2 dopamine receptors in drug-naive schizophrenics. *Science, 234*(4783), pp 1558-1563.

Wood, S. M., Potts, G. F., Hall, J. F., Ulanday, J. B., & Netsiri, C. (2006). Event-related potentials to auditory and visual selective attention in schizophrenia. *International*

Journal of Psychophysiology, 60(1), pp 67-75.

Worsley, K. J., Marrett, S., Neelin, P., Vandal, A. C., Friston, K. J., & Evans, A. C. (1996). A unified statistical approach for determining significant signals in images of cerebral activation. *Human Brain Mapping, 4*(1), pp 58-73.

World Health Organization. (1993). The ICD-10 classification of mental and behavioural disorders. Diagnostic criteria for research. Geneva: WHO.

Wu, Y., Richard, S., & Parent, A. (2000). The organization of the striatal output system: A single-cell juxtacellular labeling study in the rat. *Neuroscience Research, 38*(1), pp 49-62.

Yasuno, F., Suhara, T., Okubo, Y., Sudo, Y., Inoue, M., Ichimiya, T., et al. (2004). Low dopamine D2 receptor binding in subregions of the thalamus in schizophrenia. *American Journal of Psychiatry, 161*(6), pp 1016-1022.

Yoo, S. Y., Yeon, S., Choi, C. H., Kang, D. H., Lee, J. M., Shin, N. Y., et al. (2009). Proton magnetic resonance spectroscopy in subjects with high genetic risk of schizophrenia: Investigation of anterior cingulate, dorsolateral prefrontal cortex and thalamus. *Schizophrenia Research, 111*(1-3), pp 86-93.

Yoshihara, Y., Sugihara, G., Matsumoto, H., Suckling, J., Nishimura, K., Toyoda, T., et al. (2008). Voxel-based structural magnetic resonance imaging (MRI) study of patients with early onset schizophrenia. *Annals of General Psychiatry, 7,* pp 25.

Zheng, D., Oka, T., Bokura, H., & Yamaguchi, S. (2008). The key locus of common response inhibition network for no-go and stop signals. *Journal of Cognitive Neuroscience, 20*(8), pp 1434-1442.

Zubin, J., & Spring, B. (1977). Vulnerability: A new view of schizophrenia. *Journal of Abnormal Psychology, 86*(2), pp 103-126.